

For Reference

NOT TO BE TAKEN FROM THIS ROOM

Ex LIBRIS
UNIVERSITATIS
ALBERTAENSIS



BRUCE PEEL SPECIAL COLLECTIONS LIBRARY
UNIVERSITY OF ALBERTA LIBRARY


REQUEST FOR DUPLICATION

I wish a photocopy of the thesis by

Suko, M. (author)

entitled Inelastic Dynamic - - -

The copy is for the sole purpose of private scholarly or scientific study and research. I will not reproduce, sell or distribute the copy I request, and I will not copy any substantial part of it in my own work without permission of the copyright owner. I understand that the Library performs the service of copying at my request, and I assume all copyright responsibility for the item requested.



Digitized by the Internet Archive
in 2023 with funding from
University of Alberta Library

<https://archive.org/details/Suko1973>

Grad Studies Copy

T H E U N I V E R S I T Y O F A L B E R T A

RELEASE FORM

NAME OF AUTHOR Masaaki Suko

TITLE OF THESIS Inelastic Analysis of Multistory
 Multibay Frames Subjected to
 Dynamic Disturbances

DEGREE FOR WHICH THESIS WAS PRESENT Ph. D.

YEAR THIS DEGREE GRANTED 1973

Permission is hereby granted to THE UNIVERSITY OF ALBERTA LIBRARY to reproduce single copies of this thesis and to lend or sell such copies for private, scholarly or scientific research purposes only.

The author reserves other publication rights, and neither the thesis nor extensive extracts from it may be printed or otherwise reproduced without the author's written permission.

THE UNIVERSITY OF ALBERTA

INELASTIC ANALYSIS OF MULTISTORY MULTIBAY FRAMES
SUBJECTED TO DYNAMIC DISTURBANCES

by

Masaaki Suko



A THESIS

SUBMITTED TO THE FACULTY OF GRADUATE STUDIES AND RESEARCH
IN PARTIAL FULFILMENT OF THE REQUIREMENTS FOR THE DEGREE
OF DOCTOR OF PHILOSOPHY

DEPARTMENT OF CIVIL ENGINEERING

EDMONTON, ALBERTA

FALL, 1973

THE UNIVERSITY OF ALBERTA
FACULTY OF GRADUATE STUDIES AND RESEARCH

The undersigned certify that they have read, and recommend to the Faculty of Graduate Studies and Research, for acceptance, a thesis entitled "INELASTIC ANALYSIS OF MULTISTORY MULTIBAY FRAMES SUBJECTED TO DYNAMIC DISTURBANCES" submitted by MASAAKI SUKO in partial fulfilment of the requirements for the degree of Doctor of Philosophy.

ABSTRACT

This dissertation presents a method for the analysis of a frame subjected to either a blast load or an earthquake motion. The procedure accounts for the inelastic action of the frame members and the other significant secondary effects. A behavioral study has been performed using the procedure and as a result, a tentative design procedure for steel frames subjected to blast loads has been proposed.

The analytical model used to represent the frame has equal numbers of stories and bays as the actual frame. The frame may contain shearwalls. In the analysis, a tri-linear type of moment-curvature-thrust relationship is assumed for the structural components with a hysteresis rule employed in an attempt to account for the increasing strength under reversals of loading.

The inelastic action of the members and the $P-\Delta$ effect are considered by introducing an equivalent rotational spring at each member end. By selecting the properties of the rotational spring properly, the response of the model to lateral load can closely simulate that of an actual frame. Other secondary effects such as the shear deformations of the members and joints, the effect of semi-rigid connections, etc., may also be considered by modifying the

properties of the rotational springs.

The standard slope deflection equations are modified to meet the present situation. When these equations are used to construct the frame stiffness matrix, the computation in the inelastic range can be done in the same manner as those in the elastic range. The stiffness matrix is thus updated to be compatible with the deteriorated structure at each instant of the motion. The equations of motion are solved using a linear acceleration method.

As a result of behavioral study performed, an empirical equation for the calculation of the fundamental natural period has been proposed (the error is usually less than 5%). In addition, once the modified total impulse of a blast load is defined, the relationships between the blast load intensity and the resisting base shear can be expressed by a relatively simple formula. Once the base shear is known, the required strengths for the frame members may be estimated.

A design procedure is proposed to select a set of member sizes to resist an expected blast load. The procedure eliminates the need for a dynamic analysis for regular frames. Although the frames designed according to this procedure can be expected to behave satisfactorily, it is always desirable to perform a dynamic analysis if possible.

ACKNOWLEDGEMENTS

The author wishes to express his sincere appreciation to Prof. P. F. Adams, supervisor of the study, for his continuous encouragement and suggestions throughout the course of the research and the preparation of the manuscript. The helpful suggestions and criticisms made by Profs. L. W. Jackson, J. S. Kennedy, J. Longworth, J. G. MacGregor and R. D. Hanson, the members of the examining committee, are acknowledged with thanks. The author further wishes to acknowledge the beneficial discussions held with S. Rajasekaran, J. H. Wynhoven, B. W. Slight, and S. Hamada.

The study was supported financially by the Defense Research Board under Grant No. DRB 6301-07. This support is gratefully acknowledged as is the receipt of a fellowship awarded to the author by the Isaak Walton Killam Memorial Fellowships Committee.

The manuscript was typed by Ms. Barbara Hickey whose cooperation is appreciated.

TABLE OF CONTENTS

	Page
Library Release Form	i
Title Page	ii
Approval Sheet	iii
Abstract	iv
Acknowledgements	vi
Table of Contents	vii
List of Tables	xii
List of Figures	xiii
List of Symbols	xix
Chapter 1 INTRODUCTION	1
1-1 Purpose of Investigation	1
1-2 Previous Studies	3
1-2-1 Member and Frame Response to Static Load	3
1-2-2 Characteristics of Dynamic Loads	6
1-2-3 Dynamic Analyses in Inelastic Range	7
1-3 Scope of Dissertation	12
Chapter 2 MEMBER RESPONSE DURING STRUCTURAL VIBRATION	19
2-1 Introduction	19
2-2 Material Properties	20
2-3 Geometrical Characteristics of Wide Flange Sections	22
2-3-1 Relationship Between Cross Sectional Area and Moment of Inertia	23

2-3-2	Relationship Between Plastic Modulus and Moment of Inertia	25
2-3-3	Plastic Moment Capacity in the Presence of Axial Force	26
2-4	Moment-Curvature-Thrust Relationship	28
2-4-1	Empirical Moment-Curvature-Thrust Relationship	28
2-4-2	Derivation of Approximate Formulae	32
2-5	Use of Rotational Spring to Simulate Member Inelastic Action and P- Δ Effect	35
2-5-1	Analysis of Cantilever Column	36
2-5-2	Use of Equivalent Rotational Spring to Simulate the Actual Column Behavior	39
2-5-3	Characteristics of $M_s-\delta\theta_s$ Curves	41
2-5-4	Consideration of Reversals of Load	43
2-6	Computer Program	44
Chapter 3	FORMULATION OF EQUATIONS OF MOTION	65
3-1	Introduction	65
3-2	Analytical Model	66
3-3	Equivalent Rotational Springs in Modeled Frame	68
3-4	Influence of Semi-Rigid Connections, Deformation of Joint Panels, and Shear Deformation of Members	69
3-5	Stiffness Matrix for Frame	71
3-5-1	Slope Deflection Equations for Members with Rotational Springs and Rigid Stubs	71
3-5-2	Stiffness Matrix for Frames	75

	Page
3-6 Static Responses	79
3-7 Equations of Motion	80
3-7-1 Formulation of Equations of Motion	80
3-7-2 Numerical Integration	84
3-7-3 Natural Periods of Vibration	86
Chapter 4 BEHAVIORAL STUDY	100
4-1 Introduction	100
4-2 Relationship Between Blast Loads and Earthquake Motions	101
4-3 Empirical Formula for the Fundamental Natural Period	103
4-4 Correlation Between Input Blast Load and Structural Response	106
4-4-1 Example Blast Loads on a Structure	106
4-4-2 Properties of Example Frame	108
4-4-3 Effect of Blast Load-Time Function on Elastic Response	110
4-4-4 Effect of Blast Load-Time Function on Inelastic Response	112
4-5 Relationship Between Modified Total Impulse and Maximum Base Shear	114
4-6 Difference in Response for Various Frame Designs	116
4-6-1 The Effect of Variation in Column Stiffness	117
4-6-2 The Effect of Beam Stiffness	118
4-6-3 The Effect of Shearwalls on the Frame Response	120
4-7 Required Strength of Frame	121

		Page
4-8	Comparison of Various Designs	126
4-9	Summary	130
Chapter 5	DESIGN PROCEDURE	176
5-1	Introduction	176
5-2	Design Procedure	176
Chapter 6	SUMMARY AND CONCLUSIONS	184
REFERENCES		188
Appendix A	SUPPLEMENTARY EXPLANATION OF SECTION 2-5-1	197
A-1	Derivation of Eqs. 2-35, 2-36 and 2-39	197
A-2	Load-Deflection Relationship When Axial Load is Absent	201
A-3	Load-Deflection Relationship When the Moment Curvature Relationship is Elastic-Perfectly Plastic	202
A-4	Load-Deflection Relationship When the Base of the Column is Restrained by a Rotational Spring	203
Appendix B	COMPUTER PROGRAM I	207
B-1	Description of the Program	207
B-2	Input Data	207
B-3	Description of Subprograms and Flow Charts	208
B-4	Listing of Program	211

		Page
Appendix C	DERIVATION OF MODIFIED SLOPE DEFLECTION EQUATIONS	228
Appendix D	COMPUTER PROGRAM II	234
D-1	Description of the Program	234
D-2	Input Data	234
D-3	Presentation of Results	241
D-4	Description of Subprograms and Flow Charts	244
D-5	Listing of Program	258
Appendix E	BLAST LOADS ON A STRUCTURE	301
E-1	Determination of Blast Loads on a Structure	301
E-2	Example Calculation of the Blast Load on a Structure	308
Appendix F	EMPIRICAL METHOD FOR THE DETER- MINATION OF THE NATURAL PERIOD	331
F-1	Empirical Formula for Natural Period	331
F-2	Examples	333

LIST OF TABLES

Table		Page
4-1	Structural Properties of FRAME#1AA	133
4-2	Properties of FRAME#1BA, FRAME#1BB, FRAME#1BC and FRAME#1BD	134
4-3	Properties of FRAME#2AA and FRAME#2AB	135
4-4	Properties of FRAME#2BA and FRAME#2BB	136
4-5	Properties of FRAME#3AA and FRAME#3AB	137
4-6	Properties of FRAME#4AB and FRAME#4BB	138
4-7	Properties of FRAME#5AA	139
4-8	Properties of FRAME#5BB and FRAME#6AA	140
4-9	Responses of Various Frames	141
E-1	Drag Coefficient : C_d	312

LIST OF FIGURES

Figure		Page
1-1	Hysteretic Curve Used in Previous Studies, (1) Elastic-Perfectly Plastic	14
1-2	Hysteretic Curve Used in Previous Studies, (2) Elastic-Plastic with Negative Slope	15
1-3	Hysteretic Curve Used in Previous Studies, (3) Bilinear Relationship	16
1-4	Hysteretic Curve Used in Previous Studies, (4) Kato and Akiyama's Model	17
1-5	Hysteretic Curve Used in Previous Studies, (5) Ramberg-Osgood Model	18
2-1	Stress-Strain Relationship	47
2-2	Strain Reversals	48
2-3	Correlation Between the Moment of Inertia and the Cross Sectional Area (1)	49
2-4	Correlation Between the Moment of Inertia and the Cross Sectional Area (2)	50
2-5	Correlation Between the Moment of Inertia and the Plastic Section Modulus (1)	51
2-6	Correlation Between the Moment of Inertia and the Plastic Section Modulus (2)	52
2-7	Interaction Curve for Strong Axis Bending of Wide Flange Sections	53
2-8	Moment-Curvature-Thrust Relationship	54
2-9	Comparison of the Present Moment-Curvature- Thrust Relationship with a Rigorous Relationship	55
2-10	Schematic Expression of Stresses and Strains	56
2-11	Column with Axial Load	57
2-12	Moment-Curvature Relationship for Column	58

Figure		Page
2-13	Restrained Column	59
2-14	Cross Sectional Properties and the $M_s - \delta\theta_s$ Relationship	60
2-15	Strain Reversals in the $M_s - \delta\theta_s$ Relationship	64
3-1	Analytical Model	87
3-2	Numbering Convention	88
3-3	Typical Moment Diagram in a Frame	89
3-4	Inclusion of Secondary Effects	90
3-5	Semi-Rigid Joint	91
3-6	Shear Deformation of Joint Panel	92
3-7	Shear Deformation of Member	93
3-8	Typical Member	94
3-9	Resulting $M_s - \delta\theta_s$ Relationship	95
3-10	Static Response	96
3-11	Equilibrium of Forces in Motion	97
3-12	Chart for Numerical Integration	98
4-1	Value of T_0 for the Calculation of the Natural Period	142
4-2	Correlation Between Natural Period by Rigorous Calculation and Natural Period by Empirical Formula	144
4-3	Example Building	145
4-4	Example Frame; Dimensions and Vector $\{r\}$	146

Figure		Page
4-5	Blast Load Type A-105.2	147
4-6	Blast Load Type B-212.5	148
4-7	Blast Load Type C-358	149
4-8	Blast Load Type AA-105.2	150
4-9	Blast Load Type BA-212.5	151
4-10	Blast Load Type CA-358	152
4-11	Stress-Strain Relationship	153
4-12	Cross Sectional Properties and the $M_s - \delta \theta_s$ Relationship for FRAME#1AA	154
4-13	Maximum Base Shear vs. Total Impulse -- FRAME#1AA	157
4-14	Maximum Base Shear vs. Modified Total Impulse -- FRAME#1AA	158
4-15	Deflection at Top vs. Modified Total Impulse - FRAME#1AA	159
4-16	Maximum Base Shear vs. Modified Total Impulse for FRAME#1AA	160
4-17	Location of Yielding in FRAME#1AA Subjected to Blast Load Type A-212.5 (At Point X in Figure 4-16)	161
4-18	Location of Yielding in FRAME#1AA Subjected to Blast Load Type AA-300 (At Point Y in Figure 4-16)	162
4-19	Average Value of Q_b/I^* vs. Natural Period	163
4-20	Modified Impulse of Blast Load Type A for Standard Floor	164
4-21	Modified Impulse of Blast Load Type AA for Standard Floor	165
4-22	Maximum Intensity of Blast Load Type BA vs. Maximum Base Shear for FRAME#2AA and FRAME#2BA	166

Figure		Page
4-23	Location of Member End where Inelastic Action was Recorded for FRAME#2AA and FRAME#2BA (Blast Load Type BA-45)	167
4-24	Maximum Intensity of Blast Load Type AA vs. Maximum Base Shear for FRAME#1BA and FRAME#1BC	168
4-25	Maximum Story Shears for FRAME#1AA Subjected to Blast Load Type A-212.5	169
4-26	Maximum Story Shears Typical for Regular Type of Frames	170
4-27	Correlation Between Story Shears and Strength of Columns	171
4-28	Typical Moment Diagram at a Floor Level	172
4-29	Blast Load Intensity (Type AA) vs. Maximum Base Shear for FRAME#3AB	173
4-30	Blast Load Intensity (Type AA) vs. Maximum Base Shear for FRAME#5AA and FRAME#5BB	174
4-31	Blast Load Intensity (Type AA) vs. Maximum Relative Displacement for FRAME#5AA and FRAME#5BB	175
5-1	Design Procedure	182
A-1	Coordinate Systems in Column	206
B-1	MAIN Program	212
B-2	Subroutine KEISAN	213
C-1	Equilibrium of Forces	233
D-1	MAIN Program	259
D-2	$M_s - \delta \theta_s$ Relationship in General Situation	260
D-3	Subroutine STIFF	261
D-4	Subroutine JISHIN	262
D-5	Subroutine SAIBUN	267

Figure		Page
D-6	Subroutine SUCHI	268
D-7	Subroutine KYOTO	269
D-8	Subroutine NARA	270
E-1	Peak Overpressures on the Ground for 1-KT Burst	313
E-2	Peak Overpressure and Peak Dynamic Pressure for 1-KT Surface Burst	315
E-3	Horizontal Component of Peak Dynamic Pressure for 1-KT Burst	316
E-4	Positive Phase Duration on the Ground of Overpressure and Dynamic Pressure for 1-KT Burst	317
E-5	Rate of Decay of Pressure with Time for Various Values of the Peak Overpressure	318
E-6	Rate of Decay of Dynamic Pressure with Time for Various Values of the Peak Overpressure	319
E-7	Relation of Ideal Blast Wave Characteristics at the Shock Front to the Peak Overpressure	320
E-8	Arrival Time on the Ground of Blast Wave for 1-KT Burst	321
E-9	Reflected Overpressure Ratio as Function of Angle of Incidence for Various Side-on Overpressures.	322
E-10	Angle of Incidence, α , of Blast Wave with Reflecting Surface	323
E-11	Closed Box-Like Structure	324
E-12	Average Front Surface Pressure, p_1	325
E-13	Average Back Surface Pressure, p_2	326
E-14	Net Horizontal Load (Pressure)	327

Figure		Page
E-15	Average Pressure Applied to Front Surface (A) and to Back Surface (B)	329
E-16	Average Net Horizontal Load on the Structure	330
F-1	Frame with Shearwalls	337
F-2	Frames with Pinned-End Columns	338
F-3	Example Frame	339

LIST OF SYMBOLS

In the following list, the subscript, i , represents an appropriate number; and the subscripts, x and y , are replaced by appropriate letters in the main text.

A	:	Cross sectional area
A_i, A'_i	:	Coefficients used to describe the modified slope deflection equations
B	:	Width of a building
$\{B\}$:	Known vector (right hand side vector) in equilibrium equations
C_d	:	Drag coefficient
C_{xy}	:	Fixed end moment at x -end of member xy
CMA_i	:	Sum of the mass times the acceleration (relative to the ground) above the i -th floor (excluding the i -th floor), as defined in Eq. 3-35
CR_i	:	$\sum_{j=1}^i r_j$
CSM_i	:	Sum of the masses above the i -th floor (including the i -th floor), as defined in Eq. 3-35
c_i	:	Damping coefficient at the i -th story

D_{xy}	: Term in the modified slope deflection equations caused by U.D.L. with respect to x-end of member xy
d	: Nominal depth of a wide flange section (chapter 2); or the distance of a building from G.Z. (appendix E)
d_1	: Scaled distance of a building from G.Z.
E	: Modulus of elasticity
E_{st}	: Average ratio of the increase in stress to the increase in strain in the initial portion of the strain-hardening range
$f(t)$: Function used to calculate modified impulse
G	: Modulus of rigidity
[G]	: Frame stiffness matrix
G.Z.	: Ground zero
g	: Acceleration of gravity
H	: Height of the building
h	: Ratio of the average story height to a standard height of 12 feet (144 inches) (chapter 4, 5 and 6); or the height of burst (appendix E)
h_1	: Scaled height of burst
h_i	: Constant used to determine the damping constant at the i-th story

I	: Moment of inertia (chapter 2 and 3); or the total impulse applied to a frame (chapter 4)
I^*	: Modified total impulse applied to a frame
i^*	: Modified impulse applied at a standard floor, where the maximum intensity of a blast load is scaled to unity
K	: EI
K_b	: Average stiffness of beam members
K_c	: Average stiffness of column members
K_{st}	: $(2-m)E_{st}I$
k	: Spring constant of an elastic foundation
L	: Length of an equivalent cantilever column (chapter 2); the member length (chapter 3 and 4); or the depth of a building (appendix E)
L_1	: Length of the elastic portion of an equivalent cantilever column
L_2	: Length of the inelastic portion of an equivalent cantilever column
M_b	: Moment at the bottom of a cantilever column
M_i	: Intercept on the moment axis as shown in Fig. 2-12
M_p	: Plastic moment capacity
M_{pc}	: Reduced plastic moment capacity due to an axial load

M_s	: Moment in an equivalent rotational spring
M_u	: Ultimate moment capacity
M_{uc}	: Reduced ultimate moment capacity due to an axial load
M_{xy}	: End moment at x-end of member xy
m	: M_{pc}/M_p
m_i	: Mass concentrated at the i-th floor
N_b	: Number of bays
N_s	: Number of stories
P	: Axial load
P_y	: Yield axial load
p	: Peak overpressure
p_n	: Average net pressure applied to a building, i.e., $p_1 - p_2$
p_r	: Reflected overpressure
p_s	: Stagnation pressure
p_1	: Average pressure applied to the front surface of a building
p_2	: Average pressure applied to the back surface of a building
$p(t)$: Overpressure which is a function of time
Q	: Transverse load
Q_b	: Maximum base shear
$\{Q\}$: Story shears due to frame action

q	: Peak dynamic pressure
$q(t)$: Dynamic pressure which is a function of time
$[R]$: Coefficient matrix in equilibrium equations
$\{r\}$: Vector which indicates the ratios of blast load applied at each floor level
S	: Height of a building or the half of the width of the frontal surface of the building, whichever is less
$S_i(t)$: One of the terms in equations of motion as defined in Eq. 3-34
s	: ϵ_{st}/ϵ_y
T_i	: Natural period in the i -th mode
T_0	: Fundamental natural period of a standard 10-story frame
t	: Time in seconds
t_b	: Time required for the pressure to build up to the surrounding pressure at the back surface of a building
t_s	: Time required for stagnation at the frontal surface of a building
t_2	: Time required for the shock front to travel the depth of a building
t_{+p}	: Duration of positive phase overpressure
t_{+p1}	: Duration of positive phase overpressure for a 1 KT burst

t_{+q}	: Duration of positive phase dynamic pressure
t_{+q1}	: Duration of positive phase dynamic pressure for a 1 KT burst
U	: Shock front velocity
W	: Size of burst in KT's, TNT equivalent
w	: Uniformly distributed load
$\{x\}$: Displacement relative to the ground
$\{\dot{x}\}$: Velocity relative to the ground
$\{\ddot{x}\}$: Acceleration relative to the ground
\ddot{Y}_O	: Acceleration of ground motion
Z	: Plastic section modulus
$Z(t)$: Blast load applied at a standard floor
α	: Ratio of average stiffness of columns to a standard value of stiffness ($.500 \times 10^6$ kip·in) (chapter 4, 5 and 6); or the angle of incidence of a blast wave (appendix E)
α_1, α_2	: Coefficients used to describe the $M_s - \delta\theta_s$ relationship of an equivalent rotational spring
β	: Ratio of the average story mass divided by the number of columns to a standard value of mass ($70/g$ kip·sec ² /in), adjusted by the number of bays; as defined in Eq. 4-6

β_1, β_2	: Coefficients used to describe the M_s - $\delta\theta_s$ relationship of an equivalent rotational spring
γ	: K_b/K_c
Δ	: Deflection at the top of a cantilever column
Δt	: Increment in time when equations of motion are solved numerically
$\delta\theta_s$: Relaxation angle produced by an equivalent rotational spring
ϵ	: Strain
ϵ_{st}	: Strain at the onset of strain-hardening
ϵ_y	: Yield strain
ζ	: Quantity defined in Eq. 2-48
$\{\eta\}$: Constant vector expressing index story shears
$\{\eta_i\}$: i -th column of a stiffness matrix
$\{\eta_0\}$: $-[G]\{\xi_0\}$
θ_x, θ_y	: Joint rotations at end x and end y of member xy
$\{\theta\}$: Unknown vector in equilibrium equations
κ	: Shape factor for calculation of shear deformation
λ_1	: Ratio of length of rigid stub at the left end of a beam to the entire member length
λ_2	: Ratio of length of rigid stub at the right end of a beam to the entire member

Chapter 1.

INTRODUCTION

1-1 Purpose of Investigation.

The design of structural frames to resist forces induced during an earthquake motion or blast disturbance is generally a semiempirical procedure with the forces specified being based primarily on dynamic analyses of simplified structures and modified in the light of observations of past failures. In order to design on a more rational basis, it is first necessary to have available a procedure for the analysis of complex structures; this procedure is the subject of this dissertation.

The analytical procedure presented herein is able to determine the inelastic response of rigidly connected multibay multistory planar frames using a large capacity digital computer. Interest is focused on steel frames with or without shearwalls, although with minor modifications in the input data, concrete frames may also be treated. The disturbance applied to a structure may be either an earthquake motion or blast loading.

The secondary moments produced by the vertical loads acting through the sway displacements of the frame are treated together with the effects of inelastic action (including strain-hardening) of the members. The effects

of semirigid connections, shear deformations of joint panels and shear deformation of the members can also be taken into account without increasing the complexity of the procedure. The above effects are treated in an approximate manner due to the complexity of the overall problem.

The second objective of this dissertation is to present the results of a behavioral study, performed using the analytical procedure. The following factors are specifically considered in the study.

a) The effects of beam stiffness and column stiffness distributions over the height of a structure on the natural periods.

(b) The effects of various types of blast loads on the response of a structure.

c) The effects of beam stiffness and column stiffness distribution over the height of a structure on the response of the structure (both in elastic and inelastic ranges) to a blast load.

These factors are examined by investigating the response of several steel frames having different structural arrangements. By analyzing the results of the behavioral study, a tentative design procedure, which leads to an efficient design against blast loading, is proposed.

1-2 Previous Studies.

The objective of this section is to locate the present study in the stream of current research; the section is not intended to be a complete survey of the literature in this field. The discussion is oriented in such a way that one can realize the necessity of the present type of study and understand the background on which certain assumptions are made in the present analysis. The discussion is also limited to the literature published in English, although many reports in Japanese (and possibly in other languages) are available in the field of dynamic analysis.

The section is divided into three parts. The study of the static response of both member elements and entire frames is first discussed, since this knowledge has great influence on the analytical model on which a dynamic analysis is performed. A clear understanding of the characteristics of dynamic loads is also highly desirable. The present state of this knowledge is briefly discussed in the second part of the review. In the final part, the technique used to solve the equations describing the dynamic response are reviewed. Current topics in the field of dynamic analysis are also introduced.

1-2-1 Member and Frame Response to Static Load.

In order to analyze a frame, it is necessary to prepare

an end moment-end rotation relationship for every member for an assumed value of the axial force.

Such an end moment-end rotation relationship for a steel member has often been represented by an elastic-perfectly plastic relationship as shown in Fig. 1-1 or by a bilinear relationship having a negative slope as shown in Fig. 1-2; depending upon whether the $P-\Delta$ effect is included at this stage.

The role of strain-hardening, which was ignored in the above models, has been taken into account by Jennings and Husid¹ and Thomaides² in their dynamic analyses. The end moment-end rotation relationship employed was a bilinear relationship with a positive second branch as shown in Fig. 1-3. It has been observed that under reversals of loading, the strength of column members increases with an increased number of load applications.^{3,4,5} Kato and Akiyama³ have shown that the strength increase is caused partly by the residual $P-\Delta$ moment and partly by strain-hardening and have proposed a hysteresis rule of the type shown in Fig. 1-4. The present study complies with this idea.

Jennings⁶ and Goel and Berg⁷ have used the Ramberg-Osgood function (Fig. 1-5) to approximate the moment-curvature relationship and derived a very similar function to approximate the end moment-end rotation relationship.

The prime advantage of this approach is in the easy mathematical treatment when considering hysteresis loops.

However, the negative portion of the end moment-end rotation relationship (due to axial force) can not be represented by this function.

A number of different methods have been used for the nonlinear analysis of the complete frame. Oden⁸ has discussed the advantages and disadvantages of each presently available method. Rajasekaran and Murray⁹ have classified these methods according to the mathematical technique involved and suggested the recommended method to be used for solving an individual problem according to the physical nature. The method described in Chapter 3 is an incremental loading method in principle, although it may not be seen clearly in the process of solving dynamic equations.

The $P-\Delta$ effect has been investigated by Yarimci, Yura and Lu¹⁰ on steel frames and by Majumdar, MacGregor and Adams¹¹ on coupled steel frame-shearwall structures. The analytical method used in these studies was to apply an additional lateral load in an attempt to produce the same column end moment as the actual case. It has been shown both theoretically and experimentally that the reduction in load carrying capacity is significant in both types of frames. In the present analysis, the $P-\Delta$ effect is considered by introducing an equivalent rotational spring at

each member end; the new system is proposed to eliminate the iterative procedure.

Naka, et al.¹² have studied the effect of shear deformation of the joint panels and have indicated that the elastic response calculated by taking this effect into account could be as much as 30% greater than the elastic response for a frame with properly reinforced joints or than an elastic response ignoring the effect. Munse, Bell and Cherson¹³ have pointed out that the response could also be increased when beam to column connections are not perfectly rigid. In the present analysis, these secondary effects, together with the effect of shear deformation of a member, can also be taken into account in conjunction with the previously mentioned rotational spring, although in an approximate manner.

1-2-2 Characteristics of Dynamic Loads.

The characteristics of blast waves have been investigated by the United States Department of Defence and other affiliated agencies and research institutes. Refs. 14 through 20 provide useful information concerning the magnitude of the blast loads which should be applied to a structure at a particular site. Brode²¹ and Newmark²² have reviewed the studies in this field and have added new remarks. The blast loads applied to the example frames in this

dissertation have been determined by summarizing the above information as shown in Appendix E.

Only a few records of the ground motion induced by strong earthquakes were available before the 1950's.²³ The strong motion accelerograph networks started recording ground motions in the U.S.A. and Japan in the late 1950's. The digitized data for recent earthquake motions have been published by the California Institute of Technology,²⁴ the SERAC²⁵ and the Ministry of Transport of Japan.²⁶ Jennings, Housner and Tsai²⁷ proposed artificial ground motions to be used for the analysis of a structure. In spite of efforts made by many researchers, it is still impossible to predict the ground motion which a future earthquake might produce at a particular building site.

1-2-3 Inelastic Response of Steel Frame to Dynamic Load.

The equations describing the response of a structure to an earthquake motion and to a blast load are very similar and hence the same numerical techniques can be used to achieve a solution in both cases. The Runge-Kutta's method modified by Gill,²⁸ Milne's method,²⁹ the linear acceleration method¹⁸ and Newmark's method³⁰ are typical techniques used to solve the second order coupled differential equations. Ralston³¹ presented an excellent comparison

among these methods. In the present study, the linear acceleration method is used because of its numerical stability.

The early studies of the response of a structure in the inelastic range used single degree-of-freedom systems^{2,32,33} and were gradually extended to more complex multidegree-of-freedom structures.^{34,35} In these studies, the importance of ductility and hysteretic damping (energy absorption) was emphasized; however, because of the highly idealized models, it was impossible to study various structural effects more specifically.

Jennings and Husid¹ investigated the significance of gravity load in a study of single degree-of-freedom systems subjected to artificially generated ground accelerations. In this study, the important parameters were the height of the structure, the ratio of the earthquake strength to the yield level of the structure and the slope of the second branch of the bilinear end moment-end rotation relationship.

Clough, Benuska and Wilson^{36,37} developed a computer program to analyze more complex structures. In these studies, a 3-bay, 20-story frame was analyzed by assuming a bilinear type of end moment-end rotation relationship. The structure was subjected to the N-S component of the El Centro 1940 earthquake. One of the important conclusions from this study was that plastic deformation will be

concentrated in the weaker members, thus sudden changes in stiffness should be avoided.

Goel and Berg⁷ analyzed multistory, single bay structures (symmetric) allowing inelastic action in the girders (Ramberg-Osgood function) but not in the columns. It was shown that the inelastic action of the girders alone can be a potential source of energy dissipation in unbraced steel frames during a strong earthquake motion. Very similar conclusion was also obtained from the study of Walpole and Shepherd.³⁸ Goel³⁹ further studied the $P-\Delta$ effect during the earthquake motions using the same structural model. From this, it was concluded that the $P-\Delta$ effect on the inelastic response was insignificant.

Sun⁴⁰ also investigated the gravity load effect on dynamic stability using one or two degree-of-freedom systems with bracing members whose force-displacement relationship was assumed to be an elastic-plastic system of the slip type. In order to study the $P-\Delta$ effect more quantitatively, the equation describing the relationship between the yield or collapse of the system and the amount of input energy was proposed using the $P-\Delta$ effect parameter (defined as axial load divided by the product of stiffness and height).

Lionberger and Weaver⁴¹ showed that nonrigid beam to column connections can influence both the lateral translation and the member end moments. The study was performed

on a 10-story, 2-bay symmetric frame subjected to an idealized blast load.

The analytical procedure presented in this dissertation is an attempt to provide a tool to analyze complex frames taking many secondary effects into consideration within a feasible computational effort.

Experimental verification of analytical results has been rather sparse. Nielsen⁴² reported a series of resonance tests of a nine-story steel frame building at the time when the frame works were completed. Using the test results, the method to evaluate the elements in the stiffness matrix and the coefficient of damping for each mode was introduced. Jennings, Matthiesen and Hoerner⁴³ conducted tests on a 22-story steel frame building. The main objective was to determine first three coupled modes; i.e., the fundamental modes in two orthogonal phases and the fundamental torsional mode, all coupled, whose natural periods are close together. Tests using simulated ground motions have recently become possible within a limited capacity. The results of such tests on reinforced concrete frames have been reported.⁴⁴

Hoerner⁴⁵ indicated that a rectangular building with small eccentricities and a smooth, uniform dispersion of columns could have nearly equal fundamental periods in the three directions of motion. A strong modal coupling, which

might include both rotational and beating effects, resulted in significant increases in the elastic response of such structures.

Nigam⁴⁶ studied the inelastic response of space-frame structures. An example calculation for a simple space-frame (a rigid floor supported by four columns at corners) subjected to sinusoidal ground excitations in two perpendicular directions, indicated that mode coupling causes yielding at force levels lower than an analysis of uncoupled planer motion would indicate. Wen and Farhoomand⁴⁷ presented the analysis of truss structures, where the masses were concentrated at each nodal point and plastic hinges (of finite length) were assumed to occur at member ends. The importance of yielding condition (interaction relationship) was also emphasized.

Toridis and Khozeimeh⁴⁸ introduced a finite element method to solve a three dimensional structure subjected to a dynamic load. The stresses can be checked segment wise for each step of the calculation thus enabling each segment to follow its moment-curvature relationship more closely than any other lumped models. However, in order to enjoy the advantage of this method, each segment must be reasonably small and hence the number of degrees of freedom could become very large for even a relatively simple frame.

The present study has made no attempt to examine these many facts of the problem.

1-3 Scope of Dissertation.

This dissertation is divided into three major parts. The first part (Chapters 2 and 3) describes an analytical procedure to analyze plane structures subjected to a dynamic disturbance. The results of the behavioral study are described in the second part (Chapter 4). The third part contains the recommended design procedure (Chapter 5).

To obtain the member response for inclusion in a structural analysis, the material properties must be idealized to reduce the computational effort. This is especially important when a dynamic analysis is to be performed. In the present study, the material is assumed to have a tri-linear type of stress-strain relationship which accounts for hysteresis under strain reversals. Based on this stress-strain relationship, moment-curvature relationships are derived for various cross-sections. These are not used in the normal fashion to obtain the overall member response; instead each member is modeled as an elastic bar having nonlinear rotational springs at either end. The characteristics of the springs are selected to reflect the behavior of the actual member, while the bars are assumed to remain elastic. The pertinent derivations are included in Chapter 2.

The frame to be analyzed then consists of an assemblage of elastic members connected by means of rotational springs to the joints. The standard slope deflection equations are modified in Chapter 3 to account for the properties of the springs. The dynamic equilibrium equations are then formulated for the frame. In order to check the assumptions made in the analysis, the equations are specialized to determine the response of a given frame to the application of static loads.

For the dynamic analysis, either an earthquake motion or a blast loading may be considered. The differences between the two disturbances are briefly discussed in the beginning of Chapter 4, which is assigned for the behavioral study. The study is largely focused on the dynamic response of steel frames, with or without shearwalls, to blast loadings. The selection of design blast loads for a particular structure is presented in Appendix E by summarizing the available information. The parameters studied are listed in Sec. 1-1. Based on the results of the behavioral study, proposals are made in Chapter 5 for the design of structures subjected to blast loads.

In Chapter 6, conclusions from the study are stated. The Appendices consist of supplementary explanations of the statements and equations made in the main text. The computer programs used to perform the behavioral study are also listed in this section.

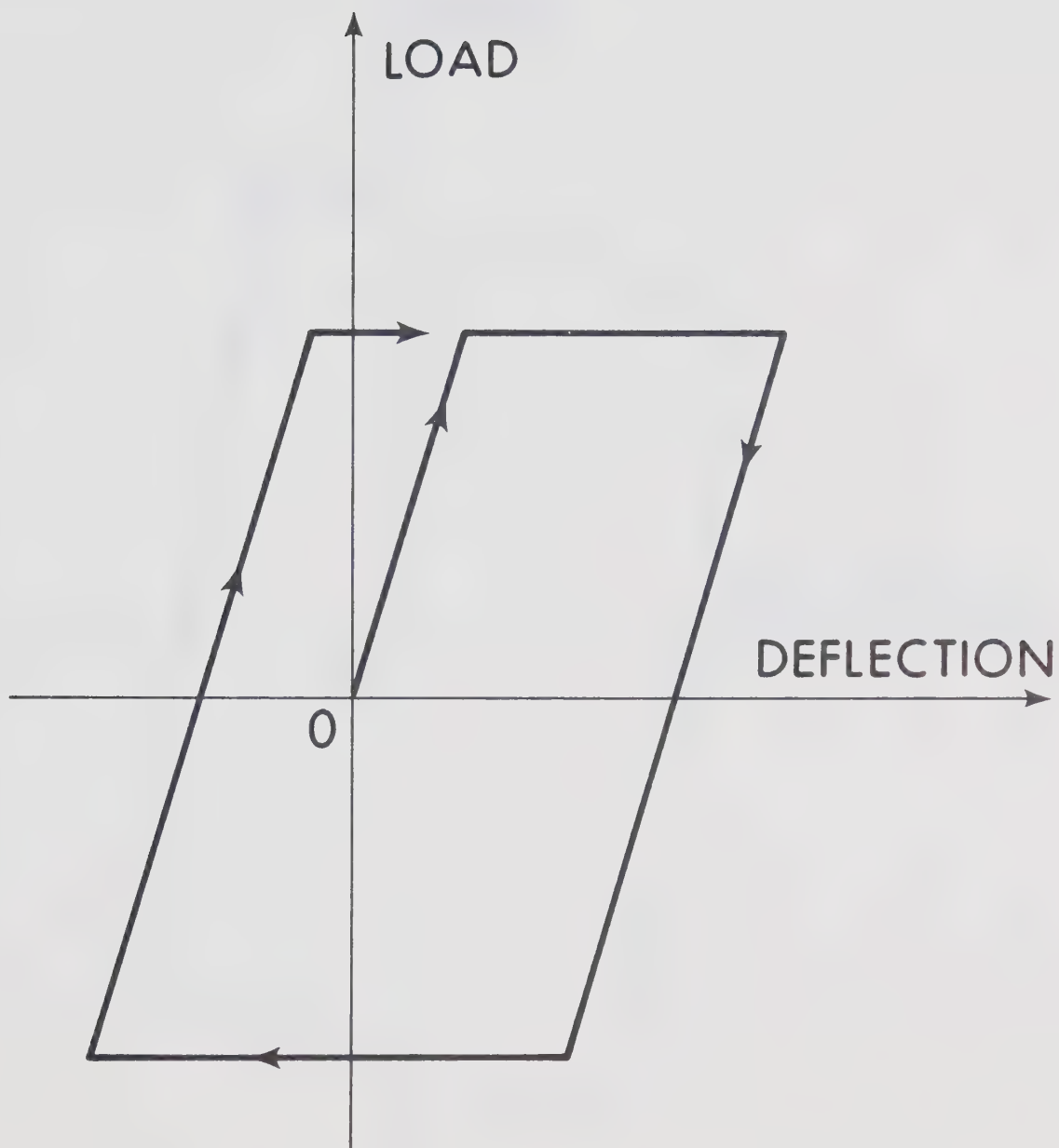


Fig. 1-1 Hysteretic Curve Used in Previous Studies,
(1) Elastic-Perfectly Plastic

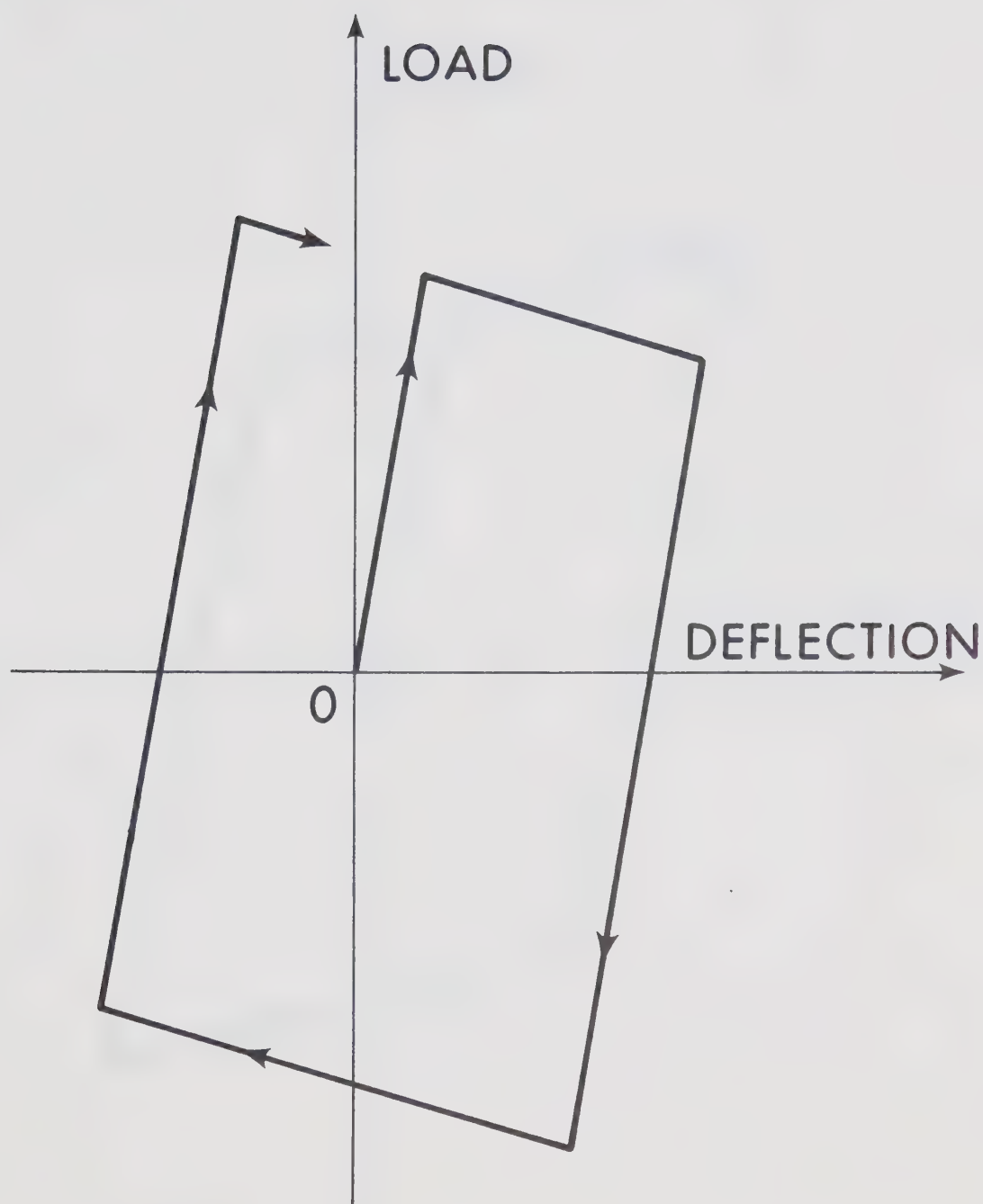


Fig. 1-2 Hysteretic Curve Used in Previous Studies,
(2) Elastic-Plastic with Negative Slope

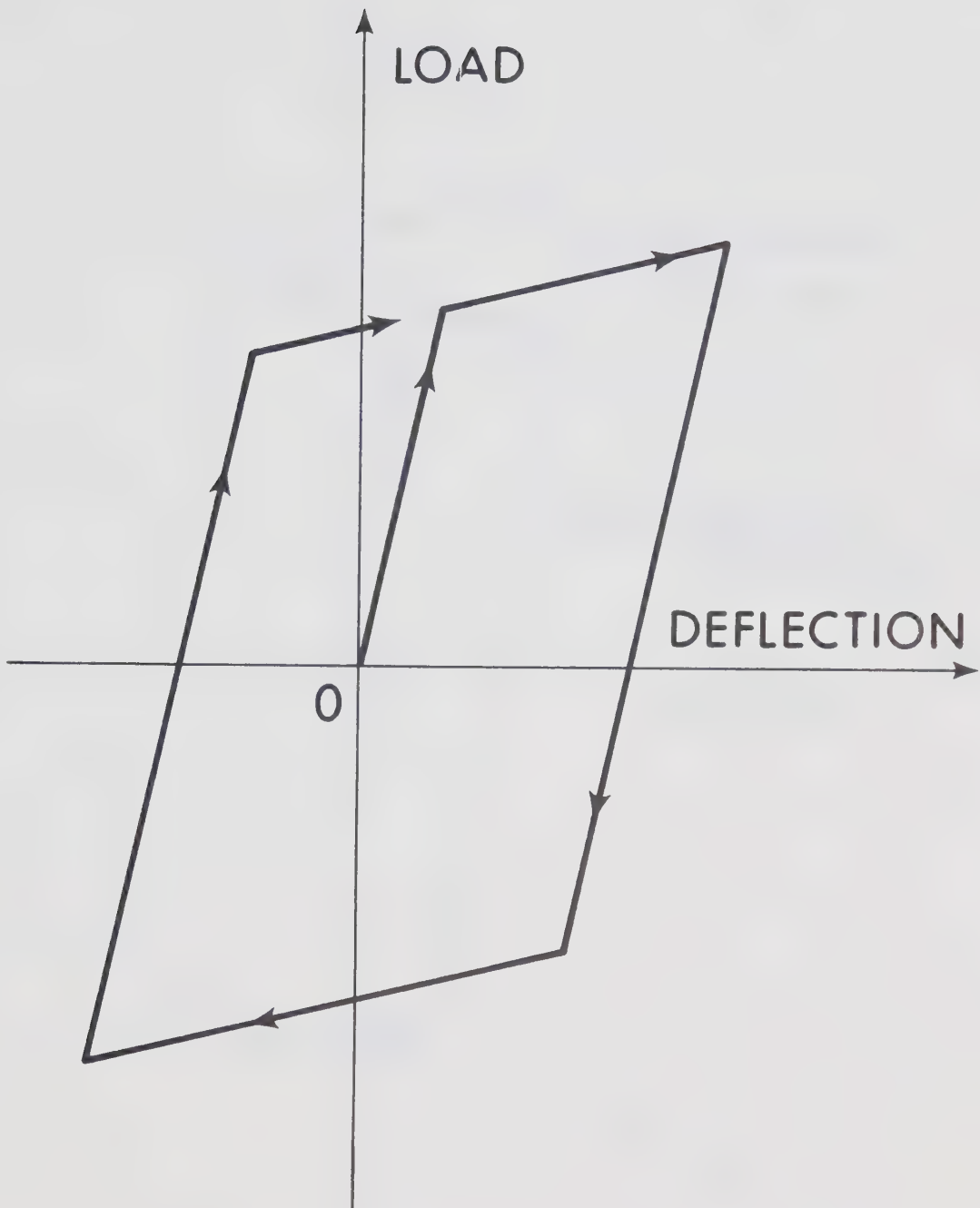


Fig. 1-3 Hysteretic Curve Used in Previous Studies,
(3) Bilinear Relationship

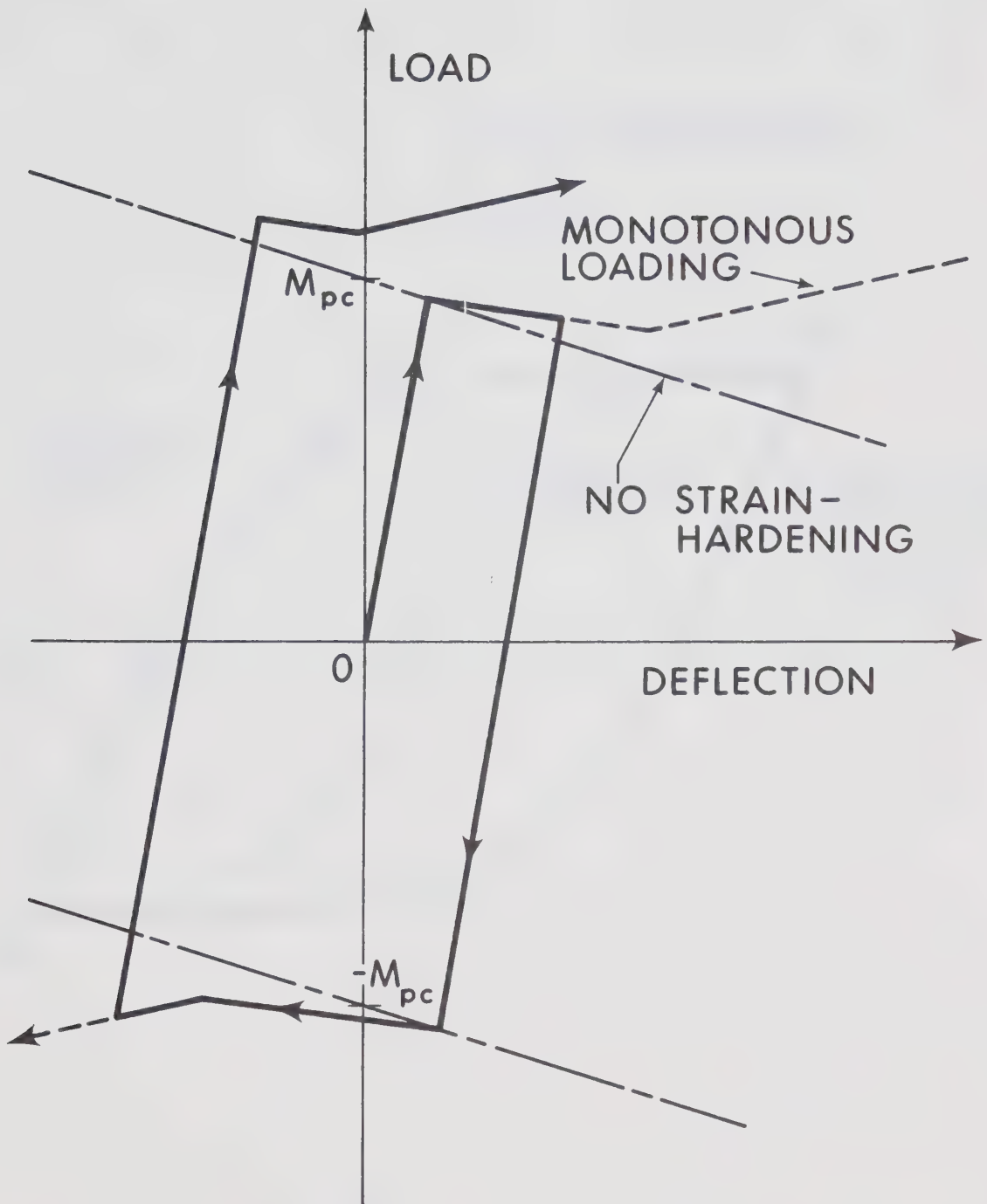


Fig. 1-4 Hysteretic Curve Used in Previous Studies,
(4) Kato and Akiyama's Model

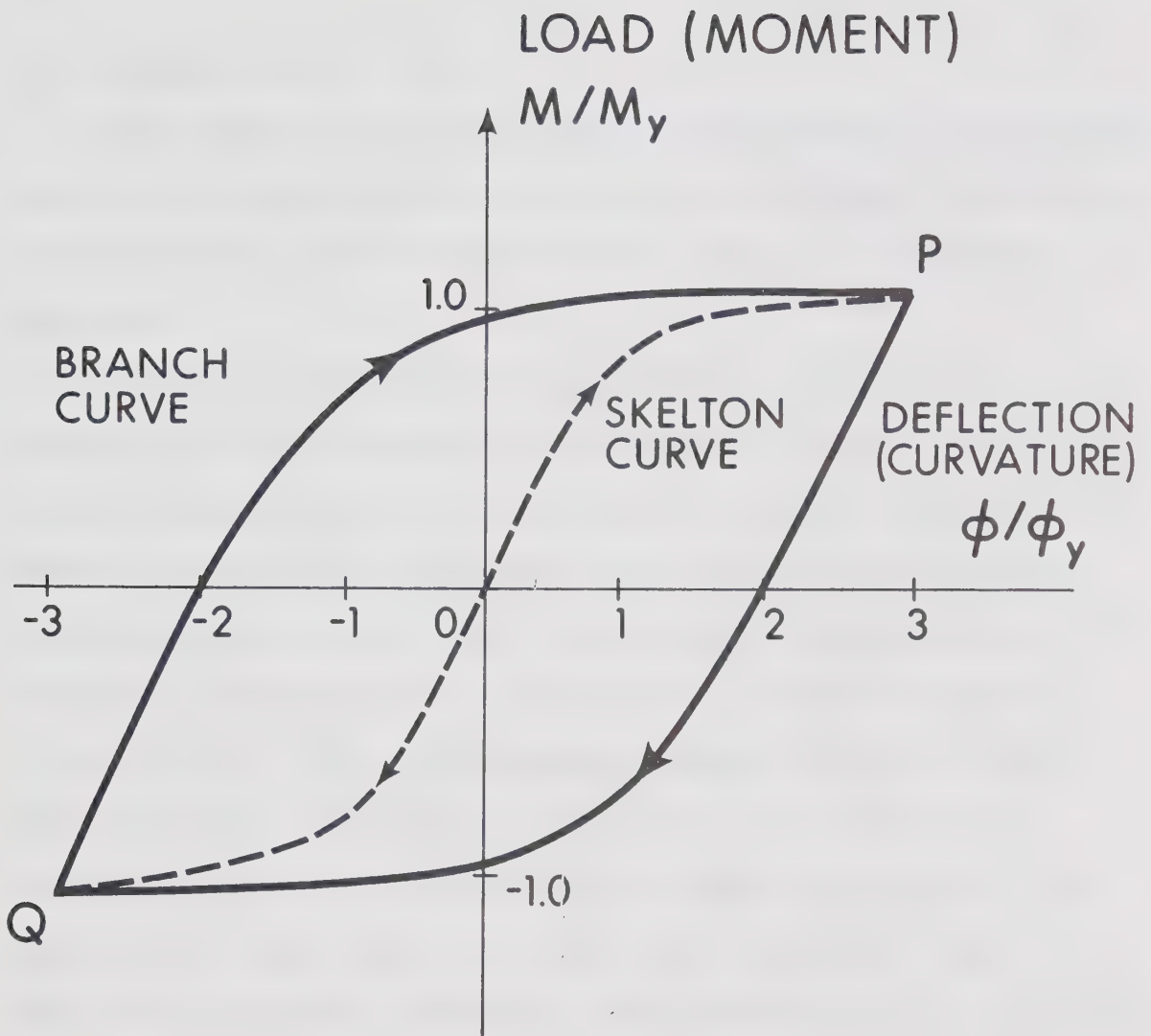


Fig. 1-5 Hysteretic Curve Used in Previous Studies,
(5) Ramberg-Osgood Model

Chapter 2.

MEMBER RESPONSE DURING STRUCTURAL VIBRATION

2-1 Introduction.

The objective of this chapter is to examine the inelastic response of members in a structure in an attempt to develop a simple model which is appropriate for use in a dynamic analysis.

The first stage is to determine the stress-strain relationship for the material of the member element. A trilinear type of stress-strain relationship is assumed. The moment-curvature-thrust relationships can then be calculated for various cross sections, and they are again approximated by trilinear relationships to reduce the subsequent computational effort. The relationships between cross sectional area and moment of inertia, plastic section modulus and moment of inertia, and the plastic moment capacity in the presence of axial force are initially formulated for a wide flange section. Thus all the necessary cross sectional properties are determined by specifying the nominal size, the moment of inertia and the amount of axial force.

If, in an actual frame, the portion of a column or beam between the point of inflection and the connection was extracted, it would be equivalent to a cantilever column subjected to a transverse load applied at top of

the column and an axial thrust. The behavior of such a cantilever column is obtained by integrating the moment-curvature-thrust relationship. This behavior is simulated in this study by that of a model consisting of an elastic bar with a nonlinear rotational spring at the end and subjected to the transverse load only. The properties of the rotational spring are selected to reflect the inelastic behavior and strain reversals of the actual member, which occur during a severe motion of a frame. The thrust is eliminated in this model, and only the actual transverse load is applied to obtain the second order inelastic deflection. An iterative procedure is not required in this model for the inclusion of $P-\Delta$ effect in contrast with presently used approximate methods.^{3,39}

2-2 Material Properties.

In the present analysis, it is assumed that the stress-strain (σ - ϵ) relationship, in either tension or compression, has three distinct regions as shown in Fig. 2-1; i.e., the initial elastic region, OA, the plastic plateau, AB, and the strain-hardening region, BC. This representation is typical for a wide range of steels used for building structures.^{3,49,50}

The initial elastic relationship terminates at point A; i.e., the yield point (the yield stress is σ_y and the yield

strain is ϵ_y). The slope of this elastic region is the modulus of elasticity (Young's modulus), E . The plastic plateau extends to point B where strain-hardening starts (the strain at this stage is ϵ_{st}). The point C corresponds to the stage at which the material attains its ultimate strength, σ_u . The strain-hardening modulus, E_{st} , is taken as the slope of the straight line which connects points B and C.

By assuming that the amount of plastic flow is zero or that the strain-hardening modulus is zero, a bilinear stress-strain relationship or an elastic-perfectly plastic stress-strain relationship can be represented, respectively.

Under conditions producing strain reversal, the stress-strain relationship of any element will remain elastic until the element is deformed beyond the yield point, σ_y . If an element is deformed beyond this limit, say to point D in Fig. 2-2, and then subjected to strain reversal, it is assumed that the unloading will take place along the line DE, which has a slope equal to that of the initial branch, OA. If the reversal continues, the stress-strain relationship is obtained by extending the line DE to the yield point F, where $\sigma = -\sigma_y$. Thereafter the stress-strain relationship will follow the curve FGH, which is symmetric to the curve ABC about the midpoint of OE (Fig. 2-2).

If the element is reloaded between points D and F, the stress-strain relationship is assumed to retrace the line DF to point D, then returns to the initial relationship on branch DC. If reloading takes place beyond point F, say point I in the same figure, the material is assumed to have the initial elastic rigidity, E , up to point D', where the stress is equal to that at point D. The stress-strain relationship will then follow the curve D'C', obtained by a parallel shift of the curve DC.

For subsequent loadings, it is assumed that the material will behave in a similar fashion. The usable limit of the material is assumed to be reached when the unused strain-hardening portion of the initial curve (in the above example, the portion DC in the positive direction, or the portion IH in the negative direction) is exhausted. (If $E_{st} \neq 0$, this corresponds to the stage at which the stress reaches the ultimate value, $\pm\sigma_u$.)

This method of tracing hysteresis loops, previously adopted by Kato and Akiyama,³ produces a reasonable approximation to the actual behavior^{51,52} except that the Bauschinger effect is neglected.

2-3 Geometrical Characteristics of Wide Flange Sections.

To simplify the development of the moment-curvature-thrust relationship, it is first necessary to determine the relationship between the cross sectional area, A , and the

moment of inertia, I ; the plastic section modulus, Z , and the moment of inertia, I ; and the axial thrust, P , and the reduced plastic moment capacity, M_{pc} , for a variety of cross sectional shapes.

In this section, these relationships are determined for standard wide flange sections, since they are used extensively in the behavioral study in Chapter 4.

2-3-1 Relationship Between Cross Sectional Area and Moment of Inertia.

The relationship between the cross sectional area, A , and the moment of inertia, I , was examined for standard wide flange sections.⁵³ A similar study has been done by Nakamura and Little.⁵⁴

Figs. 2-3 and 2-4 plot the relationships between these properties for each series of wide flange shapes. The equations describing the regression lines (calculated between $\log A$ and $\log I$) for each group are:

$$\begin{array}{ll}
 \text{for W36X} & A = 0.0210 I^{0.84} \\
 \text{W33X} & A = 0.0198 I^{0.86} \\
 \text{W30X} & A = 0.0287 I^{0.83} \\
 \text{W27X} & A = 0.0257 I^{0.86} \\
 \text{W24X} & A = 0.0404 I^{0.83}
 \end{array} \quad (2-1)$$

$$\text{for } W21X \quad A = 0.0331 \pm 0.88$$

$$W18X \quad A = 0.0397 \pm 0.89$$

$$W16X \quad A = 0.0419 \pm 0.91$$

$$W14X \quad A = 0.0843 \pm 0.83$$

(2-1)
cont'd

$$W12X \quad A = 0.0751 \pm 0.88$$

$$W10X \quad A = 0.0998 \pm 0.89$$

$$W8X \quad A = 0.1457 \pm 0.88$$

The slopes of these lines have a mean value of 0.87.
If these lines are adjusted to maintain the best fit while
holding the slope at 0.87, the following equations result:

$$\text{for } W36X \quad A = 0.0159 \pm 0.87$$

$$W33X \quad A = 0.0179 \pm 0.87$$

$$W30X \quad A = 0.0209 \pm 0.87$$

$$W27X \quad A = 0.0243 \pm 0.87$$

(2-2)

$$W24X \quad A = 0.0283 \pm 0.87$$

$$W21X \quad A = 0.0353 \pm 0.87$$

$$W18X \quad A = 0.0442 \pm 0.87$$

for W16X	$A = 0.0531 I^{0.87}$	
W14X	$A = 0.0630 I^{0.87}$	
W12X	$A = 0.0804 I^{0.87}$	(2-2) cont'd
W10X	$A = 0.1087 I^{0.87}$	
W8X	$A = 0.1515 I^{0.87}$	

This set of equations may be expressed by:

$$A = \frac{3.4}{d^{1.5}} I^{0.87}, \quad (2-3)$$

where d represents the nominal depth in inches. The lines shown in Figs. 2-3 and 2-4 are those given by Eq. 2-3.

2-3-2 Relationship Between Plastic Modulus and Moment of Inertia.

The correlation between the plastic section modulus, Z , and the moment of inertia, I ,^{54,55} is shown by the plots of Figs. 2-5 and 2-6. The equations for the regression lines for each series of wide flange sections are found to be:

for W36X	$Z = 0.102 I^{0.95}$	
W33X	$Z = 0.100 I^{0.96}$	
W30X	$Z = 0.120 I^{0.95}$	(2-4)
W27X	$Z = 0.114 I^{0.96}$	

for W24X	$Z = 0.148 I^{0.94}$
W21X	$Z = 0.141 I^{0.96}$
W18X	$Z = 0.162 I^{0.96}$
W16X	$Z = 0.169 I^{0.97}$
W14X	$Z = 0.273 I^{0.92}$
W12X	$Z = 0.250 I^{0.95}$
W10X	$Z = 0.285 I^{0.95}$
W8X	$Z = 0.346 I^{0.95}$

(2-4)
cont'd

Proceeding as before, the equations can be approximated by the formula:

$$Z = \frac{1.79}{d^{0.8}} I^{0.95}. \quad (2-5)$$

The lines shown in Figs. 2-5 and 2-6 are those given by Eq. 2-5.

2-3-3 Plastic Moment Capacity in the Presence of Axial Force.

The plastic moment capacity, M_{pc} , under an axial force, P , must be determined for various cross sectional configurations. Fig. 2-7 shows the interaction curves for strong axis bending of wide flange sections, using the nondimensionalized parameters, M_{pc}/M_p and P/P_y . The quantities, M_p and

and P_y are the full plastic moment capacity and the yield axial load, respectively; i.e.,

$$M_p = Z\sigma_y, \quad (2-6)$$

and

$$P_y = A\sigma_y. \quad (2-7)$$

Curves A and B in this figure indicate the upper and lower envelopes of interaction curves among the standard wide flange sections, respectively. Based on this observation, the following relationships are used in the present study.

$$\text{For } 1 \geq \frac{P}{P_y} \geq \frac{1}{3},$$

$$\frac{M_{pc}}{M_p} = 1.2 \left(1 - \frac{P}{P_y}\right), \quad (2-8)$$

$$\text{and for } \frac{1}{3} > \frac{P}{P_y} \geq 0,$$

$$\frac{M_{pc}}{M_p} = 1 - 1.8 \left(\frac{P}{P_y}\right)^2, \quad (2-9)$$

which is indicated by curve C in Fig. 2-7.

This relationship is almost identical to the one recommended by the ASCE⁵⁶ for P/P_y greater than one third, but the present relationship gives a slightly better approximation to the actual results when P/P_y is less than one third.

2.4 Moment-Curvature-Thrust Relationship.

Assuming that a cross section which is plane before deformation will remain plane during the loading process, a theoretical moment-curvature-thrust relationship for a given cross section may be determined either for the elastic-perfectly plastic stress-strain relationship^{57,58} or for the trilinear stress-strain relationship of Fig. 2-1.^{3,59}

2-4-1 Empirical Moment-Curvature-Thrust Relationship.

Using the method given in Ref. 3, empirical moment-curvature-thrust relationships have been generated for the present study. The method described below is applicable to wide flange sections bent about their strong axes and having a stress-strain relationship similar to that shown in Fig. 2-1. The effect of residual stresses is ignored.

The moment-curvature relationship in the absence of axial thrust is first calculated and is approximated by a trilinear relationship such as curve A in Fig. 2-8. Moment is proportional to curvature up to point a. The moment at this point is the full plastic moment, M_p , defined by Eq. 2-6. The corresponding curvature, ϕ_p , is given by

$$\phi_p = \frac{M_p}{K} \quad (2-10)$$

where K represents the elastic flexural rigidity of the

cross section, or the slope of the line oa; i.e., letting I be the moment of inertia,

$$K = EI . \quad (2-11)$$

It is assumed that plastic flow starts at point a and ends at point b where some rigidity is recovered due to strain-hardening. The curvature at point b is $s\phi_p$, where s is the ratio of the strain at the onset of strain-hardening to the yield strain (Fig. 2-1); i.e.,

$$s = \epsilon_{st}/\epsilon_y . \quad (2-12)$$

After reaching point b, the moment increases at a rate of $E_{st}I$ per unit of curvature, until the ultimate moment, M_u (point e), is reached. M_u is given by:

$$M_u = Z\sigma_u . \quad (2-13)$$

Curve B in Fig. 2-8 represents the response of a cross section subjected to a constant axial load, P , as well as a bending moment, M , for $s \geq 3$ (which is typical for mild steel⁵⁰). A trilinear moment-curvature relationship is also assumed for this case with the elastic stiffness the same as that for the pure bending case; i.e., K . The proportional limit (point a') is the reduced plastic moment capacity, M_{pc} , which is calculated using the method described in the

preceding section. The corresponding curvature, ϕ_{pc} , is given by

$$\phi_{pc} = \frac{M_{pc}}{M_p} \phi_p . \quad (2-14)$$

The length of the plastic plateau, $a'b'$, is given by ϕ_{st} minus ϕ_{pc} , where

$$\phi_{st} = [s - 0.5\sqrt{1-m}(s+1)]\phi_p , \quad (2-15)$$

and

$$m = \frac{M_{pc}}{M_p} . \quad (2-16)$$

It is assumed that the locus of point b' for various m ($0 \leq m \leq 1$) forms a parabola having its vertex at point b and an axis of symmetry parallel to the M -axis and intersecting the ϕ -axis at $0.5(s-1)\phi_p$. The coordinates of point b' , (ϕ_{st}, M_{pc}) , satisfy:

$$M_{pc} = M_p - \left[\frac{2(\phi_{st} - s\phi_p)}{(s+1)\phi_p} \right]^2 M_p . \quad (2-17)$$

The flexural rigidity after point b' for $M_{pc}/M_p = 0$ (pure compression) is twice that for $M_{pc}/M_p = 1$ (pure bending). (See Sec. 2-4-2 for the rationale for this statement.) The rigidity for an arbitrary value of $m = M_{pc}/M_p$, which is represented by K_{st} , is obtained by interpolation as:

$$K_{st} = (2-m)E_{st}I . \quad (2-18)$$

The increase in moment between point b' and the ultimate condition (point c') is equal to that for the pure bending case, regardless of the value of m. The ultimate moment, M_{uc} , under this axial thrust is, therefore,

$$M_{uc} = M_{pc} + M_u - M_p \quad (2-19)$$

If the quantity s is between 1 and 3 (which is possible for high strength steel), the locus of point b' in the above procedure is modified for m less than $\frac{1}{4}(3 + 2s - s^2)$.

In this case, ϕ_{st} is given by:

$$\phi_{st} = [m + 0.5(s-1)]\phi_p . \quad (2-20)$$

The moment-curvature-thrust relationship obtained in this manner is compared with the exact solution³ in Fig. 2-9. The stress-strain relationship used in this calculation was a trilinear type such as that shown in Fig. 2-1; the pertinent data are shown in Fig. 2-9. The cross sectional configuration is also shown in the inset to the figure. When using Eqs. 2-3 and 2-5; $d = 6$ and $I = 57.1$ were input. The relationships calculated using the present method are shown by broken lines while the solid lines represent rigorous relationships.

2-4-2 Derivation of Approximate Formulae.

Some of the quantities used in the formulae above may be explained briefly by considering a wide flange section represented by the model shown in Fig. 2-10(a). All of the cross sectional area is concentrated in two flanges, each having an area $A/2$, and placed a distance, d , apart.

Figs. 2-10(b) and (d) show the strain distributions for various loading conditions. Diagram 1 corresponds to point a in Fig. 2-8; i.e., the attainment of the full plastic moment capacity under pure bending. Diagram 2 corresponds to point b in the same figure, the onset of strain hardening. The corresponding curvatures, ϕ_1 and ϕ_2 , are:

$$\begin{aligned}
 \phi_1 &= \frac{\epsilon_y}{d/2} \\
 &= \frac{(A/2)d\epsilon_y E}{2(A/2)(d/2)^2 E} \\
 &= \frac{Z\sigma_y}{EI} \\
 &= \frac{M_p}{EI}
 \end{aligned} \tag{2-21}$$

and

$$\begin{aligned}
 \phi_2 &= \frac{\epsilon_{st}}{d/2} \\
 &= \frac{s\epsilon_y}{d/2} \\
 &= s\phi_1
 \end{aligned} \tag{2-22}$$

respectively, which provide the rationale for Eq. 2-10. Diagram 3 shows the strain distribution for a section yielded under pure compression; i.e., the case when $P/P_Y = 1.0$ or $m = 0$. If this section is subjected to additional bending, plastic flow takes place without the development of resisting moments until the strain condition indicated by diagram 4 is reached. The curvature at this stage, ϕ_4 , is

$$\begin{aligned}
 \phi_4 &= \frac{\epsilon_{st} - \epsilon_y}{d} \\
 &= \frac{s-1}{d} \epsilon_Y \\
 &= \frac{s-1}{2} \phi_1 \\
 &= \frac{s-1}{2} \phi_p
 \end{aligned} \tag{2-23}$$

which can also be obtained from Eq. 2-15 by letting $m = 0$. For an arbitrary value of m , the curvature at the onset of strain-hardening is assumed to have a locus which is a parabola connecting this point and point b as described previously.

Fig. 2-10(c) shows the equilibrium of internal forces when the cross section is deformed into the strain-hardening range for the pure bending case and corresponds to the strain distribution of diagram 5. The bending moment is increased from that at the onset of strain-hardening by an

amount:

$$\delta M = \delta \epsilon \cdot E_{st} \cdot \frac{A}{2} \cdot d, \quad (2-24)$$

while the increase in curvature is:

$$\delta \phi = \frac{\delta \epsilon}{d/2} . \quad (2-25)$$

Therefore the slope of the moment-curvature relationship in the strain-hardening range is:

$$\begin{aligned} \frac{\delta M}{\delta \phi} &= \frac{\delta \epsilon \cdot E_{st} \cdot A/2 \cdot d}{\delta \epsilon / (d/2)} \\ &= E_{st} \cdot A/2 \cdot (d/2)^2 \cdot 2 \\ &= E_{st} I \end{aligned} \quad (2-26)$$

as shown in Fig. 2-8. On the other hand, starting from the strain condition shown in diagram 4 (for the case $P/P_Y = 1.0$), in order to increase the moment by the amount given by Eq. 2-24, the equilibrium of internal forces must be that shown in Fig. 2-10(e), which corresponds to the strain distribution of diagram 6 in Fig. 2-10(d). The increase in the compressive force in the top flange is equal to the decrease in force in the bottom flange, thus if the decrease in strain in the bottom flange is $\delta \epsilon'$,

$$\begin{aligned} \delta \epsilon \cdot E_{st} \cdot A/2 &= \delta \epsilon' \cdot E \cdot A/2 \\ \delta \epsilon' &= \frac{E_{st}}{E} \delta \epsilon . \end{aligned} \quad (2-27)$$

Since the value, $\delta\epsilon'$, is small compared with $\delta\epsilon$, the change in curvature to increase the moment by the amount given by Eq. 2-24 is approximately

$$\delta\phi = \frac{\delta\epsilon}{d} . \quad (2-28)$$

Therefore the slope in this case is:

$$\begin{aligned} \frac{\delta M}{\delta\phi} &= \frac{\delta\epsilon \cdot E_{st} \cdot A/2 \cdot d}{\delta\epsilon/d} \\ &= 2E_{st}I \end{aligned} \quad (2-29)$$

Eq. 2-18 is derived by interpolating the values given by Eqs. 2-26 and 2-29 for an arbitrary value of m . Some of these quantities are explained in the derivation of the rigorous solution given in Ref. 3.

2-5 Use of Rotational Spring to Simulate Member Inelastic Action and P- Δ Effect.

In accordance with the scope given in the beginning of this chapter, the behavior of a cantilever column, subjected to a transverse load and an axial load, is examined. The actual behavior of this column, which is obtained using the moment-curvature-thrust relationships derived in the preceding sections, is simulated by the response of an elastic bar having a nonlinear rotational spring at the lower end. The bar is subjected to the same transverse load but is not

subjected to an axial load. The objective of employing a rotational spring is to simplify the treatment of inelastic action with strain reversals and to include the $P-\Delta$ effect. (In Sec. 3-3, the function of this rotational spring is expanded to include other secondary effects.)

2-5-1 Analysis of Cantilever Column.

If a cantilever column is subjected to a constant axial load, P , and a varying transverse load, Q , as shown in Fig. 2-11, the column will behave elastically, until the moment at the lower end, M_b , given by:

$$M_b = QL + P\Delta \quad (2-30)$$

reaches the reduced plastic moment capacity, M_{pc} . In this expression, L is the column length and Δ is the deflection at the top of the column.

The moment-curvature relationship for the column under the given axial load is assumed to be that shown in Fig. 2-12. This relationship may be obtained by the approximate method explained in the previous section if the column has a wide flange section. For other types of cross sections (or also for a wide flange section), moment-curvature-thrust relationships may be obtained by employing other reasonable methods^{3,56,59,60} or by modifying the pertinent equations above to fit the individual case.

The deflection at the top of the column, Δ , is:

$$\Delta = \frac{QL^3}{3K} \cdot \frac{3(\tan \mu L - \mu L)}{(\mu L)^3} \quad (2-31)$$

for $Q \leq \frac{\mu M_{pc}}{\tan \mu L} \quad (2-32)$

implying that the column behaves elastically. In the above expressions,

$$\mu = \sqrt{P/K} . \quad (2-33)$$

If the column is forced to deflect beyond this limit, the inelastic region spreads from the lower end of the column, resulting in an increased end moment because of strain-hardening in this region, in accordance with the relationship shown in Fig. 2-12. The deflection, Δ , in this case is expressed as

$$\Delta = \Delta_e + \Delta_p , \quad (2-34)$$

where

$$\Delta_e = \frac{M_{pc} - QL_1}{P} , \quad (2-35)$$

and

$$\begin{aligned} \Delta_p = \frac{Q}{P} \left(\frac{\tan v L_2}{v} - L_2 \right) \\ + \frac{M_i}{P} (\sin v L_2 \tan v L_2 + \cos v L_2 - 1) , \end{aligned} \quad (2-36)$$

for the value of Q such that the inelastic region increases in length. In the above equations:

$$\nu = \sqrt{\frac{P}{K_{st}}} , \quad (2-37)$$

L_1 = the length of the column which behaves elastically, and

L_2 = the length of the column which has strain hardened,

as shown in Fig. 2-11. Obviously,

$$L_1 + L_2 = L . \quad (2-38)$$

Further, M_i represents the intercept on the moment axis shown in the moment curvature relationship of Fig. 2-12. In the inelastic range, the transverse load, Q , may decrease, particularly if the axial load, P , or the column length, L , is relatively high or the stiffness in the strain hardening range K_{st} , is comparatively small.

Since the length of the inelastic zone, L_2 , is dependent on the value of the transverse load, Q , or vice versa, the following relation between Q and L_2 must be introduced in order to determine the $Q-\Delta$ relationship in this range.

$$Q = \mu M_{pc} \frac{\cos \nu L_2}{\tan \mu L_1} - M_i \nu \sin \nu L_2 \quad (2-39)$$

Once the value of L_2 has been selected, Q is calculated using the above equation, and the corresponding Δ is obtained from Eqs. 2-34, 2-35 and 2-36.

Similar load deflection relationships must be computed for special cases: when the axial load, P , is zero; when the

stiffness in the strain hardening range is zero (i.e., the elastic-perfectly plastic case); and when the column is not fixed at the lower end but is connected to an elastic foundation. The $Q-\Delta$ relationships for these cases, as well as the derivation of the appropriate equations are given in Appendix A.

2-5-2 Use of Equivalent Rotation Spring to Simulate the Actual Column Behavior.

The behavior of the actual member discussed above can be approximated by considering the system shown in Fig. 2-13. The spring at the base of the column is forced through a rotation, $\delta\theta_s$, for a given transverse load, Q (corresponding to a moment in the spring, $M_s = -QL$). The spring is selected so that the deflection at the top of the column is equal to that given by Eq. 2-31 or Eq. 2-34 even though the axial load is eliminated. The stiffness of the column is assumed to remain equal to the elastic stiffness, K , throughout the complete column length, regardless of the end moment at the base of the actual column.

In order to satisfy the preceding conditions, the spring at the base of the column must produce a rotation, $\delta\theta_s$ (which will be called a relaxation angle), that should satisfy:

$$\Delta = \delta\theta_s L + \frac{QL^3}{3K} \quad (2-40)$$

in which Δ is the value given by either Eq. 2-31 or Eq. 2-34 depending upon the condition of the actual column. Therefore the member end moment, M_S , and the relaxation angle, $\delta\theta_S$, are related by:

$$\delta\theta_S = \frac{\Delta}{L} + \frac{M_S L}{3K} . \quad (2-41)$$

The end moment and the relaxation angle are both positive in a clockwise sense, thus the relationship

$$M_S = -QL \quad (2-42)$$

is used to obtain Eq. 2-41.

Some typical moment-relaxation angle (M_S - $\delta\theta_S$) relationships for the rotational springs are shown in the upper portions of Fig. 2-14a to 2-14d by the full lines. In these relationships, the slope in the elastic range is calculated as below. From Eq. 2-31, Δ is given in terms of end moment (moment in the spring), M_S , by:

$$\Delta = -\frac{M_S L^2}{3K} \cdot \frac{3(\tan\mu L - \mu L)}{(\mu L)^3} . \quad (2-43)$$

Substituting this into Eq. 2-41,

$$\begin{aligned} \delta\theta_S &= -\frac{M_S L}{3K} \frac{3(\tan\mu L - \mu L)}{(\mu L)^3} + \frac{M_S L}{3K} \\ &= -\left[\frac{3(\tan\mu L - \mu L)}{(\mu L)^3} - 1\right] \frac{M_S L}{3K} \end{aligned} \quad (2-44)$$

Thus the slope is:

$$\frac{M_S}{\delta\theta_S} = -\frac{3K}{L} \left[\frac{3(\tan\mu L - \mu L)}{(\mu L)^3} - 1 \right]^{-1} . \quad (2-45)$$

And the limit of elastic behavior of this spring, (M_{S-y} , $\delta\theta_{S-y}$), is given by:

$$\delta\theta_{S-y} = \left[\frac{1}{PL} - \left(\frac{1}{PL} + \frac{L}{3K} \right) \cdot \frac{\mu L}{\tan\mu L} \right] M_{pc} , \quad (2-46)$$

and

$$M_{S-y} = \frac{\mu L}{\tan\mu L} M_{pc} . \quad (2-47)$$

For the inelastic region, points on the $Q-\Delta$ relationship (given by Eq. 2-34) correspond to similar points on the $M_S-\delta\theta_S$ curve through the relationships given by Eqs. 2-41 and 2-42. The broken lines in the $M_S-\delta\theta_S$ curves represent the behavior in the absence of strain-hardening. The slopes of these lines, ζ , are given by:

$$\zeta = \frac{PL}{(1 + PL^2/3K)} . \quad (2-48)$$

By selecting the $M_S-\delta\theta_S$ relationship as shown above, the model shown in Fig. 2-13 produces a load-deflection ($Q-\Delta$) curve exactly the same as that of the actual column shown in Fig. 2-11.

2-5-3 Characteristics of $M_S-\delta\theta_S$ Curves.

Fig. 2-14a shows the $M_S-\delta\theta_S$ relationship when the axial load, P , is zero. The section considered here is a W12X85.

The column length is 60 inches. The moment-curvature relationship used in this calculation is also shown in this figure. This was obtained by assuming a stress-strain relationship typical of G40.12 steel ($\sigma_y = 44$ ksi, $\sigma_u = 1.35\sigma_y$, $E = 29600$ ksi, $E/E_{st} = 40$, $s = 10$). In this case, $\delta\theta_s$ is zero until M_s reaches the plastic moment capacity of the member, $M_{pc} = M_p$. If strain-hardening occurs, the spring moment is increased until it reaches the ultimate moment, $M_{uc} = M_u$, with a corresponding increase in the relaxation angle, $\delta\theta_s$.

The effect of axial load on the M_s - $\delta\theta_s$ relationship is shown in Figs. 2-14a, 2-14b, and 2-14c, where the applied axial load is 0.0, $0.3P_y$, and $0.6P_y$ respectively. Other properties are the same for comparison. With an increase in the axial load, the slope of the elastic branch of the curve is reduced and the yield moment of the spring, M_{s-y} , is decreased. For relatively high axial loads, the M_s - $\delta\theta_s$ relationships exhibit negative slopes in the inelastic range, although strain-hardening does provide an increased strength relative to the elastic-perfectly plastic case (Note the difference between the solid curves and the broken lines). The contribution of strain-hardening is relatively greater for columns subjected to higher axial loads.

Figure 2-14d shows an M_s - $\delta\theta_s$ curve with the same axial load ($0.3P_y$) as in Fig. 2-14b, but the column length is

increased by 50% (90 inches). The other parameters are the same in both cases. The comparison between these two curves indicates that the increase in column length has a small effect on the yield moment of the spring, M_{S-y} , although the inelastic curves are somewhat different.

2-5-4 Consideration of Reversals of Load.

The $M_S-\delta\theta_S$ relationship can account for reversals of load by using a method analogous to that discussed in Sec. 2-1, used to account for strain reversals when considering the stress-strain relationship of the material.

For a symmetric column section, the initial $M_S-\delta\theta_S$ relationship is also symmetric about the origin as shown by curve $B_1-A_1-O-A'_1-B'_1$ in Fig. 2-15(a). When the reversals of load are within the elastic range (between point A_1 and point A'_1), the $M_S-\delta\theta_S$ relationship need not be modified. Once the moment has reached the yield moment, M_{S-y} or $-M_{S-y}$, and unloading occurs between A_1 and B_1 (for example, at point S_1), the $M_S-\delta\theta_S$ curve must be changed to that shown by $B_1-S_1-A'_2-B'_2$ in the same figure. In this figure, the dashed lines have slopes given by Eq. 2-48. The line $S_1-A'_2$ is assumed to be parallel to the line $A_1-A'_1$, where point A'_2 is on the dashed line passing through point A'_1 . Curve $A'_2-B'_2$ is obtained by a translation of curve $A'_1-B'_1$.

If subsequent reversals of load are within line S_1-A_2' , this curve need not be changed.

If after reversals of load, however, the moment in the opposite direction exceeds that corresponding to point A_2' , and unloading is to take place at, for example, point S_2' , the $M_S-\delta\theta_S$ curve must be modified to that shown as $B_2'-S_2'-S_2-B_2$ in Fig. 2-15(b). Again the unloading stiffness corresponds to the initial loading stiffness. The point S_2 lies on the dashed line passing through point S_1 , with a slope given by Eq. 2-48. Curve S_2-B_2 is again obtained by a translation of curve S_1-B_1 .

A similar process is repeated for subsequent reversals of load. Collapse is assumed to occur when the above procedure is no longer possible; that is, when the $M_S-\delta\theta_S$ curve in either direction is completely exhausted.

This method of tracing the response of a member implies that the member strength may be increased under an increased number of reversals of load in the inelastic range. This phenomenon has been reported in several references.^{3,61-68} The present method is based on the theoretical explanation by Kato and Akiyama.³

2-6 Computer Program

In this section, a brief explanation of the computer program developed to construct the $M_S-\delta\theta_S$ relationships

for a wide flange section with the stress-strain curve shown in Fig. 2-1 will be presented. This section also serves as a summary of this chapter.

The necessary input data for the program are as follows:

- (1) E : Modulus of elasticity,
- (2) σ_y : Yield stress,
- (3) s : ϵ_{st}/ϵ_y as in Fig. 2-1,
- (4) E_{st}/E : as in Fig. 2-1,
- (5) σ_u/σ_y : as in Fig. 2-1,
- (6) d : Nominal size of wide flange section,
- (7) I : Moment of inertia of the section,
- (8) P : Axial force, and
- (9) L : Column length.

The first five parameters are necessary to describe the stress-strain relationship. The column section is described only by its nominal size and moment of inertia. The cross sectional area, A , is calculated using the relationship given by Eq. 2-3. The ratio of axial load, P , to the yield load, P_y , is then computed. The plastic section modulus, Z , is found from the relationship of Eq. 2-5. The moment-curvature relationship under pure bending corresponding to curve A in Fig. 2-8 is next computed. The reduced plastic moment capacity, M_{pc} , under the axial load, P , is found from curve C in Fig. 2-7 or from Eq. 2-8 or 2-9. Once the

value of M_{pc} is determined, the moment-curvature relationship for the given axial load is constructed according to the procedure described in Sec. 2-3.

The properties of the rotational spring ($M_S-\delta\theta_S$ relationship) are determined as explained in Secs. 2-4-1 and 2-4-2. The resulting $M_S-\delta\theta_S$ relationships are drawn by the CalComp Plotter (Model 770/663) as shown in Figs. 2-14a to 2-14d. The computer program is listed in Appendix B.

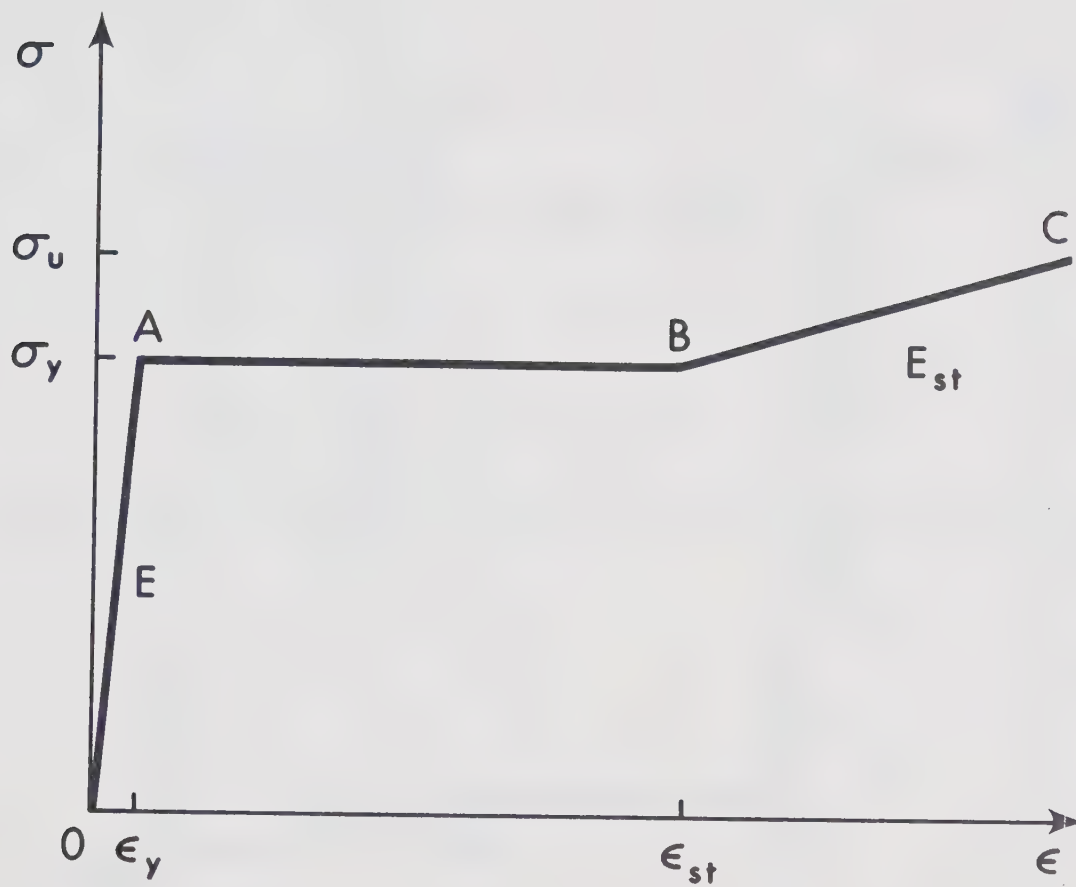


Fig. 2-1 Stress-Strain Relationship

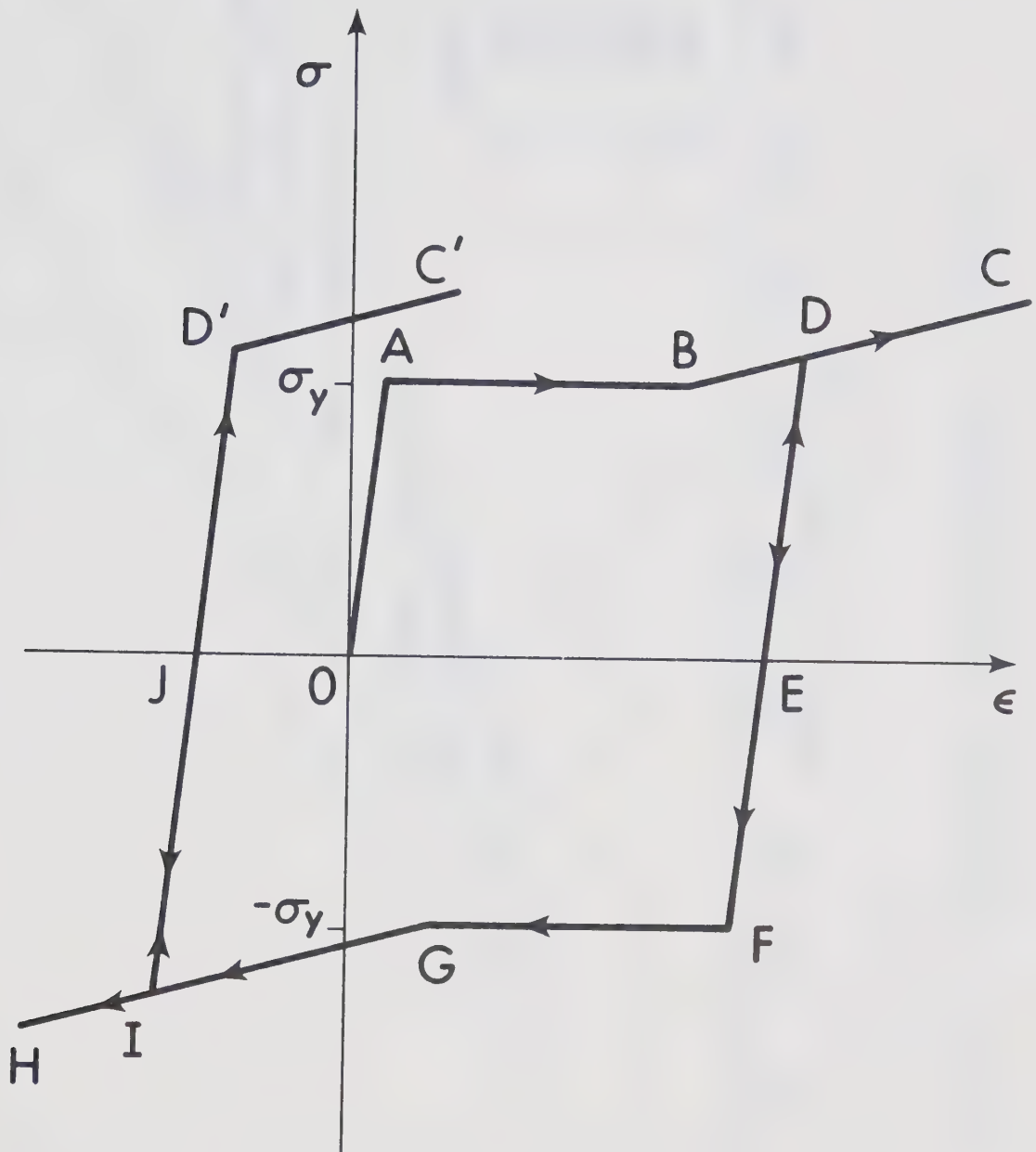


Fig. 2-2 Strain Reversals

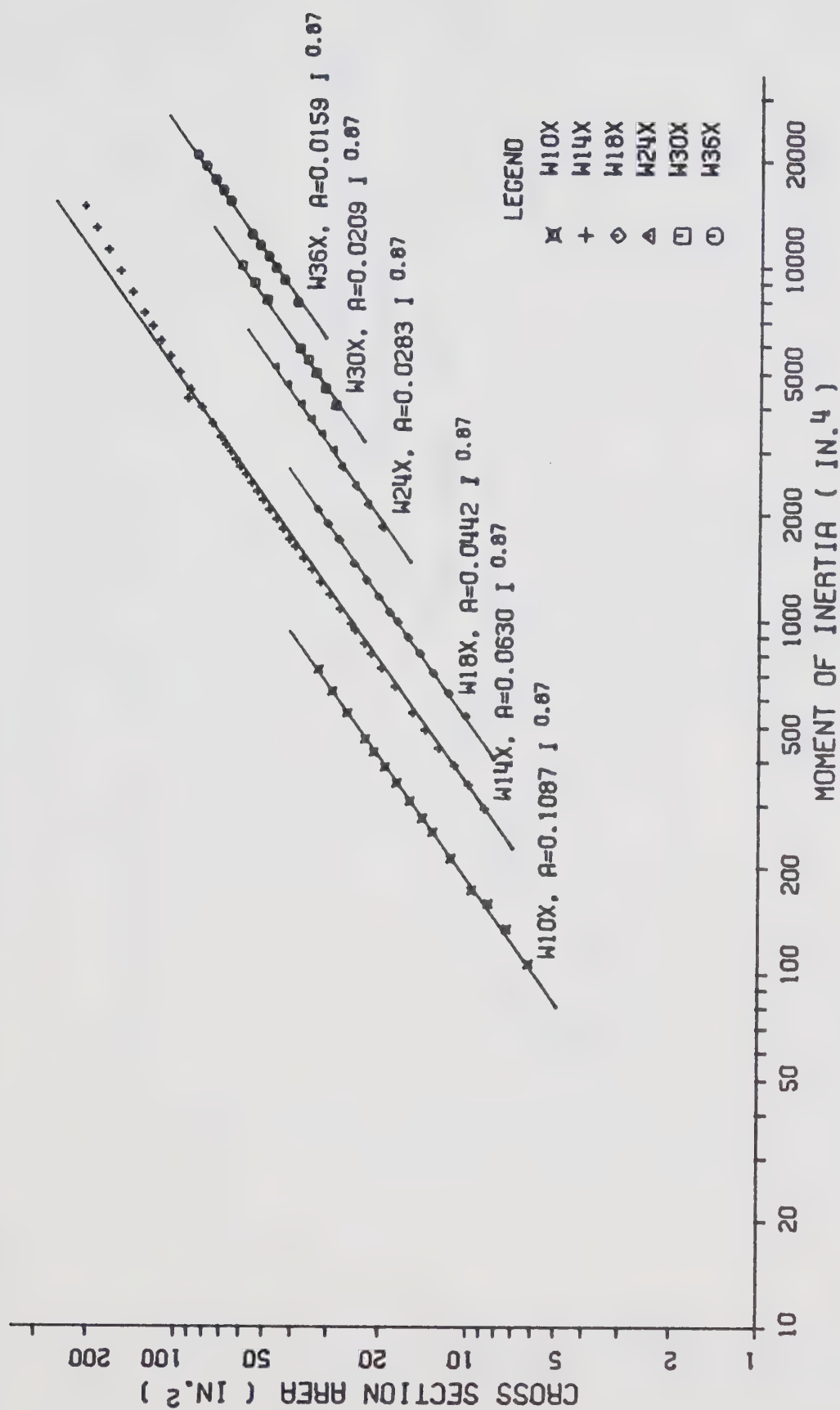


Fig. 2-3 Correlation Between the Moment of Inertia and the Cross Sectional Area (1)

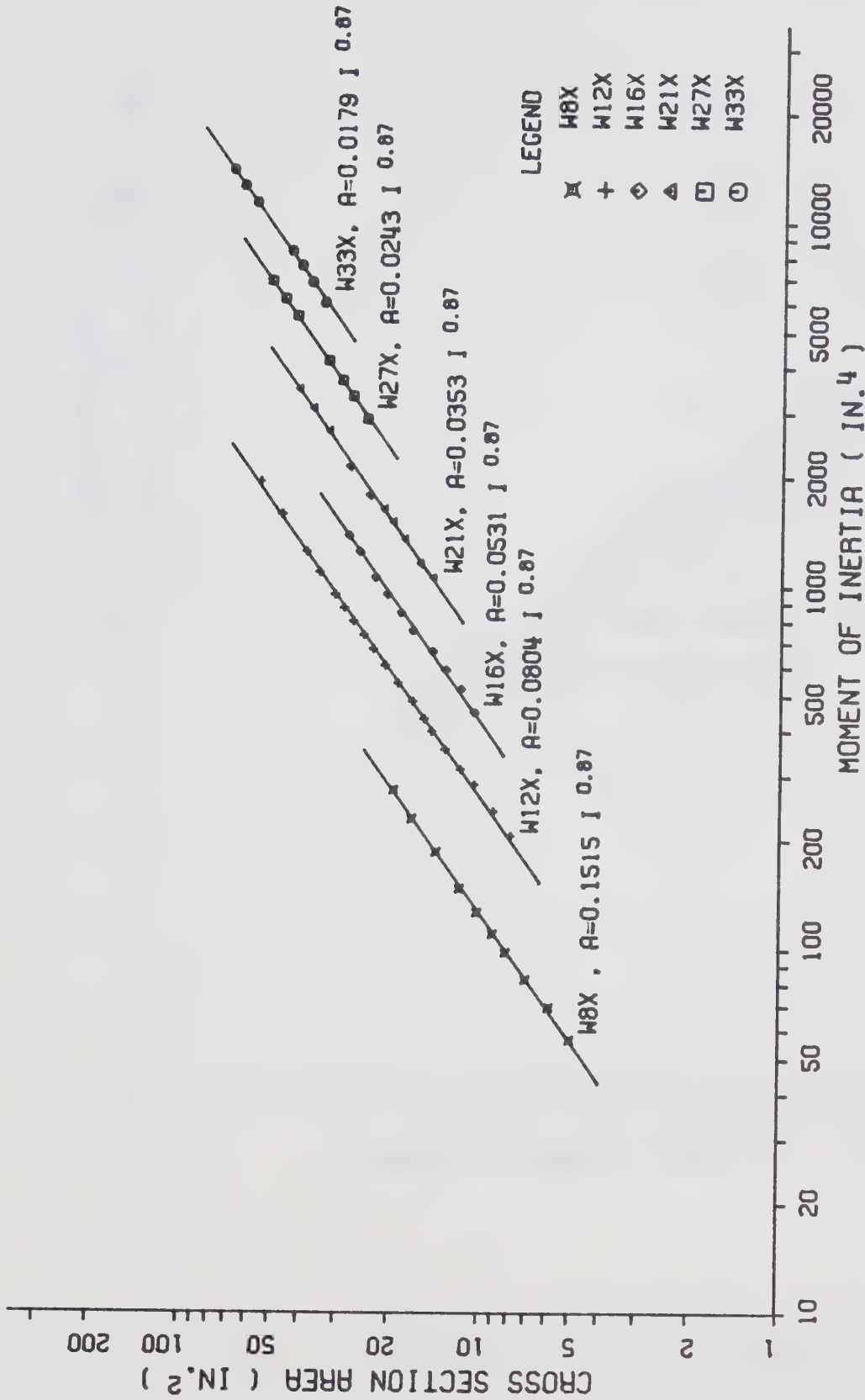


Fig. 2-4 Correlation Between the Moment of Inertia and the Cross Sectional Area (2)

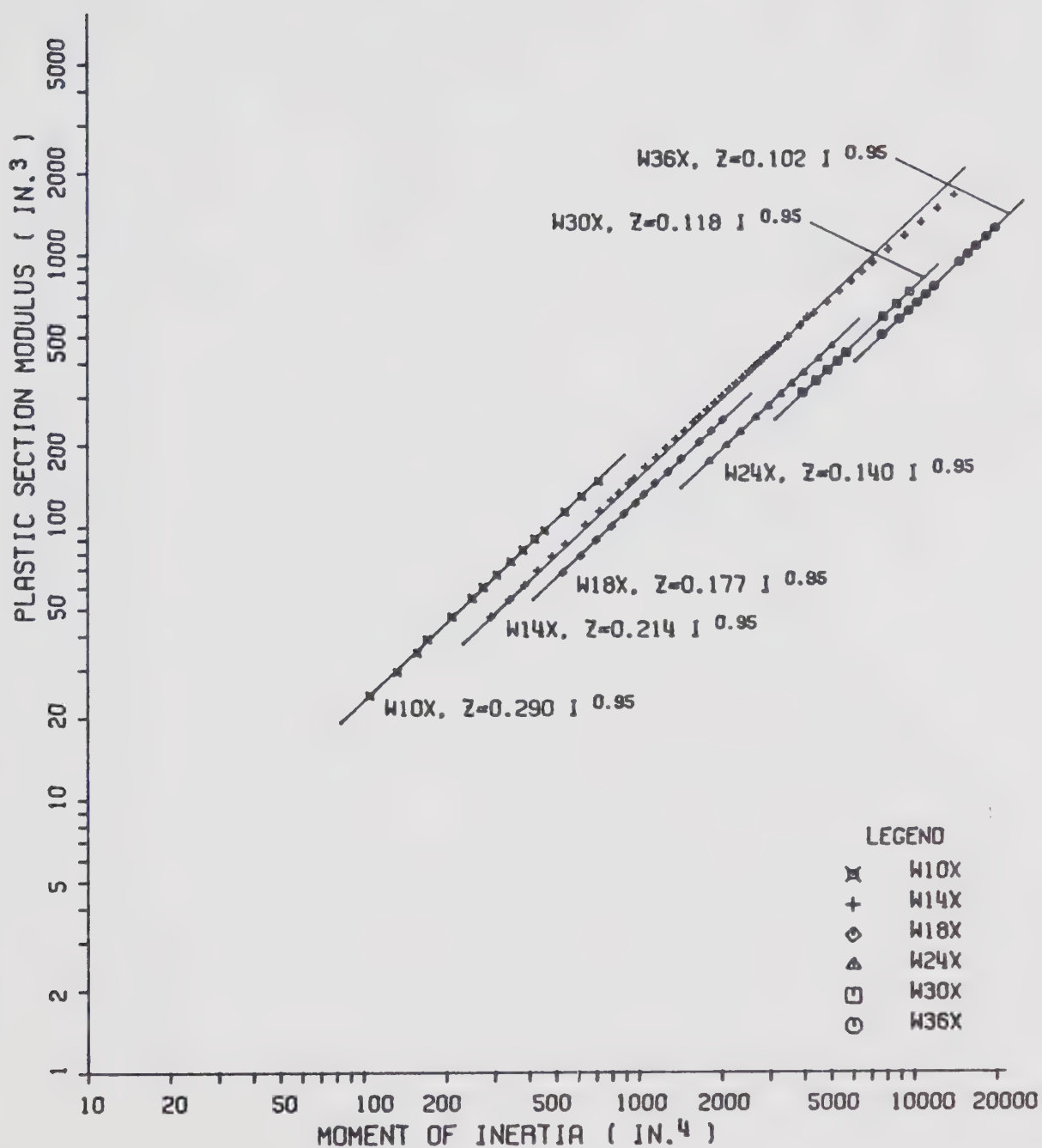


Fig. 2-5 Correlation Between the Moment of Inertia and the Plastic Section Modulus (1)

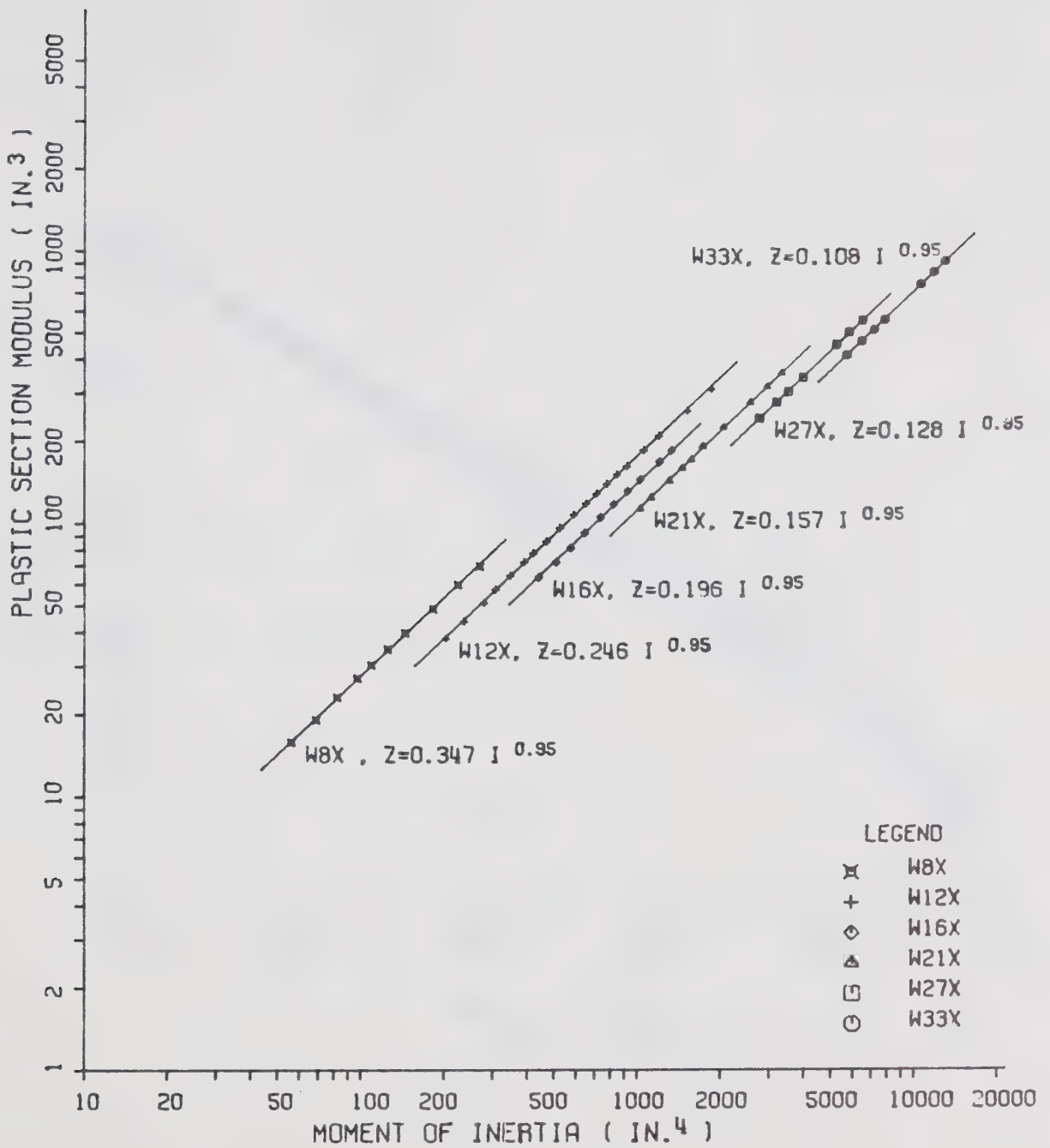


Fig. 2-6 Correlation Between the Moment of Inertia and the Plastic Section Modulus (2)

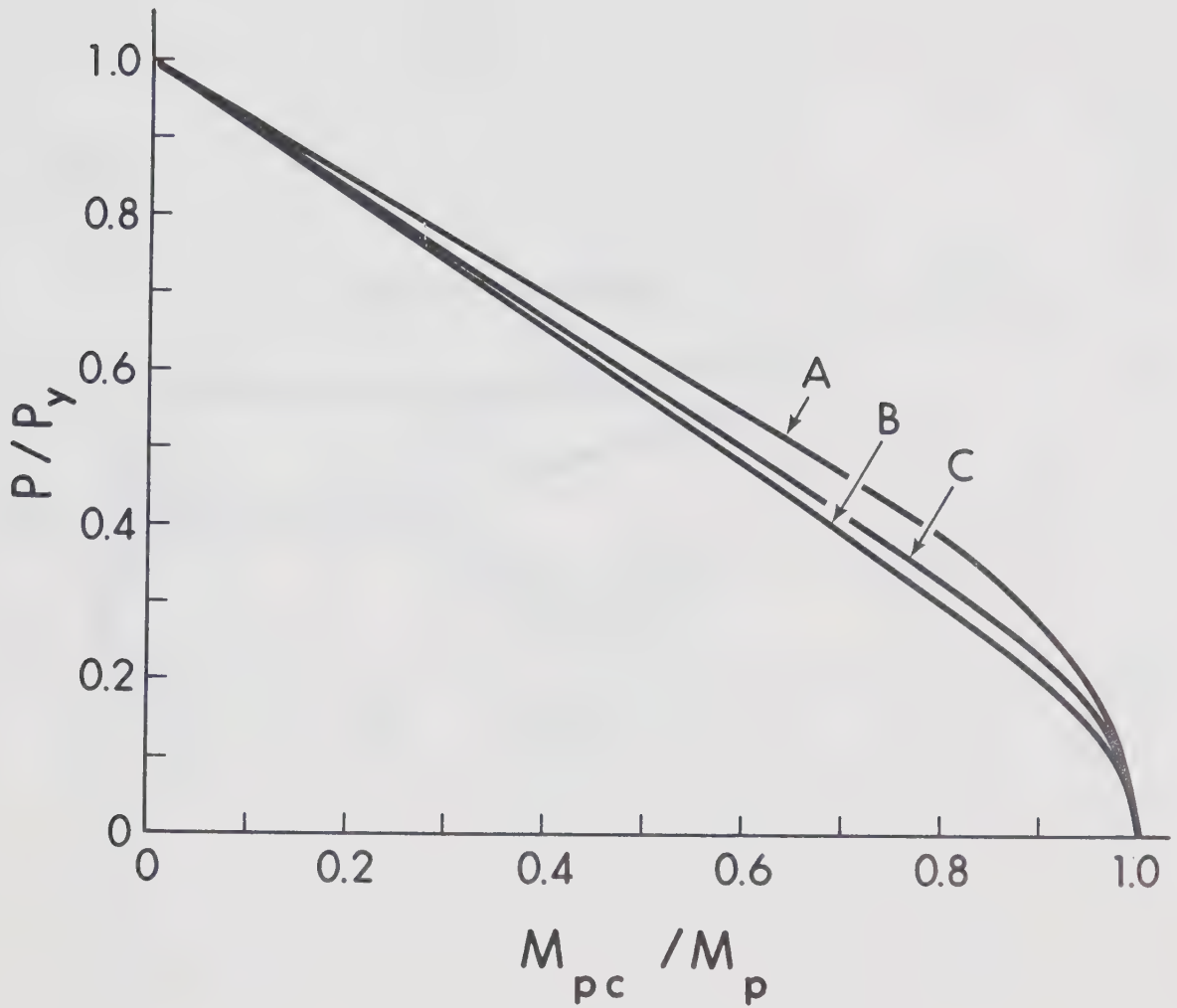


Fig. 2-7 Interaction Curve for Strong Axis Bending of Wide Flange Sections

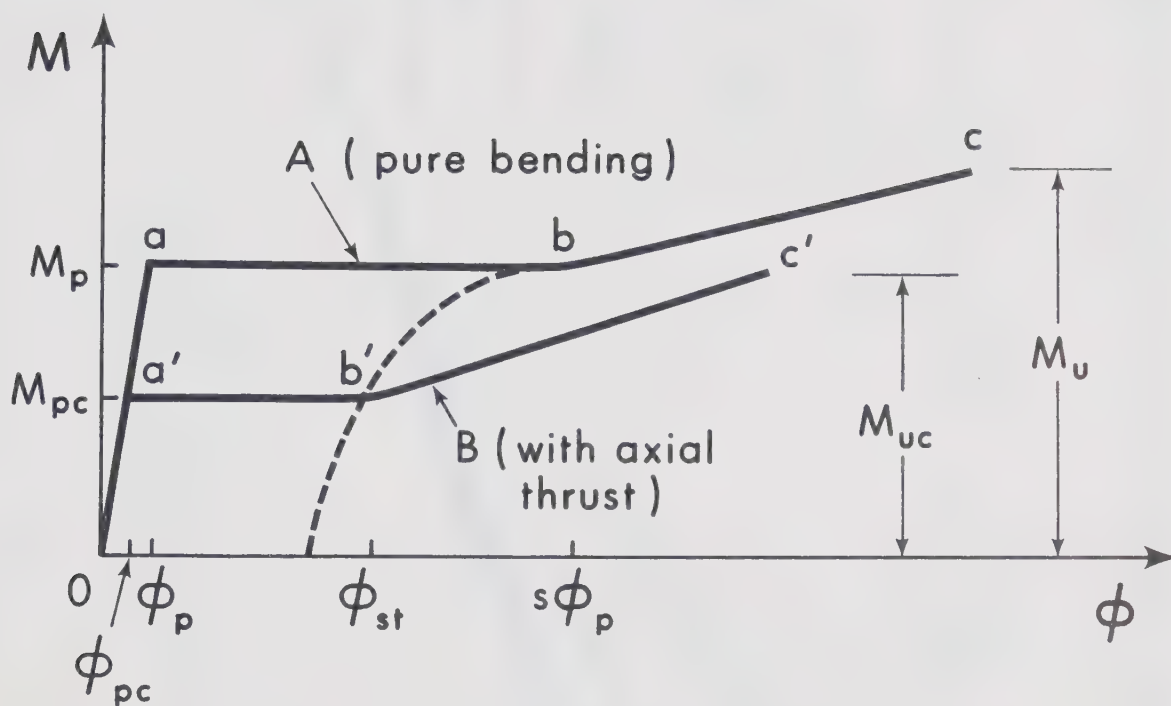


Fig. 2-8 Moment-Curvature-Thrust Relationship

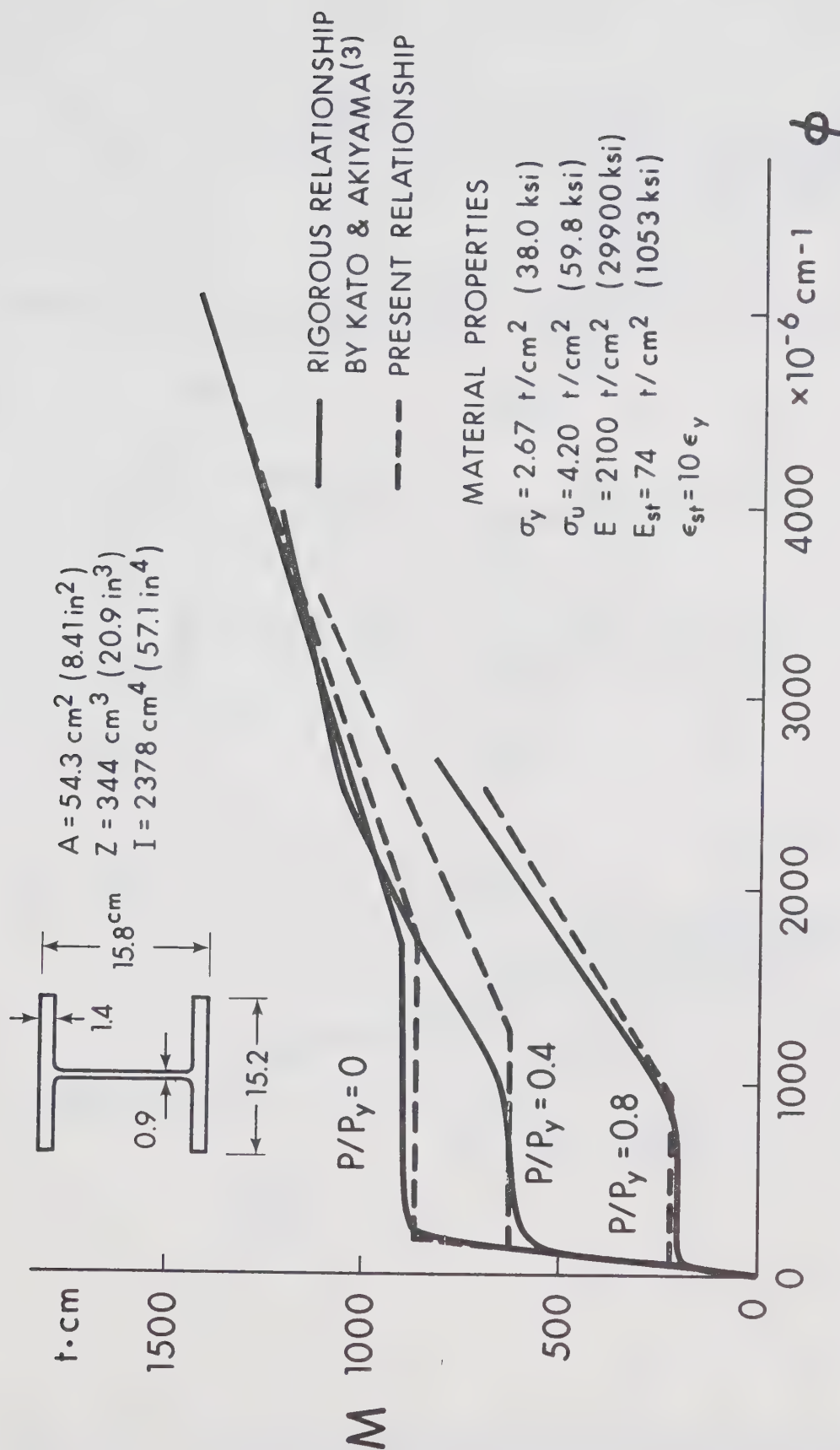


Fig. 2-9 Comparison of the Present Moment-Curvature-Thrust Relationship with a Rigorous Relationship

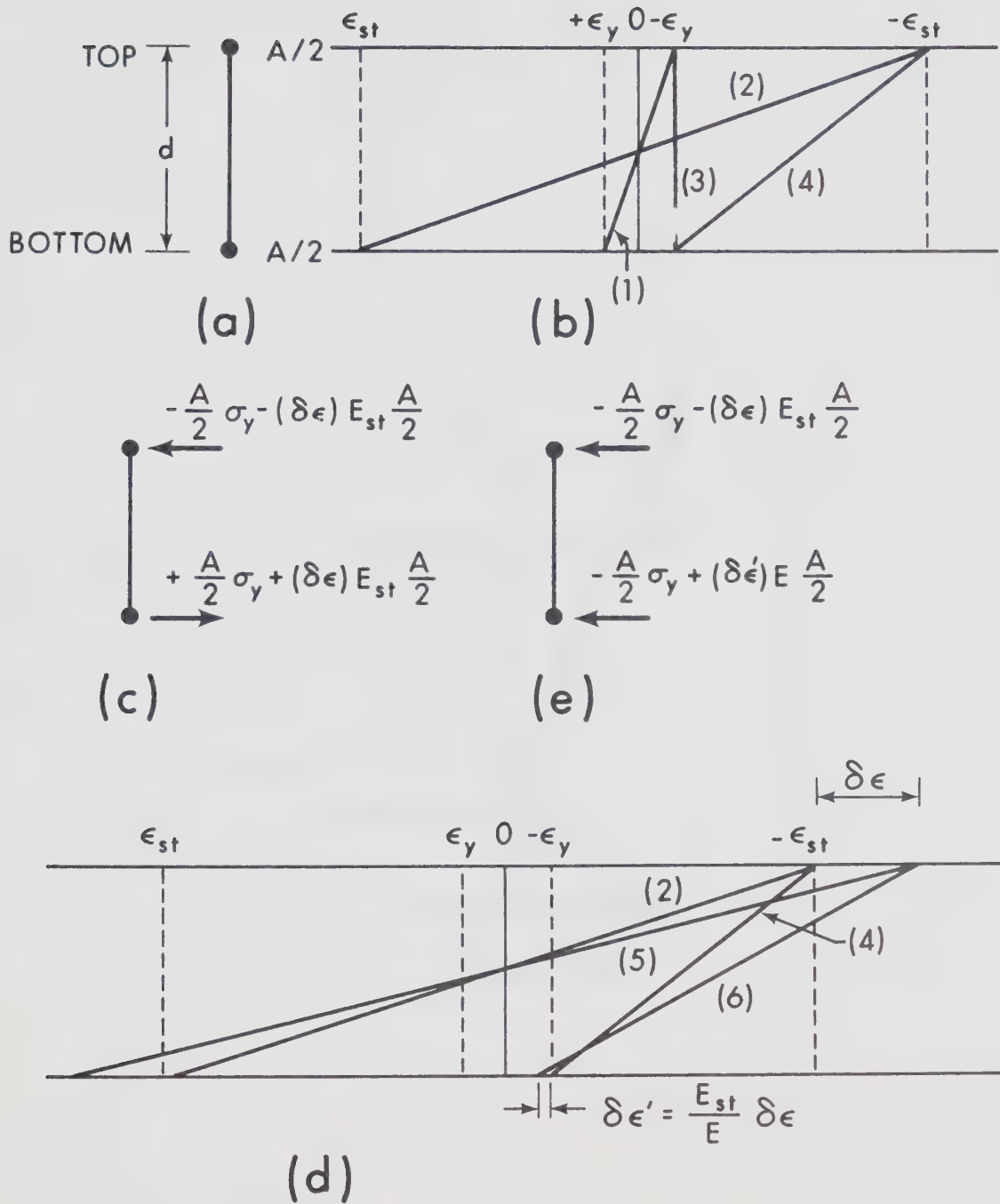


Fig. 2-10 Schematic Expression of Stresses and Strains

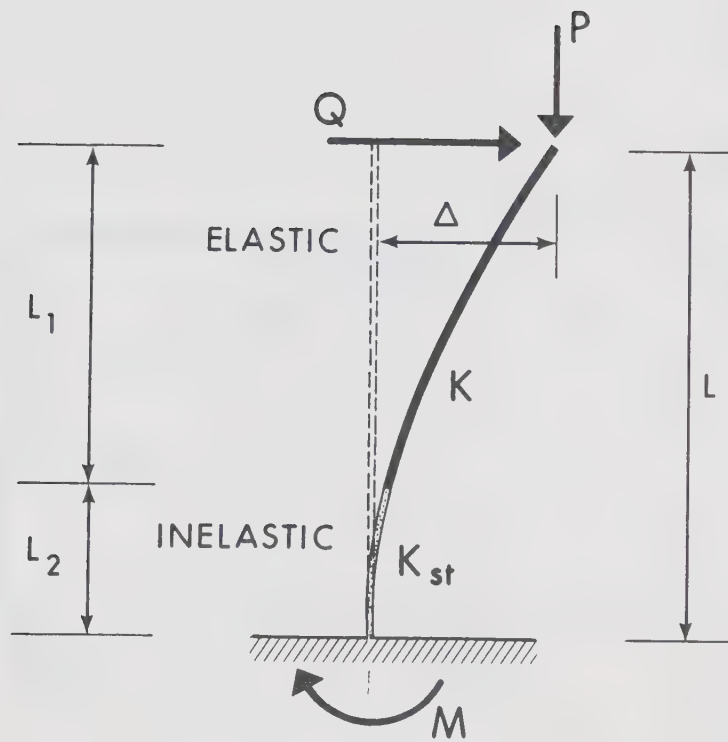


Fig. 2-11 Column with Axial Load

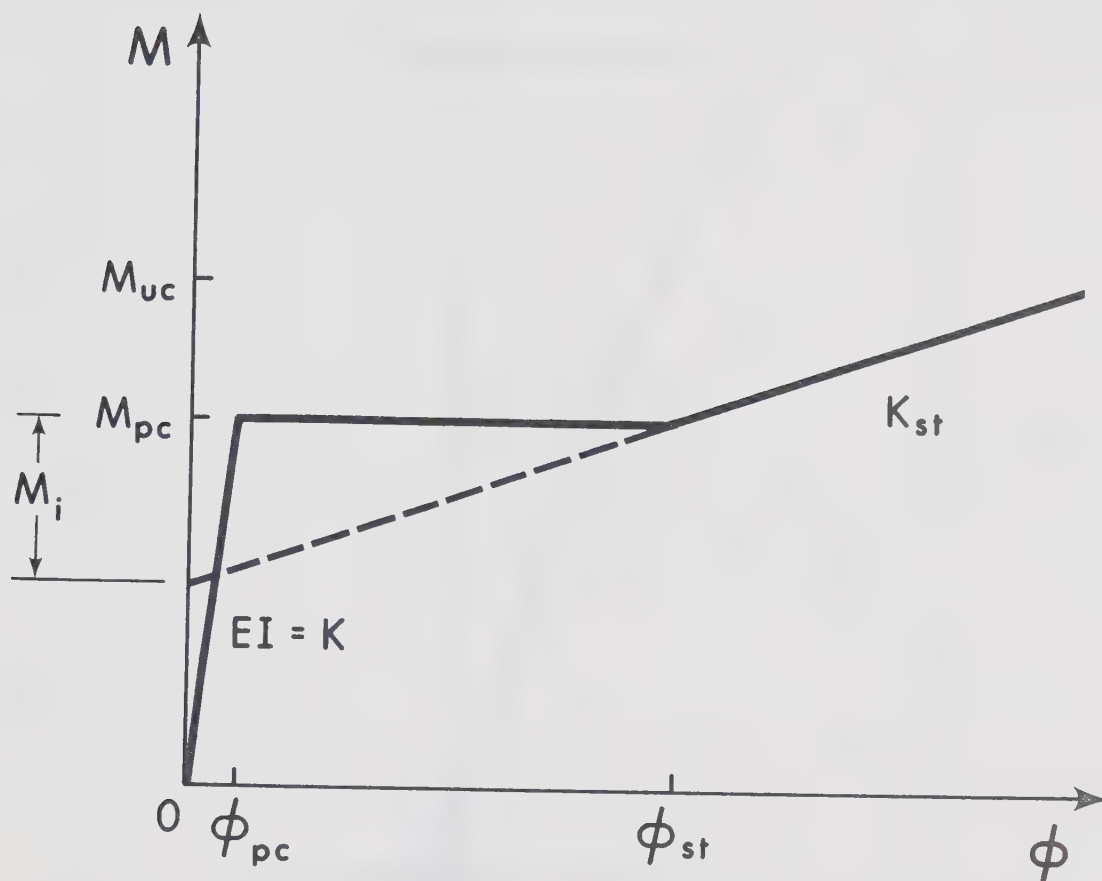


Fig. 2-12 Moment-Curvature Relationship for Column

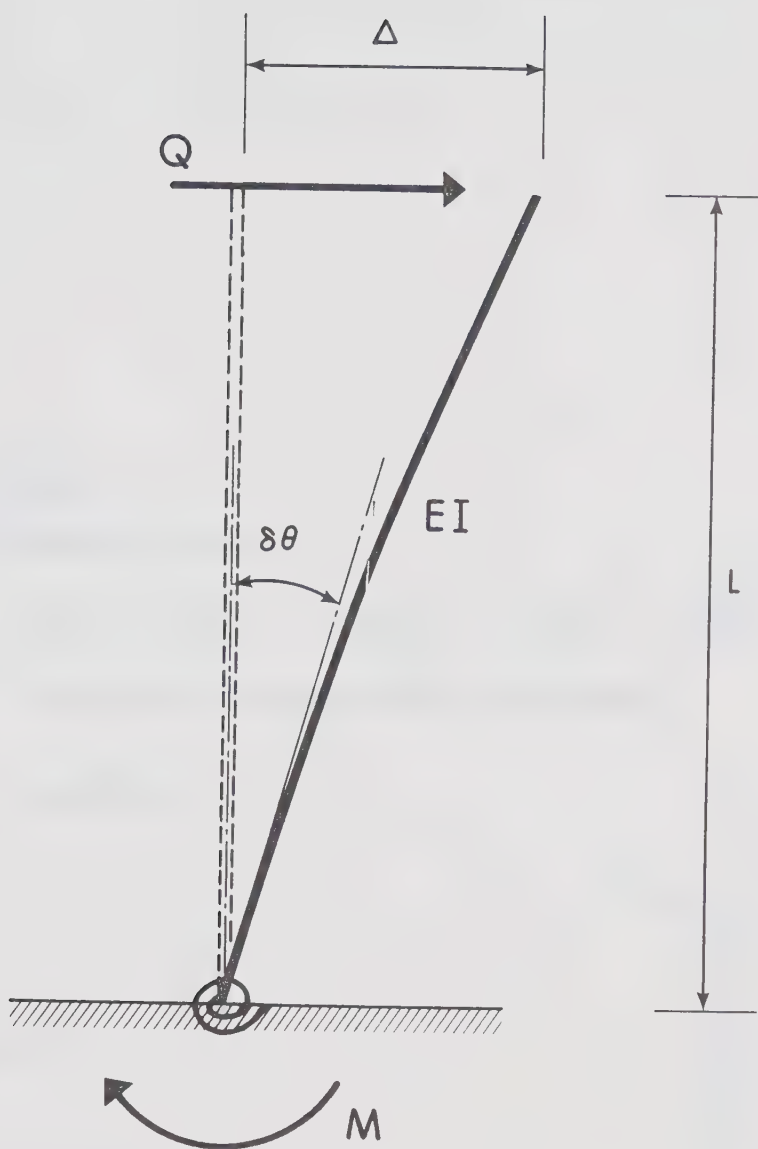
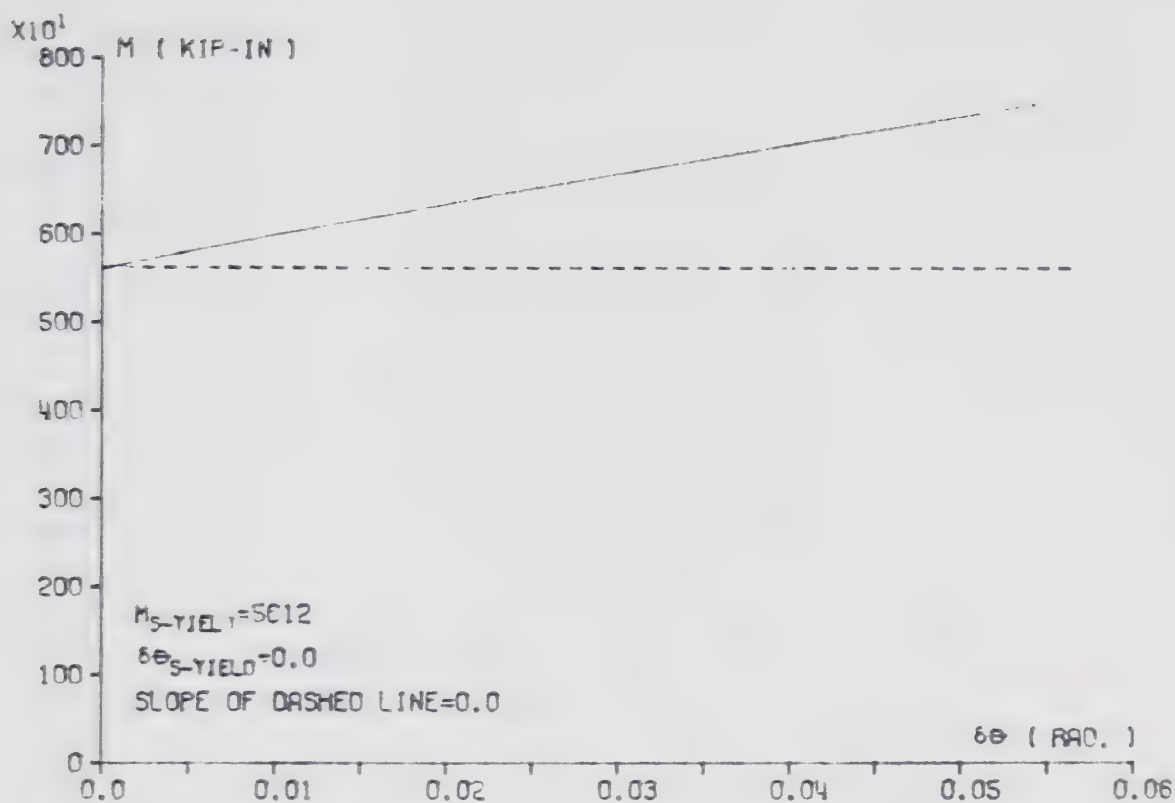
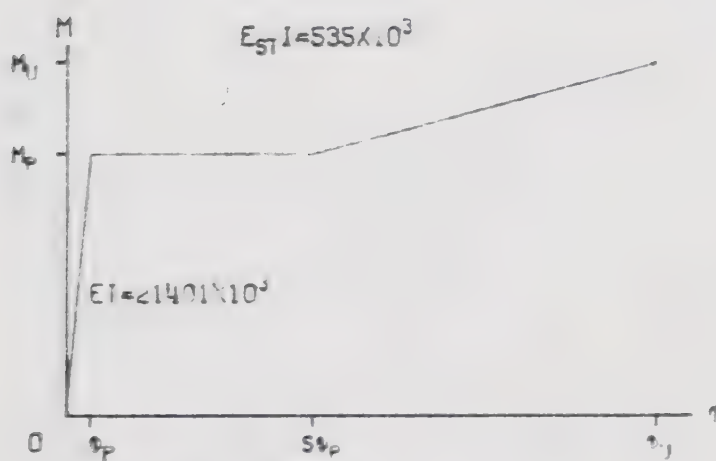


Fig. 2-13 Restrained Column



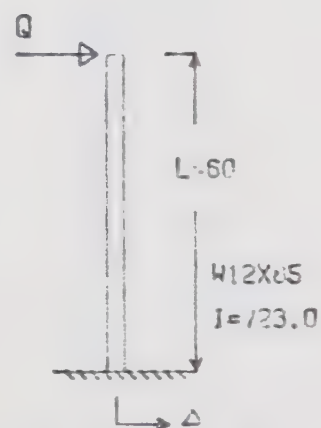
END MOMENT RELAXATION ANGLE RELATIONSHIP



$$M_p = 5612.3, M_u = 7576.6$$

$$\phi_p = 0.262 \times 10^{-3}, 5\phi_p = 10.0\phi_p, \phi_u = 24.0\phi_p$$

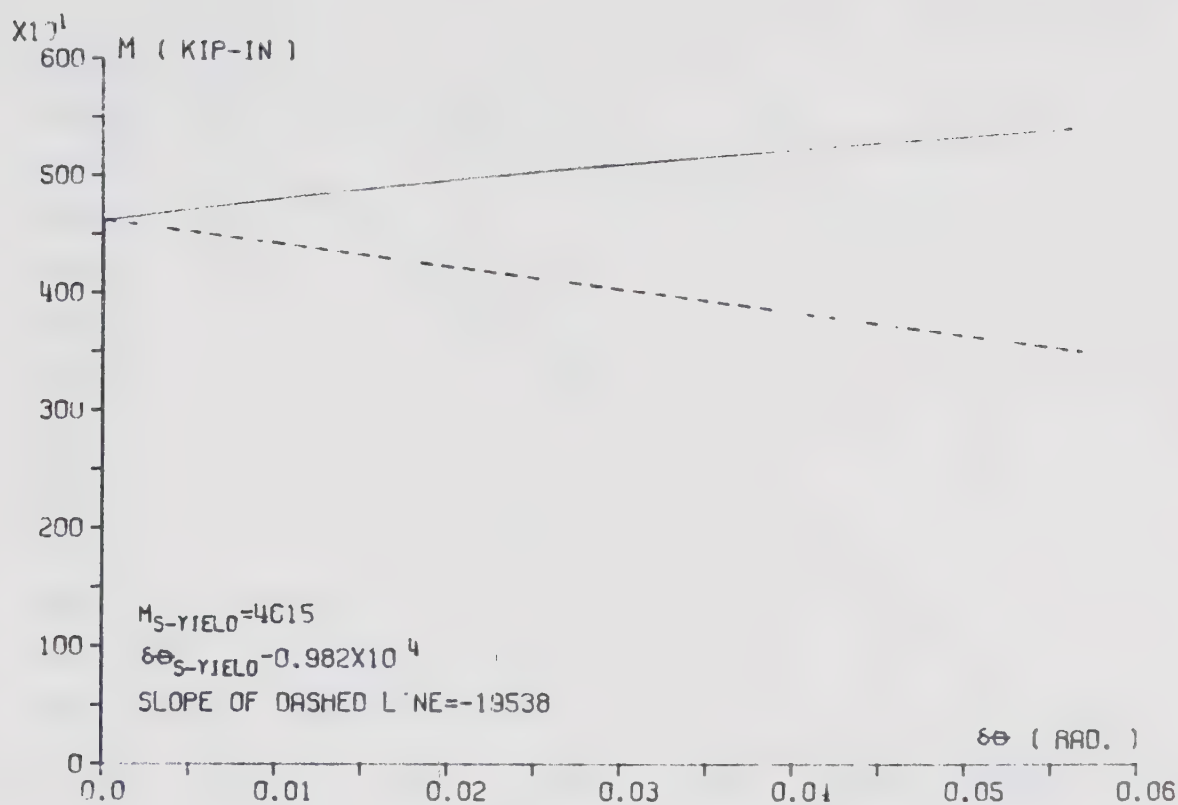
MOMENT CURVATURE RELATIONSHIP



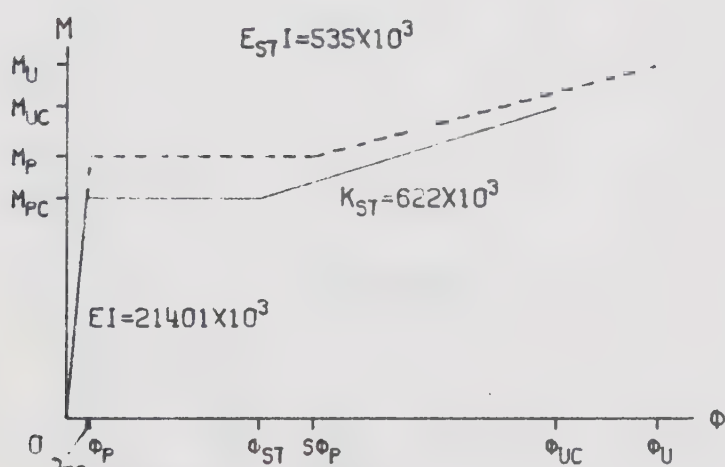
UNIT OF FORCE: KIP.

UNIT OF LENGTH: IN.

Fig. 2-14a CROSS SECTIONAL PROPERTIES AND M- $\delta\theta$ RELATIONSHIP



END MOMENT-RELAXATION ANGLE RELATIONSHIP



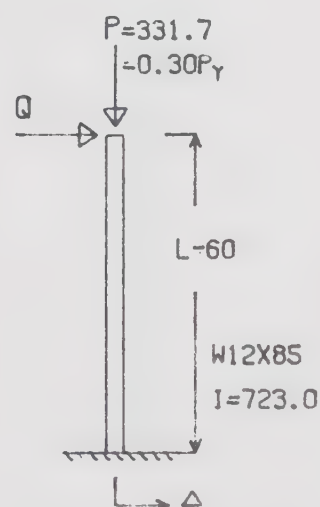
$$M_P = 56.2.3, M_U = 7576.6$$

$$M_{PC} = 4703.1, M_{UC} = 6667.4$$

$$\Phi_P = 0.262 \times 10^{-3}, \Phi_{ST} = 10.0 \Phi_P, \Phi_U = 24.0 \Phi_P$$

$$\Phi_{PC} = 0.220 \times 10^{-3}, \Phi_{ST} = 9.3 \Phi_{PC}, \Phi_{UC} = 23.7 \Phi_{PC}$$

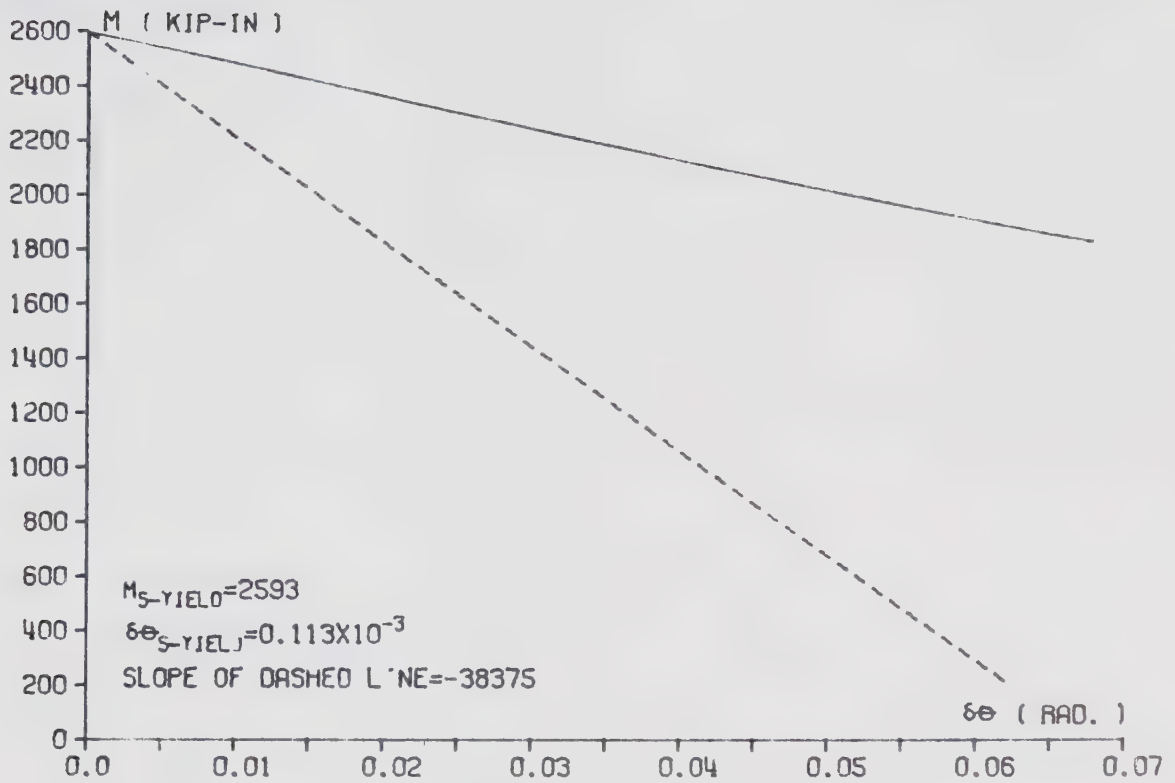
MOMENT CURVATURE RELATIONSHIP



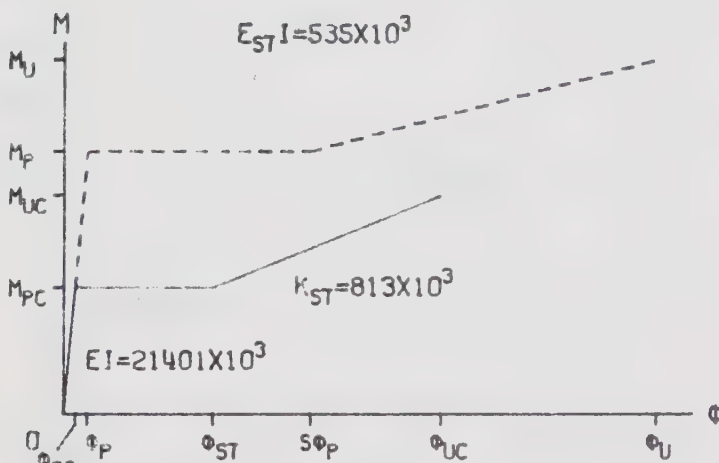
UNIT OF FORCE: KIP.

UNIT OF LENGTH: IN.

Fig. 2-14b CROSS SECTIONAL PROPERTIES AND $M-\Delta\theta$ RELATIONSHIP

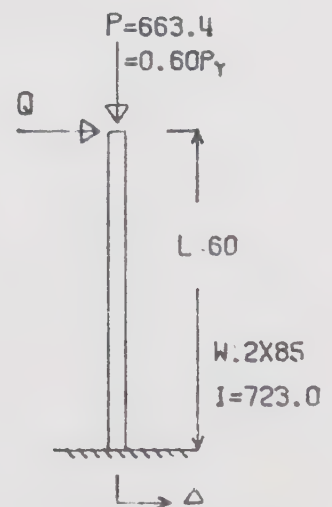


END MOMENT-RELAXATION ANGLE RELATIONSHIP



$M_P=5612.3, M_U=7576.6$
 $M_{PC}=2693.9, M_{UC}=4658.2$
 $\phi_P=0.262 \times 10^{-3}, \phi_{ST}=10.0\phi_P, \phi_U=24.0\phi_P$
 $\phi_{PC}=0.126 \times 10^{-3}, \phi_{ST}=12.6\phi_{PC}, \phi_{UC}=31.8\phi_{PC}$

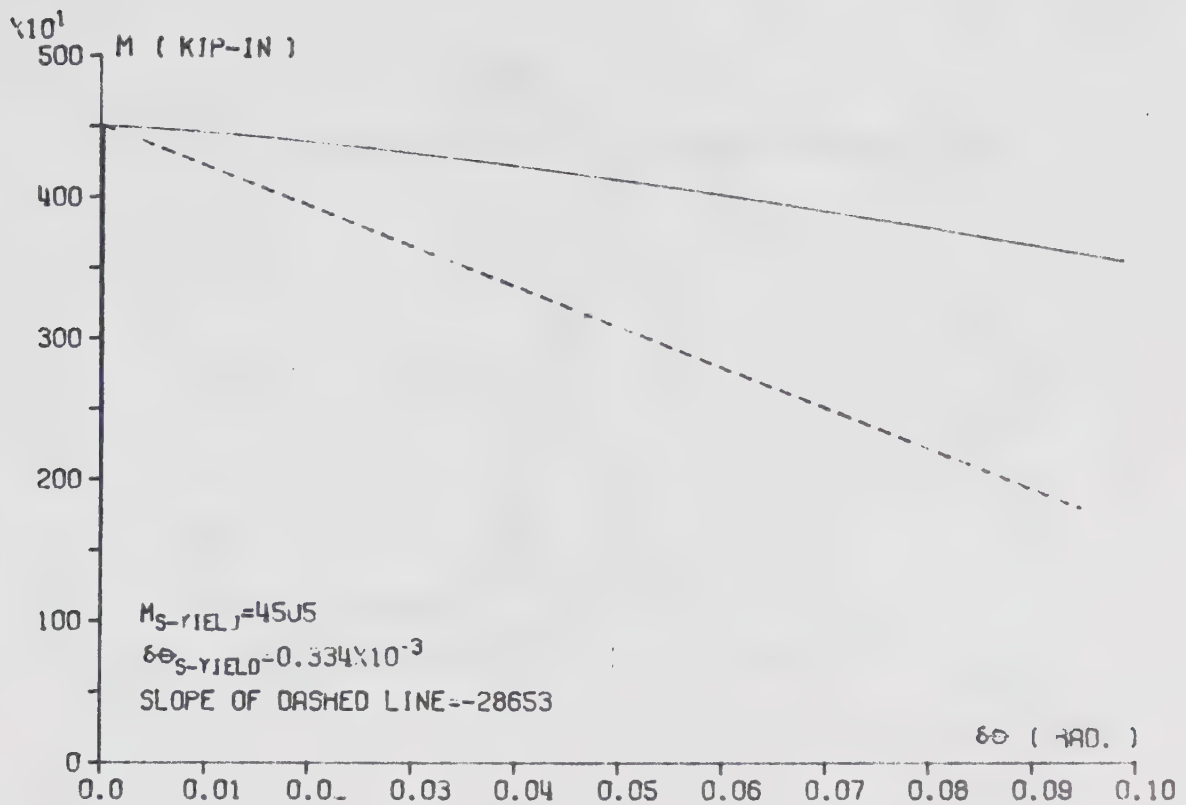
MOMENT CURVATURE RELATIONSHIP



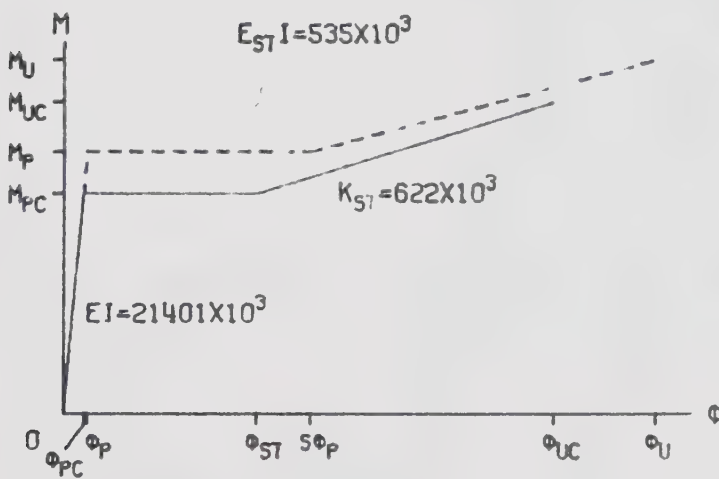
UNIT OF FORCE: KIP.

UNIT OF LENGTH: IN.

Fig. 2-14c CROSS SECTIONAL PROPERTIES AND M- $\delta\theta$ RELATIONSHIP



END MOMENT-RELAXATION ANGLE RELATIONSHIP



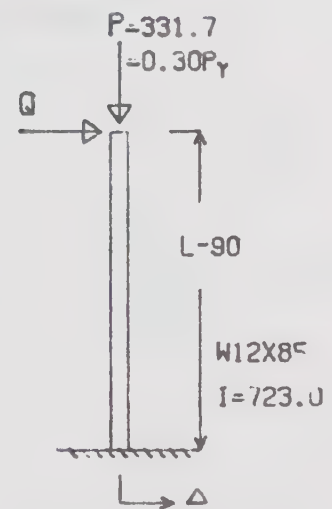
$$M_P = 5612.3, M_U = 7576.6$$

$$M_{PC} = 4703.1, M_{UC} = 6667.4$$

$$\Phi_P = 0.262 \times 10^{-3}, \Phi_{ST} = 10.0 \Phi_P, \Phi_U = 24.0 \Phi_P$$

$$\Phi_{PC} = 0.220 \times 10^{-3}, \Phi_{ST} = 9.3 \Phi_{PC}, \Phi_{UC} = 23.7 \Phi_{PC}$$

MOMENT CURVATURE RELATIONSHIP



UNIT OF FORCE: KIP.

UNIT OF LENGTH: IN.

Fig. 2-14d CROSS SECTIONAL PROPERTIES AND M- $\Delta\theta$ RELATIONSHIP

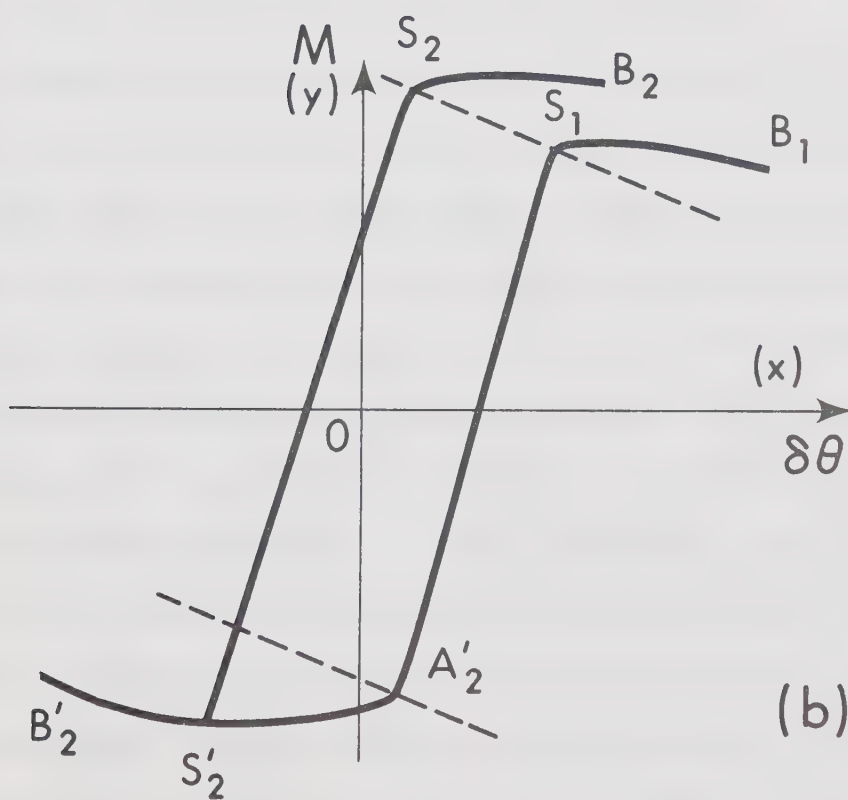
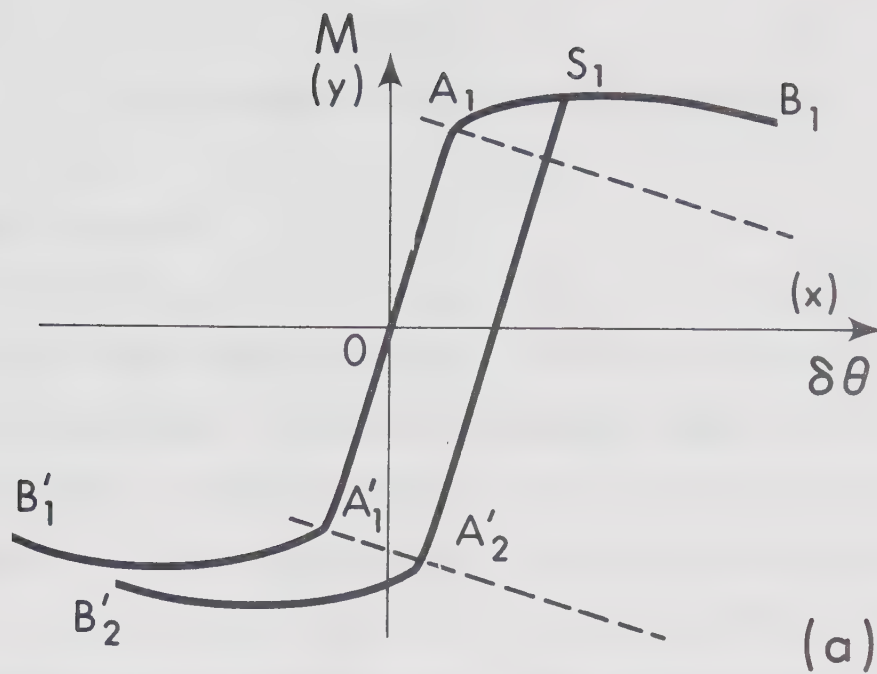


Fig. 2-15 Strain Reversals in the $M_s - \delta\theta_s$ Relationship

Chapter 3.

FORMULATION OF EQUATIONS OF MOTION

3-1 Introduction.

In this chapter, an actual frame is represented by an analytical model which consists of elastic members, rigid bars and equivalent rotational springs, which account for the inelastic properties and the $P-\Delta$ effect, as described in Chapter 2. The function of a rotational spring is expanded to include the influence of semi-rigid connections, deformation of joint panels and shear deformation of members.

In order to solve the equations of motion, it is first necessary to evaluate the static load-deflection relationship. The standard slope deflection equations must be modified for a member with nonlinear rotational springs. It is only necessary to change some of the coefficients in the modified slope deflection equations, when the $M_S-\delta\theta_S$ relationship of a rotational spring is changed from one stage to another. Because of this simplicity, the inelastic response with reversals of load is calculated efficiently. The static load-deflection relationships obtained from this method have been checked against the published test results. When the static load-deflection curve is known, the equations of motion can readily be solved. A linear acceleration method is used to integrate the equations of motion.

3-2 Analytical Model.

The frame to be analyzed is modeled as shown in Fig. 3-1. The number of stories, N_s , and the number of bays, N_b , as well as the story height for each story and the bay width for each bay in the model correspond to those of the original frame.

The stiffness of a member in the modeled frame is taken to be equal to the elastic stiffness of the corresponding member in the actual frame and is assumed to be unchanged throughout the response regardless of the stress level. A rotational spring of the type explained in Chapter 2 is placed between each member and the corresponding joint (or a rigid stub) as shown in the figure, to account for the inelastic action of the member and the secondary effects. The procedures used to determine the properties of this spring will be discussed in the following section. If a shearwall is present, it is simulated by a column which has a bending stiffness and strength equivalent to those of the original shearwall and is attached to the adjacent beams through rigid stubs. The stub length simulates the wall width effect.⁶⁹ This column is then treated in the usual manner.

The bottom story columns are attached to the foundation by elastic rotational springs in an attempt to account for the flexibility of the foundation. The secondary effects

produced by axial shortening or elongation of the columns are ignored. Uniformly distributed loads may be applied to the beams although the possibility of forming a plastic zone within the span length of a member is not checked.

The masses are assumed to be concentrated at each floor level and to translate in a horizontal direction only as shown graphically in Fig. 3-1. A mass concentrated at a floor level is denoted by m_i , in which the subscript i identifies the floor level.

Damping forces are assumed to be developed by the relative motion of adjacent floors.⁷⁰ Thus the damping force at the i -th story is expressed as $c_i(\dot{x}_i - \dot{x}_{i+1})$, in which c_i represents the damping coefficient which is constant throughout the motion within a story; and \dot{x}_i and \dot{x}_{i+1} represent the velocities relative to the ground at immediate upper and lower floors, respectively, with respect to this story.

Each nodal point and member are numbered as shown in Fig. 3-2. Floors and stories are numbered from the top. Bays and columns are numbered from the left. The joint of the i -th floor (from the top) and the j -th column row (from the left) is called the $\{(N_b+1)(i-1)+j\}$ -th joint. The beam of the i -th floor and the j -th bay is called the $\{(2N_b+1)(i-1)+j\}$ -th member and the column of the i -th story and the j -th column row is similarly called the

$\{(2N_b+1)i-(N_b+1)+j\}$ -th member. Thus a N_b -bay, N_s -story frame consists of $(N_b+1)N_s$ joints and $(2N_b+1)N_s$ members.

3-3 Equivalent Rotational Springs in Modeled Frame.

Equivalent rotational springs are placed at the ends of each member of the frame (Fig. 3-1) to account for the influence of axial load and the inelastic behavior (including the strain-hardening effect) of the actual member.

The properties of these rotational springs are determined in the following steps. The axial load and the point of inflection are estimated for each member in the actual frame (Fig. 3-3). These values are then assumed to remain constant during the motion of the frame. Under these conditions, the portion from the point of inflection to the joint (for instance, the portion a-b in Fig. 3-3) would be equivalent to the system shown in Fig. 2-11. This cantilever column is then simulated by the system shown in Fig. 2-13, in which the properties of the rotational spring is obtained in accordance with the method discussed in Sec. 2-5. It is the above-obtained rotational spring that is placed between the member and the corresponding joint in the model of Fig. 3-1.

In the actual frame, the positions of the points of inflection and the values of axial forces are not known beforehand, and moreover may change during the loading

processes. Consequently it is impossible to account exactly for these effects by the present method. Generally, however, these values would not change drastically during the motion of a structure, especially for the interior members of regular frames. Reasonably small changes in the equivalent cantilever column length, L in Fig. 2-11, (the length from the point of inflection to the joint, $a-b$ in Fig. 3-3) produce relatively small changes in the $M_S-\delta\theta_S$ relationship as discussed in Sec. 2-5-3. Thus the $M_S-\delta\theta_S$ relationship is primarily a function of the axial load and the material and cross sectional properties.

3-4 Influence of Semi-Rigid Connections, Deformation of Joint Panels, and Shear Deformation of Members.

The $M_S-\delta\theta_S$ relationship obtained in the manner discussed in the preceding section (for example, curve A in Fig. 3-4) will be modified to include the influence of semi-rigid connections, deformation of joint panels, and shear deformation of members.

The connection of members at a joint may not be rigid; i.e., a relative rotation between ends of adjacent members will be observed, for example, in a bolted joint¹³ as shown in Fig. 3-5. The relaxation angle is a function of the end moment and may be represented by curve B in Fig. 3-4.

The shear deformation in a joint panel may sometimes

have a significant influence on the overall response of a frame.^{12,71} The moment diagram shown in Fig. 3-6(a) can be expected when a frame is subjected to lateral loads. The stress condition in a joint panel is shown in Fig. 3-6(b) corresponding to the moment diagram of Fig. 3-6(a), and the deformed shape of the panel in Fig. 3-6(c). Curve C in Fig. 3-4 indicates the average end moment vs. change in angles between the ends of beams and columns. (In the case where combined vertical and lateral loads are to be considered, it would become difficult to relate the relaxation angle to the end moment.)

Shear deformations of a member may also be taken into account, if desired. The deflection due to shear for the member shown in Fig. 2-11 is given by (ref. Fig. 3-7):

$$\Delta = \frac{\kappa Q}{GA} L, \quad (3-1)$$

where G is the modulus of rigidity, A is the cross sectional area, and κ is the shape factor.⁷² Therefore, the end moment, $M_S = QL$, and the relaxation angle, $\delta\theta_S = \Delta/L$, are related by:

$$M_S = \frac{GAL}{\kappa} \delta\theta_S. \quad (3-2)$$

This relationship is shown schematically by curve D in Fig. 3-4.

If the curves A through D are combined, the resulting curve is that shown by curve E in Fig. 3-4. If the

rotational spring at the end of the member has an $M_S - \delta\theta_S$ relationship which follows this curve, it is then possible to approximate all of these secondary effects together with the inelastic action of the member.

The unloading of the member will be considered by applying the procedure described in Sec. 2-5-4 to the resultant $M_S - \delta\theta_S$ curve.

3-5 Stiffness Matrix for Frame.

3-5-1 Slope Deflection Equations for Members with Rotational Springs and Rigid Stubs.

The actual structure has been modeled according to the procedure described in the previous sections (Sec. 3-2 to 3-4). In order to calculate the response of the frame, it is first necessary to modify the standard slope deflection equations to accommodate the presence of rotational springs at the member ends and, if required, the presence of rigid stubs which simulate the wall width effect.

The member, a-c-d-b, shown in Fig. 3-8 is considered as a general example. The entire member length is denoted by L and the rigid stubs placed at the left and right ends have lengths of $\lambda_1 L$ and $\lambda_2 L$, respectively. Thus the length of the elastic portion of the member is $\lambda_3 L$, where

$$\lambda_1 + \lambda_2 + \lambda_3 = 1$$

and

$$\lambda_1 \geq 0; \quad \lambda_2 \geq 0; \quad \lambda_3 > 0.$$

A sway rotation, ρ (between the end a and the end b), is permitted for a column but not for a beam. A uniformly distributed load, w , may be applied to a beam over its entire length. Equivalent rotational springs are located at the ends of the rigid stubs at points c and d. The portion c-d is assumed to remain elastic regardless of the deflected shape of the member.

The $M_S - \delta\theta_S$ relationship for the rotational spring for each member end has been determined by the method described in Secs. 3-3 and 3-4. These relationships are now approximated by the trilinear relationships as shown in Fig. 3-9 to simplify the calculations. Thus the additional angle change at point c, $-\delta\theta_c$, and the end moment, M_{cd} , are related by:

$$M_{cd} = \alpha_1(-\delta\theta_c) + \beta_1 \quad (3-3)$$

and similarly at point d:

$$M_{dc} = \alpha_2(-\delta\theta_d) + \beta_2 \quad (3-4)$$

with appropriate values of α_1 , β_1 , α_2 and β_2 depending upon which branch of the moment-relaxation angle relationship is describing the present condition.

The end moments, M_{ab} and M_{ba} , are calculated as:

$$M_{ab} = \frac{\frac{2K}{\lambda_3 L} (A_1 \theta_a + A_2 \theta_b + A_3 \rho + A_4 \frac{\beta_1}{\alpha_1} + A_5 \frac{\beta_2}{\alpha_2}) + A_6 C_{cd}}{A_7} + A_8 D_{ab} \quad (3-5)$$

$$M_{ba} = \frac{\frac{2K}{\lambda_3 L} (A_2 \theta_a + A_1' \theta_b + A_3' \rho + A_5' \frac{\beta_1}{\alpha_1} + A_4' \frac{\beta_2}{\alpha_2}) + A_6' C_{dc}}{A_7} + A_8' D_{ba} \quad (3-6)$$

in which

$$C_{cd} = -\frac{1}{12} w (\lambda_3 L)^2 \quad (3-7)$$

$$C_{dc} = \frac{1}{12} w (\lambda_3 L)^2 \quad (3-8)$$

$$A_8 D_{ab} = -\frac{1}{2} w \lambda_1 (1 - \lambda_2) L^2 \quad (3-9)$$

$$A_8' D_{ba} = \frac{1}{2} w \lambda_2 (1 - \lambda_1) L^2 \quad (3-10)$$

and

$$A_1 = 2 + 6 \frac{\lambda_1}{\lambda_3} + 6 \left(\frac{\lambda_1}{\lambda_3} \right)^2 + 6 \frac{K}{L} \left(\frac{1}{\alpha_2 \lambda_3} + \frac{2 \lambda_1}{\alpha_2 \lambda_3^2} + \frac{\lambda_1^2}{\alpha_1 \lambda_3^3} + \frac{\lambda_1^2}{\alpha_2 \lambda_3^3} \right) \quad (3-11)$$

$$A_1' = 2 + 6 \frac{\lambda_2}{\lambda_3} + 6 \left(\frac{\lambda_2}{\lambda_3} \right)^2 + 6 \frac{K}{L} \left(\frac{1}{\alpha_1 \lambda_3} + \frac{2 \lambda_2}{\alpha_1 \lambda_3^2} + \frac{\lambda_2^2}{\alpha_1 \lambda_3^3} + \frac{\lambda_2^2}{\alpha_2 \lambda_3^3} \right) \quad (3-12)$$

$$\begin{aligned}
 A_2 = 1 + 3\frac{\lambda_1}{\lambda_3} + 3\frac{\lambda_2}{\lambda_3} + 6\frac{\lambda_1\lambda_2}{\lambda_3^2} \\
 + 6\frac{K}{L}\left\{\frac{\lambda_1}{\alpha_1\lambda_3^2} + \frac{\lambda_2}{\alpha_2\lambda_3^2} + \left(\frac{1}{\alpha_1} + \frac{1}{\alpha_2}\right)\frac{\lambda_1\lambda_2}{\lambda_3^3}\right\} \quad (3-13)
 \end{aligned}$$

$$A_3 = -(A_1 + A_2) \quad (3-14)$$

$$A'_3 = -(A'_1 + A_2) \quad (3-15)$$

$$A_4 = 2 + 3\frac{\lambda_1}{\lambda_3} + 6\frac{K}{L}\left(\frac{1}{\alpha_2\lambda_3} + \frac{\lambda_1}{\alpha_2\lambda_3^2}\right) \quad (3-16)$$

$$A'_4 = 2 + 3\frac{\lambda_2}{\lambda_3} + 6\frac{K}{L}\left(\frac{1}{\alpha_1\lambda_3} + \frac{\lambda_2}{\alpha_1\lambda_3^2}\right) \quad (3-17)$$

$$A_5 = 1 + 3\frac{\lambda_1}{\lambda_3} + 6\frac{\lambda_1 K}{\alpha_1\lambda_3^2 L} \quad (3-18)$$

$$A'_5 = 1 + 3\frac{\lambda_2}{\lambda_3} + 6\frac{\lambda_2 K}{\alpha_2\lambda_3^2 L} \quad (3-19)$$

$$A_6 = 1 + 6\frac{K}{L}\left(\frac{1}{\alpha_2\lambda_3} - \frac{\lambda_1}{\alpha_1\lambda_3^2} + \frac{\lambda_1}{\alpha_2\lambda_3^2}\right) \quad (3-20)$$

$$A'_6 = 1 + 6\frac{K}{L}\left(\frac{1}{\alpha_1\lambda_3} + \frac{\lambda_2}{\alpha_1\lambda_3^2} - \frac{\lambda_2}{\alpha_2\lambda_3^2}\right) \quad (3-21)$$

$$A_7 = 1 + 4\frac{K}{L}\left\{\frac{1}{\lambda_3}\left(\frac{1}{\alpha_1} + \frac{1}{\alpha_2}\right) + \frac{3}{\alpha_1\alpha_2\lambda_3}\frac{K}{L}\right\} \quad (3-22)$$

$$\text{where } K \equiv EI. \quad (3-23)$$

If the sway rotation, ρ , is set equal to zero in the preceding equations, the behavior of a beam is simulated.

If

$$w = 0$$

and

$$\lambda_1 = \lambda_2 = 0; \lambda_3 = 1$$

are substituted, the equations simulate the action of a column. The derivation of Eqs. 3-5 and 3-6 is detailed in Appendix C.

It is noted that the inelastic behavior (in this case, the $M_s - \delta\theta_s$ relationships for the rotational springs deviate from the initial linear branch passing through the origin) is expressed by the same equations, by changing the coefficients α_1 and β_1 or α_2 and β_2 in Eqs. 3-3 and 3-4, and in Eqs. 3-5 and 3-6.

3-5-2 Stiffness Matrix for the Frame.

When the end moments for each member have been expressed by Eqs. 3-5 and 3-6, it is possible to formulate the moment equilibrium condition at each nodal point and the shear equilibrium equation for each story. In these equations,

the joint rotations and story shears are written in terms of the horizontal deflections at each floor level.

Using the notation defined in Sec. 3-2, the number of unknowns is equal to the sum of the number of stories, N_S , and the number of joints, $N_S(N_b+1)$; i.e., a total of $N_S(N_b+2)$. The coefficient matrix, $[R]$, is therefore $N_S(N_b+2) \times N_S(N_b+2)$ in size. Letting the vector $\{\theta\}$ denote the unknowns (consisting of joint rotations and story shears), the equilibrium equations are expressed as:

$$[R]\{\theta\} = \{B\} \quad (3-24)$$

where the vector $\{B\}$ consists of fixed end moment terms and the sway rotation terms. By arranging the equilibrium equations in an appropriate order, the coefficient matrix $[R]$ becomes a band matrix with a width of $2N_b+3$ and will have the diagonal elements dominant in most cases. Then, the LU decomposition of $[R]$ by Gaussian elimination without pivoting technique can be employed without losing accuracy.^{73,74} Thus, by preparing a space for an array of $N_S(N_b+2) \times (2N_b+3)$ for the matrix $[R]$, Eq. 3-24 is solved for any right hand side vector $\{B\}$. If a multiplier, in the process of Gaussian elimination, grows greater than one, there is a possibility that accuracy is lost by one digit and if it grows greater than ten, the loss of accuracy could be 2 digits. Should it be the case that the loss of

accuracy could be more than two digits in this process, the computer program is made to indicate this situation. This critical condition, however, has not happened throughout the behavioral study included in this study.

The horizontal loads (or story shears) compatible with the assumed deflected shape used to obtain the vector $\{B\}$ are determined by extracting the story shear terms from the solution $\{\theta\}$. If the vector $\{B\}$ is computed by assuming the sway rotations are zero at every story, the story shears (the sum of the horizontal loads applied at floor levels above a particular story) required to restrain the frame in this position are calculated. This vector is denoted by $\{\eta_0\}$, which is a zero vector unless the uniformly distributed loads on the beams produce lateral sways. If the vector $\{B\}$ is calculated by permitting a unit displacement only at the i -th floor level (from the top), the story shears required to maintain the other floor levels in the undeflected position can be calculated as $\{\eta'_i\}$. Then, the i -th column of frame stiffness matrix, $[G]$, is given by $\{\eta_i\}$, which is:

$$\{\eta_i\} = \{\eta'_i\} - \{\eta_0\} . \quad (3-25)$$

Repeating the computation of $\{\eta_i\}$ for $i = 1$ to N_s , the elements of the complete frame stiffness matrix are obtained. Thus the story shears $\{Q\}$, and the corresponding deflections

at each floor level, $\{x\}$, are related by:

$$\{Q\} = [G](\{x\} - \{\xi_0\}) \quad (3-26)$$

where the vector $\{\xi_0\}$ is the initial deflection at each floor level produced by vertical loads alone applied to the beams, and is obtained by:

$$\{\xi_0\} = -[G]^{-1}\{\eta_0\} . \quad (3-27)$$

Eq. 3-26 is valid if the $M_s-\delta\theta_s$ relationship for every rotational spring in the frame remains elastic. If any of the rotational springs are forced into the inelastic branches of the $M_s-\delta\theta_s$ relationships, the stiffness matrix must be adjusted. Let the vector $\{\xi\}$ be the deflections at each floor level and let the vector $\{\eta\}$ be the story shears at the instant that changes are required in the stiffness matrix. Equilibrium equations, similar to Eq. 3-24, are constructed using new branches of the $M_s-\delta\theta_s$ relationships (substituting a new set of α_1 and β_1 or a new set of α_2 and β_2 in the modified slope deflection equations) at the pertinent member ends. The new stiffness matrix, $[G]$, is calculated in exactly the same manner as before. The deflection at the floor levels, $\{x\}$, and the story shears, $\{Q\}$, are now related by:

$$\{Q\} = [G](\{x\} - \{\xi\}) + \{\eta\} . \quad (3-28)$$

This procedure is repeated as required to obtain

the updated stiffness matrix and the corresponding relationship between the story shears and deflections.

3-6 Static Responses.

In order to check the adequacy of the static load-deflection relationships obtained from the present models, they have been compared with the published results of experimentally obtained responses.^{11,75} It has been concluded that the present procedure can simulate the actual behavior satisfactorily.

One example is given in Fig. 3-10. The frame analyzed by Yarimci⁷⁵ is shown in the inset. The ordinate represents the horizontal load at each floor, H , and the abscissa the sway at the first floor (from the bottom in this case), Δ . The solid curve shows the test result and the broken line A the theoretical calculation by Yarimci. The result from the present calculation is shown by broken line B.

When calculating the response by the present method, the concentrated loads on beams were replaced by the uniformly distributed loads that were to produce the same fixed end moments. The $M_s - \delta\theta_s$ relationship for the equivalent rotational springs were calculated assuming the points of inflection at midpoint of each column. The axial loads on the columns were assumed as follows for the purpose of

calculating the $M_s - \delta\theta_s$ relationships.

3rd Story (top) : $Q + P = 43$ kips (per column)

2nd Story : $Q + 2P = 66$ kips

1st Story (bottom): $Q + 3P = 89$ kips

Other secondary effects such as the shear deformations of members and joint panels were ignored. The $M_s - \delta\theta_s$ relationships obtained in this manner are the same for the top and bottom ends of a column within a story. Axial loads were taken to be zero and the points of inflection were assumed at midspan when calculating the $M_s - \delta\theta_s$ relationships for each beam end. The effect of strain-hardening was ignored in both this analysis and the original analysis.

Thus it is seen that the present method can trace the actual behavior reasonably well, in spite of the fact that the assumptions made to determine the properties of rotational springs have been somewhat crude.

3-7 Equations of Motion.

3-7-1 Formulation of Equations of Motion.

If the masses, m_i , are assumed to be concentrated at each floor level and damping is assumed to be developed by the relative motion of adjacent floors as stated in Sec. 3-2 or as shown in Fig. 3-1, the equations of motion are formulated as outlined below.

Let x_i , \dot{x}_i , and \ddot{x}_i be the deflection, velocity and acceleration, respectively, at the i -th floor relative to the ground and let vectors $\{x\}$, $\{\dot{x}\}$, and $\{\ddot{x}\}$ represent sets of such values from the top floor to the bottom floor at any instant during the motion.

The restoring shear at the i -th story, Q_i , is the i -th element of the vector $\{Q\}$, which is a function of $\{x\}$ and is expressed in general by Eq. 3-28; i.e.,

$$\{Q\} = [G](\{x\} - \{\xi\}) + \{\eta\}$$

where the stiffness matrix, $[G]$, and the vectors, $\{\xi\}$ and $\{\eta\}$, depend upon the behavioral history of the frame from the initiation of motion to the instant under consideration.

If the acceleration of the ground motion is given by $\ddot{y}_0(t)$, the acceleration at the i -th floor with respect to the absolute axis is $\ddot{x}_i + \ddot{y}_0$, and thus the inertia force due to D'Alembert's principle is $-m_i(\ddot{x}_i + \ddot{y}_0)$.⁷⁶

The evaluation of the damping effect is complex. However, it is simply assumed here that the damping force is proportional to the relative velocity of adjacent floors⁷⁰ and is given by $c_i(\dot{x}_i - \dot{x}_{i+1})$, where the damping coefficient, c_i , is taken as:

$$c_i = \frac{2h_i G_{ii}}{\omega_1} \quad (3-29)$$

in which G_{ii} is the i -th diagonal element of the initial

stiffness matrix $[G]$ (which is expressed in terms of story shears), and ω_1 is the circular frequency in the first natural mode of the undamped frame; h_i is an arbitrary constant serving the same purpose as does the percentage of critical damping in the analysis of single degree-of-freedom systems.

Since the applied loads (inertia forces) must be in equilibrium with the frame restoring forces and the forces developed by damping as shown in Fig. 3-11, the following conditions must be satisfied.

At the first story:

$$-m_1(\ddot{x}_1 + \ddot{y}_0) = Q_1(\{x\}) + c_1(\dot{x}_1 - \dot{x}_2) \quad (3-30)$$

At the i -th story ($i = 2, 3, \dots, N_s - 1$):

$$\sum_{j=1}^i \{-m_j(\ddot{x}_j + \ddot{y}_0)\} = Q_i(\{x\}) + c_i(\dot{x}_i - \dot{x}_{i+1}) \quad (3-31)$$

At the bottom story (the N_s -th story):

$$\sum_{j=1}^{N_s} \{-m_j(\ddot{x}_j + \ddot{y}_0)\} = Q_{N_s}(\{x\}) + c_{N_s}\dot{x}_{N_s} \quad (3-32)$$

Or in a concise form:

$$\ddot{x}_i = -\frac{1}{m_i}\{c_i\dot{x}_i + Q_i(\{x\}) + S_i(t)\} \quad (3-33)$$

for $i = 1, 2, \dots, N_s$. These equations are termed the equations of motion. Where:

$$S_i(t) = CMA_i + \ddot{y}_0(t) \cdot CSM_i - c_i \dot{x}_{i+1} \quad (3-34)$$

and the last term, $c_i \dot{x}_{i+1}$, is zero for $i = N_s$. CMA_i and CSM_i are given by:

$$\begin{aligned} \text{for } i = 1 & : CMA_i = 0 ; CSM_i = m_1 \\ \text{for } i = 2 \text{ to } N_s - 1 & : CMA_i = \sum_{j=1}^{i-1} m_j \ddot{x}_j ; \\ & CSM_i = \sum_{j=1}^i m_j \\ \text{for } i = N_s & : CMA_i = \sum_{j=1}^{N_s-1} m_j \ddot{x}_j ; CSM_i = \sum_{j=1}^{N_s} m_j \end{aligned} \quad (3-35)$$

The equations of motion under a blast loading are obtained in a similar manner, if the loads are assumed to be concentrated at each floor level and to vary in proportion to one another during the blast.⁴¹ In the actual case, pressures act on all surfaces of the structure. Both the dynamic pressure and the overpressure have distributions which depend upon the characteristics of the blast, distance of the structure from the blast, the terrain surrounding the building and the shape of the structure.^{77,78} It is possible in many cases to approximate the ratio of the blast loads acting on each floor level.

Let the vector $\{r\}$ denote this ratio. The blast load applied at the i -th floor is then expressed by $Z(t)r_i$,

where $Z(t)$ is a function of time and represents the blast load applied at the floor level where the value of r_i is equal to one. Evaluation of $Z(t)$ will be explained in Appendix E. The external loads which are in equilibrium with the inner forces (restoring frame forces and the forces developed by the damping action) are the sum of the blast loads and the inertia forces; i.e., at the i -th floor, $-m_i \ddot{x}_i + Z(t)r_i$. Defining a vector $\{CR\}$ such that

$$CR_i = \sum_{j=1}^i r_j \quad (3-36)$$

for $i = 1, 2, \dots, N_s$, and replacing $\ddot{y}_0(t)$ and CSM_i in Eq. 3-34 by $-Z(t)$ and CR_i respectively, Eq. 3-33 now represents the equations of motion under blast loading conditions.

3-7-2 Numerical Integration.

To solve the coupled second order differential equations such as Eq. 3-33, a numerical integration method is employed. The linear acceleration method¹⁸ is used in this study.

The acceleration at any floor is assumed to change linearly within the time interval, Δt ; i.e., if the acceleration at a time $n\Delta t$ (from the initiation of vibration; n is an integer) at the i -th floor is $\ddot{x}_i(n)$ and the acceleration at time Δt later at that floor is $\ddot{x}_i(n+1)$, then

the derivative at time $n\Delta t$, $\ddot{x}_i(n)$, is assumed to be:

$$\ddot{x}_i(n) = \frac{\ddot{x}_i(n+1) - \ddot{x}_i(n)}{\Delta t}, \quad (3-37)$$

and the fourth (and higher degree) derivative of x_i vanishes. Therefore, assuming that $x_i(t)$ is differentiable for at least three times between $n\Delta t$ and $(n+1)\Delta t$, Taylor's expansion is written as:

$$x_i(n+1) = x_i(n) + \frac{\dot{x}_i(n)}{1!} \Delta t + \frac{\ddot{x}_i(n)}{2!} \Delta t^2 + \frac{\ddot{\ddot{x}}_i(n)}{3!} \Delta t^3 \quad (3-38)$$

and by differentiating:

$$\dot{x}_i(n+1) = \dot{x}_i(n) + \frac{\ddot{x}_i(n)}{1!} \Delta t + \frac{\ddot{\ddot{x}}_i(n)}{2!} \Delta t^2. \quad (3-39)$$

Substituting Eq. 3-37 into Eqs. 3-38 and 3-39, $x_i(n+1)$ and $\dot{x}_i(n+1)$ are, respectively, expressed as:

$$x_i(n+1) = x_i(n) + \dot{x}_i(n)\Delta t + \frac{1}{3}\ddot{x}_i(n)\Delta t^2 + \frac{1}{6}\ddot{\ddot{x}}_i(n+1)\Delta t^2 \quad (3-40)$$

and

$$\dot{x}_i(n+1) = \dot{x}_i(n) + \frac{1}{2}\ddot{x}_i(n)\Delta t + \frac{1}{2}\ddot{\ddot{x}}_i(n+1)\Delta t. \quad (3-41)$$

Eqs. 3-40 and 3-41 together with Eq. 3-33 determine the deflection, velocity and acceleration at each floor at every instant of the motion. For determination of these values, however, an iterative procedure is required. The chart shown in Fig. 3-12 describes this procedure.

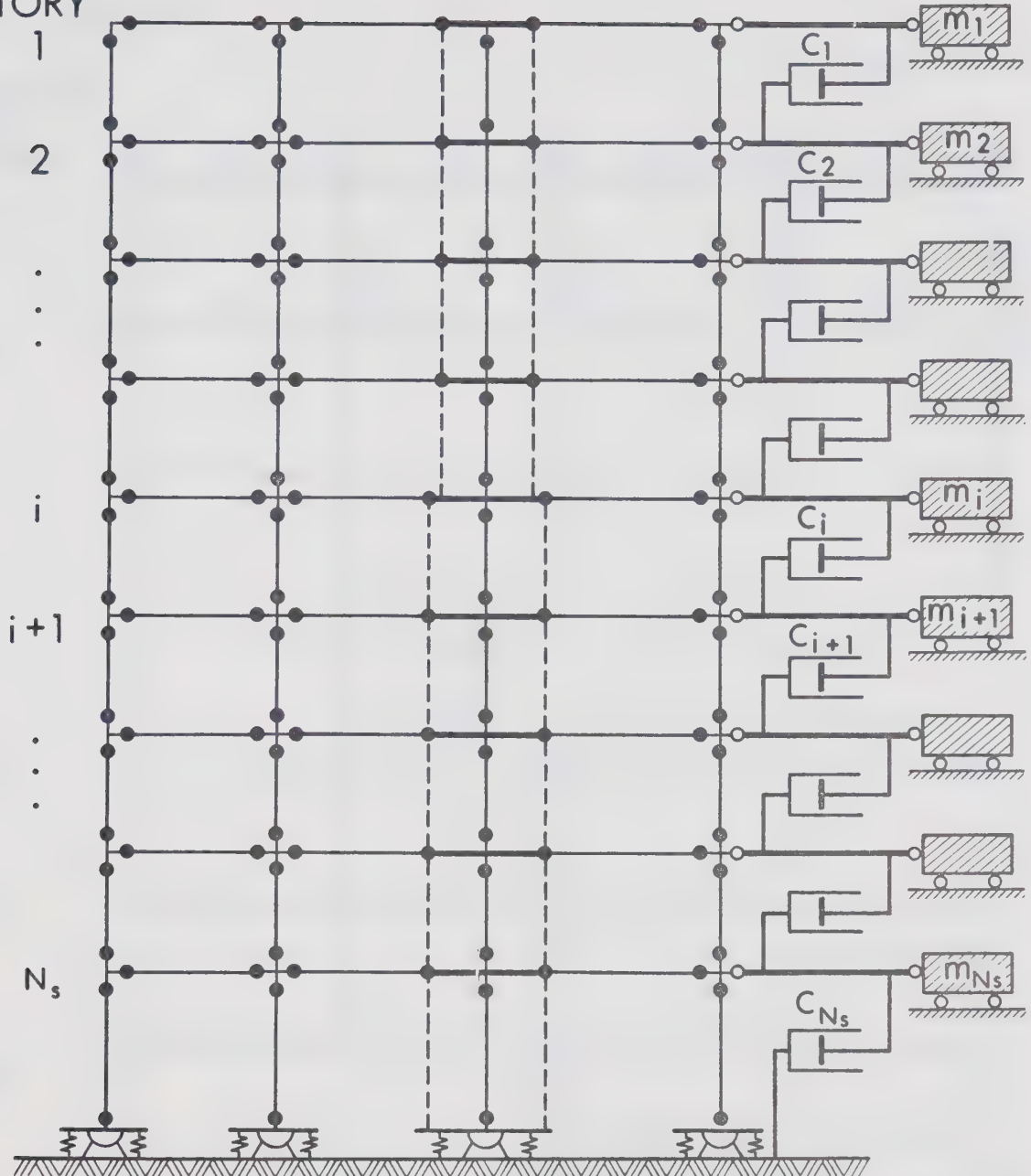
The computer program which is used to perform the dynamic analysis of a frame shown in Fig. 3-1, using the above method of numerical technique, is listed in Appendix D.

3-7-3 Natural Periods of Vibration.

It is sometimes necessary to know the smallest natural period of a frame to select a proper time interval for the numerical integration process. When the linear acceleration method is used to solve Eq. 3-33, the time step, Δt , in Eqs. 3-40 and 3-41 must be less than approximately one-tenth of the smallest natural period in order to obtain convergence.⁷⁹

The natural periods are also used as reliable parameters to classify the overall stiffness of frames. For this purpose, however, only the first two or three modes would be sufficient.

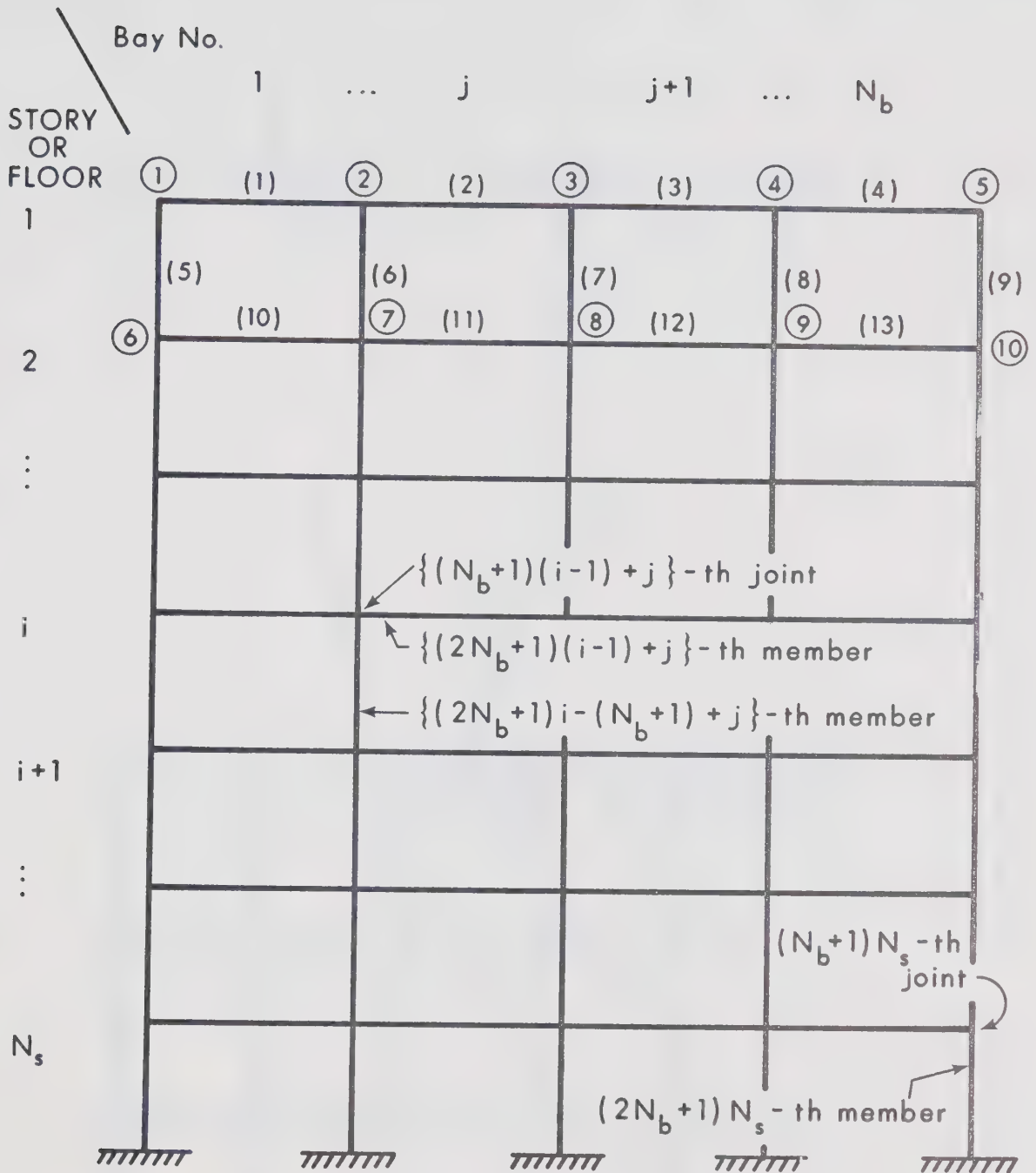
In the computer program listed in Appendix D, the minimum natural period and the first three natural periods and their corresponding natural modes are calculated prior to the response calculation. The smallest and the largest natural periods are computed using Stodola's method¹⁸ (power iteration method). Knowing the first eigenvalue (largest natural period) and the corresponding eigenvector (mode), the second and the third eigenvalues and the corresponding eigenvectors are obtained successively using Wielandt's deflation method.⁷⁴

FLOOR/
STORY

LEGEND

- FLEXIBLE MEMBER
- RIGID MEMBER
- EQUIVALENT ROTATIONAL SPRING
- PINNED JOINT
- ▨ MASS ON ROLLERS
- DASHPOT TO SIMULATE VISCOUS DAMPING
(C_i : DAMPING FORCE PER UNIT VELOCITY)

Fig. 3-1 Analytical Model



ENCIRCLED NUMBER : JOINT NUMBER
BRACKETED NUMBER : MEMBER NUMBER

Fig. 3-2 Numbering Convention

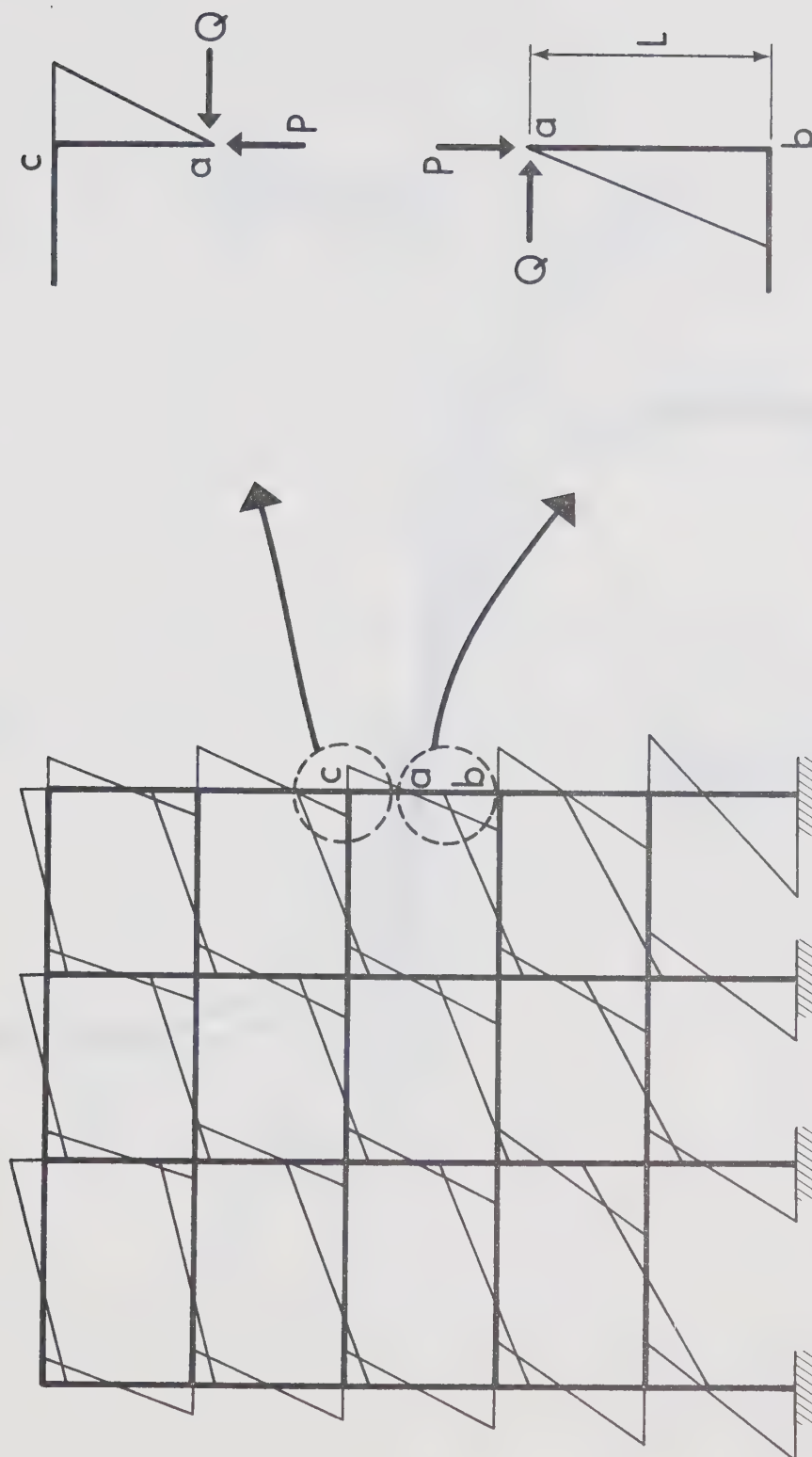


Fig. 3-3 Typical Moment Diagram in a Frame

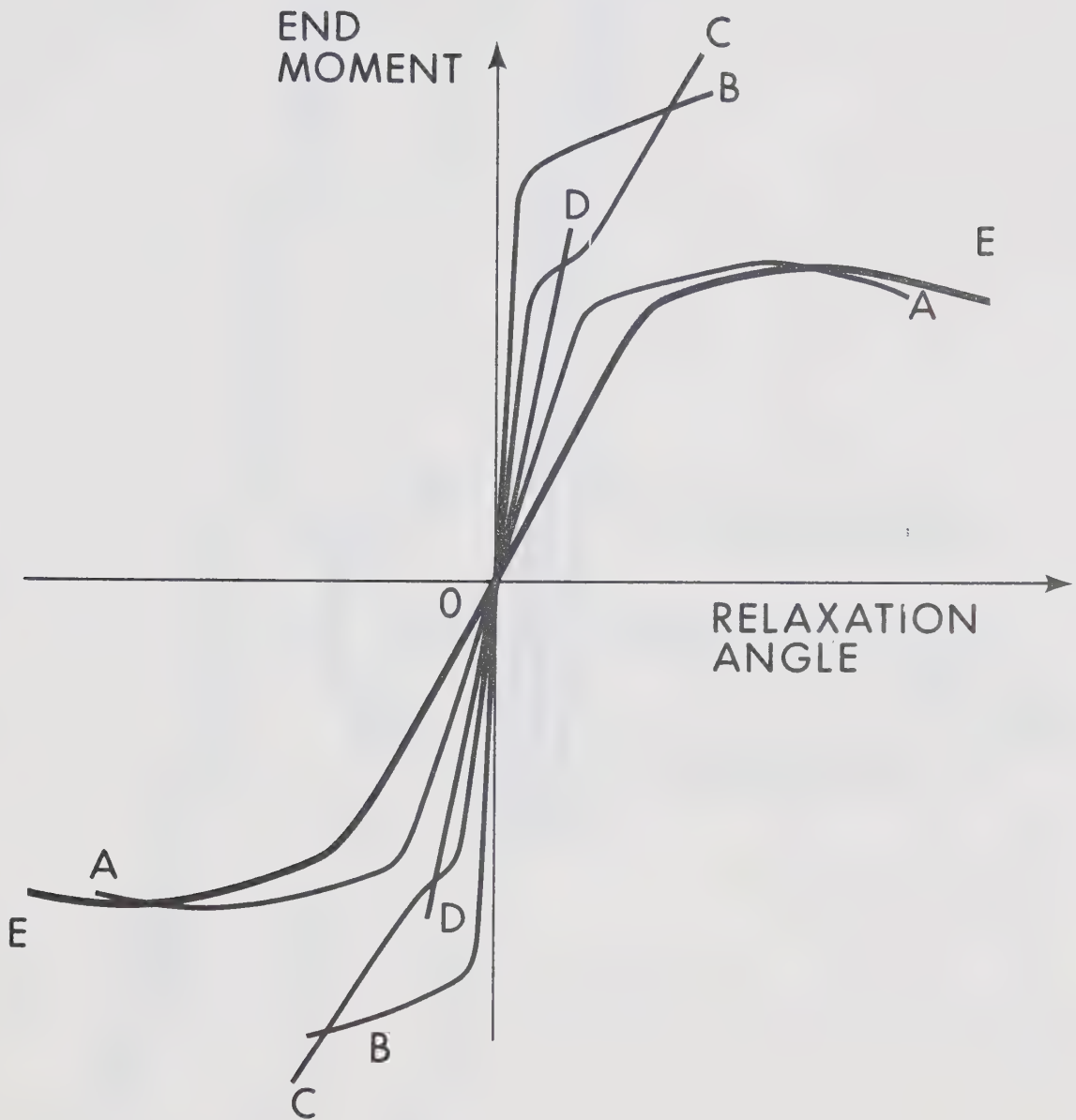


Fig. 3-4 Inclusion of Secondary Effects

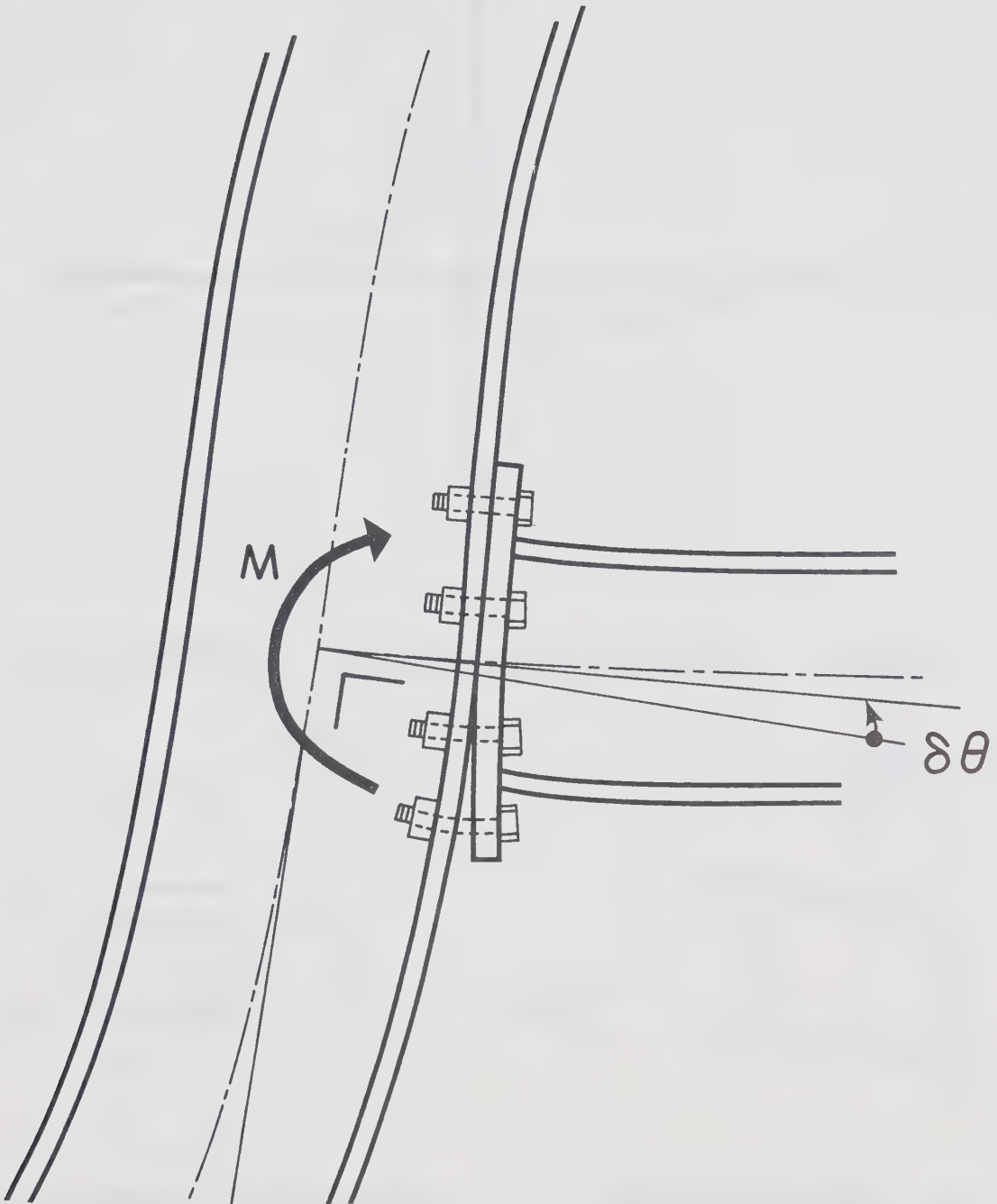
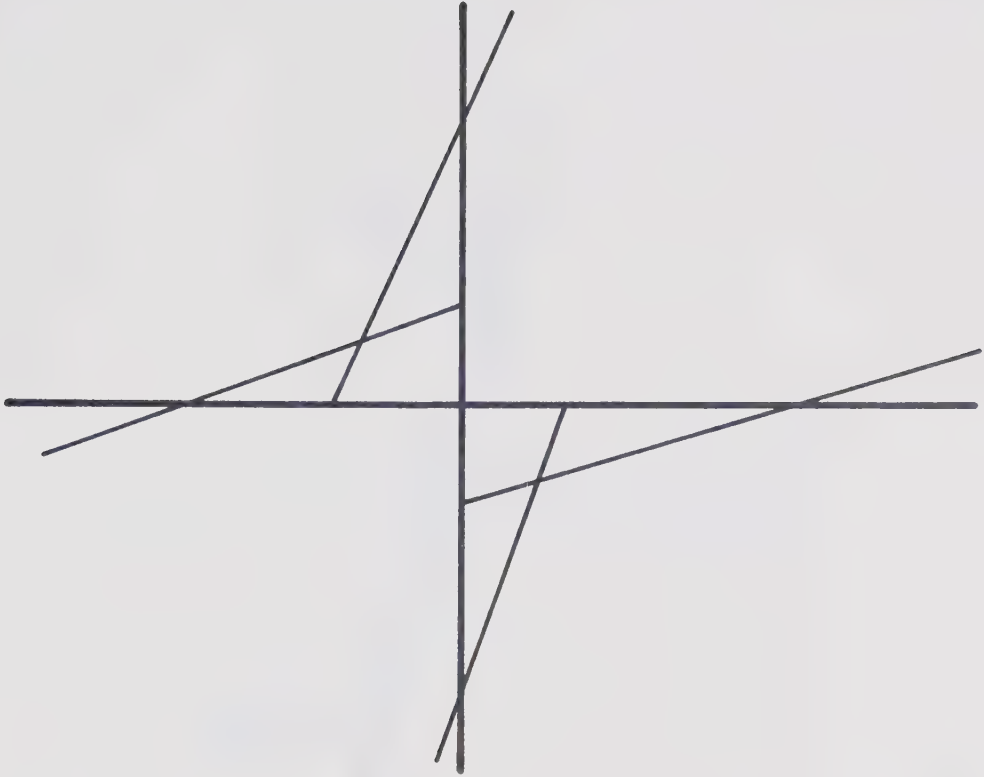
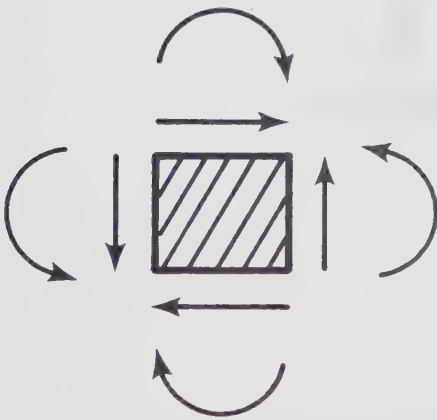


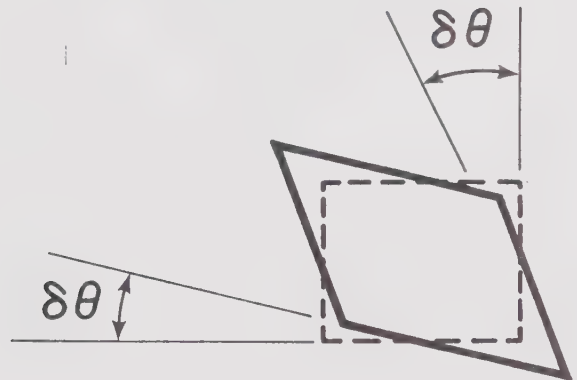
Fig. 3-5 Semi-Rigid Joint



(a) MOMENT DIAGRAM AROUND A JOINT



(b) STRESS CONDITION
IN A JOINT PANEL



(c) DEFORMATION OF
JOINT PANEL

Fig. 3-6 Shear Deformation of Joint Panel

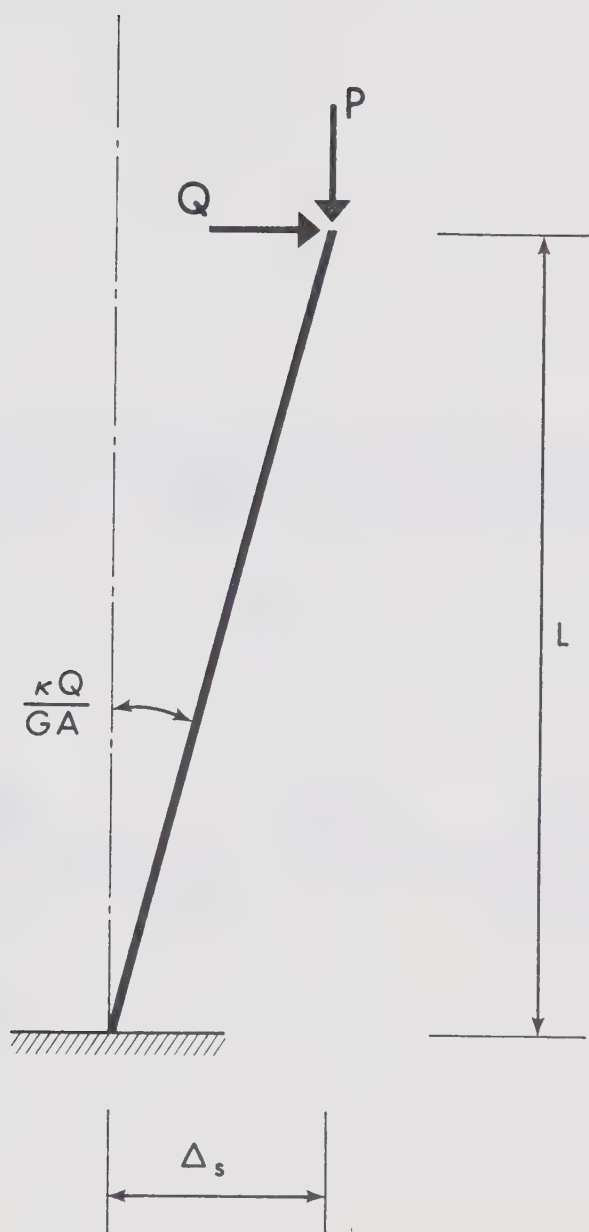


Fig. 3-7 Shear Deformation of Member

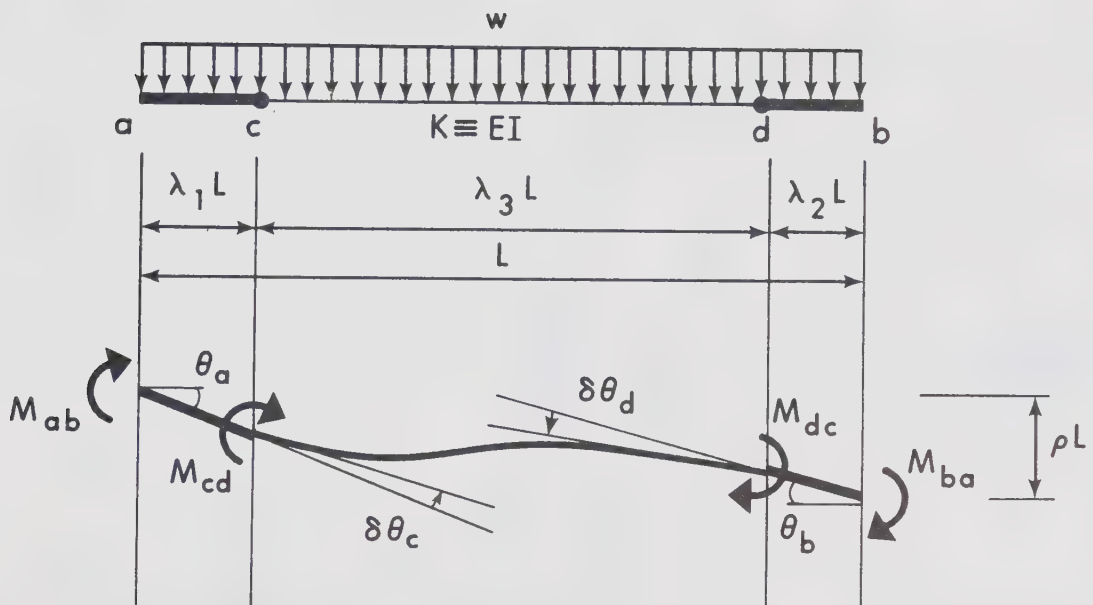


Fig. 3-8 Typical Member

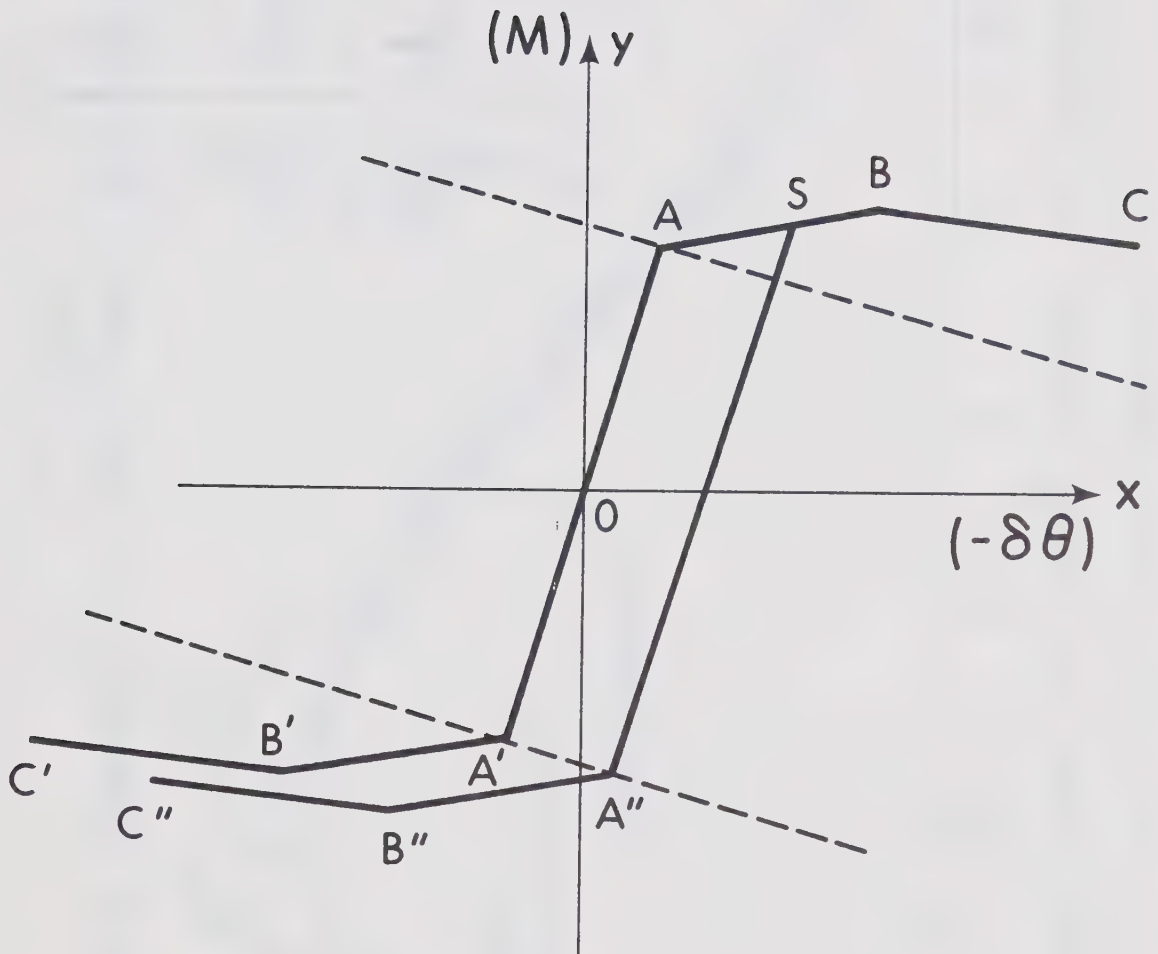


Fig. 3-9 Resulting $M_s - \delta\theta_s$ Relationship

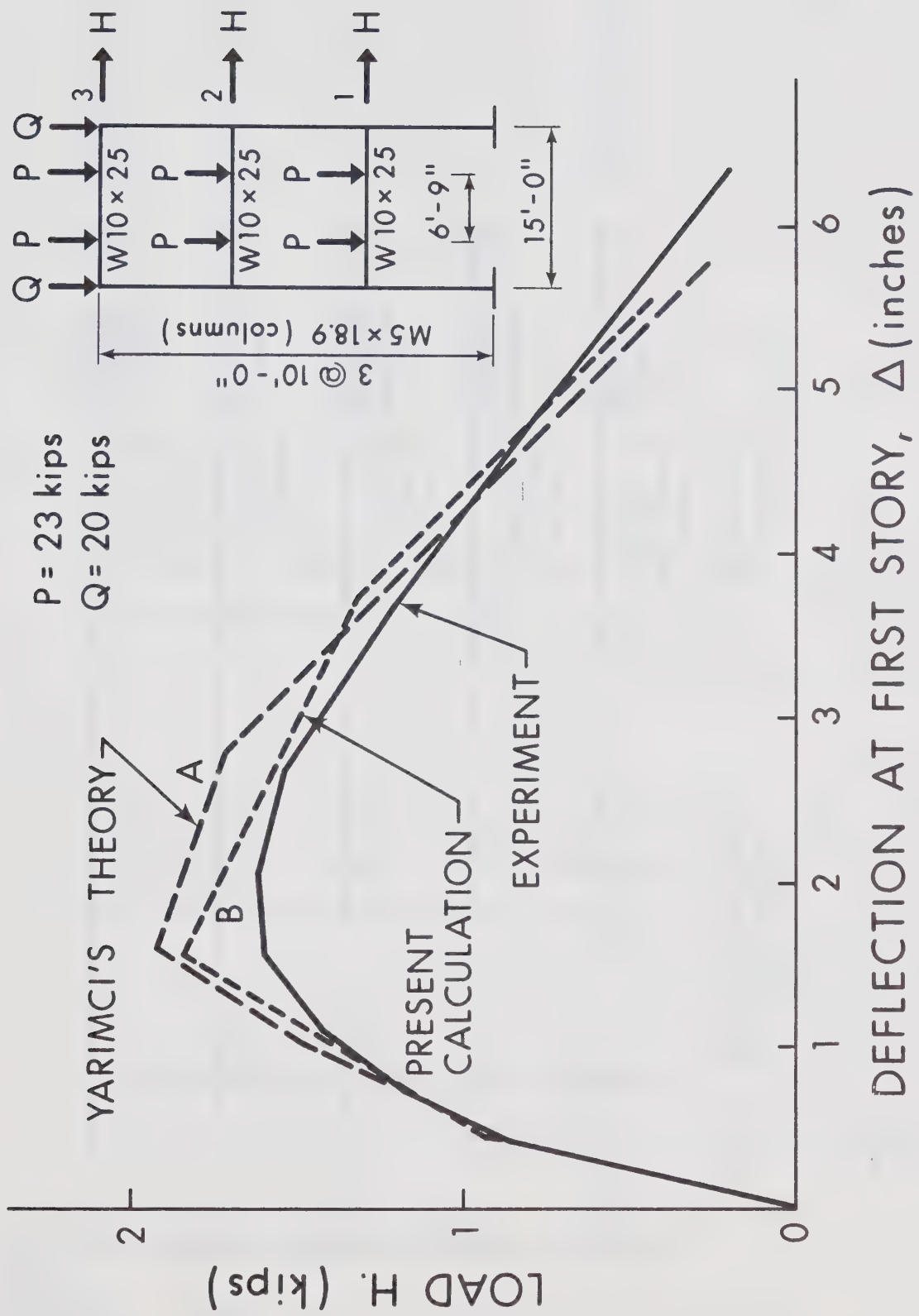


Fig. 3-10 Static Response

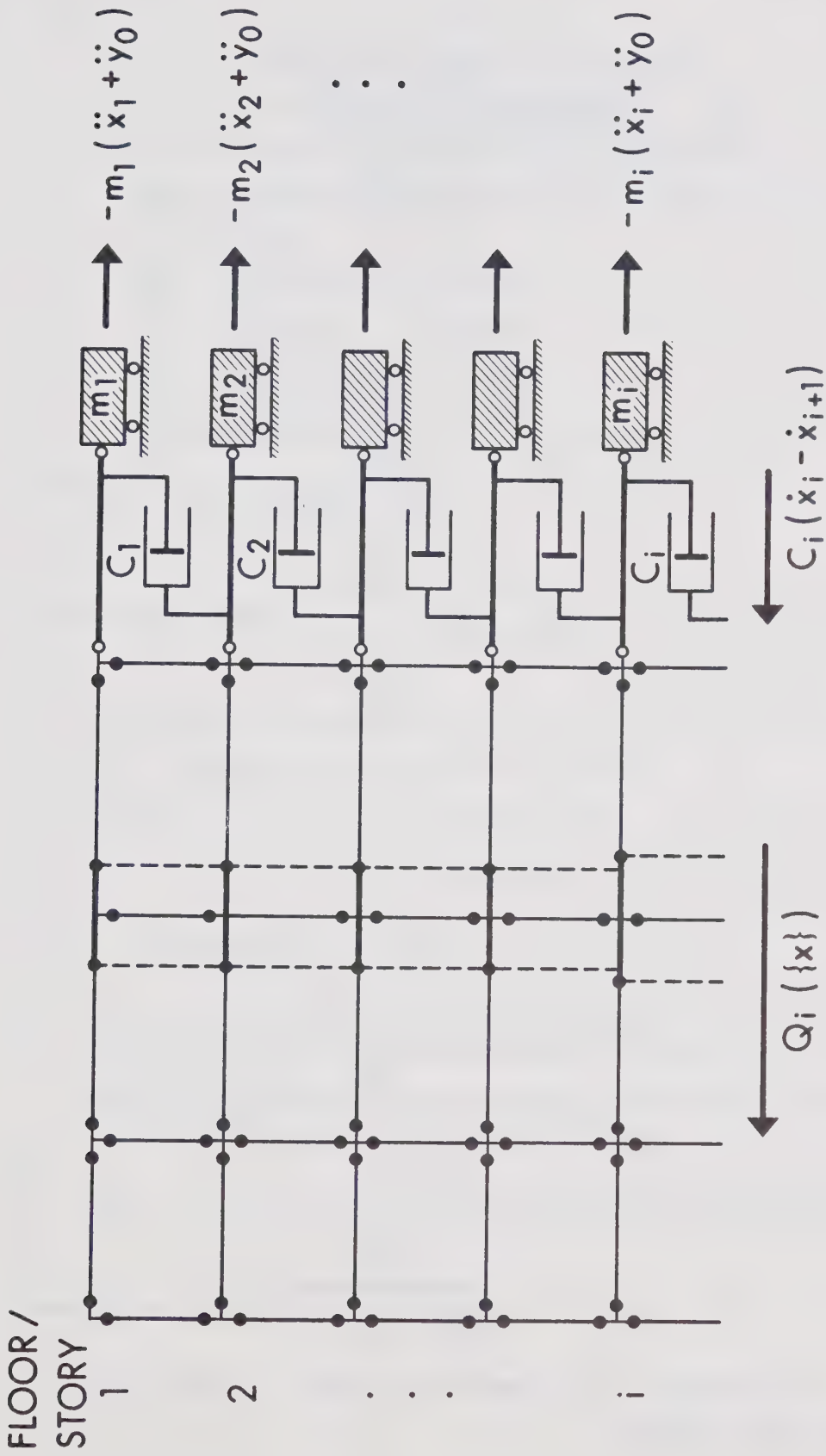


Fig. 3-11 Equilibrium of Forces in Motion

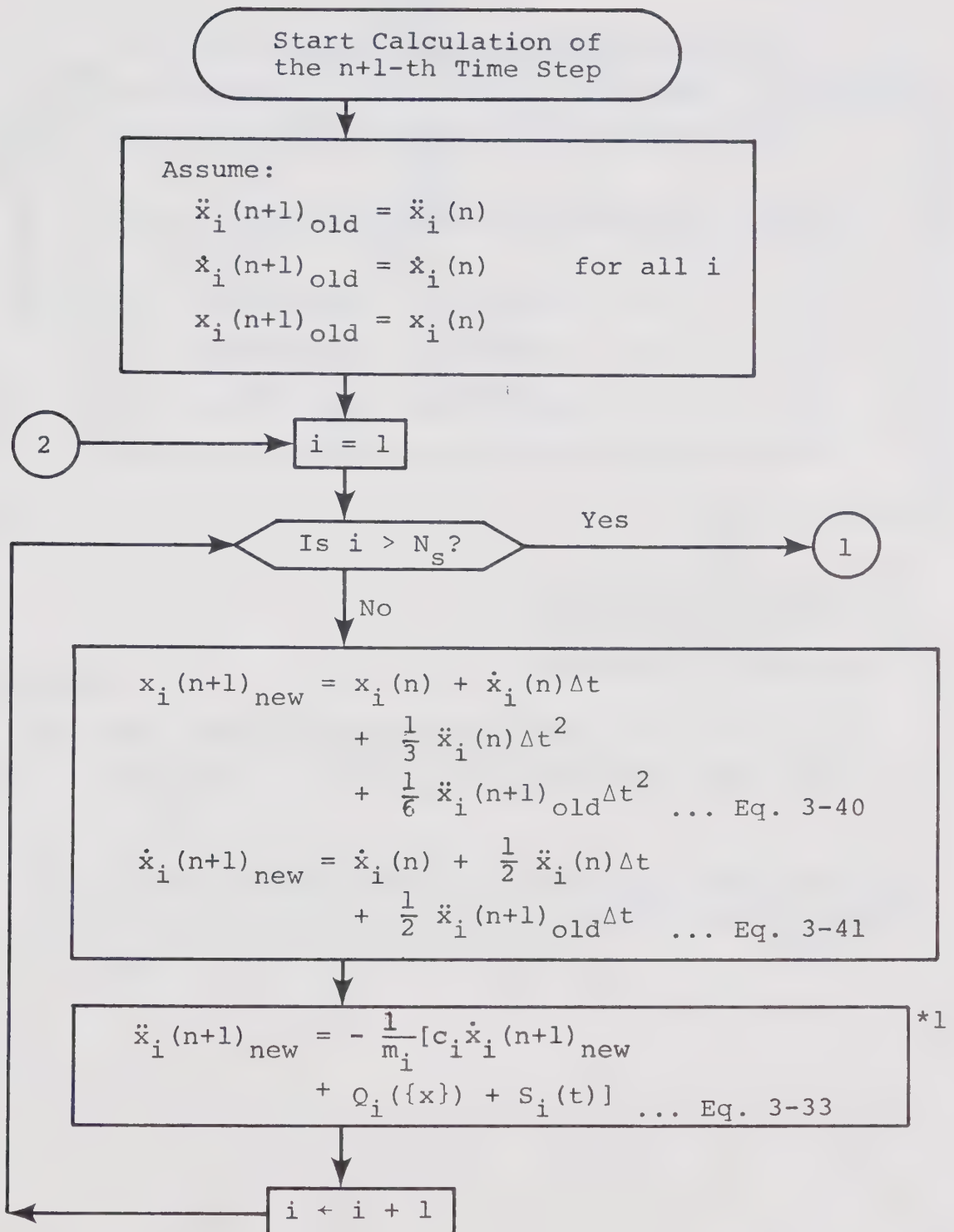
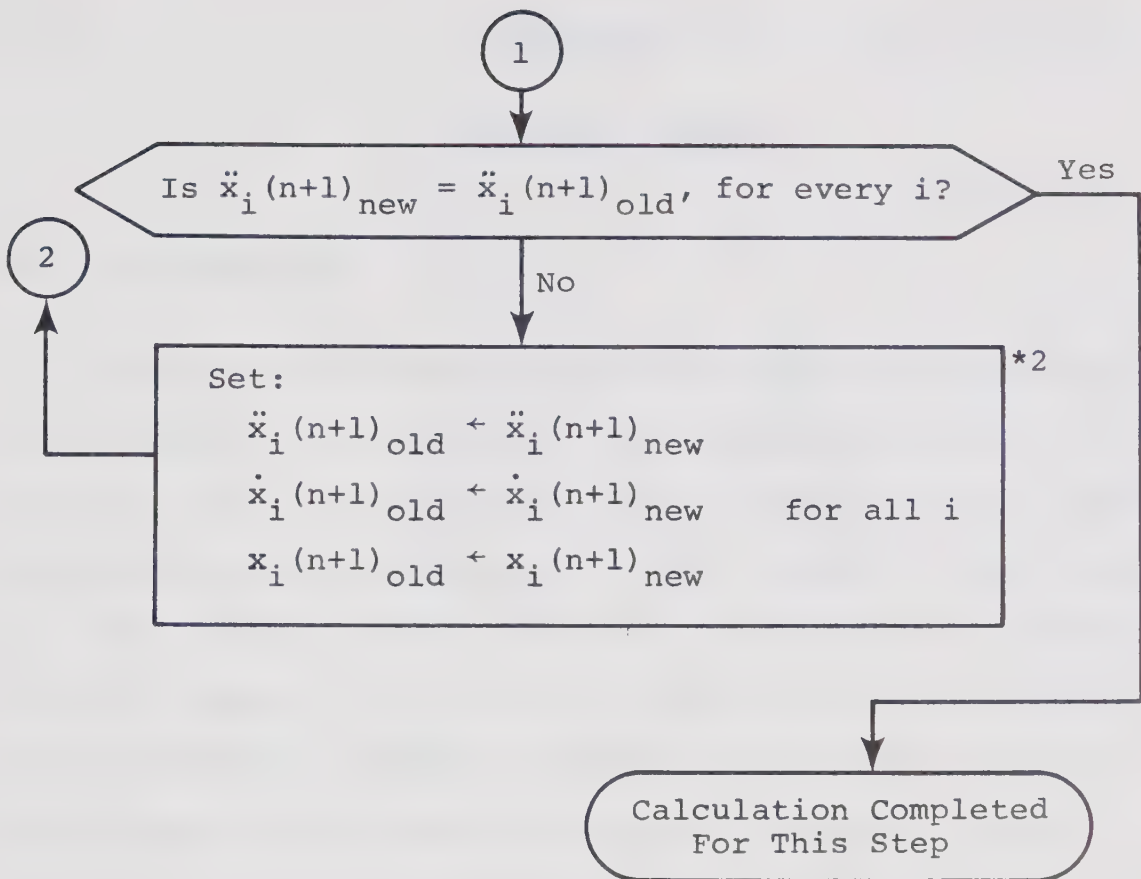


Fig. 3-12 Chart for Numerical Integration
(to be continued)



Notes:

- *1 When calculating $Q_i(\{x\})$ and $S_i(t)$, new values of $\ddot{x}_j(n+1)$, $\dot{x}_j(n+1)$ and $x_j(n+1)$ are used for $j < i$.
- *2 In the computer program, $\dot{x}_i(n+1)_{\text{new}}$ and $x_i(n+1)_{\text{new}}$ are overwritten on $\dot{x}_i(n+1)_{\text{old}}$ and $x_i(n+1)_{\text{old}}$ as soon as they are calculated.

Fig. 3-12 (continued) Chart for Numerical Integration

Chapter 4.

BEHAVIORAL STUDY

4-1 Introduction.

After a brief discussion of the relationship between the response of a structure to an earthquake motion and to a blast load, the behavioral study included in this chapter is focused on the response of a steel frame to blast loads.

The theme of this portion of the study is to investigate the general pattern of response of various structures under different loading situations, so that the structure can be designed to respond to dynamic loads in a satisfactory manner. In keeping with this theme, the following factors were considered:

- 1) The use of an approximate method to estimate the fundamental natural period.
- 2) The effect of the shape of the pressure-time curves (due to blast loads) on the response of a structure.
- 3) The relationship between the applied load and the base shear.
- 4) The effect of variations in column stiffness on the overall response; the effect of beam stiffness on the overall response; and the response characteristics of shear-wall structures.

5) The relationship between the maximum story shear and the required strength.

6) A comparison of overall behavior among various structures in search of an optimum design.

The structures studied in this chapter are limited to 10 stories in height and 4 bays in width. The effect of strain-hardening and the $P-\Delta$ effect are included in the analyses; however these effects are not evaluated specifically. Other secondary effects are ignored in the present behavioral study.

4-2 Relationship Between Blast Loads and Earthquake Motions.

The lateral loads that a structure may experience during its lifetime are, in general, of two different types. One type is the result of pressure applied to the exterior walls of the building. The pressure could be a dynamic pressure (wind pressure) or a combination of dynamic pressure and an overpressure induced by nuclear explosions,^{14,22} gas explosions²² or sonic booms.^{80,81} The magnitudes of the lateral loads caused by these pressures depend upon the area of the exterior walls, the type of cladding, the width and height of the frontal wall and the depth of the building. The duration of the loading for nuclear blasts, gas explosions or sonic booms is relatively short, however, the

intensity of the pressure could be very high in the immediate neighborhood of an explosion site.

The second type of lateral load is caused by the motion of the ground on which the building is situated. Earthquakes or underground explosions are sources of this motion. The lateral loads induced by the ground motion are inertia forces, and thus the magnitudes of these forces depend upon the distributions of mass and stiffness in the building and the intensity of ground acceleration.

In general, lateral loads caused by nuclear blasts and those produced by earthquake motions may be compared as follows:

1. The duration of the portion of high pressure of a blast load is usually shorter than the natural period in the first mode of most common highrise buildings. On the other hand, the ground motion due to an earthquake occurs over a period many times longer than the natural period of the building; the intensity varies during the motion and the most severe vibration would be of short duration. A blast load may be regarded as a single shock or impulse while an earthquake disturbance may be regarded as a series of shocks occurring successively.

2. The distribution of lateral loads over the height of a building will not be drastically different from the two types of loads, that is, the vector {CSM} in Eq. 3-35

and the vector $\{CR\}$ in Eq. 3-36 are rather similar.

3. Because of these factors, structures which are well designed to resist blast loads are generally also suitable to resist earthquake motions, and vice versa, if the input energy in each case is approximately the same.

4. In an earthquake, resonance could become a problem if peaks of loading are repeated with a frequency that is approximately equal to the natural frequency of vibration of the structure. This would not be the case for blast loading since the pressure application is usually completed within a short time and would not be repeated.

5. The acceptability of structural damage could also be different for the two types of loadings since many political, financial and social judgements are differently involved.

In the following sections of this chapter, the responses of different types of steel frames to blast loads are presented. The method of determining the blast load on a structure is explained in Appendix E. A design procedure against blast loads is proposed in Chapter 5.

4-3 Empirical Formula for the Fundamental Natural Period.

The natural period in the fundamental mode is one of the most important structural parameters when a dynamic analysis is to be performed, and yet the existing

formulae^{18,76} to estimate this property are rather crude, resulting in some cases in more than 100% error.

The present study has suggested the necessity of having a more accurate formula to predict the fundamental natural period of a structure. The following empirical formula is proposed:

$$T_1 = T_0 h \sqrt{\frac{\beta}{\alpha}} \cdot \frac{N_s}{10} \quad (4-1)$$

where T_1 : the estimated fundamental natural period of a given frame (in seconds),

T_0 : the value read from the chart given in Fig. 4-1a or 4-1b, depending upon the value of γ ,

γ : K_b/K_c , where K_b is the average stiffness of beams; i.e.,

$$K_b = \left\{ \sum_{\text{for all beams}} \left(\frac{EI}{L} \right)_b \right\} / (N_s \cdot N_b) \quad (4-2)$$

in which $\left(\frac{EI}{L} \right)_b$ is the stiffness of an individual beam, and K_c is the average stiffness of columns; i.e.,

$$K_c = \left\{ \sum_{\text{for all columns}} \left(\frac{EI}{L} \right)_c \right\} / \{N_s (N_b + 1)\} \quad (4-3)$$

in which $\left(\frac{EI}{L} \right)_c$ is the stiffness of an individual column,

h : the ratio of the average story height to a standard height of 12 feet (144"); i.e.,

$$h = \frac{H}{144 N_s} \quad (4-4)$$

in which H is the overall height (in inches) of the structure,

α : the ratio of the average stiffness of columns to a standard value of stiffness of $.500 \times 10^6$ kip·in; i.e.,

$$\alpha = 2K_c / 10^6, \quad (4-5)$$

β : the ratio of the average story mass per column, m , to a standard value of mass ($70/g$ kip·sec²/in) adjusted by the number of bays; i.e.,

$$\beta = \frac{mg}{70} \cdot \frac{(N_b + 0.4)}{N_b} \quad (4-6)$$

in which g is the acceleration of gravity (≈ 386 in/sec²),

N_s : the number of stories, and

N_b : the number of bays.

This formula has been tested on many regular types of frames; the deviation from the rigorously calculated value is usually less than 5% as seen in Fig. 4-2. Example frames plotted here include 5 frames used by Goel,⁵⁵ 4 frames used by Blume,⁸² 1 frame by Lionberger and Weaver,⁴¹ 1 frame by Newmark and Rosenblueth⁷⁶ and 10 frames from the present

study. The frames tested ranged from 2 to 40 stories and 1 to 4 bays.

The application of this formula to a structure with unusual framing schemes is explained in Appendix F, where some example calculations are also displayed.

4-4 Correlation Between Input Blast Load and Structural Response.

The blast load applied to a structure is a function of the magnitude and height of the detonation, the location (distance from ground zero) and the type of the building. In this section, various types of blast loads are applied to an example structure and the responses are analyzed to find a correlation between input loads and responses.

4-4-1 Example Blast Loads on a Structure.

It is assumed that a 10-story building shown in Fig. 4-3 is exposed to a nuclear blast (perpendicular to the frontal exterior wall). The building has a width and depth of 100 feet each and a height of 120 feet. Structurally, it consists of 5 bents in either direction. Exterior walls and windows are made strong enough to resist the pressure caused by a possible blast, but do not contribute to the frame action. It is assumed that the pressure is transmitted to the frames at each floor level and that each one

of five bents (whose dimensions are shown in Fig. 4-4) will carry the same amount of lateral load at every instant during a vibration. The relative ratio of the load applied at each floor level is simply assumed to be proportional to the tributary area as indicated in Fig. 4-4. This ratio corresponds to the vector $\{r\}$ mentioned in Sec. 3-7-1.

If a detonation, whose energy yield is 1 MT, TNT equivalent, takes place at 5,000 feet above the ground level and 42,000 feet away from the building, the blast load applied to a standard floor (where $r_i = 1$ in Fig. 4-4) of each frame is calculated as shown in Fig. 4-5. This curve is a function of time as explained in Sec. 3-7-1. The calculations used to obtain this curve are fully demonstrated in Appendix E. This blast load-time function, $Z(t)$, will be referred to as 'Blast Load Type A-105.2', hereafter.

If the same building is exposed to the same detonation but at 29,000 feet away from G.Z., the same frame will now be subjected to the blast load shown in Fig. 4-6. The calculation required to obtain this curve is very similar to the previous example. This blast load-time function will be referred to as 'Blast Load Type B-212.5', hereafter.

A new case is the previous building with the windows which occupy 40% of the exterior surface) that are now assumed (partially open box-like structure).

Assuming the average distance from the center of a wall section to an open edge (window) of the wall is 7 feet, the blast load applied to each of the frames is now calculated as shown in Fig. 4-7. In this calculation, the detonation is assumed to be the same as before but the building is located at 15,000 feet away from G.Z. (Ground Zero). This load-time function will be referred to as 'Blast Load Type C-358'.

In addition to these blast loads, three more types of blast loads are used for the response calculations for the purpose of comparison. They will be referred to as 'Blast Load Type AA-105.2', 'Blast Load Type BA-212.5', and 'Blast Load Type CA-358'. Their load-time functions coincide with the major portions of type A-105.2, type B-212.5 and type C-358 blast loads respectively, but are truncated at a shorter duration as shown in Figs. 4-8 through 4-10.

•

4-4-2 Properties of Example Frame.

The frame shown in Fig. 4-4 is assumed to have the structural properties as listed in Table 4-1 (FRAME#1AA). The stress-strain relationship assumed for this example is shown in Fig. 4-11. In this example, the values for both the strain-hardening modulus and the ultimate strength are deliberately taken rather lower than usual, since no attempt is made to evaluate the effect of strain-hardening

specifically in this chapter and it is not desirable to over estimate this effect. Based on this curve, the $M_S-\delta\theta_S$ relationships are calculated using the program listed in Appendix B. For the purpose of this calculation, the axial load in each column within a story is assumed to be equal; the point of inflection is assumed at the midpoint of each member. Thus the $M_S-\delta\theta_S$ relationships are the same for either end of a member within a story. The $M_S-\delta\theta_S$ relationships are shown in Figs. 4-12a through 4-12c, for some examples. In these calculations, the effects of shear deformations of members and joint panels, and the effect of the connection flexibility are ignored.

In addition to these static properties, some dynamic properties are evaluated. The damping coefficient, c_i , is calculated assuming $h_i = .005$ (refer to Eq. 3-29) for each story. (Most of the damping coefficients used in the example calculations in this chapter have been obtained assuming $h_i = 0.005$ or 0.01 .) Observations have indicated that the maximum damping force developed by assuming $h_i = 0.005$ is usually less than 5% of the maximum resistance due to frame action and that developed by assuming $h_i = 0.01$ less than 8%. The elastic, undamped natural period of FRAME#1AA was calculated to be 2.24 sec. when the P- Δ effect was ignored and 2.25 sec. when it was included.

4-4.3 Effect of Blast Load-Time Function on Elastic Response.

The blast loads prepared in Sec. 4-4-1 were applied to the example frame shown in Sec. 4-4-2. Responses were calculated using the program listed in Appendix D. The $M_s-\delta\theta_s$ relationships were represented by trilinear relationships.

The responses to blast loads type B-212.5, type BA-212.5 and type C-358 were inelastic. For these types of blast loads, the intensity was then reduced so that the maximum intensities were 130 kips, 130 kips and 200 kips respectively (in other words, the $Z(t)$ values for these types of blast loads were multiplied by 130/212.5, 130/212.5 and 200/358, respectively) and were called 'Blast Load Type B-130', 'Blast Load Type BA-130' and 'Blast Load Type C-200' respectively. The responses to the blast loads of reduced intensities were elastic.

The results of the response calculations are shown in Fig. 4-13. The maximum base shear developed due to frame action, Q_b , is plotted against the total impulse, I , which is defined by:

$$I = \int_0^{\infty} Z(t) dt \cdot \sum_{i=1}^{N_s} r_i \quad (4-7)$$

The ratios of the maximum base shear to the total impulse of the applied blast load for type AA-105.2, BA-130 or

CA-358 blast loads are similar (this ratio for blast load type AA is shown in the figure).

The observation that these ratios for type A-105.2, B-130 and C-200 blast loads are smaller than those for other types indicates that the elastic response is significantly influenced by the initial, major portion of the blast load-time functions. For this reason, the modified total impulse, I^* , for an input blast load is defined as:

$$I^* = \int_0^{\infty} f(t) Z(t) dt \sum_{i=1}^{N_s} r_i, \quad (4-8)$$

where

$$f(t) = \begin{cases} \frac{1}{2}(1 + \cos \frac{2\pi}{T_1} t) & \text{for } \frac{T_1}{2} \geq t \geq 0 \\ 0 & \text{for } t > \frac{T_1}{2} \end{cases} \quad (4-9)$$

and T_1 is the fundamental natural period of the frame to which the blast load is being applied. The modified impulse ignores the effect of the portion of load that is applied after one half of the fundamental period of the frame, and more emphasis is placed on initial portion of the loading. The correlation between the maximum base shear, Q_b , and the modified total impulse, I^* , is found to be much stronger than before as shown in Fig.4-14. The average ratio of maximum base shear to modified total impulse for FRAME #1AA is calculated to be 1.97, or

$$Q_b = 1.97 I^*, \quad (4-10)$$

which is also shown in the figure. In fact, the strong correlation has also been found in other frames throughout the behavioral study. The same was true of the relationship between the deflection (either maximum roof deflection or maximum relative displacement) and the modified total impulse. As one example, the maximum roof deflection is plotted against the modified total impulse in Fig. 4-15.

Thus the elastic response does not depend significantly on the shape of a blast load-time function, but depends strongly on the value of the modified total impulse; since the major portion of a blast load is within say, one quarter of the fundamental natural period of a frame. This is the case under most of the situations considered in this study. For this reason, the subsequent behavioral study has been performed against a limited number of blast load-time functions, although the intensity has been amplified or reduced as in the case of type B-212.5 and type B-130. (Hereafter, the alphabetic letter indicates the type of load-time function; the digits indicate the maximum intensity.)

4-4-4 Effect of Blast Load-Time Function on Inelastic Response.

The effect that a different type of blast load might have on the inelastic response is examined in this section. The responses of FRAME#1AA to blast load type A and type AA,

with the intensity varied in several steps, so that varying degrees of inelastic response are observed, are shown (up to collapse) in Fig. 4-16. The collapse of a structure is defined as the point where any one of the $M_s-\delta\theta_s$ relationships of the equivalent rotational springs comes to the failure point; which is defined in Sec. 2-5-4.

The plot shows the relationship between maximum base shear and modified total impulse. The ratio of the maximum base shear to the modified total impulse is similar to that in the elastic range, where the inelastic action is minor or rather moderate. (Say, up to point X; i.e., the response to the blast load type A-212.5 ($I^* = 325 \text{ kip}\cdot\text{sec}$); or point Y; i.e., the response to blast load type AA-300 ($I^* = 371 \text{ kip}\cdot\text{sec}$), in Fig. 4-16. The locations of member ends where the elastic limit was exceeded during the responses corresponding to points X and Y are shown in Figs. 4-17 and 4-18, respectively.)

The maximum base shear is a little greater when the structure is subjected to blast load type A than to type AA with the same amount of modified total impulse, up to about these points; hereafter, however, the situation reverses. The modified total impulse corresponding to collapse of the structure is almost the same regardless of the type of blast load. The base shears corresponding to collapse are also approximately the same in both cases.

The response of a structure thus may be described in terms of the modified total impulse, in the inelastic range. Thus the shape of a blast load-time function is not an important factor.

4-5 Relationship Between Modified Total Impulse and Maximum Base Shear.

In the preceding section, it was shown that the ratio of the maximum base shear due to frame action, Q_b , to the modified total impulse of the blast load, I^* , is constant for a frame up to the point of moderate inelastic response (say, up to point X or point Y in Fig. 4-16), regardless of the type of blast load. In this section, a closer investigation of this ratio is performed.

The responses of FRAME #1AA with damping coefficient, $h_i = .001$ or $.01$ for every story (in the previous example calculations, h_i was assumed to be $.005$) were calculated for several blast loads. The same degree of correlation was found between Q_b and I^* ; the average ratios of Q_b/I^* were 2.25 and 1.84 for $h_i = .001$ and $.01$, respectively, in comparison with 1.97 for $h_i = .005$. Thus it is shown that the degree of damping causes slight change in the ratio of Q_b to I^* .

The average ratios of Q_b to I^* have been obtained for many example frames, whose basic properties are listed in Tables 4-2 through 4-8. (Other properties are the same

unless otherwise noted or may be derived in the same manner as for FRAME#1AA. A frame is classified by a number followed by two letters. Those frames that have the same numbering have the same dimensions. The first letter indicates the type of column design and the second the type of beam design.) The ratios of Q_b to I^* for these frames are listed in Table 4-9 (natural periods listed here are determined by rigorous calculations); and are also plotted against the fundamental natural period of the frame in Fig. 4-19.

The plot in Fig. 4-19 suggests that the ratio, Q_b/I^* is inversely proportional to the fundamental natural period, T_1 , of the frame. Assuming that Q_b , I^* and T_1 have a relationship of the form

$$Q_b = \frac{\rho I^*}{T_1} , \quad (4-11)$$

the quantity, ρ , is calculated for each frame and listed in the last column of Table 4-9. The coefficient, ρ , has a value between 4 and 5, where the variation is caused by the differences in the damping characteristics and in the type of structure.

Eq. 4-11 may be used to predict the maximum base shear (up to the range of moderate inelastic response) for a frame whose natural period is known (by either a rigorous calculation or by the approximate method explained in

Sec. 4-3) against a given blast load. The value of I^* is calculated by Eq. 4-8, if the blast load-time function and the natural period of a frame are known. However, it would be convenient to prepare a chart which gives the value of modified impulse for a given natural period. Such charts are shown for type A and type AA blast loads in Figs. 4-20 and 4-21. The value in ordinate axis indicates the modified impulse, i^* , per story where $r_i = 1$, for a blast load whose maximum intensity is equal to unity. The total modified impulse, I^* , is then given by:

$$I^* = \left(\sum_{i=1}^{N_s} r_i \right) i^* Z_{\max} \quad (4-12)$$

where Z_{\max} is the maximum intensity of the blast load being considered. The value of ρ ranges from 4.0 to 5.0 and may be selected in accordance with the expected damping situation and the type of structure.

4-6 Difference in Response for Various Frame Designs.

In this section, the discussion focuses on the differences between the responses of frames having varying column stiffnesses and those having column stiffnesses which are relatively constant over the height of the building; and between the responses of frames with strong and stiff beams and those with weak and flexible beams. A brief discussion of shearwall structures is also included.

4-6-1 The Effects of Variation in Column Stiffness.

The effect of variation in column stiffness on the fundamental natural period is minor for the frames considered, as shown by the comparisons between FRAME#2AA and FRAME#2BA or between FRAME#2AB and FRAME#2BB. (The ratio of column stiffness at the bottom story to that at the top story is 8.46 for FRAME#2AA and FRAME#2AB, while the corresponding ratio is 1.55 for FRAME#2BA and FRAME#2BB.)

The responses of FRAME#2AA and FRAME#2BA subjected to various intensities of blast load type BA are compared in Fig. 4-22. As seen here, the maximum base shears developed are almost the same for the two frames in the elastic or moderately inelastic range. Initial yielding occurred at a maximum intensity of approximately 20 kips for FRAME#2AA and 40 kips for FRAME#2BA.

The maximum base shear in FRAME#2AA increased in an almost linear manner up to the collapse point, as the applied blast load intensity was increased. On the other hand, the ratio of maximum base shear to the applied blast load intensity decreased substantially in the case of FRAME#2BA as yielding progressed through the frame.

The blast load intensity corresponding to the collapse of FRAME#2BA is approximately 1.5 times that for FRAME#2AA. Locations where inelastic action occurred during the

response to type BA-45 blast load are shown in Fig. 4-23. The inelastic action is more concentrated for FRAME#2AA, thus leading to collapse at a relatively low intensity of blast load. Thus FRAME#2BA is considered to be superior to FRAME#2AA.

Similar studies have shown that the desirable range of the ratio of column stiffness at the bottom story to that at the top story is approximately 2 to 5 for 10-story buildings and approximately 1 to 3 for 5-story buildings. For instance, this ratio for FRAME#1AA is 3.7. In this case, the ratio of the maximum resisting base shear to the blast load intensity gradually decreased as shown in Fig. 4-16, indicating the gradual spread of inelastic action in the frame.

4-6-2 The Effect of Beam Stiffness.

FRAME#1BC contains beams having stiffnesses 3 to 4 times those for the beams of FRAME#1BA. The other members are the same for the two frames. The response of these frames are compared in Fig. 4-24.

As expected from the preceding studies, a much higher resisting base shear was recorded in FRAME#1BC than in FRAME#1BA, when subjected to the same intensity of blast load; since FRAME#1BC is stiffer than FRAME#1BA. In fact, the value of ρ , as seen in Table 4-9, is also higher for FRAME#1BC than the other, which may indicate the inefficiency

(in this sense) of frames with higher beam stiffness.

The maximum resisting base shear vs. input blast load intensity relationship for FRAME#1BC is almost linear up to collapse, while a gradual reduction is observed for FRAME#1BA at higher load intensities. It is normally true that a higher strength is attained by the use of stiffer members. However, by doing so, the force attracted to the frame, for the same blast load, increases as discussed in Sec. 4-5. It is often observed that the increase in force developed in the frame is greater than the increase in strength; thus a stiffer frame comes to collapse earlier than the more flexible frame. This fact is clearly seen in Fig. 4-24.

Thus it is not desirable to make the beam stiffness high except when the deflections must be controlled. At the other extreme, if the beams are too flexible, the moments to be resisted by the column become excessive, and the overall resisting capacity is again lost. The responses of many frames with various beam stiffnesses were compared. The observation indicated that the desirable stiffness for beam members is slightly below the average column stiffness (say, 50% to 100% of the average column stiffness), with little variation along the height.

4-6-3 The Effect of Shearwalls on the Frame Response.

The equation proposed to predict the fundamental natural period (Eq. 4-1) was also found to be applicable to frames with shearwalls, although some parameters will need to be modified as explained in Appendix F.

Assuming the relationship between the maximum resisting base shear and input blast load is also expressed by Eq. 4-11, the quantity, ρ , has been evaluated for about 10 frames with shearwalls. As seen in two typical examples (FRAME#4AB and FRAME#4BB, whose properties are shown in Table 4-6), ρ for such frames generally lies below the median (which is about 4.4); as indicated in Table 4-9.

Although the deflections of a structure can sometimes be controlled by using shearwalls, it should be noted again that the intensity of a blast load that the frame can withstand does not increase proportionally as the strength provided in the frame increases; and that severe inelastic action could take place at beam ends which are attached to shearwalls. If shearwalls are located in an asymmetric manner in a building, the torsional effect may become dominant.⁸³ When a frame with shearwalls is designed, these factors must be considered from both technical and economical points of view.

4-7 Required Strength of Frame.

Since the normal design for static loads is based on strength, it would be very convenient if the required strength of a frame against an assumed blast load could be determined. In this section, the relationship between the maximum resisting story shear at every story and the column strength provided is examined for a regular type of frame.

The maximum story shears developed during the response of FRAME#1BA to type AA-250 blast load are shown in Fig. 4-25. In this case, the frame exhibited moderate inelastic action (point X in Fig. 4-24). The shapes of the corresponding diagrams for other 10-story frames are similar over a wide range of frame configurations. That is, the average diagram of maximum story shears would indicate the ratio of a maximum story shear to the maximum base shear as about .9 at the seventh floor, .6 at the third floor, and between .15 and .3 at the first (top) floor, as shown by curve A in Fig. 4-26. The corresponding diagram for 5-story frames is also shown by curve B in the same figure.

It has been shown in Sec. 4-5 that the maximum base shear can be predicted for an assumed blast load. Therefore it is now possible to predict the maximum shear for every story for the assumed load.

The correlation between the maximum story shears and

the required column strengths is best explained in the following example calculation. FRAME#3AB (10-story, 3-bay frame) was designed against blast load type AA-105.2, allowing moderate inelastic action (the range indicated by point X or Y in Fig. 4-16). The example calculation is an attempt to determine if the assumed frame is adequate without performing a dynamic analysis.

The fundamental natural period of this frame was calculated to be 1.24 sec. Assuming the vector, $\{r\}$, is the same as that shown in Fig. 4-4 (i.e., $\sum r_i = 9.5$), the modified total impulse, I^* , is calculated, using the chart given in Fig. 4-21, as:

$$\begin{aligned} I^* &= Z_{\max} i^* \sum r_i \\ &= 105.2 \times .125 \times 9.5 \\ &= 125. \quad (\text{kip}\cdot\text{sec}) \end{aligned}$$

Then, the expected base shear, Q_b , is given, assuming $\rho = 4.5$, as:

$$\begin{aligned} Q_b &= \frac{\rho I^*}{T_1} \\ &= \frac{4.5 \times 125}{1.24} \\ &= 450. \quad (\text{kips}) \end{aligned}$$

The maximum story shears divided by the number of columns per story (4 in this case) are now assumed as shown by curve A in Fig. 4-27.

If the shears shown here develop simultaneously, the

moments in columns would be those shown by diagram (1) if the stiffness of beams are zero; or by diagram (2) if the beams are infinitely rigid and strong. In the actual frame, the moments developed in columns lie between these two diagrams, depending upon the actual moment capacities of the beams.

A part of the moment diagram for a frame in which the beams here reached their plastic moment capacities is shown in Fig. 4-28. In this figure, the following symbols are used:

- M_i^{uc} : Moment at the bottom of upper column #i,
- M_i^{lc} : Moment at the top of lower column #i,
- M_i^b : Plastic moment capacity of beam #i,
- M_a^{uc} : Average moment at the bottom of upper columns,
and
- M_a^{lc} : Average moment at the top of lower columns.

The latter two quantities are given by:

$$M_a^{uc} = \frac{1}{N_b + 1} \sum_{i=1}^{N_b+1} M_i^{uc} \quad (4-13)$$

$$M_a^{lc} = \frac{1}{N_b + 1} \sum_{i=1}^{N_b+1} M_i^{lc} \quad (4-14)$$

Adding the equilibrium equations at each joint, the following equation is obtained:

$$\sum_{i=1}^{N_b+1} M_i^{uc} + \sum_{i=1}^{N_b+1} M_i^{lc} + 2 \sum_{i=1}^{N_b} M_i^b = 0$$

or,

$$M_a^{uc} + M_a^{lc} = - \frac{2N_b}{N_b+1} M_p \quad (4-15)$$

where M_p is the average plastic moment capacity of the beams at this floor. This equation indicates that the difference between the moment at the bottom of the column immediately above a given beam and the moment at the top of the column immediately below the beam can not be greater than the amount shown in the right hand side of Eq. 4-15, on the average. In the present case, $N_b = 3$, therefore the difference in moments between two adjacent column ends is not more than $1.5 M_p$, on the average.

Based on this consideration, the minimum required moment capacities for the columns are obtained as shown by diagram (3) in Fig. 4-27. Starting from the top story; if the difference between the moments at two adjacent column ends in diagram (2) is less than $1.5 M_p$, diagram (3) is assumed to coincide with diagram (2); however, if the difference is greater than $1.5 M_p$ in diagram (2), then diagram (3) at a particular story is drawn by sliding diagram (2) in parallel toward diagram (1), so that the difference between the moment at the bottom of the upper column and the moment at the top of the column of this story becomes

$1.5 M_p$; as seen in the 5th and the lower stories.

The moment capacities provided by the columns are shown by diagram (4). Since the required strengths are within the provided capacities, it may be concluded that the frame would be adequate for this blast load. From the way diagram (3) was constructed, it may also be possible to predict that the inelastic action in the beams would take place at the 5th and the lower floors.

In the derivation of Eq. 4-15, the beams were assumed to have reached their full plastic moment capacities, which might seem unconservative. However, as seen in Fig. 4-17 or 4-18, many beam ends do reach their plastic moment capacities in the range of the expected response. On the other hand, the maximum story shears do not occur simultaneously in each story and therefore the approximate moment diagram is somewhat conservative.

A dynamic analysis was performed to see how well a frame designed using the above procedure would resist the blast loads. The response to the given blast load was located at point X in the maximum base shear vs. the intensity of blast load relationship in Fig. 4-29. The maximum story shears recorded during the dynamic analysis are shown by curve B; these may be compared with the assumed values shown by curve A in Fig. 4-27. As expected, inelastic action was observed in the 5th and lower floor beams.

One more rather crude estimate of the required average strength of a column at the bottom story, M_b , is given by:

$$M_b = Q_b L / (N_b + 1) \quad (4-16)$$

where L is equal to 70% to 100% of the bottom story height. This equation is derived assuming that the moment diagram shown by diagram (3) in Fig. 4-27 is typical for a regular frame. This equation may be useful for the first estimate of the required member sizes.

4-8 Comparison of Various Designs.

When a structure is designed against any type of loading, it must develop sufficient strength to withstand the applied loads and in addition the deflections must be within the specified limits. Among many possible designs which satisfy these two criteria, some effort is usually made to find the most economical frame.

If a frame is designed for a static loading condition, adding more strength (which is usually accompanied by additional stiffness) can be expected to reduce the deflections.

On the other hand, when a frame is designed to resist a dynamic loading, an increase in the stiffness (and strength) of the members to reduce the deflections during the motion does not automatically mean that the intensity of dynamic loading which the frame can withstand is increased. In fact, as seen in the responses of FRAME#1BA

and FRAME#1BC (Fig. 4-24), by making a frame stiffer, the intensity of a blast load that the frame can withstand was decreased, although there was a slight decrease in the observed displacements. Thus the two design criteria often conflict with one another.

The job of finding the most economical frame involves many factors when a frame is designed to withstand a dynamic loading. The next example shows one comparison of two frames both designed against similar blast loads. The frames compared are FRAME#5AA and FRAME#5BB. FRAME#5AA possesses about 35% more static strength than FRAME#5BB, at the bottom story. The average column stiffness of FRAME#5AA is 1.15 times that of FRAME#5BB, and the average beam stiffness of the former frame is 2.90 times that of the latter. The total weight of material used in the structural members of FRAME#5AA is 1.28 times that used in FRAME#5BB.

The maximum base shears are shown as functions of the intensity of applied loads (Blast Load Type AA) for both FRAME#5AA and FRAME#5BB in Fig. 4-30. The relationship between the intensity of applied blast load and the maximum relative displacement of any two adjacent floors are shown for the same frames in Fig. 4-31.

When these two frames are compared, the intensity of blast load that each frame can withstand is approximately

the same (frames having stiffnesses between those of the two example frames had a reduced capacity to withstand blast loads); but the maximum relative displacement in FRAME#5BB is approximately twice that developed in FRAME#5AA subjected to the same intensity of blast load. Thus it may be said that FRAME#5AA is superior to FRAME#5BB. However, before making the final selection, the economical factors must be taken into consideration.

Suppose the cost of the structural components of FRAME#5AA is \$W and that the corresponding cost for FRAME#5BB is \$X. For similar type of framings, the cost may be assumed to be proportional to the weight of material used for columns and beams, thus, $W = 1.28X$. Suppose also the total of the cost of cladding (including windows), partitioning and other non-structural elements; and the cost of constructing and installing them is \$Y for FRAME#5AA. If this cost is 'a' times the cost of structural components of the same frame, $Y = aW$. The corresponding cost for FRAME#5BB may be estimated equal to bY, where $b > 1$ if the deflection of FRAME#5BB is greater than the allowable limit set on the basis of the design of FRAME#5AA (because a new detail and careful installation are required to ensure enough deflection capacities for the windows, precast exterior walls and other elements in order to avoid dislodgement); otherwise $b = 1$.

The total cost for FRAME#5AA, C_{5AA} , is then calculated as:

$$\begin{aligned} C_{5AA} &= W + Y \\ &= 1.28(1 + a)X \end{aligned} \quad (4-17)$$

The corresponding cost for FRAME#5BB, C_{5BB} , is similarly calculated as:

$$\begin{aligned} C_{5BB} &= X + bY \\ &= (1 + 1.28ab)X \end{aligned} \quad (4.18)$$

The economy of two frames may be decided by comparing Eqs. 4-17 and 4-18. If, for instance, $a = .70$ and $b = 1.2$ are assumed, C_{5AA} and C_{5BB} are calculated respectively as:

$$\begin{aligned} C_{5AA} &= 1.28(1 + .70)X \\ &= 2.18X, \end{aligned}$$

and

$$\begin{aligned} C_{5BB} &= (1 + 1.28 \cdot 0.70 \cdot 1.2)X \\ &= 2.07X. \end{aligned}$$

Thus it is seen FRAME#5BB is more economical under these conditions.

By designing claddings and non-structural elements so that they can follow a larger deflection, a more flexible frame may safely be designed with a reduction in cost. Further, if, as in the above discussion, the quantities 'a' and 'b' are obtained as function of the type of frame, the frame stiffness (or the fundamental natural period), the

required maximum relative displacement and so on, it would be possible to obtain an optimum design for a given blast load by repeating comparisons similar to that shown here.

4-9 Summary.

The behavioral study included in this chapter was performed using the procedure developed in Chapter 3. The study focussed on the dynamic behavior of steel frame subjected to various types of blast loads. The results of the study are summarized as follows.

1) An empirical formula to predict the fundamental natural period was proposed as shown in Eq. 4-1; i.e.,

$$T_1 = T_0 h \sqrt{\frac{\beta}{\alpha}} \frac{N_s}{10}$$

in which the symbols are explained in Sec. 4-3. This formula has been tested on many frames ranging from 2 to 40 stories and 1 to 4 bays, and resulted in close agreement with the period computed from a rigorous analysis.

2) The shape of blast load-time function, $Z(t)$, does not significantly affect the response either in the elastic range or in the inelastic range. The response is mainly influenced by the modified total impulse of the blast load, I^* , which is defined in Eq. 4-8; i.e.,

$$I^* = \int_0^\infty f(t) Z(t) dt \sum_{i=1}^{N_s} r_i$$

where

$$f(t) = \begin{cases} \frac{1}{2}(1 + \cos \frac{2\pi}{T_1} t) & \text{for } \frac{T_1}{2} \geq t \geq 0 \\ 0 & \text{for } t > \frac{T_1}{2} \end{cases}$$

Therefore a subsequent study was performed using a limited number of blast load-time functions. The frames used in the study had 5 or 10 stories and ranged from 1 to 4 bays. Some frames had a shearwall.

3) The maximum base shear developed, Q_b , can be estimated by Eq. 4-11; i.e.,

$$Q_b = \frac{\rho I^*}{T_1}$$

where ρ has a value between 4 and 5 with its median approximately 4.4. This formula is valid both in the elastic range and for moderate inelastic action.

4) The variation in column stiffness along the height should be as small as practicable. The recommended value for the ratio of the column stiffness at the bottom story to that at the top story ranges from 2 to 5 for ten-story frames, and 1 to 3 for five-story frames.

The average stiffness of beam members should be less (say, 50% to 100%) than the average stiffness of column members.

Although the deflection of a structure can sometimes be controlled by stiffening the members or by introducing

shearwalls, it should be noted that the intensity of a blast load that the frame can withstand does not increase proportionally (sometimes, even decreases) as the strength provided in the frame increases.

5) The maximum resisting shear for every story is distributed approximately as shown by curve A for ten-story frames, and by curve B for five-story frames; both in Fig. 4-26.

Using this fact together with the relationship in moments between two adjacent column ends (refer to Eq. 4-15), it was shown, in Sec. 4-7, that a frame can be checked to ensure adequate strength against a given blast load.

A crude estimate of required strength for the bottom story columns, M_b , is given by Eq. 4-16; i.e.,

$$M_b = \frac{Q_b}{N_b + 1} L,$$

on the average, where L may be taken equal to 70% to 100% of the bottom story height.

6) A structure must develop sufficient strength to withstand the applied loads and in addition the deflection must be within the specified limits. When a frame is subjected to dynamic loads, the two design criteria often conflict with one another. One comparison between two frames designed against the same type of blast loads is shown in Sec. 4-8.

Table 4-1 Structural Properties of FRAME #1AA

Story or Floor	Weight per Floor (kips)	Axial Load per Column (kips)	Column			Beam
			Section	I (in ⁴)	M _{pc} (kip-in)	
1	250	50	W14x105	1200	6545	W 18 x 113 I = 2000 in ⁴ M _p =8728 kip-in
2	500	150	W14x105	1200	6355	
3	500	250	W14x105	1200	5975	
4	500	350	W14x179	2200	10960	
5	500	450	W14x179	2200	10490	
6	500	550	W14x179	2200	9900	
7	500	650	W14x254	3300	15370	
8	500	750	W14x254	3300	14770	
9	500	850	W14x326	4400	20110	
10	500	950	W14x326	4400	19500	

(1) Section was determined by specifying nominal depth and moment of inertia in accordance with Eq. 2-3.

(2) M_p and M_{pc} were determined in accordance with Eq. 2-5 and Eq. 2-8 or 2-9.

Table 4-2 Properties of FRAME #1BA, FRAME #1BB, FRAME #1BC & FRAME #1BD
10-Stories, 4-Bays. Dimensions as shown in Fig. 4-4.

Story or Floor	Weight*1 per Floor (kip)	Column*1		Beams*3		
		Axial Load*2 (kip)	Section*2	Sections*4 for FRAME #1BB	Sections*4 for FRAME #1BC	Sections*4 for FRAME #1BD
1	125	25	W14x105 I=1200 in ⁴	W24x104 I=3000 in ⁴	W33x118 I=6000 in ⁴	I=3.0x10 ⁵ (rigid beams)
2	250	75				
3	250	125				
4	250	175				
5	250	225	W14x179 I=2200 in ⁴			
6	250	275		W24x134 I=4000 in ⁴	W33x152 I=8000 in ⁴	
7	250	325	W14x254 I=3300 in ⁴			
8	250	375				
9	250	425	W14x326 I=4400 in ⁴			
10	250	475				

*1 Same for all frames

*2 Same for all columns within a story

*3 Beams for FRAME #1BA are the same as in FRAME #1AA (see Table 4-1)

*4 Same for all beams within a floor

Footnotes (1) and (2) in Table 4-1 are also applicable.

Table 4-3 Properties of FRAME #2AA*1 and FRAME #2AB

10-Stories, 2-Bays. Story height: 12'; Bay length: 24' (each)

Story or Floor	Weight*2 per Floor (kip)	Columns*2		Beams	
		Axial Load (kip)		Sections for FRAME #2AA	Sections for FRAME #2AB
		Exterior Columns	Interior Columns		
1	60	18.0	24.0	W21x55 I=1141 in ⁴ W16x41 I=516 in ⁴	
2	105	49.5	66.0		
3	105	81.0	108.0		
4	105	112.5	150.0		
5	105	144.0	192.0		
6	105	175.5	234.0		
7	105	207.0	276.0		
8	105	238.5	318.0		
9	105	270.0	360.0		
10	105	301.5	402.0		

*1 Very similar to the example frame used by Lionberger and Weaver (41).

*2 Same for both frames.

*3 Same for all columns within a story.

Footnotes (1) and (2) in Table 4-1 are also applicable.

Table 4-4 Properties of FRAME #2BA and FRAME #2BB

10-Stories, 2-Bays. Story height: 12', Bay length: 24' (each)							
Story or Floor	Weight*1 per Floor (kip)	Columns*1			Section*2	Moment of Inertia (in ⁴)	Beams
		Axial Load (kip)		Interior Columns			
		Exterior Columns					
1	60	18.0	24.0		W12x52	408	For FRAME #2BA: same as in FRAME #2AA (see Table 4-3)
2	105	49.5	66.0		W12x55	433	
3	105	81.0	108.0		W12x57	458	
4	105	112.5	150.0		W12x60	483	
5	105	144.0	192.0		W12x63	508	For FRAME #2BB: same as in FRAME #2AB (see Table 4-3)
6	105	175.5	234.0		W12x66	533	
7	105	207.0	276.0		W12x68	558	
8	105	238.0	318.0		W12x71	583	
9	105	270.0	360.0		W12x73	608	
10	105	301.5	402.0		W12x76	633	

*1 Same for both frames

*2 Same for all columns within a story

Footnotes (1) and (2) in Table 4-1 are also applicable

Table 4-5 Properties of FRAME #3AA and FRAME #3AB

10-Stories, 3-Bays. Story height: 12', Bay length: 25' (exterior), 10' (interior)

Story or Floor	Weight*1 per Floor (kip)	Column*1		Beams	
		Axial Load*2 (kip)	Section*2	Sections*3 for FRAME #3AA	Sections*3 for FRAME #3AB
1	120	30	W14x105 I=1200 in ⁴	W18x88 I=1500 in ⁴	Same as in FRAME #3AA
2	180	75			
3	180	120			
4	180	165	W14x179 I=2200 in ⁴	W21x89 I=2000 in ⁴	
5	180	210			
6	180	255			
7	180	300	W14x254 I=3300 in ⁴	W24x119 I=3500 in ⁴	W24x89 I=2500 in ⁴
8	180	345			
9	180	390	W14x326 I=4400 in ⁴	W27x136 I=5000 in ⁴	W24x104 I=3000 in ⁴
10	180	435			

*1 Same for both frames.

*2 Same for all columns within a story.

*3 Same for all beams within a floor.

Footnotes (1) and (2) in Table 4-1 are also applicable.

Table 4-6 Properties of FRAME #4AB, FRAME #4BB

- 1) FRAME #4AB: 10-Stories, 2-Bays.

Central bay of FRAME #3AB is replaced by a shearwall whose width is 10'.

$(EI)_{\text{shearwall/E}_{\text{steel}}}$ are given as:

Stories	$(EI)_{\text{shearwall/E}_{\text{steel}}}$
1, 2, 3	192000 in ⁴
4, 5, 6	352000
7, 8	528000
9, 10	704000

Exterior columns and beams are the same as the exterior columns and exterior beams in FRAME #3AB, respectively.

- 2) FRAME #4BB: 10-Stories, 2-Bays.

Stiffness of shearwall in FRAME #4AB is reduced to 1/100, while the wall width remain the same. Other properties are the same.

Table 4-7 Properties of FRAME #5AA

5-Stories, 3-Bays. Story height: 144", Bay length: 250" (for all bays)								
Story or Floor	Weight per Floor (kip)	Axial Load (kip)	Columns		Section		Beams	
			Exterior Columns	Interior Columns	Exterior Beams	Interior Beams	Section	
1	200	50	W14x164 I=2000 in ⁴	W14x427 I=6000 in ⁴	W27x112 I=4000 in ⁴	W36x189 I=12000in ⁴		
2	300	125						
3	300	200						
4	300	275	W14x234 I=3000 in ⁴	W14x549 I=8000 in ⁴	W27x160 I=6000 in ⁴	W36x243 I=16000 in ⁴		
5	300	350						

Footnotes (1) and (2) in Table 4-1 are also applicable.

Table 4-8 Properties of FRAME #5BB and FRAME #6AA

1) FRAME #5BB. 5-Stories, 3-Bays. Dimension same as FRAME #5AA						
Story or Floor	Weight per Floor	Axial Load	Columns		Beams	
			Section		Section	
			Exterior Columns	Interior Columns	Exterior Beams	Interior Beams
1	Same as in FRAME #5AA (See Table 4-7)		W14x164	W14x427	W21x89	W27x112
.			I=2000 in ⁴	I=6000 in ⁴	I=2000 in ⁴	I=4000 in ⁴
.						
.						
5						

Footnotes (1) and (2) in Table 4-1 are also applicable.

2) FRAME #6AA.

5-Stories, 3-Bays. This is identical to the top five stories of FRAME #1AA.
For properties, see Table 4-1.

Table 4-9 Response of various frames

FRAME #	Size (Story x bay)	T_1 (Sec.)	h_i^{*1}	Q_b/I^*	ρ
1AA	10 x 4	2.248	.001	2.25	5.05
1AA	"	"	.005	1.97	4.43
1AA	"	"	.01	1.84	4.14
1BA	"	1.588	.005	2.64	4.19
1BA	"	"	.01	2.61	4.14
1BB	"	1.273	.01	3.50	4.45
1BC	"	1.065	.005	4.80	5.10
1BC	"	"	.01	4.30	4.58
1BD	"	.784	.01	6.59	5.15
2AA	10 x 2	2.388	.01	1.93	4.60
2AB	"	2.986	.01	1.50	4.49
2BA	"	2.304	.01	1.87	4.31
2BB	"	2.931	.01	1.44	4.21
3AA	10 x 3	1.241	.005	4.10	5.09
3AB	"	1.326	.005	3.66	4.85
4AB ^{*2}	10 x 2	.994	.01	4.06	4.04
4BB ^{*2}	"	1.294	.01	3.14	4.07
5AA	5 x 3	.539	.05	8.35	4.50
5BB	"	.779	.05	5.60	4.36
6AA	5 x 4	1.165	.005	4.00	4.66

*1 Same value is assumed throughout the stories.

*2 Contains a shearwall.

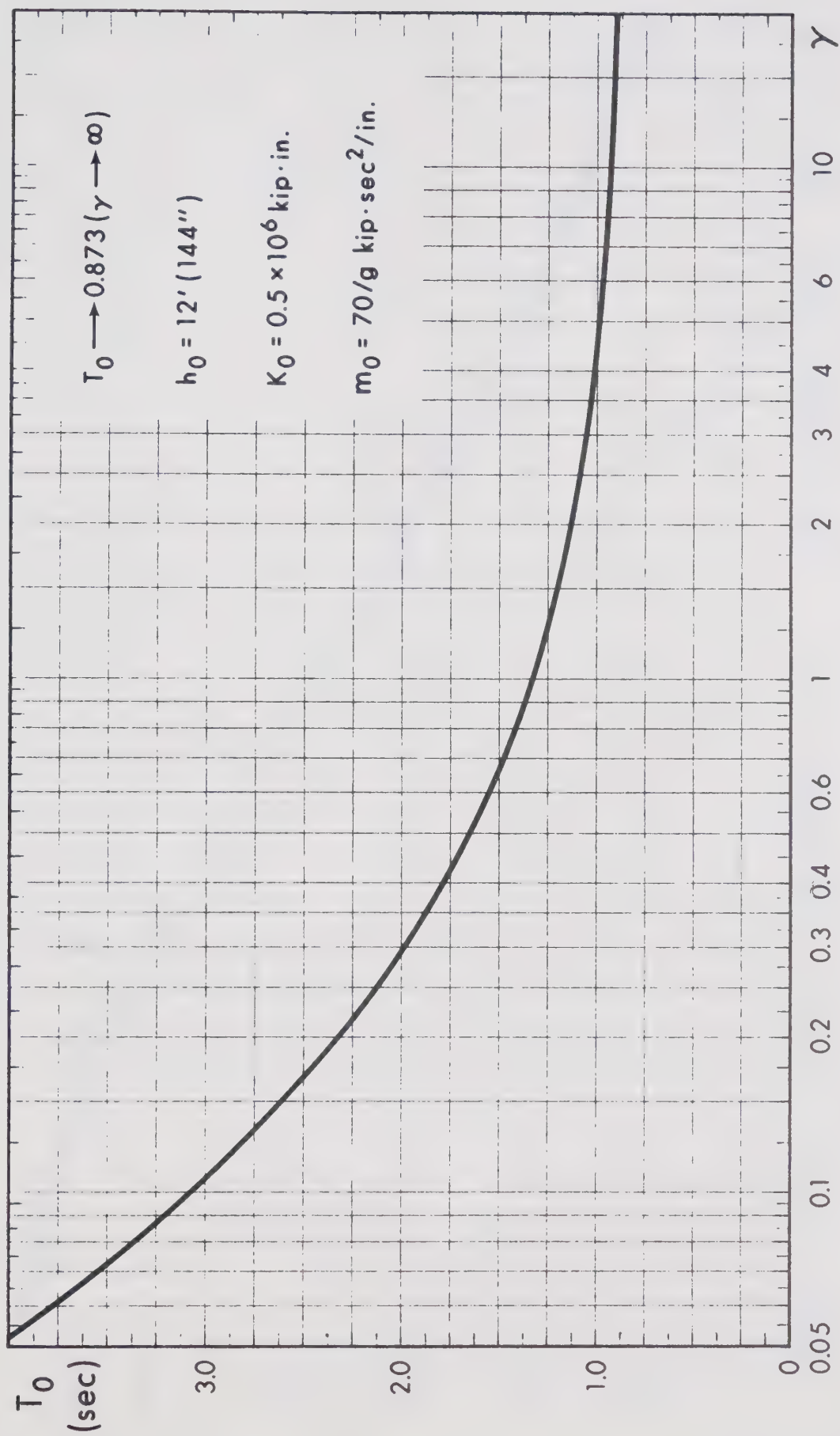


Fig. 4-1a Value of T_0 for the Calculation of the Natural Period (1)

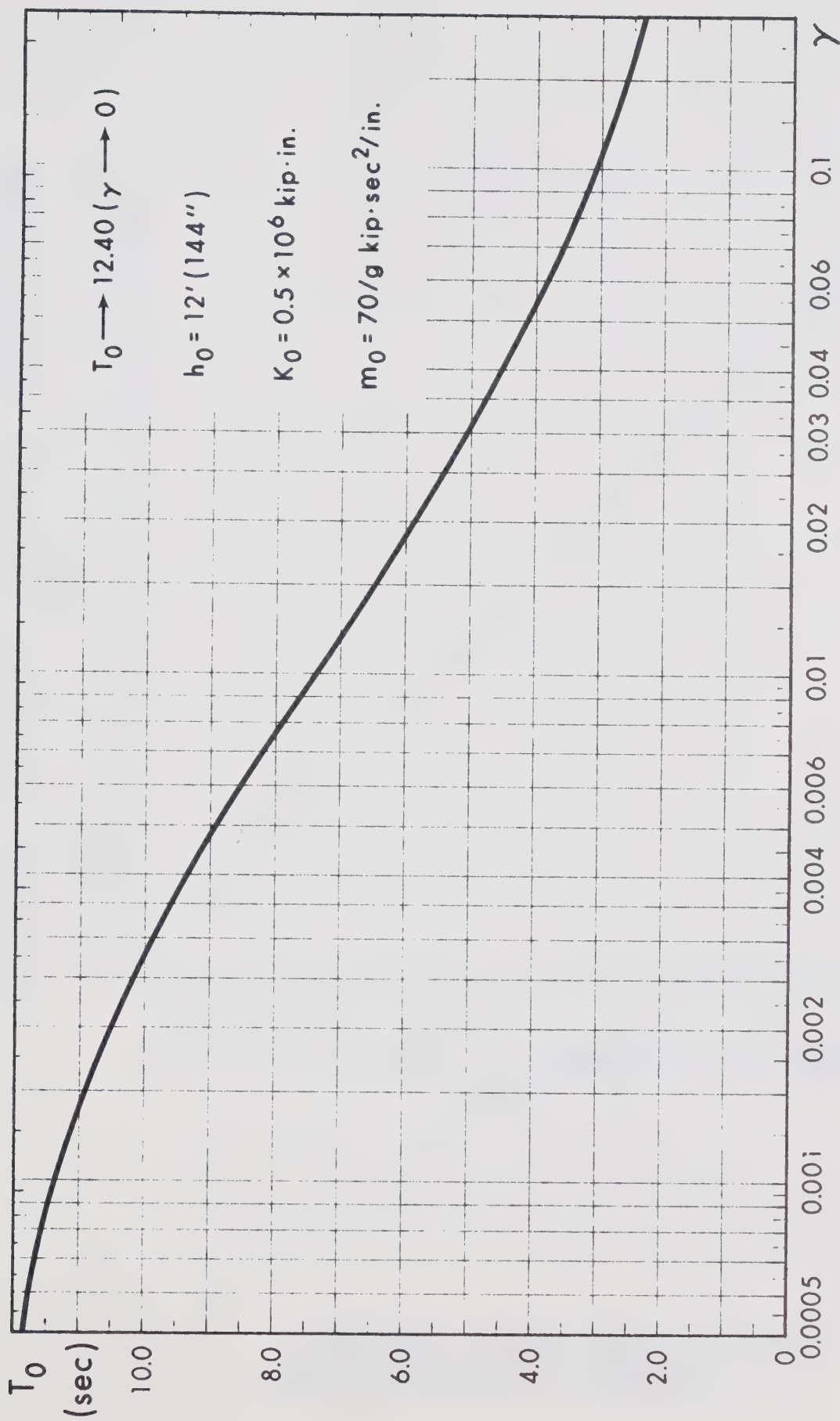


Fig. 4-1b Value of T_0 for the Calculation of the Natural Period (2)

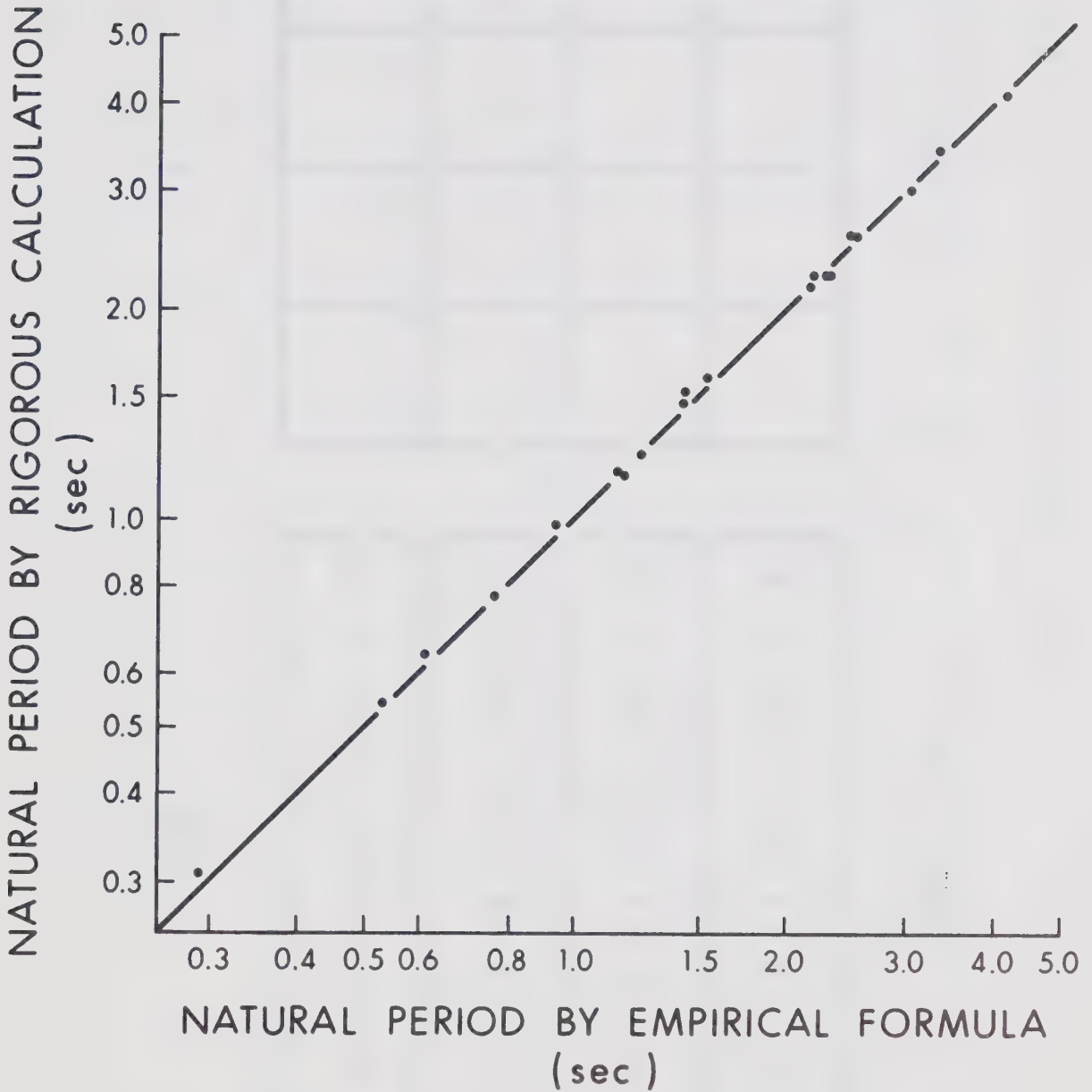
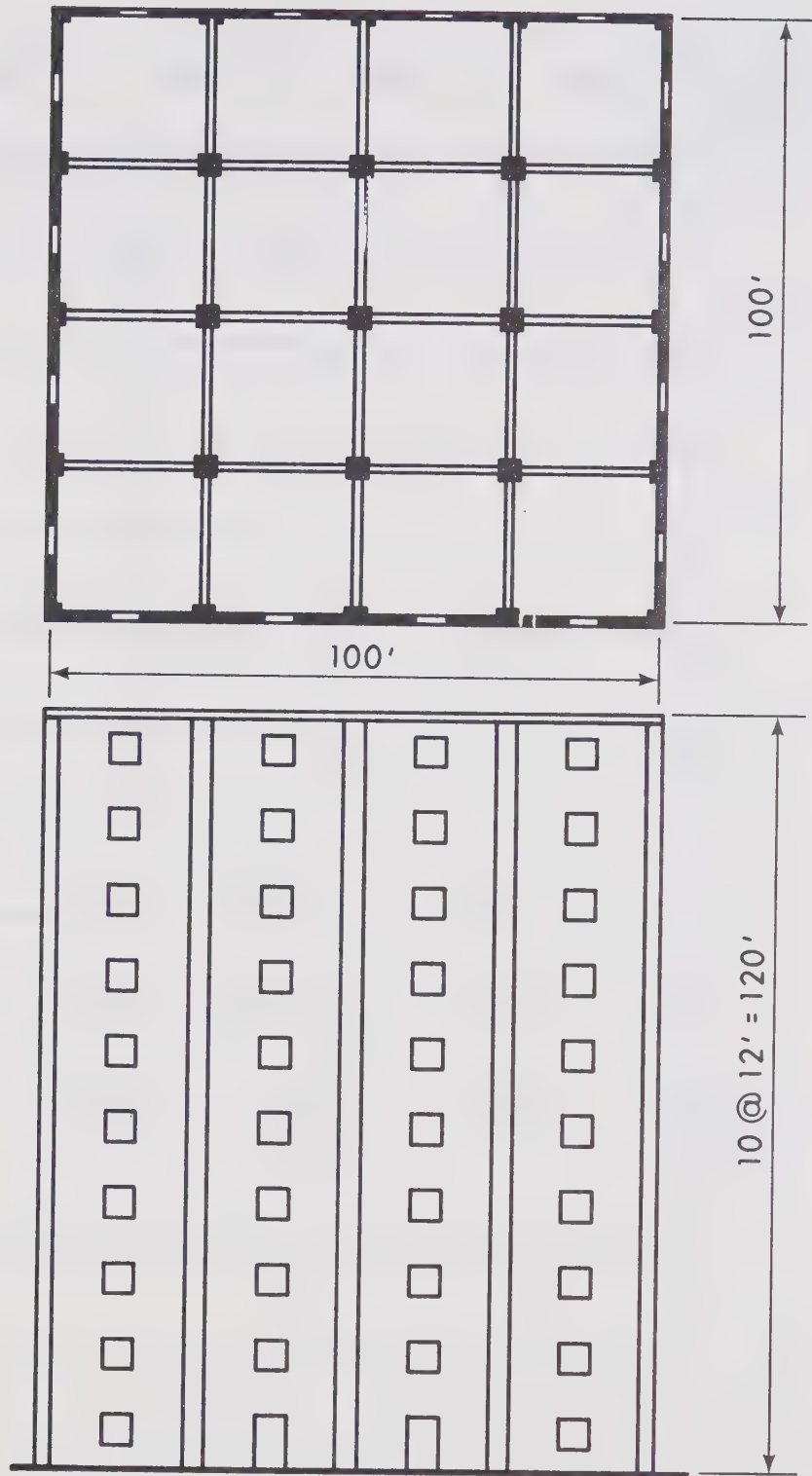


Fig. 4-2 Correlation Between Natural Period
by Rigorous Calculation and Natural
Period by Empirical Formula

PLAN



FRONT
VIEW

Fig. 4-3 Example Building

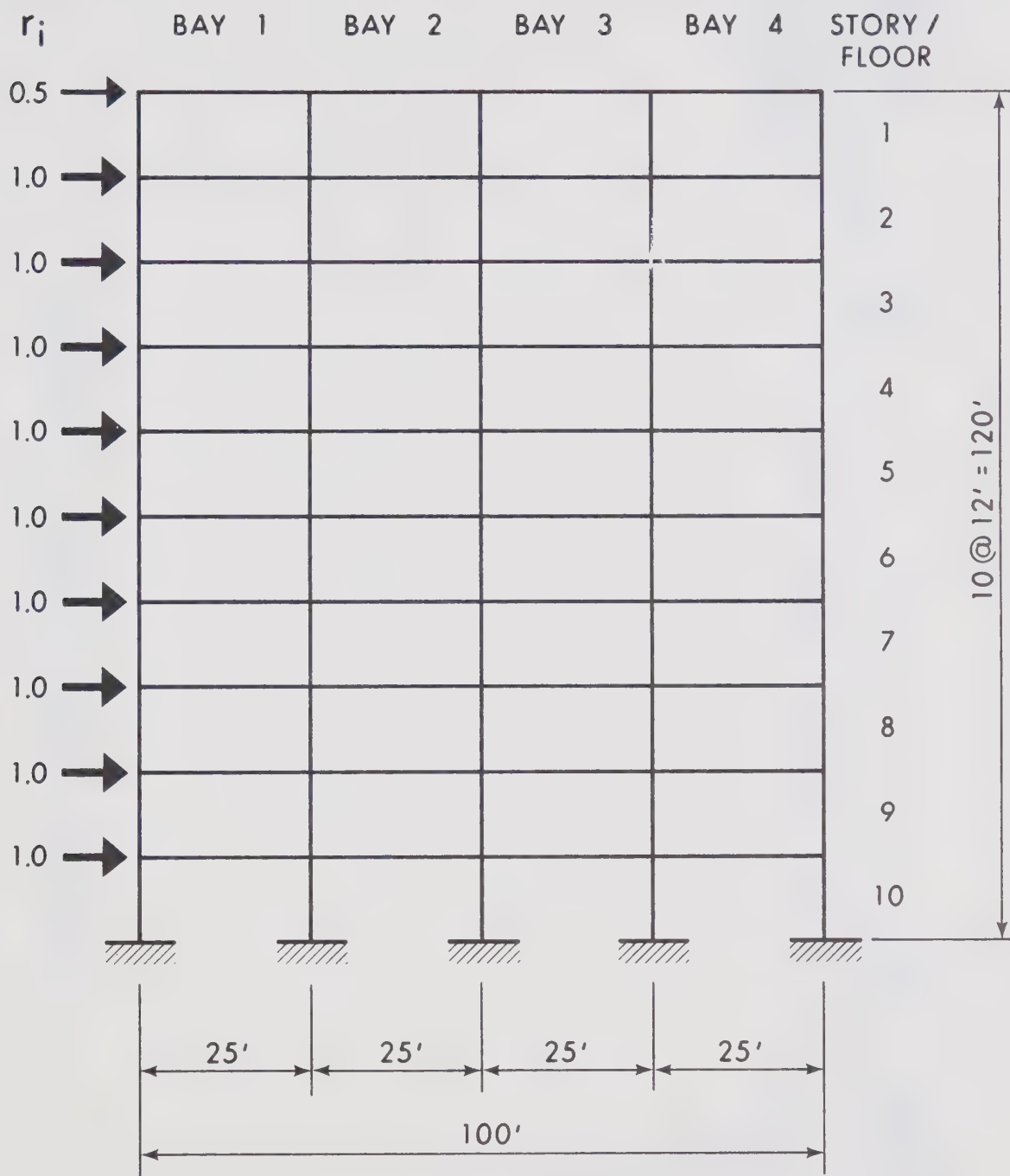


Fig. 4-4 Example Frame; Dimensions and Vector $\{r\}$

BLAST LOAD TYPE A-105.2

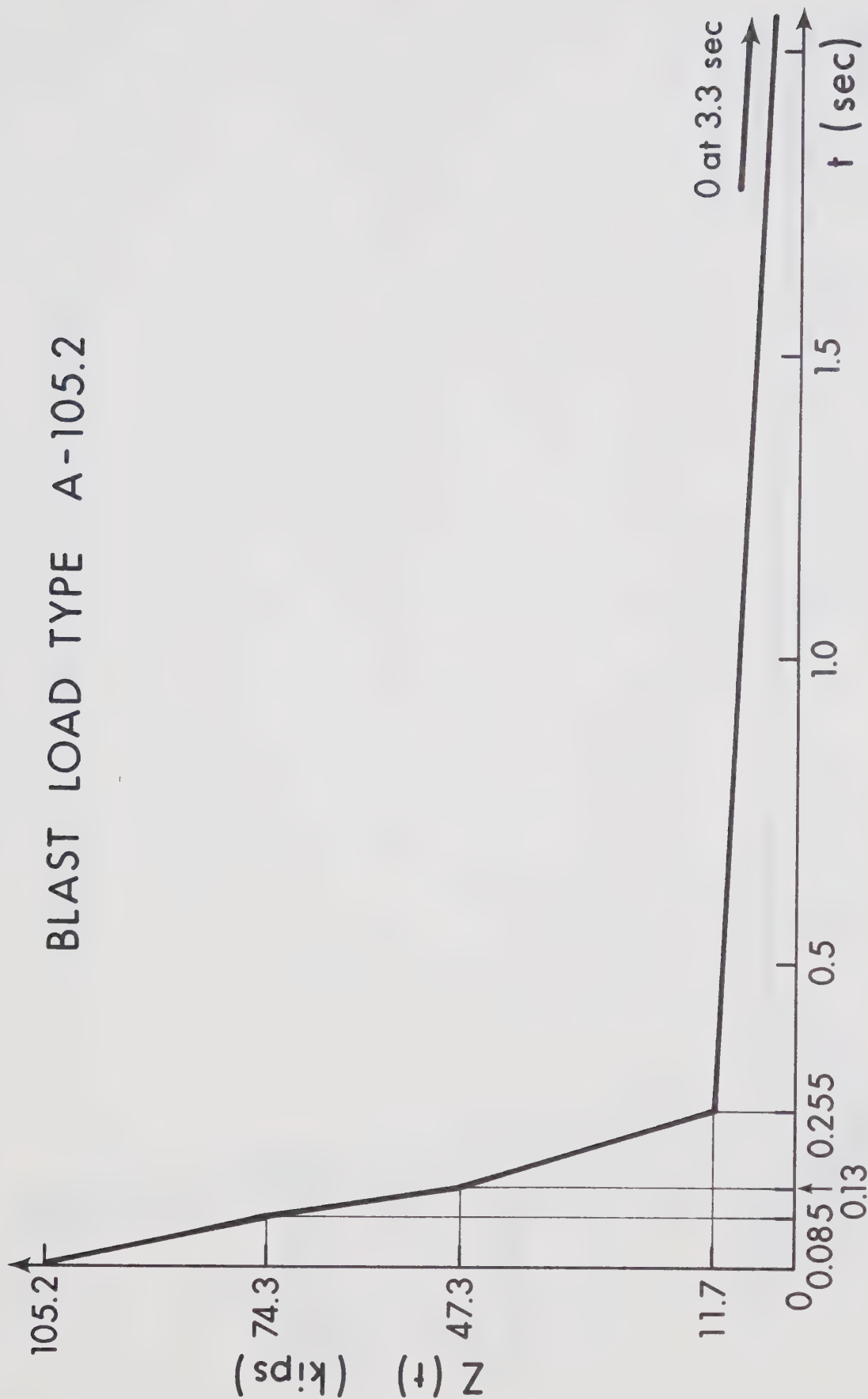


Fig. 4-5 Blast Load Type A-105.2

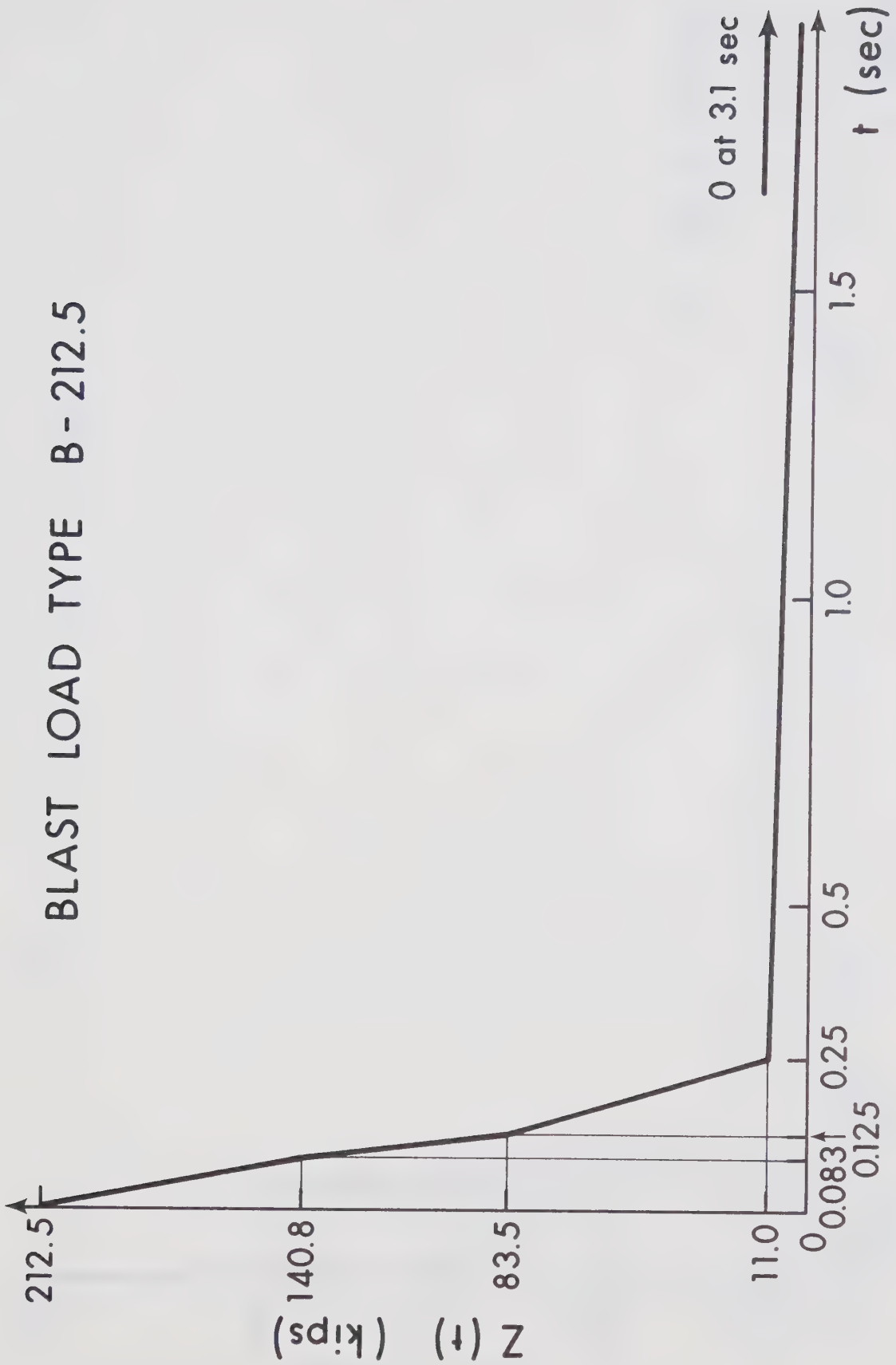


Fig. 4-6 Blast Load Type B-212.5

BLAST LOAD TYPE C-358

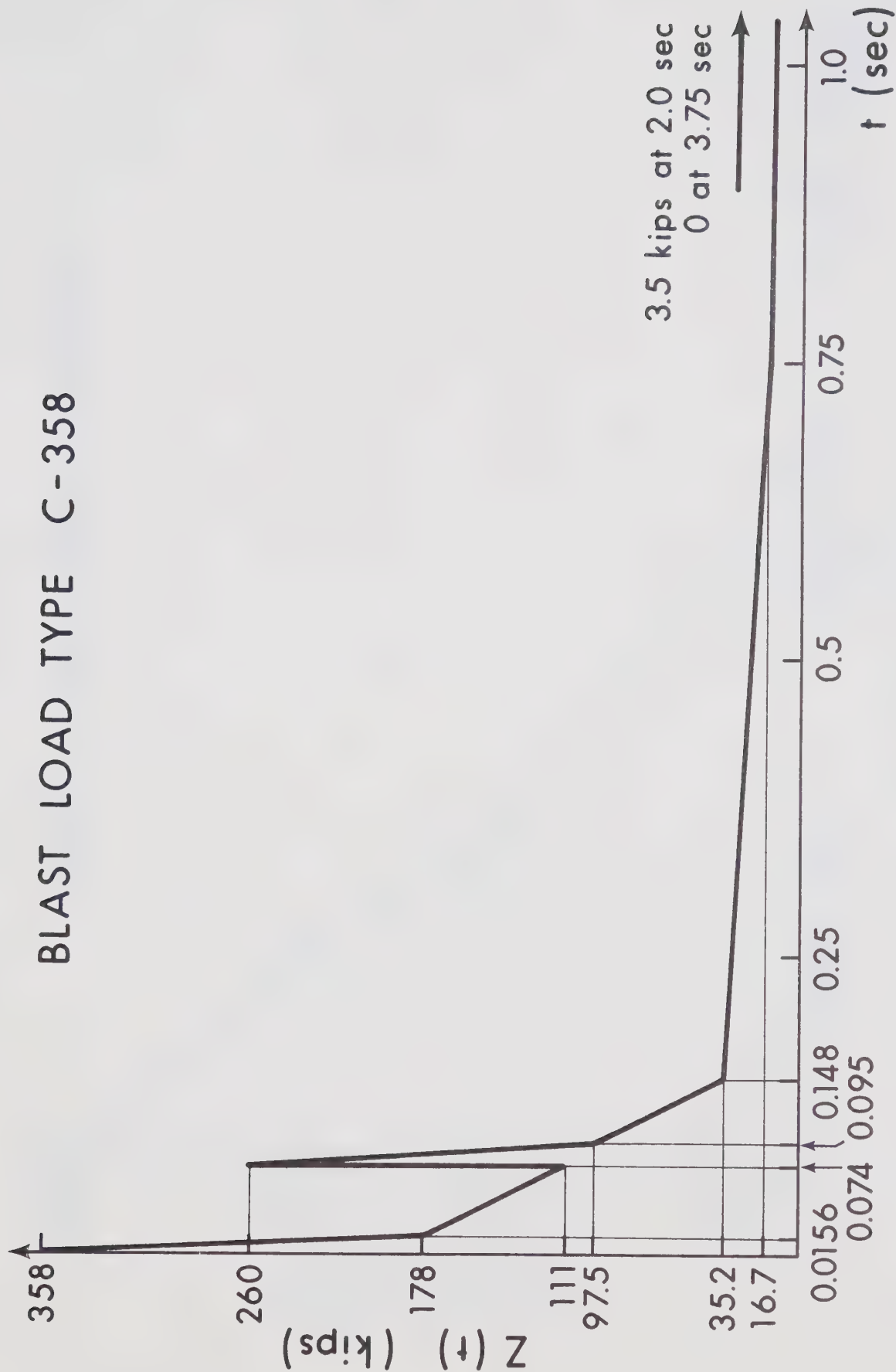


Fig. 4-7 Blast Load Type C-358

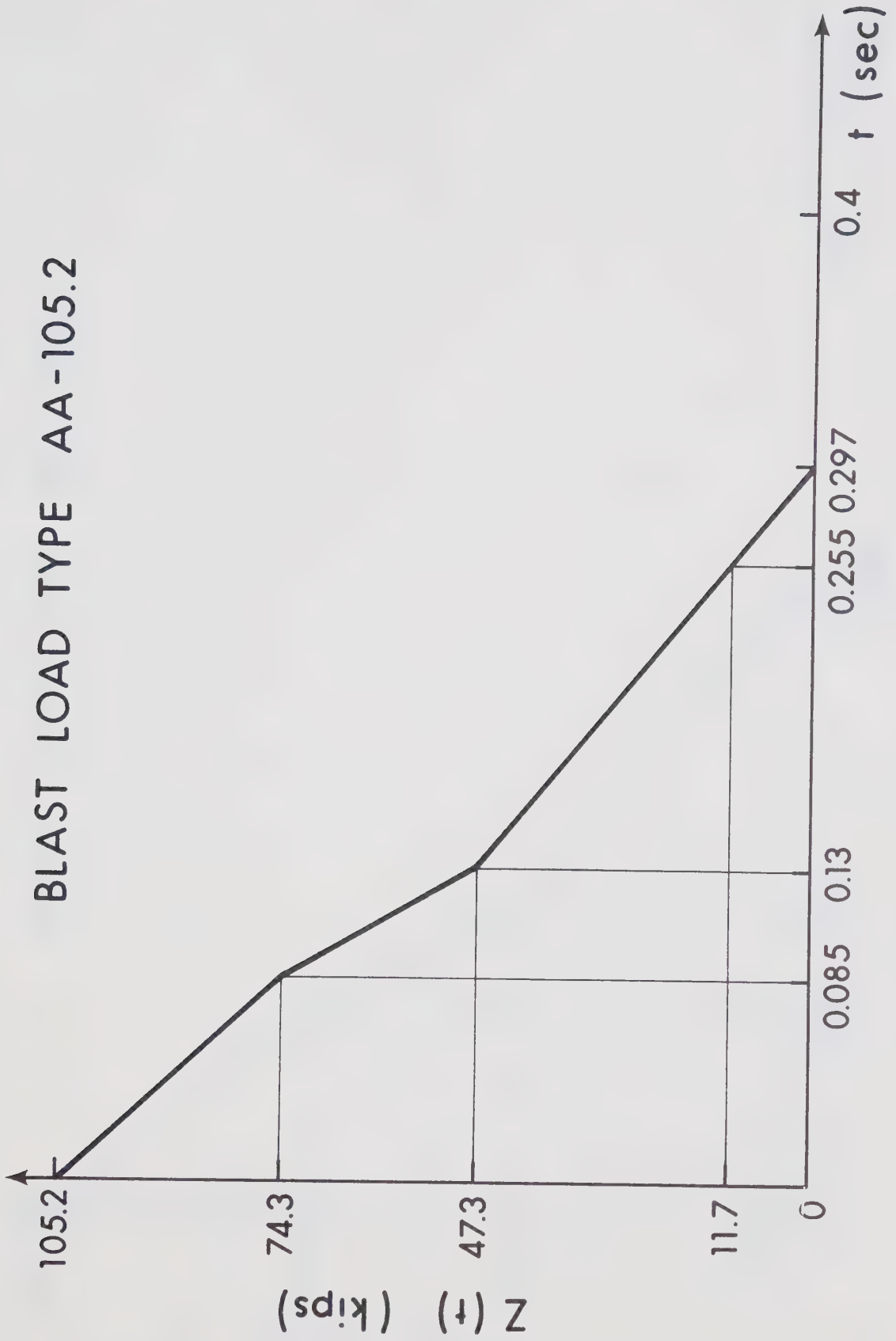


Fig. 4-8 Blast Load Type AA-105.2

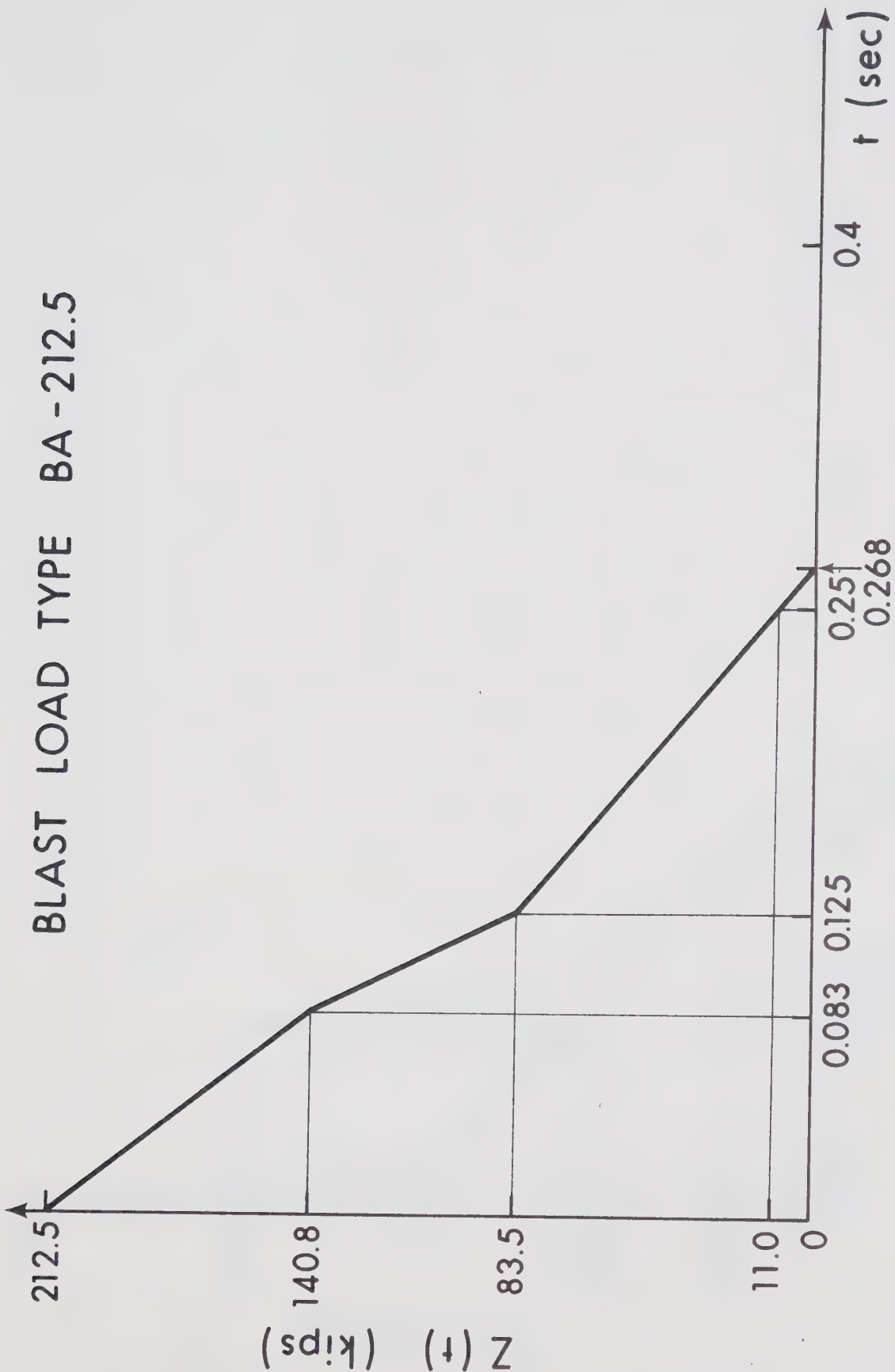


Fig. 4-9 Blast Load Type BA-212.5

BLAST LOAD TYPE CA-358

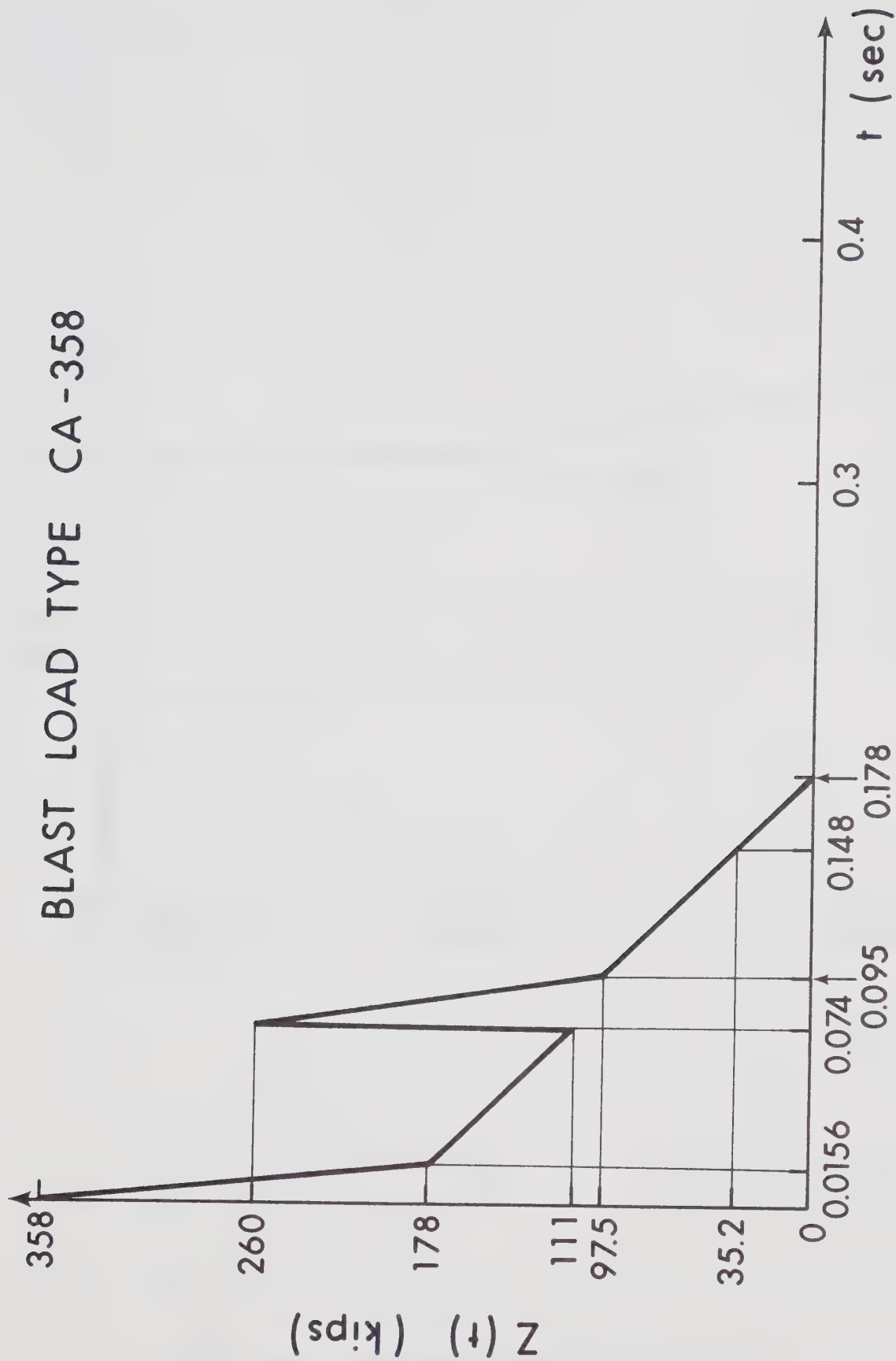


Fig. 4-10 Blast Load Type CA-358

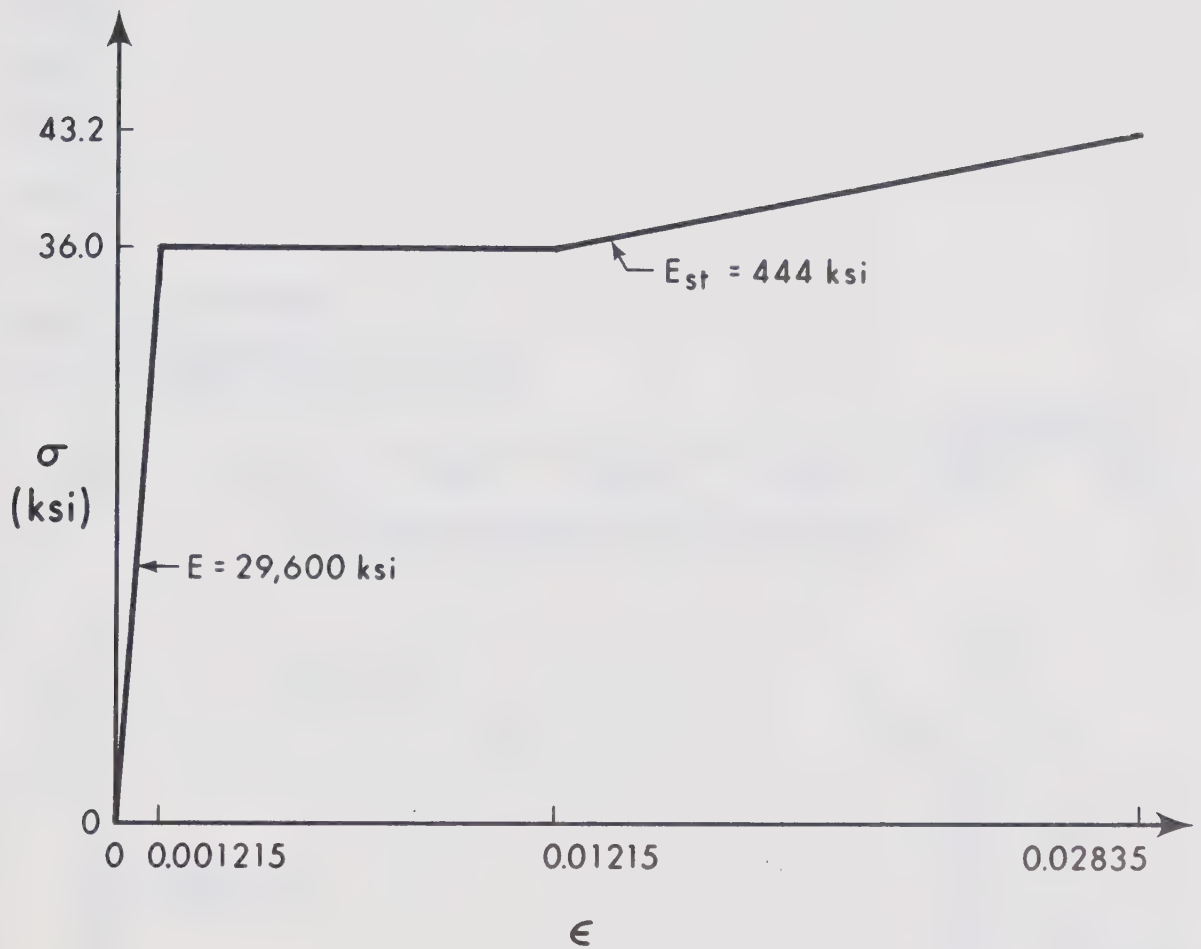
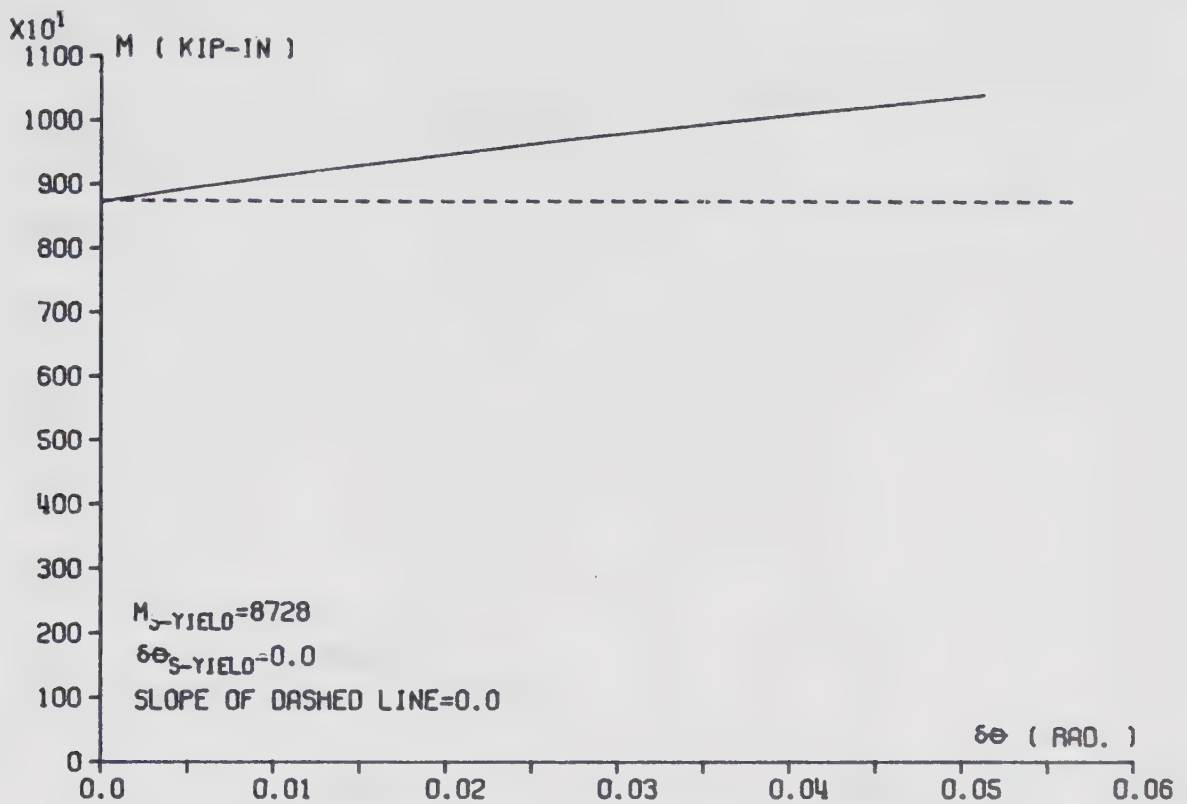
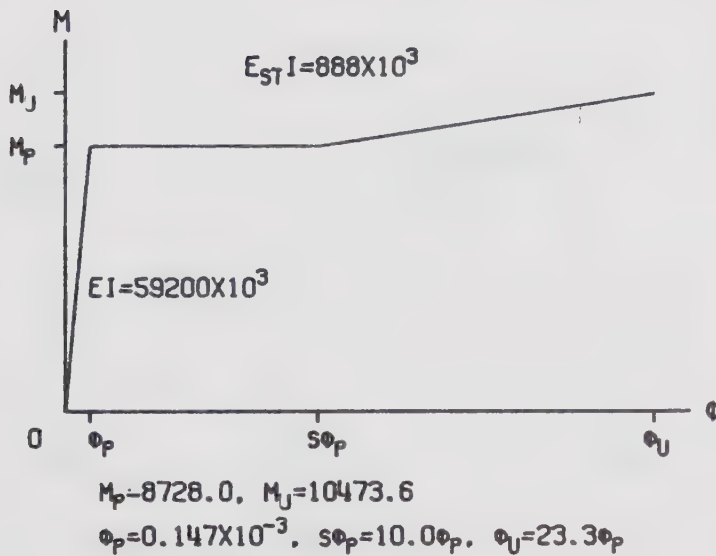


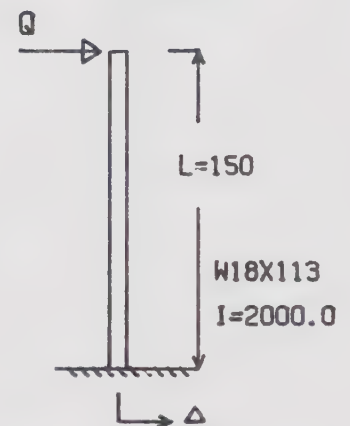
Fig. 4-11 Stress-Strain Relationship



END MOMENT-RELAXATION ANGLE RELATIONSHIP

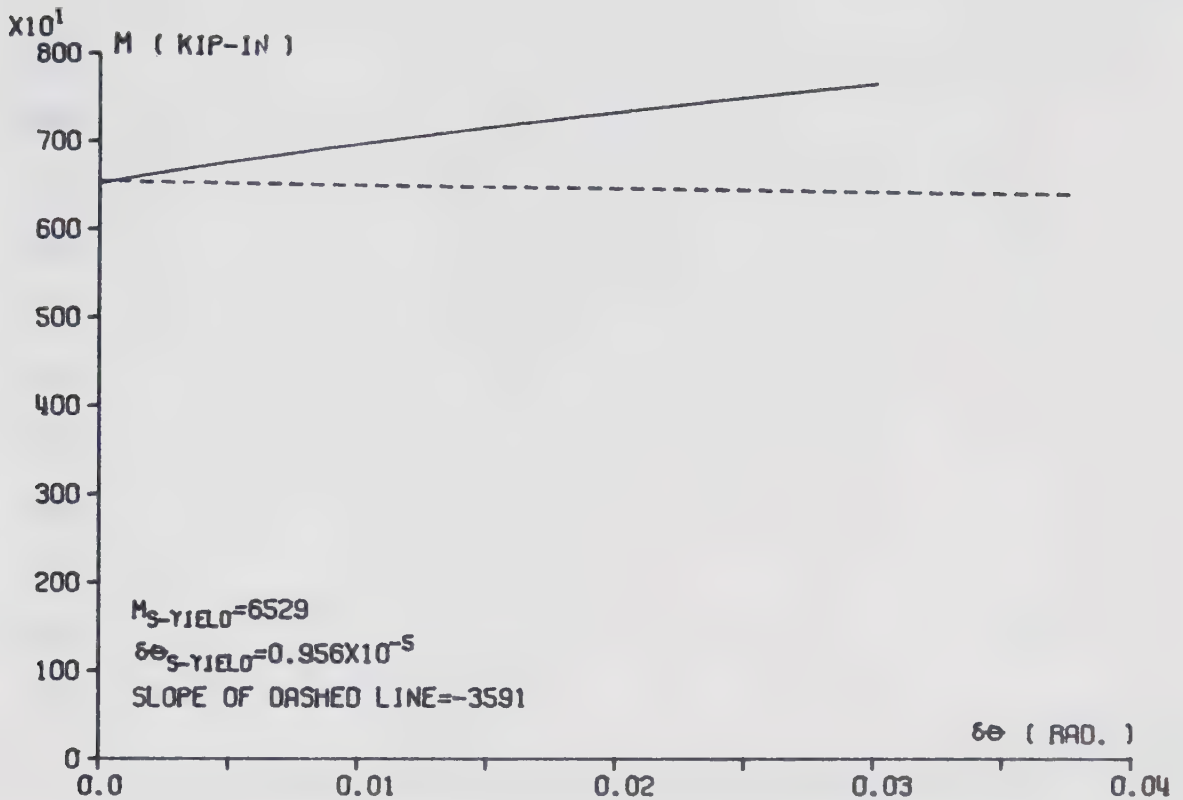


MOMENT CURVATURE RELATIONSHIP

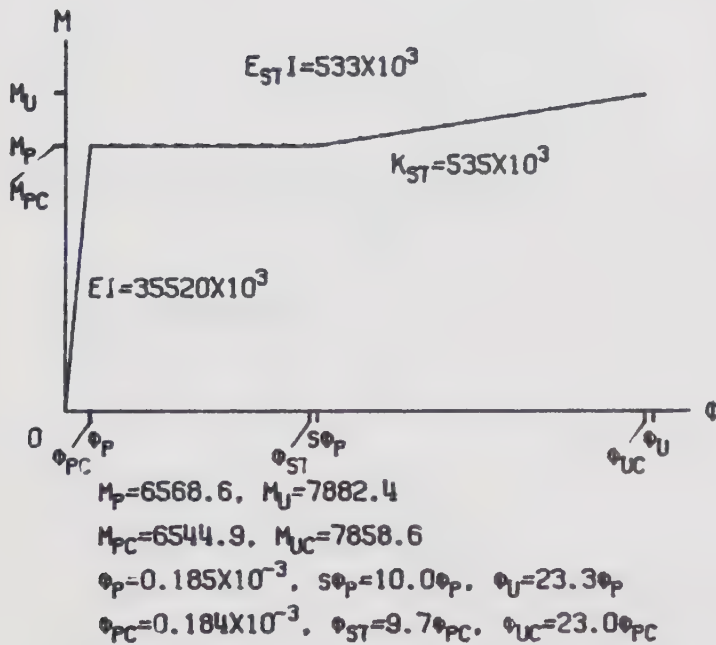


UNIT OF FORCE: KIP.
UNIT OF LENGTH: IN.

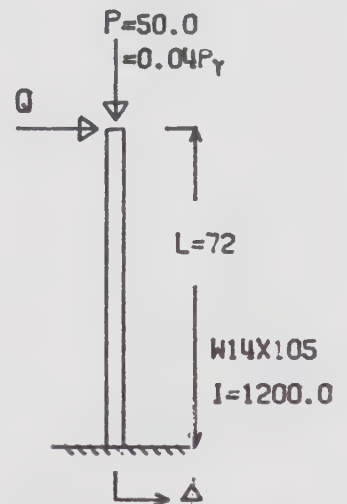
Fig. 4-12a CROSS SECTIONAL PROPERTIES AND $M-\Delta\theta$ RELATIONSHIP
(FRAME#1AA, Beams)



END MOMENT-RELAXATION ANGLE RELATIONSHIP

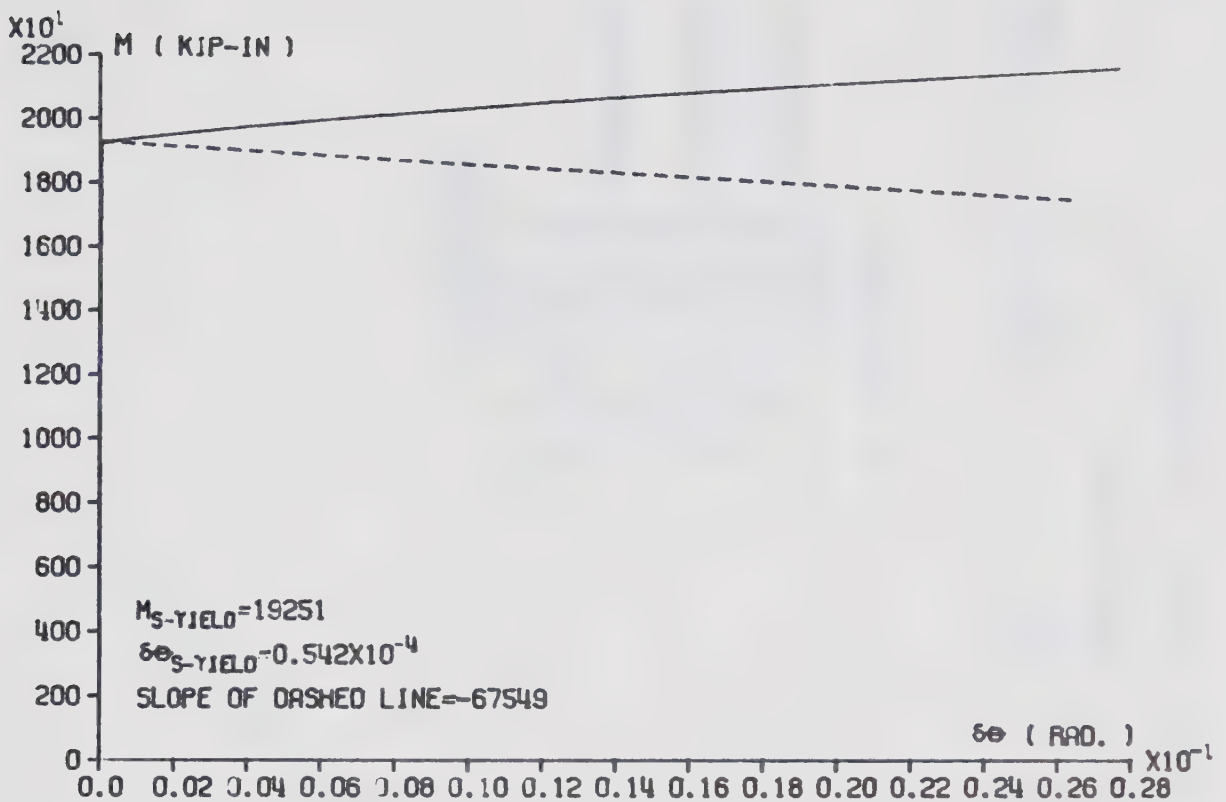


MOMENT CURVATURE RELATIONSHIP

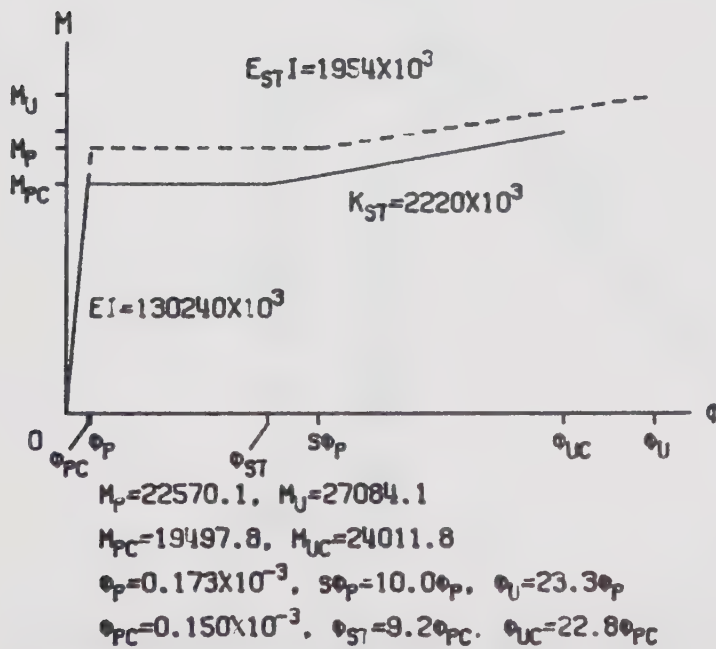


UNIT OF FORCE: KIP.
UNIT OF LENGTH: IN.

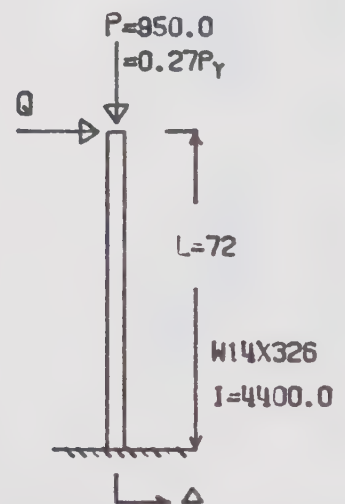
Fig. 4-12b CROSS SECTIONAL PROPERTIES AND $M-\delta\theta$ RELATIONSHIP
(FRAME#1AA, Top Story Columns)



END MOMENT-RELAXATION ANGLE RELATIONSHIP



MOMENT CURVATURE RELATIONSHIP



UNIT OF FORCE: KIP.
UNIT OF LENGTH: IN.

Fig. 4-12c CROSS SECTIONAL PROPERTIES AND $M-\Delta\theta$ RELATIONSHIP
(FRAME#1AA, Bottom Story Columns)

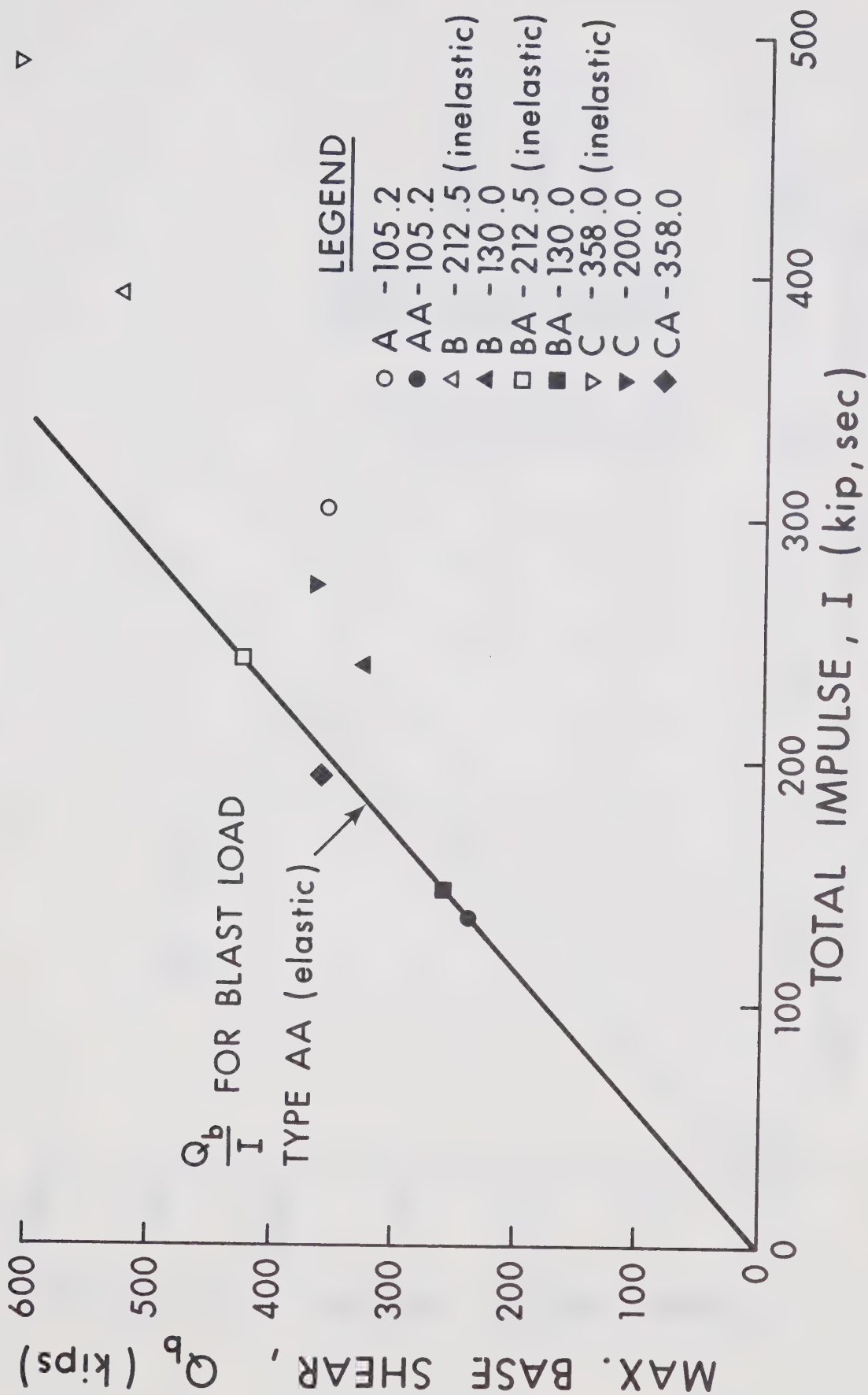


Fig. 4-13 Maximum Base Shear vs. Total Impulse -- FRAME#1AA

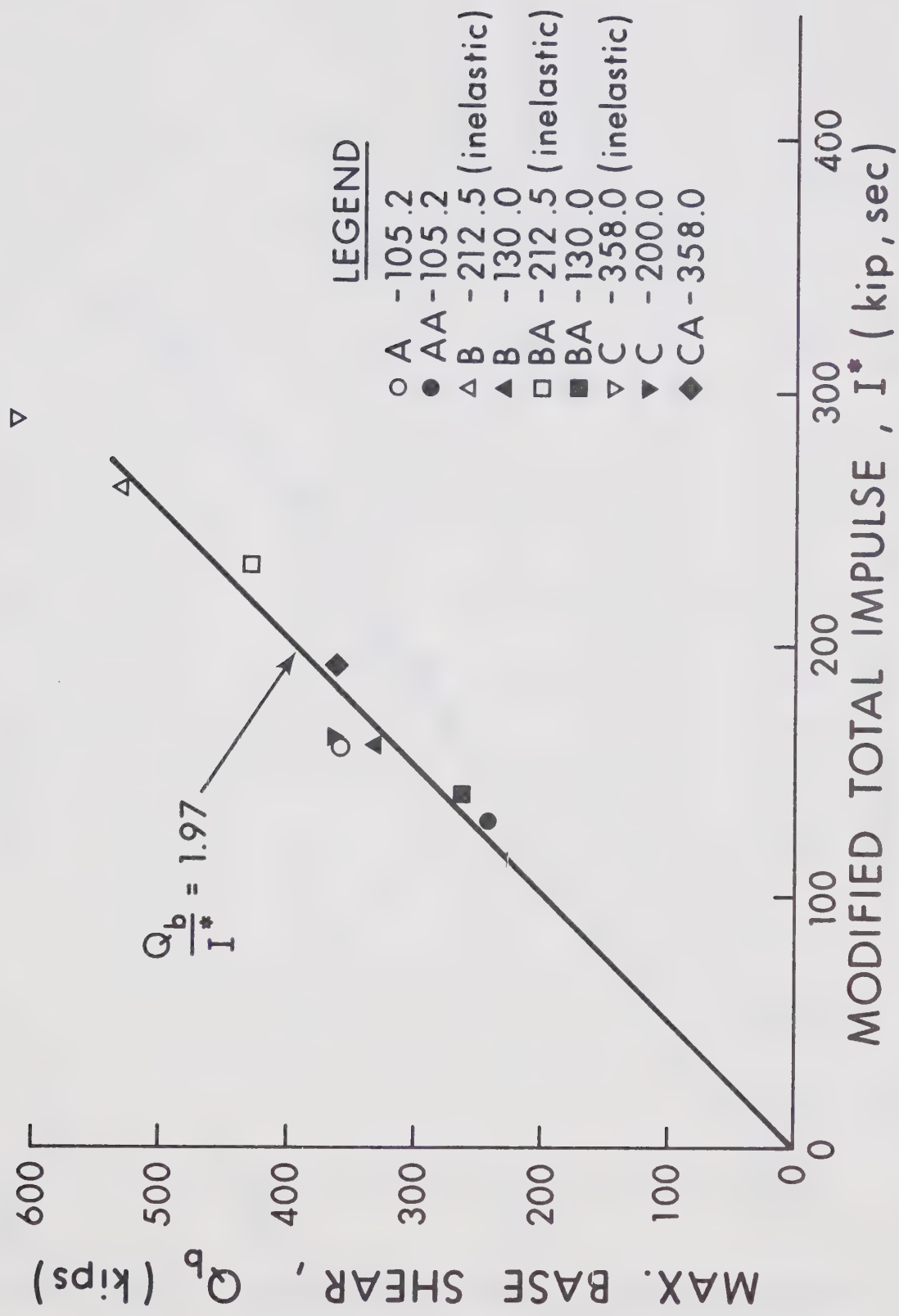


Fig. 4-14 Maximum Base Shear vs. Modified Total Impulse -- FRAME#1AA

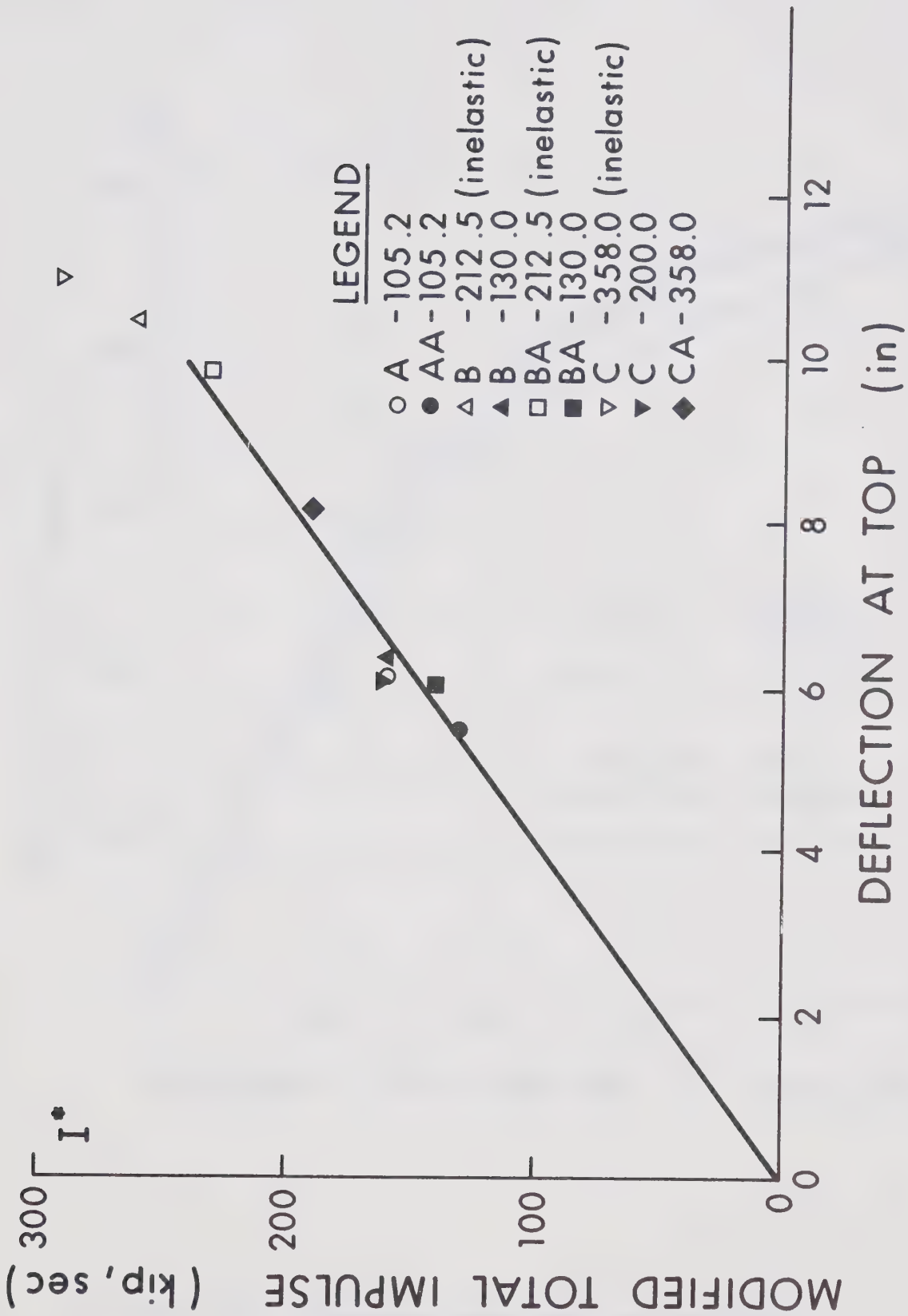


Fig. 4-15 Deflection at Top vs. Modified Total Impulse -- FRAME#1AA

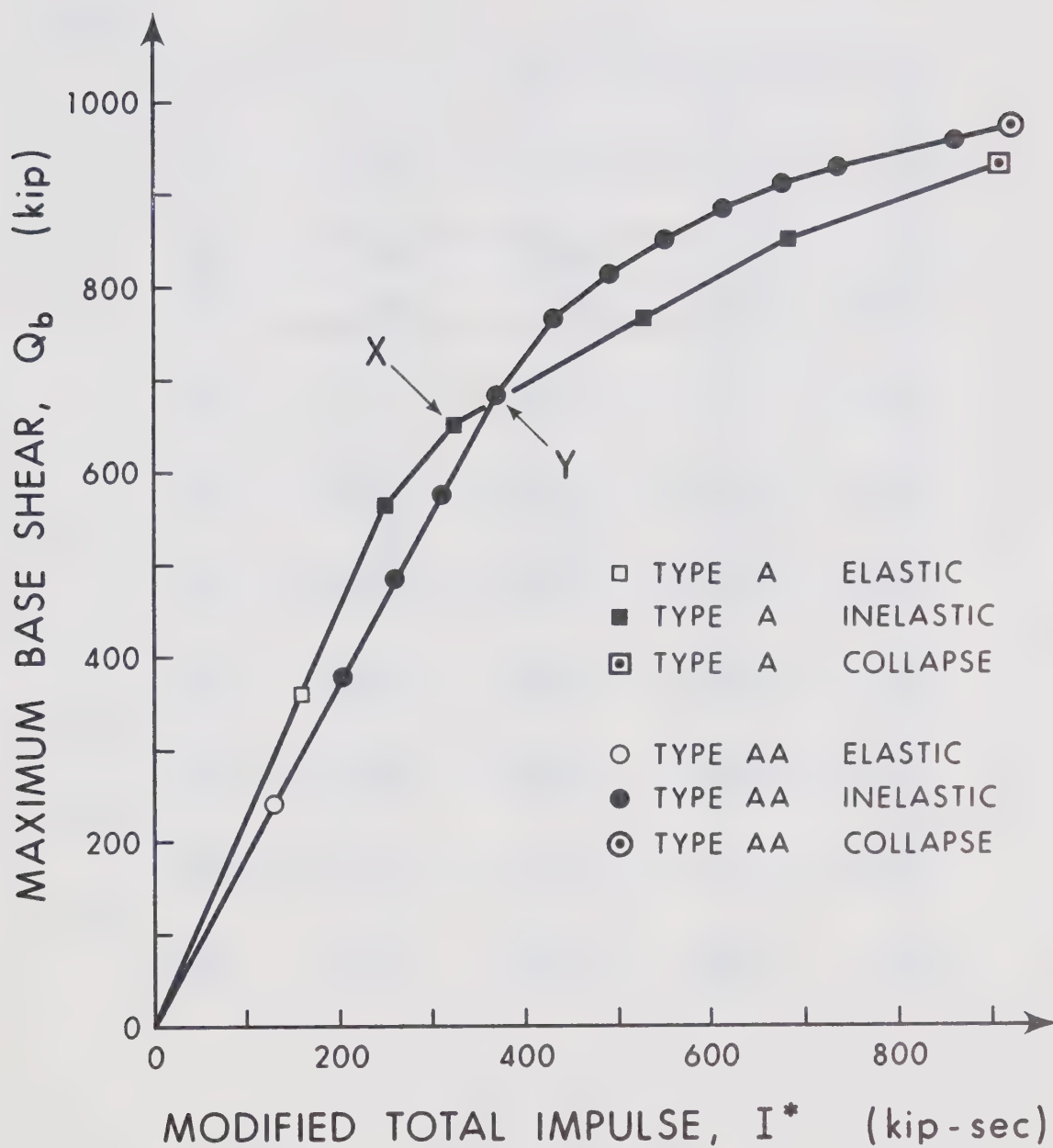


Fig. 4-16 Maximum Base Shear vs. Modified Total Impulse for FRAME#1AA

STORY

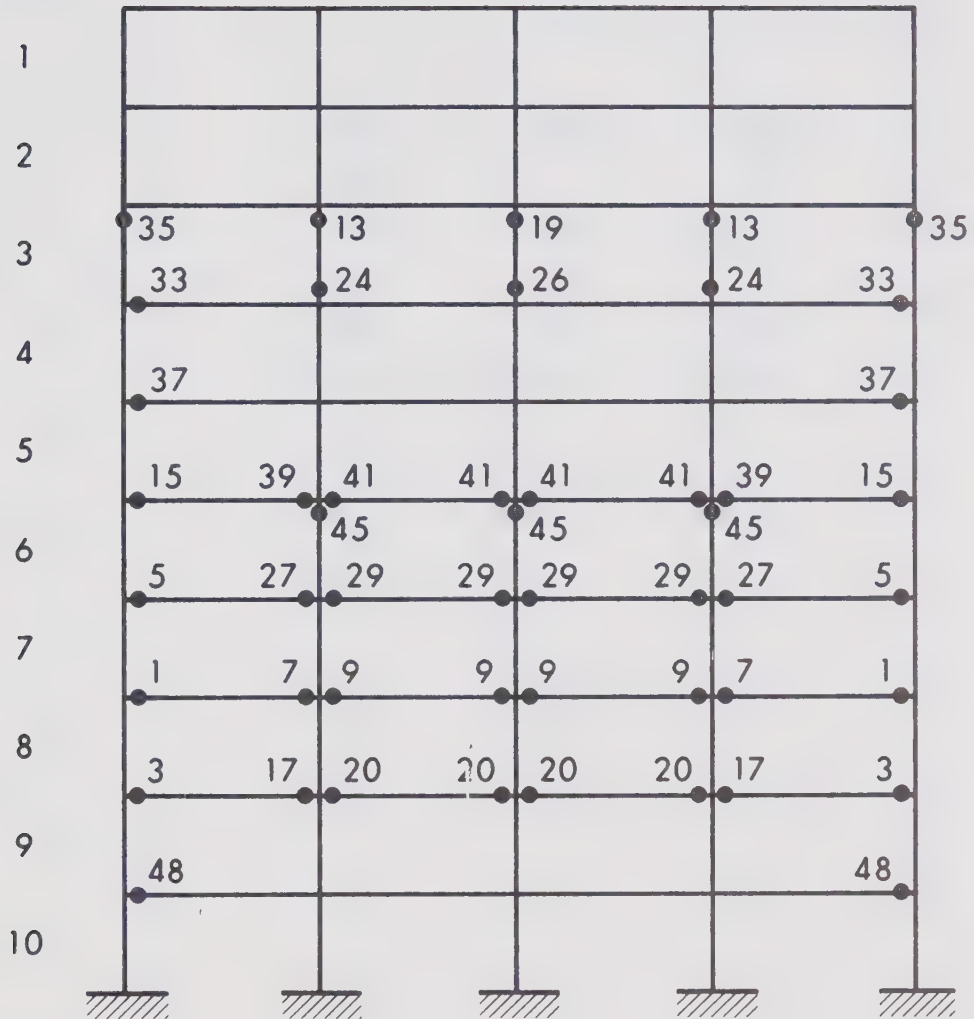


Fig. 4-17 Location of Yielding in FRAME#1AA
 Subjected to Blast Load Type A-212.5
 (At Point X in Figure 4-16)

STORY

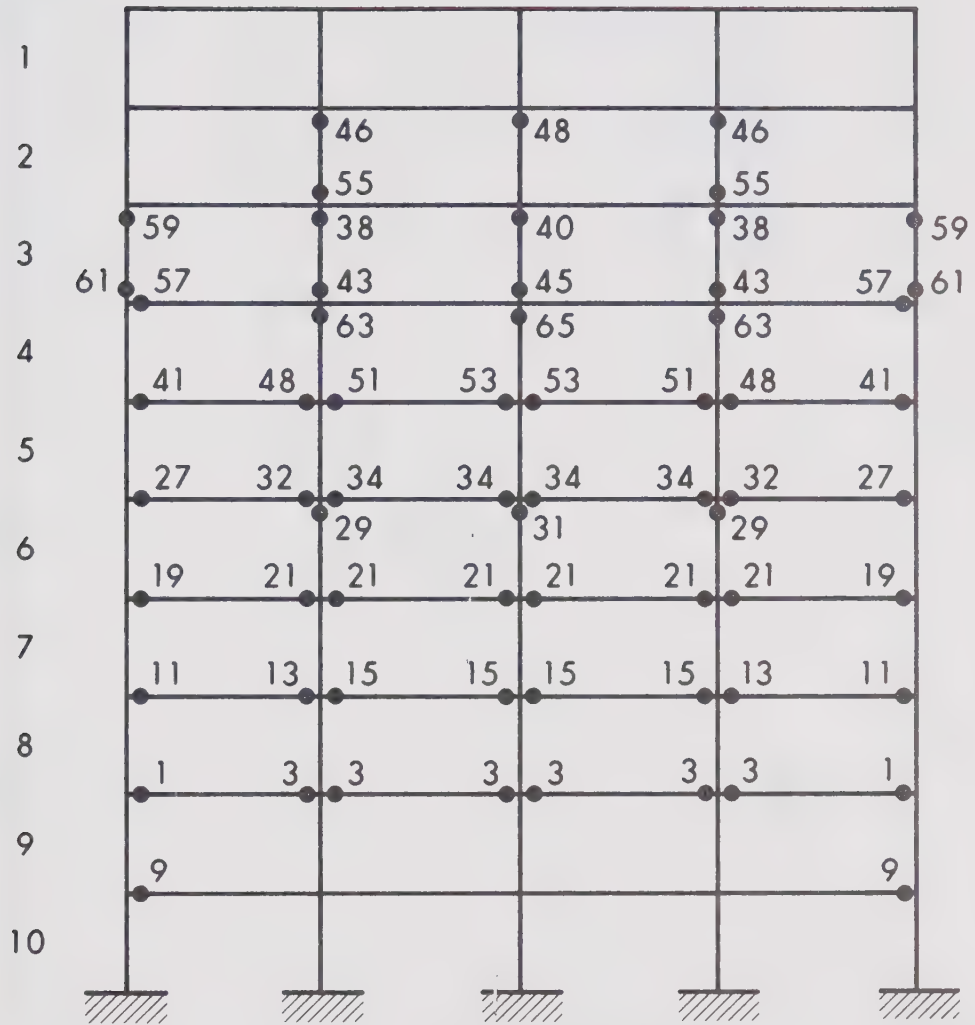


Fig. 4-18 Location of Yielding in FRAME#1AA
Subjected to Blast Load Type AA-300
(At Point y in Figure 4-16)

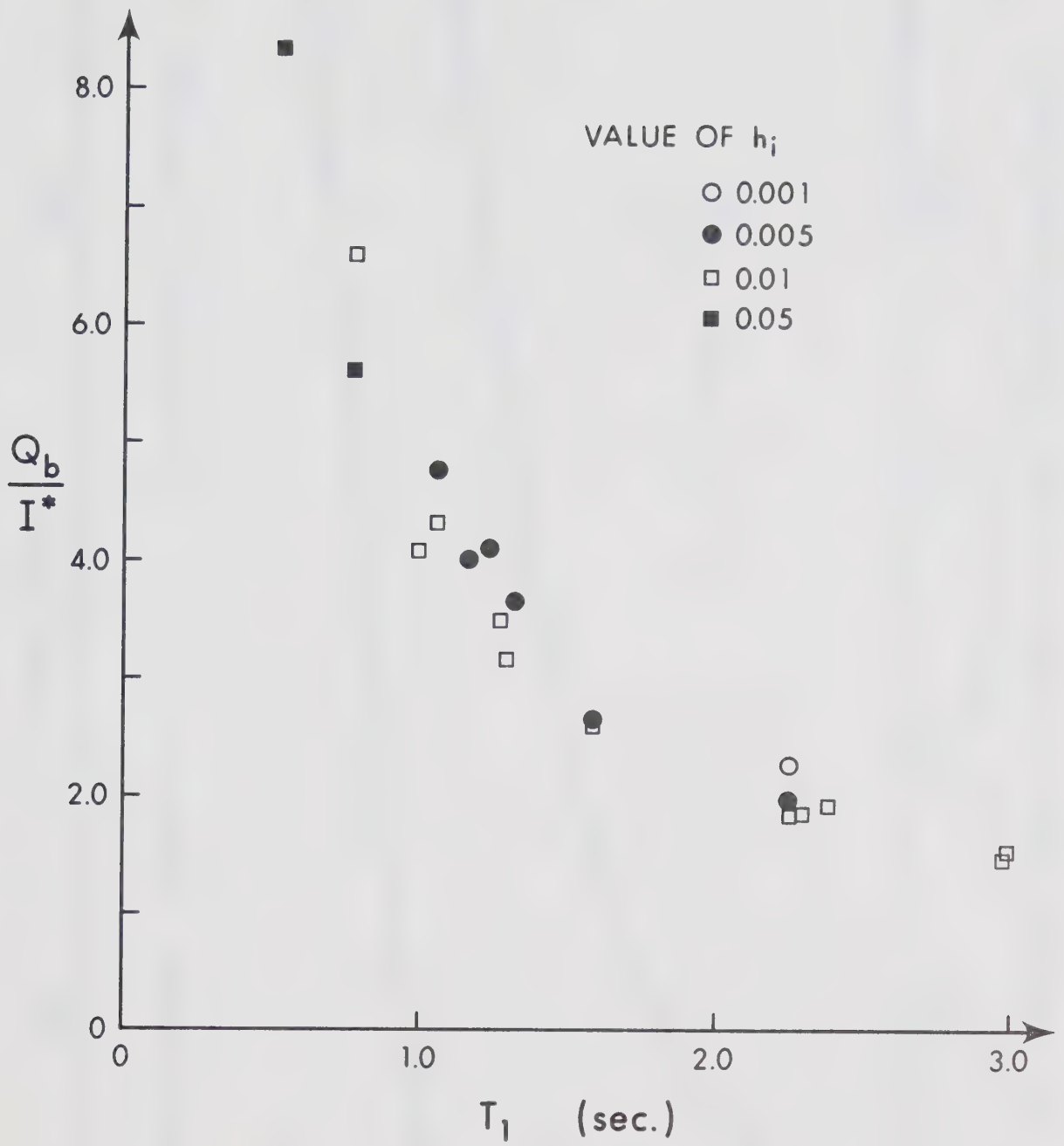


Fig. 4-19 Average Value of Q_b/I^* vs. Natural Period

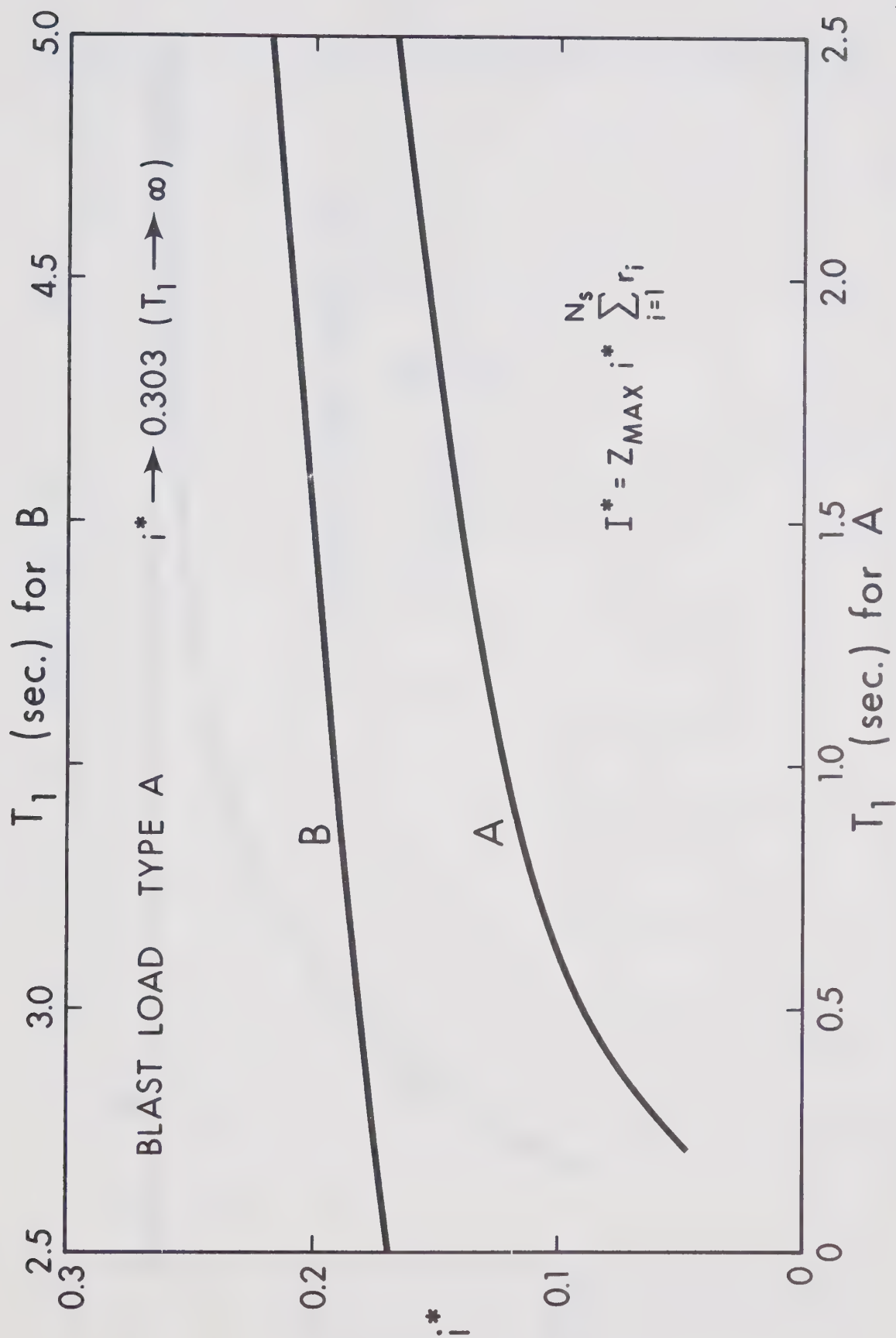


Fig. 4-20 Modified Impulse of Blast Load Type A for Standard Floor

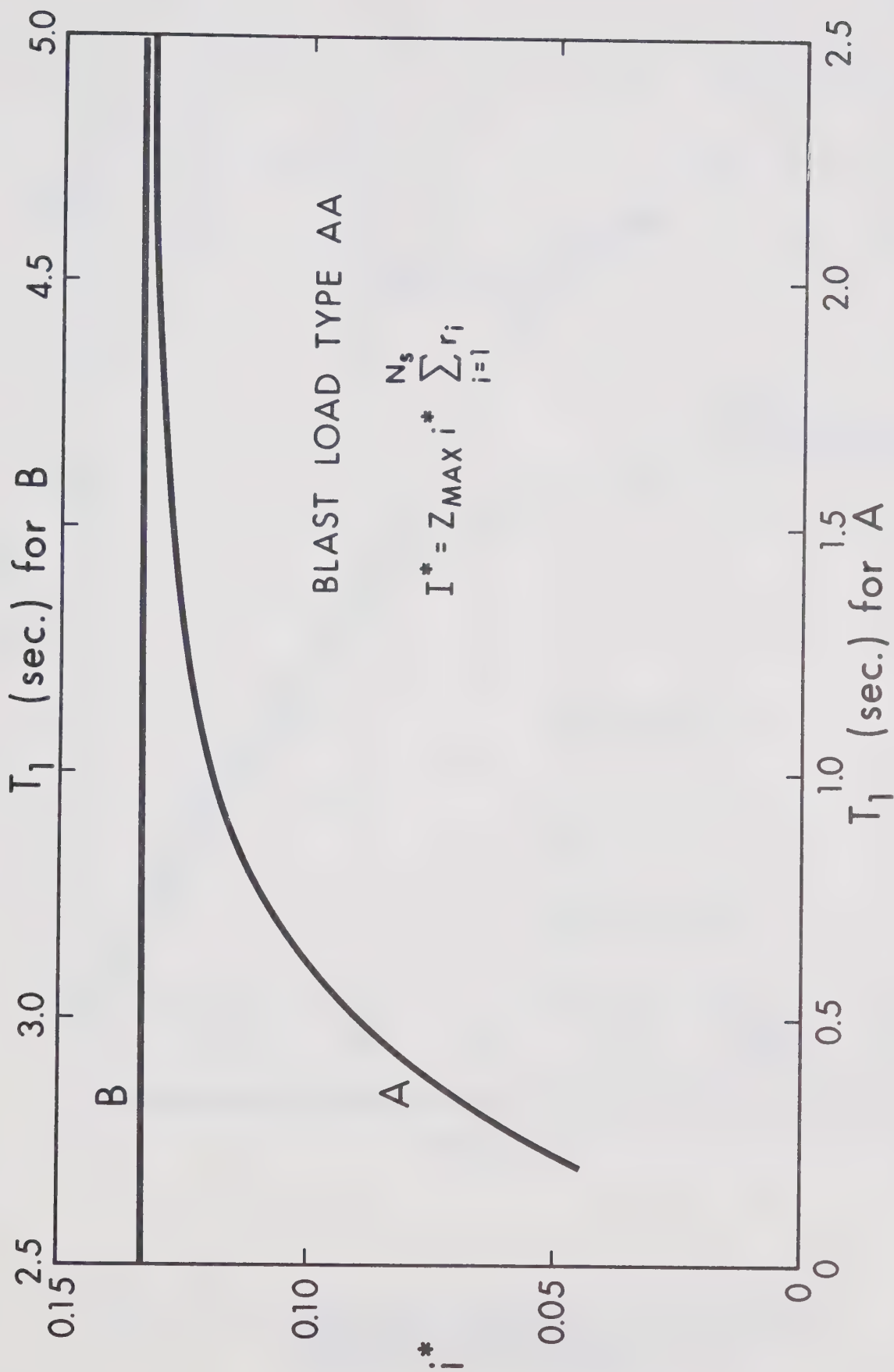


Fig. 4-21 Modified Impulse of Blast Load Type AA for Standard Floor

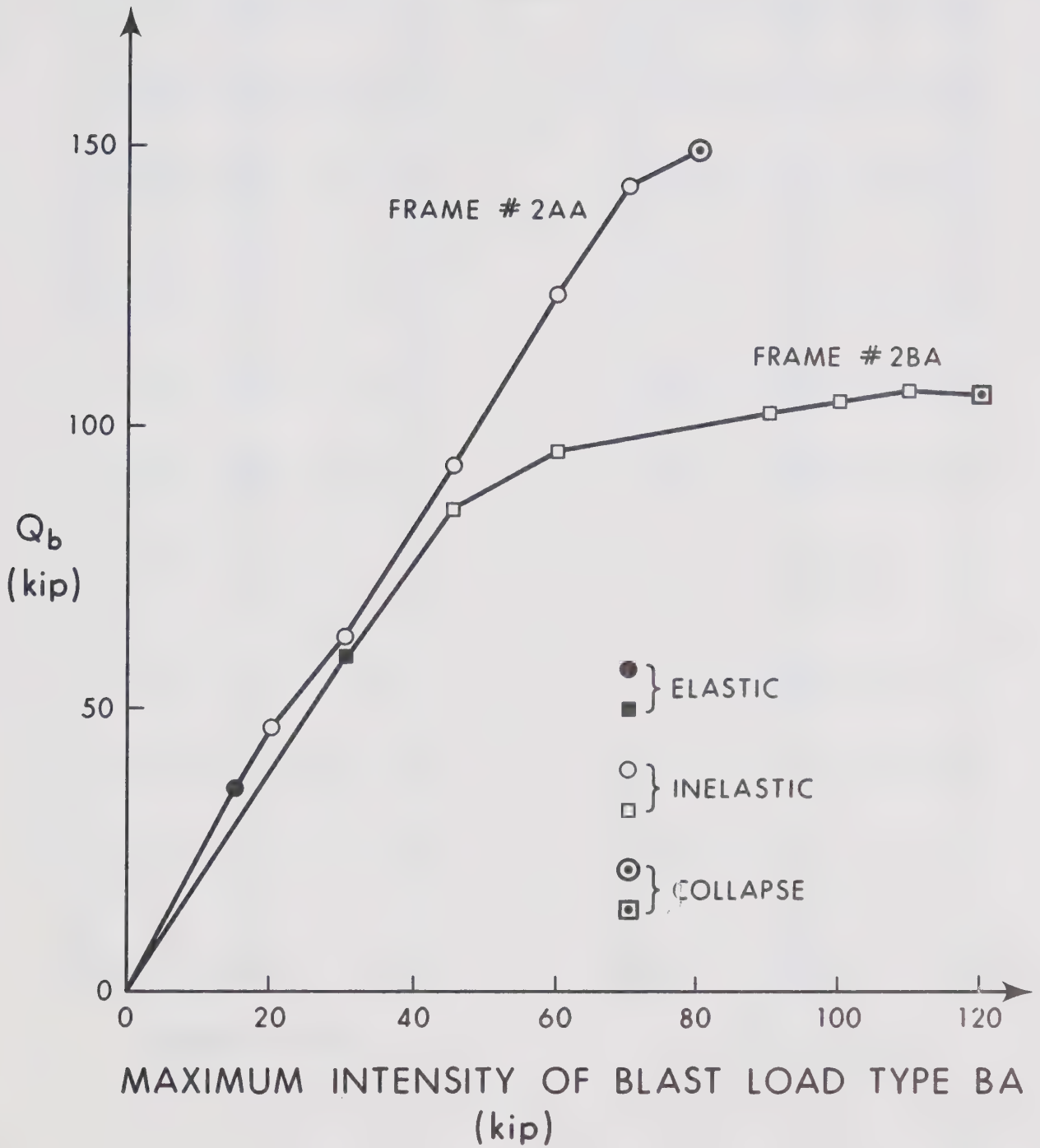


Fig. 4-22 Maximum Intensity of Blast Load Type BA vs. Maximum Base Shear for FRAME#2AA and FRAME#2BA.

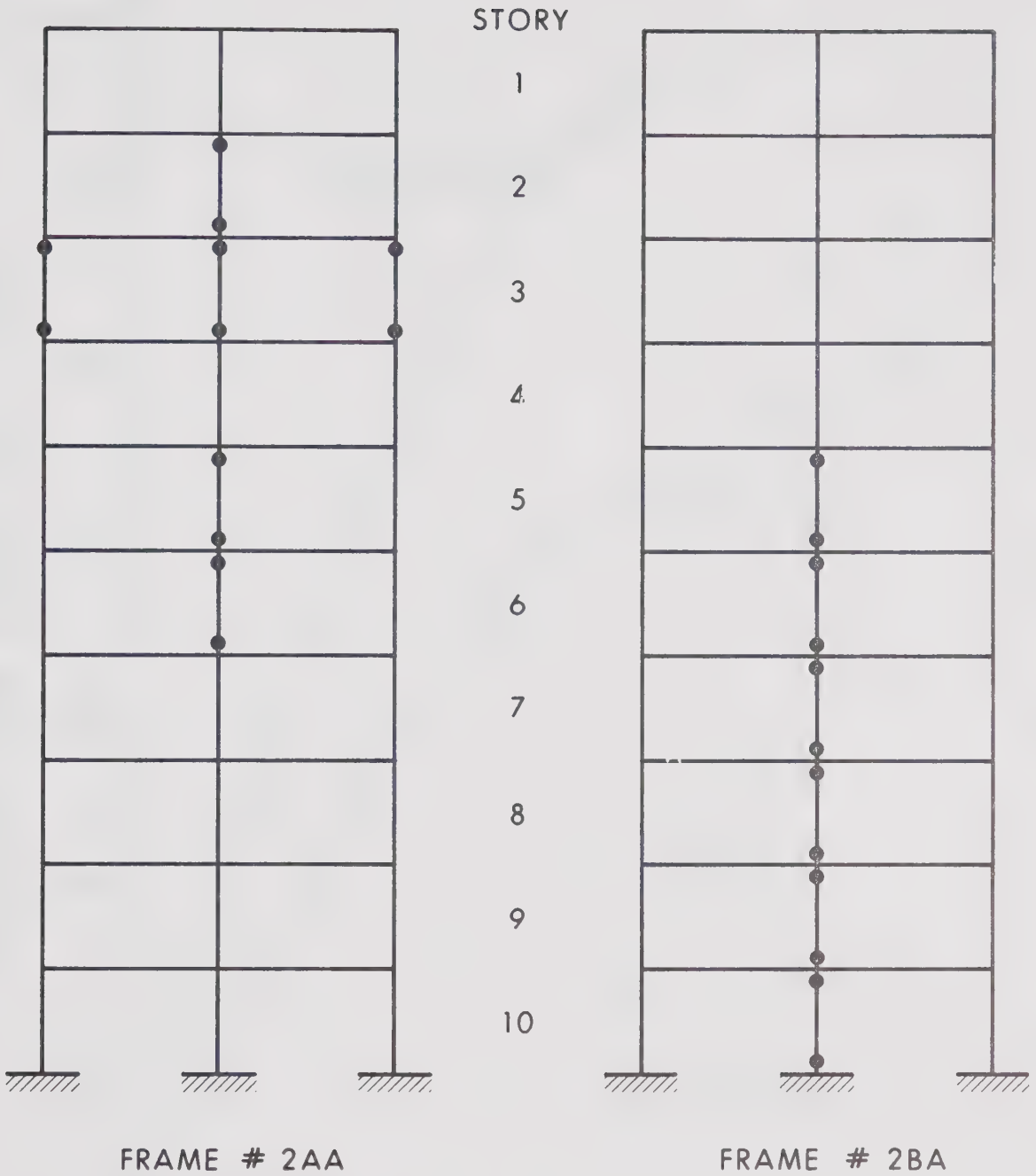


Fig. 4-23 Location of Member End where Inelastic Action was Recorded for FRAME#2AA and FRAME#2BA (Blast Load Type BA-45)

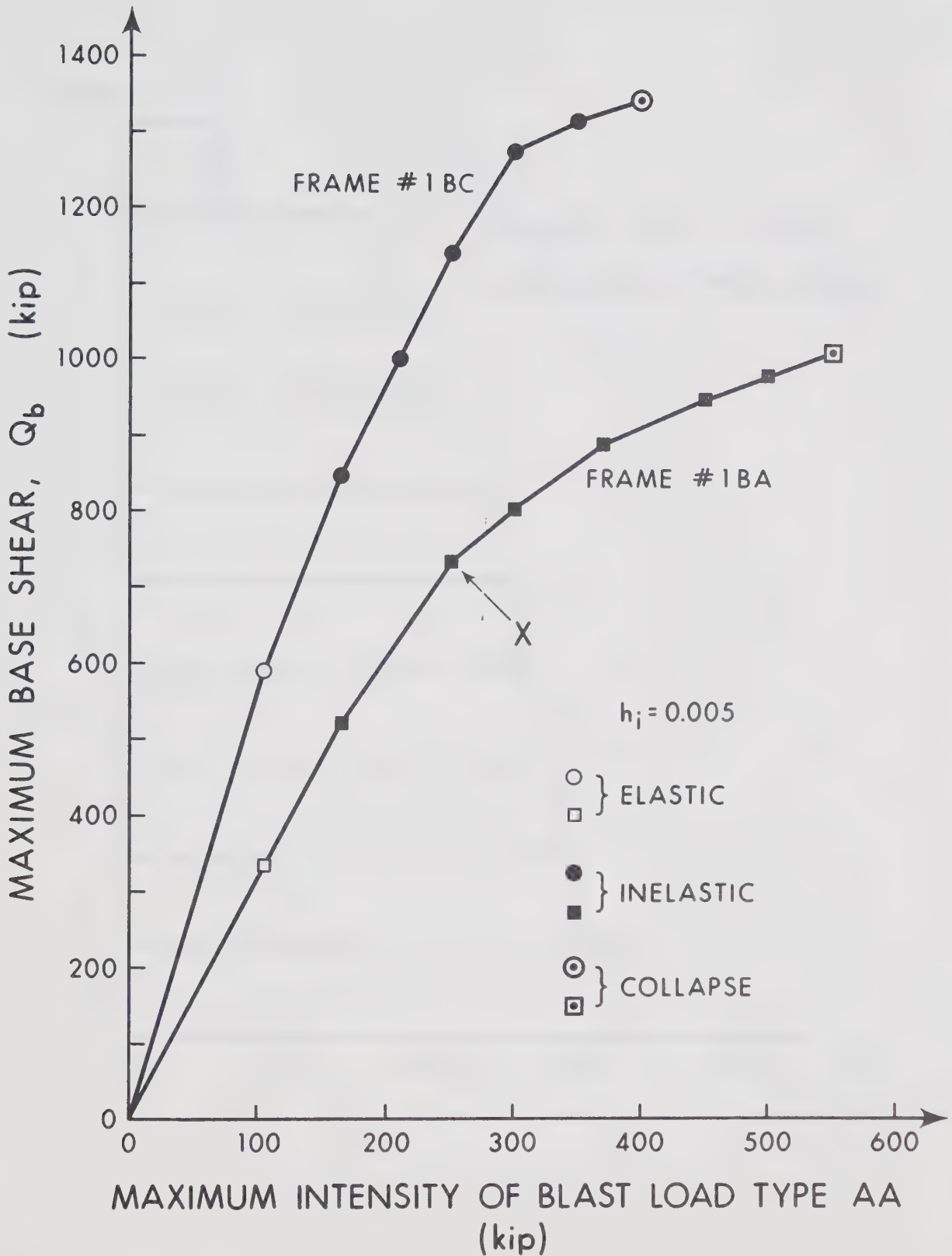


Fig. 4-24 Maximum Intensity of Blast Load Type AA vs. Maximum Base Shear for FRAME#1BA and FRAME#1BC

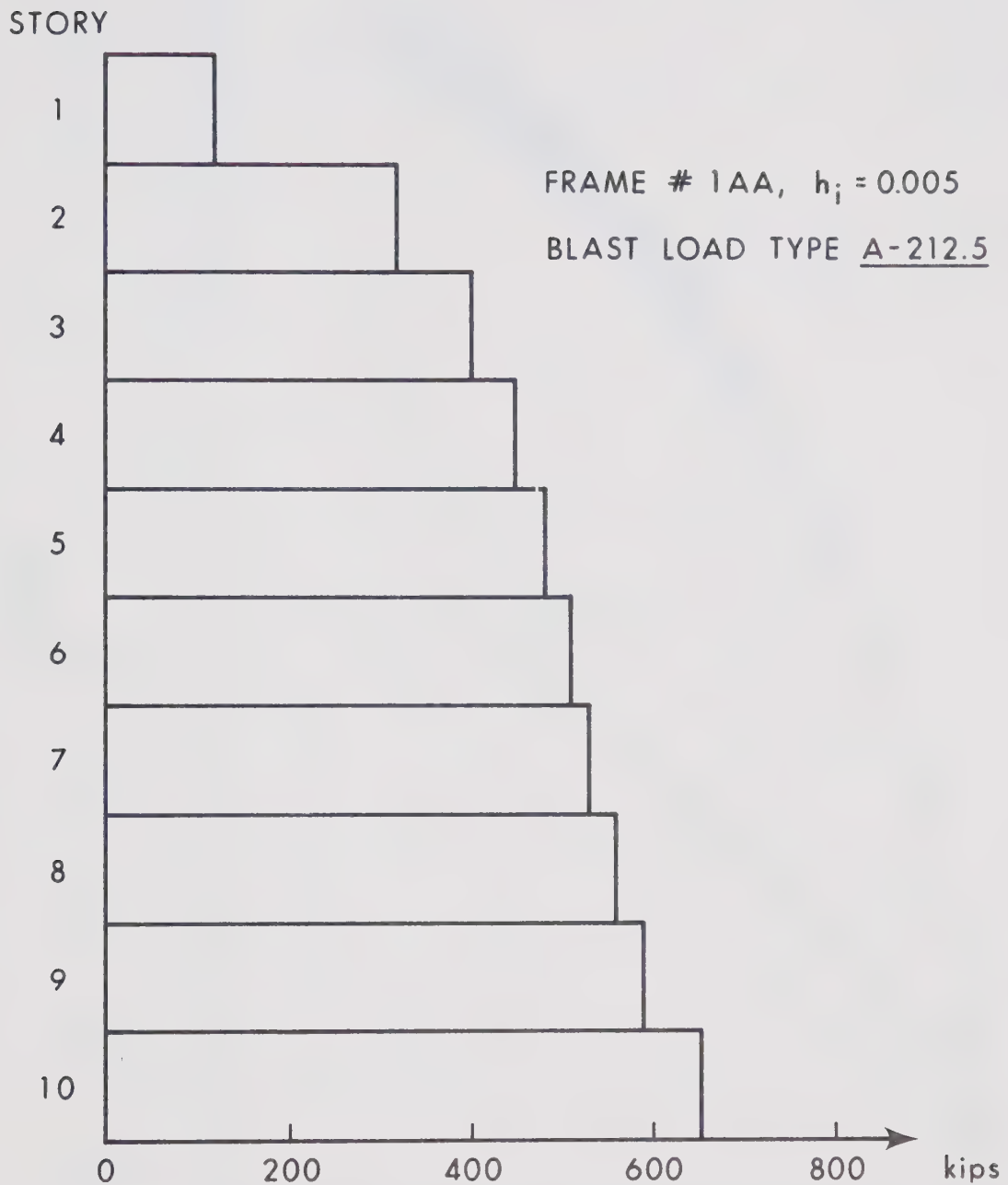


Fig. 4-25 Maximum Story Shears for FRAME#1AA
Subjected to Blast Load Type A-212.5

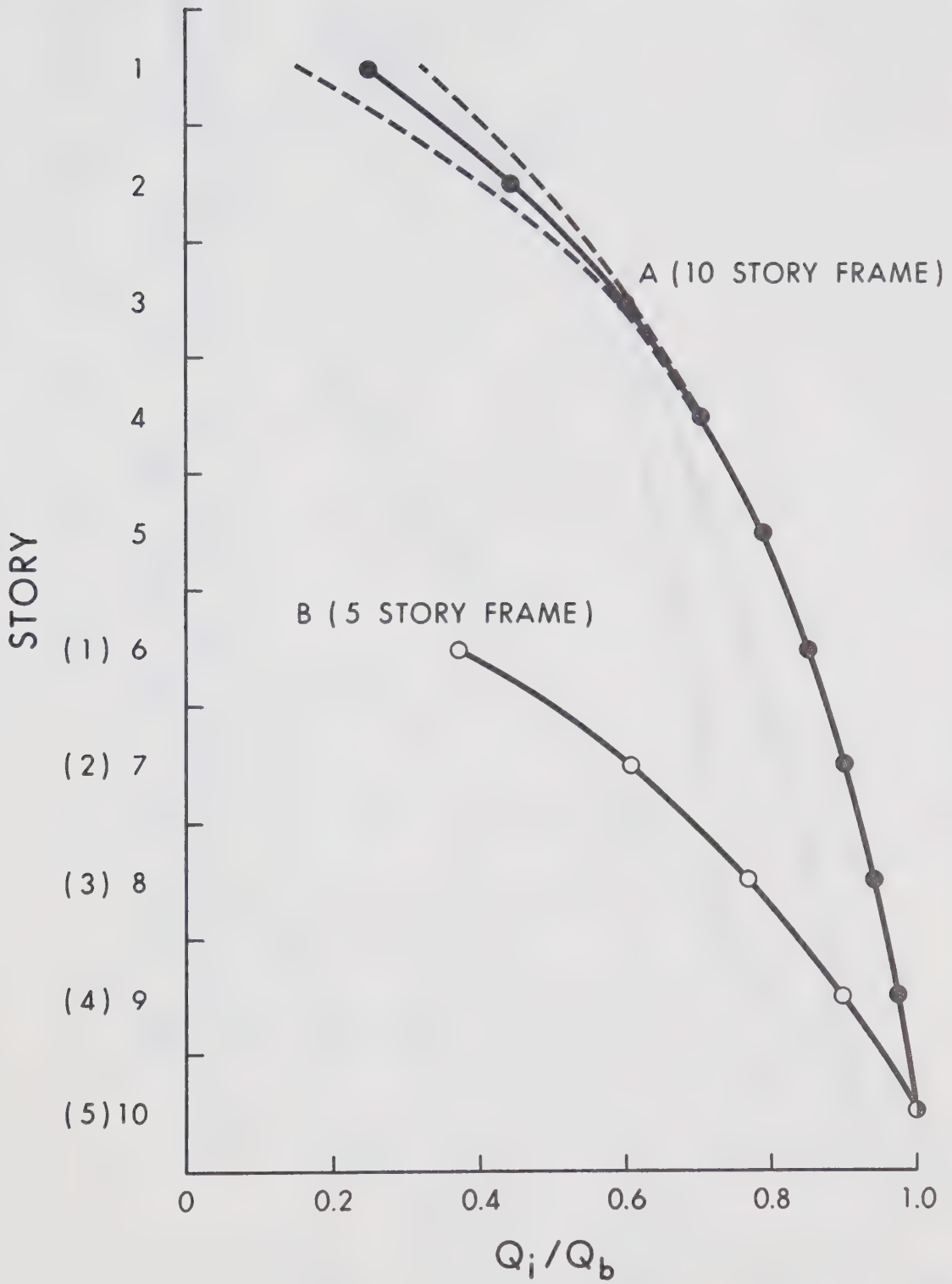


Fig. 4-26 Maximum Story Shears Typical for Regular Type of Frames

STORY

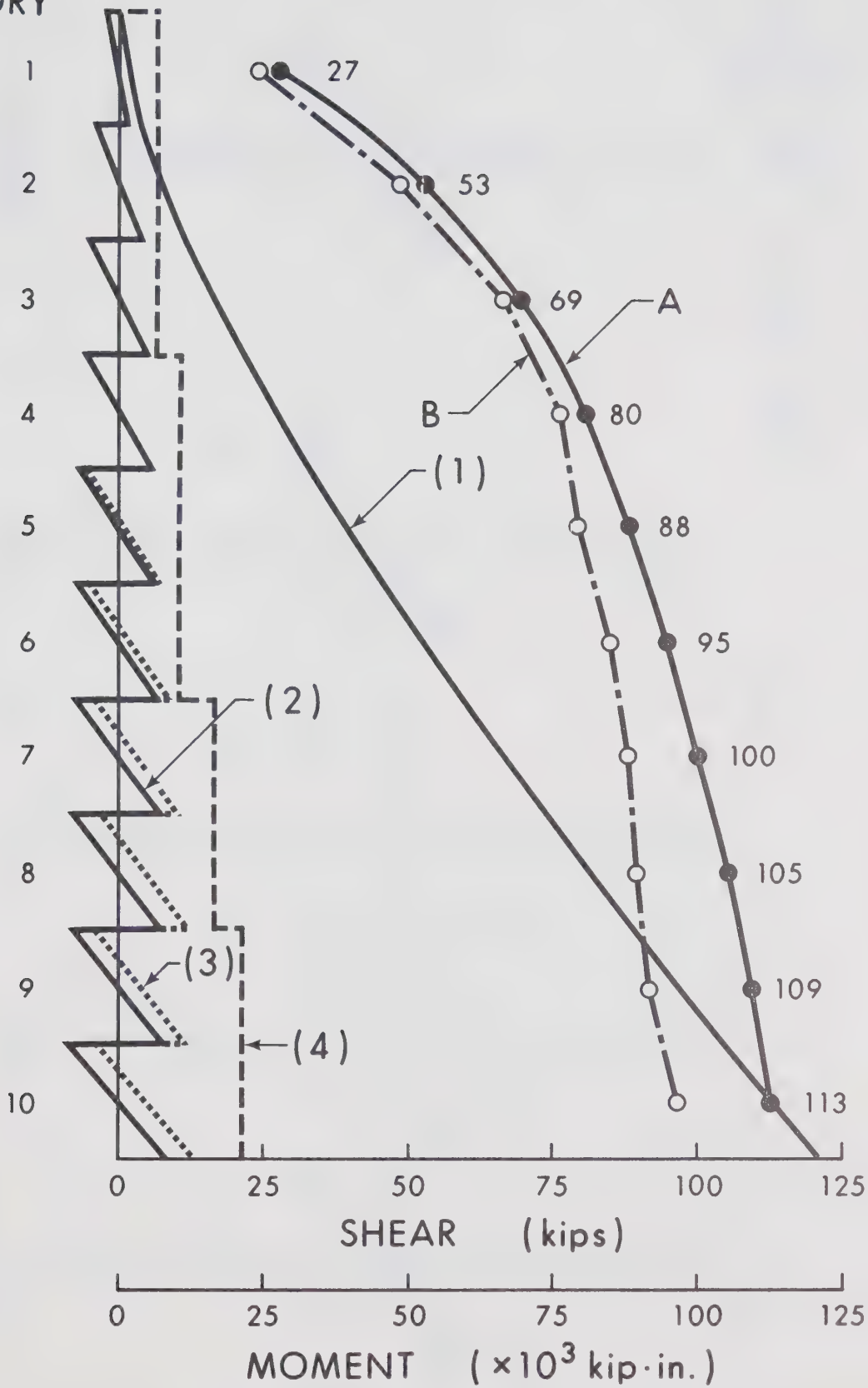


Fig. 4-27 Correlation Between Story Shears and Strength of Columns

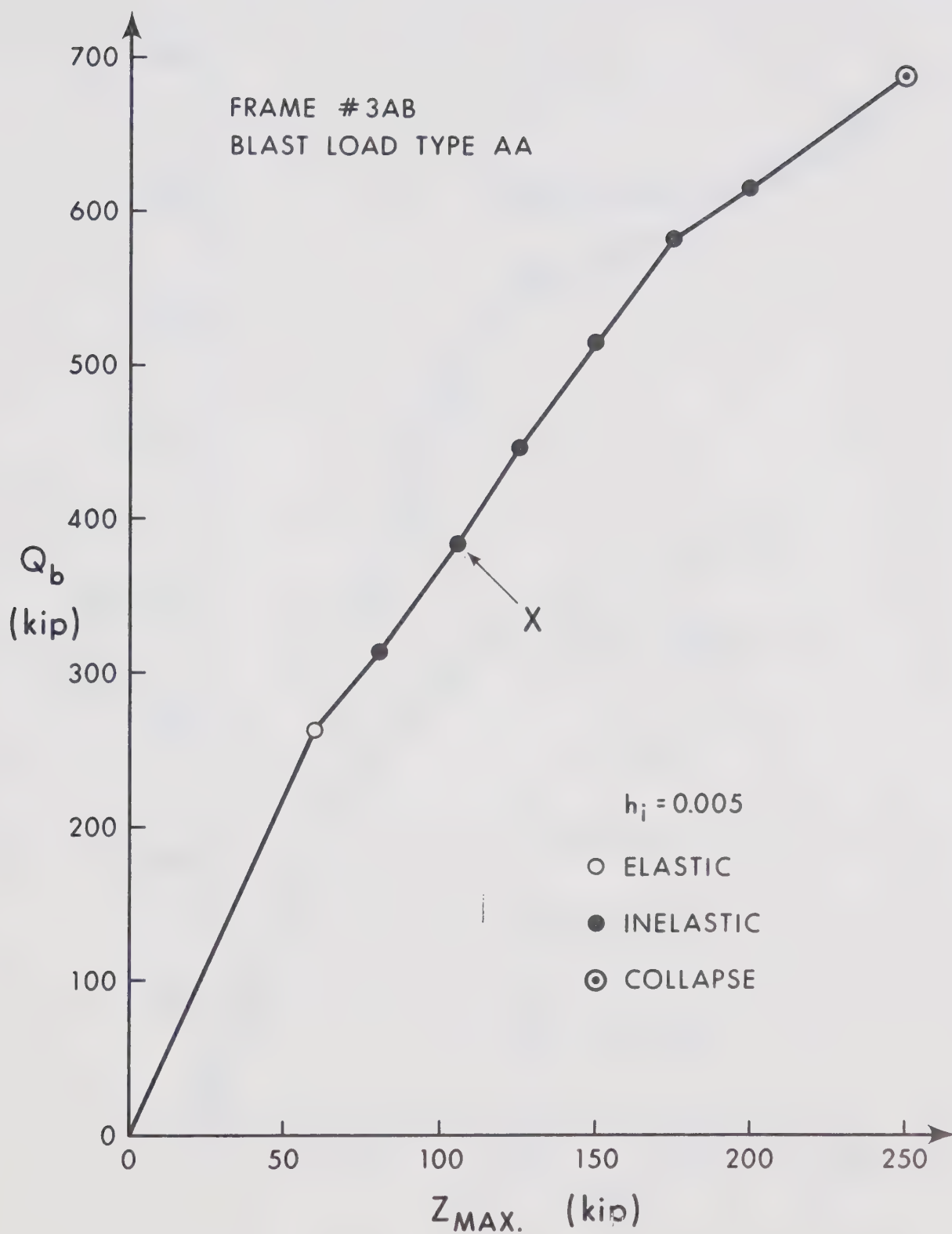


Fig. 4-29 Blast Load Intensity (Type AA) vs. Maximum Base Shear for FRAME#3AB

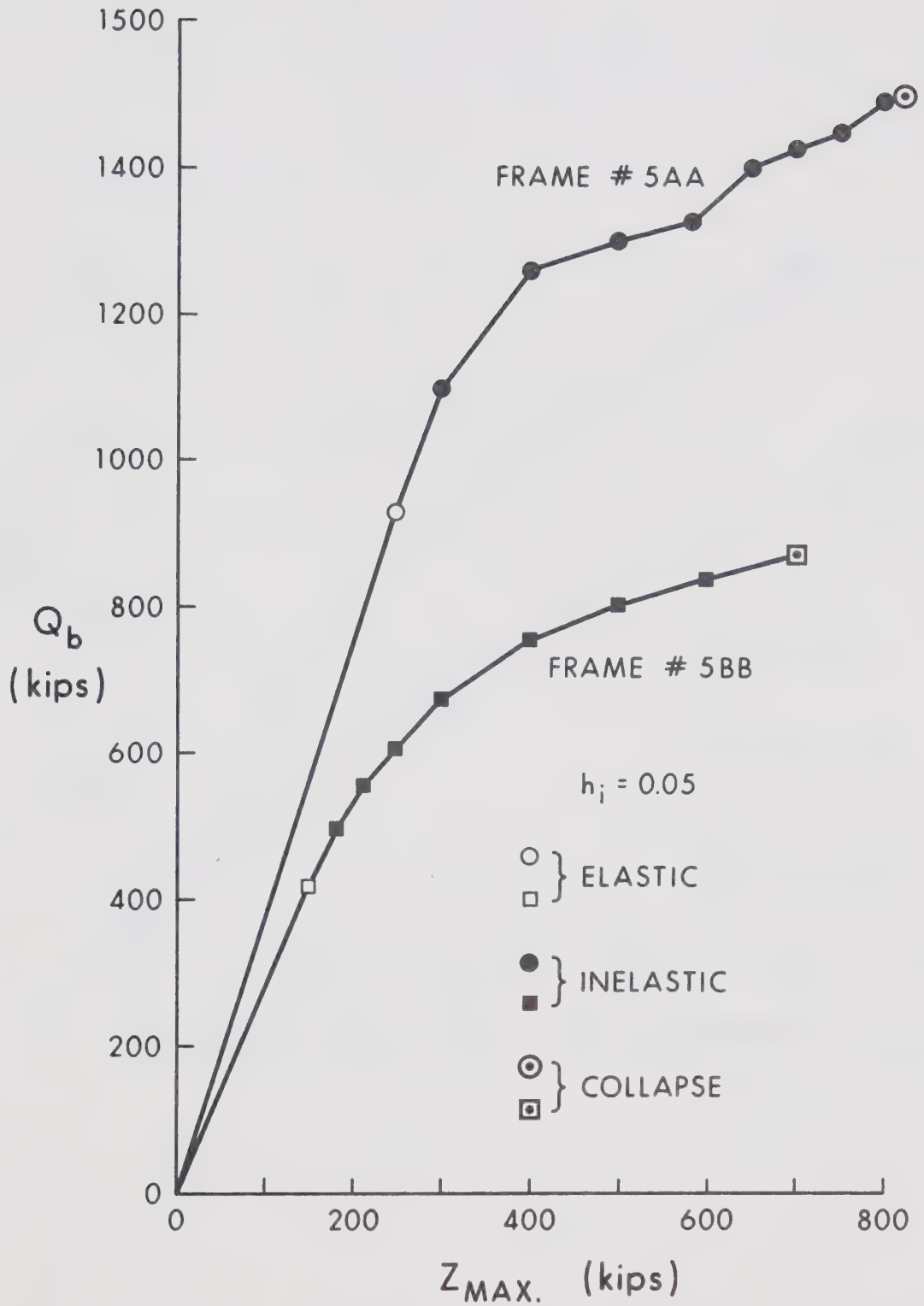


Fig. 4-30 Blast Load Intensity (Type AA) vs. Maximum Base Shear for FRAME#5AA and FRAME#5BB

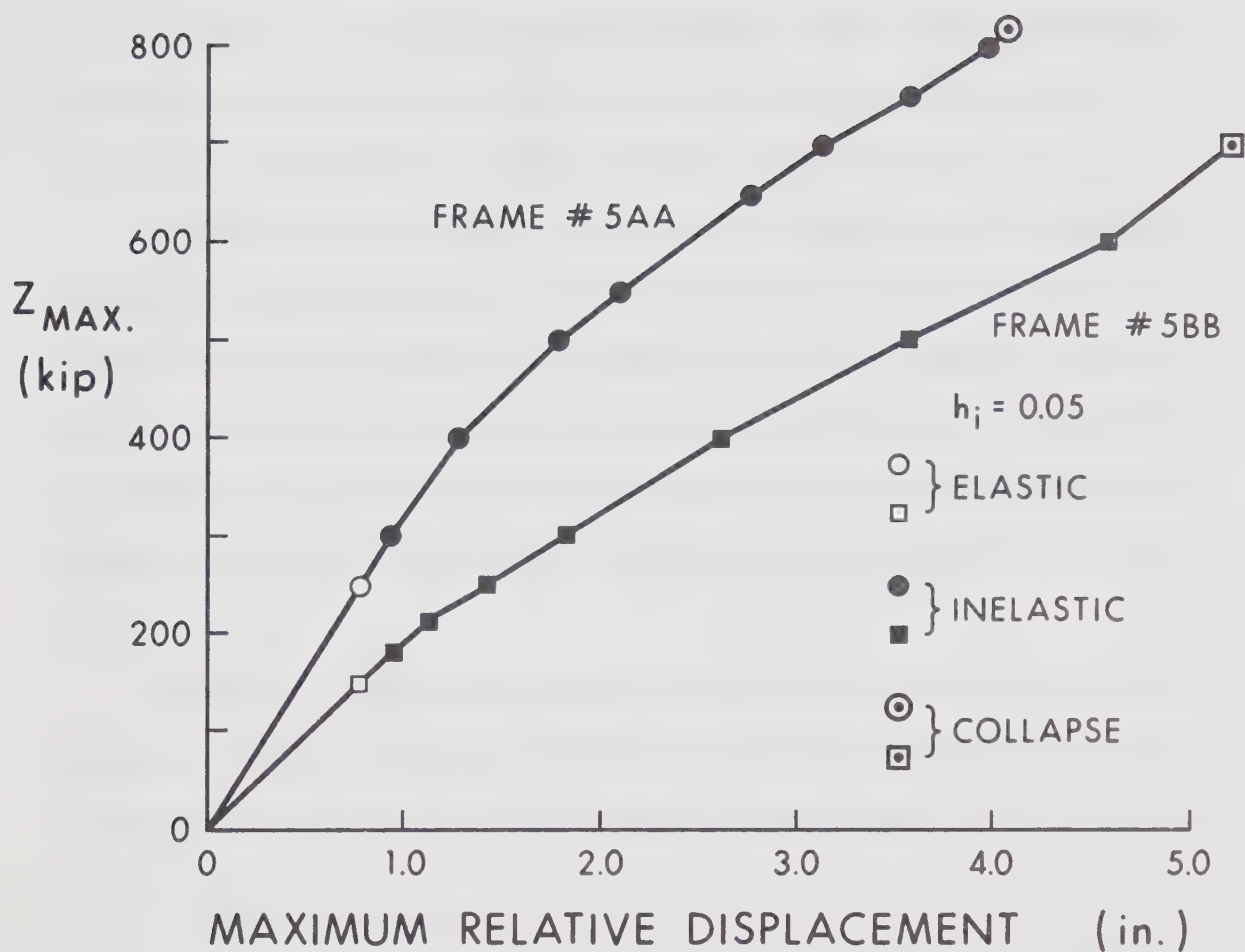


Fig. 4-31 Blast Load Intensity (Type AA) vs. Maximum Relative Displacement for FRAME#5AA and FRAME#5BB

Chapter 5.

DESIGN PROCEDURE

5-1 Introduction.

Based on the knowledge obtained from the behavioral study, a design procedure for steel frames required to resist blast loads is proposed in this chapter.

If this procedure is followed, a designer should be able to select a proper (if not optimum) set of members for columns and beams with relatively few steps. After the members are selected, the details should be designed carefully enough so that the ductility is not reduced by premature lateral or local buckling or by connection failure.

Special attention should be paid to irregular structures as the present procedure may require modification and additional checks for these structures.

5-2 Design Procedure.

The procedure presented in this section attempts to assist in selecting member sizes for a frame subjected to a blast load. The frame determined by this procedure is expected to have a response characterized by moderate inelastic action with yielding occurring mainly in the beam members (the response as indicated by point X or Y

in Fig. 4-16, or by point X in Fig. 4-24). The frame will have, in addition, a reserve capacity to withstand a blast load with an intensity at least twice that of the design blast load.

The procedure may also be used for checking the adequacy of existing frames against possible blast loads. However, if the structural arrangement of the frame is very different from that recommended in Sec. 4-6, there is a possibility that the procedure is not applicable. It is advisable to carry out a detailed dynamic analysis for such a frame.

The procedure is described in the next eight steps. These steps are also shown in the format of a flow chart diagram in Fig. 5-1.

STEP 1: Determine the configuration of the building, the dimension of the frames and the type of exterior walls.

The first step in a design is to determine the overall dimensions, number of stories and number of bays. It is also necessary to investigate if the finished building would act as a closed box-like structure or a partially open box-like structure when subjected to a blast load.

STEP 2: Determine the average pressure-time function of the possible blast. Determine the vector $\{r\}$ and the function $Z(t)$ in the sense explained in Sec. 3-7-1.

The magnitude of the detonation and the location of

the building must be specified. Then, the blast load function, $Z(t)$, and the vector, $\{r\}$, are calculated in accordance with the procedure shown in Appendix E.

STEP 3: Estimate the fundamental natural period, T_1 , of the structure.

It should be noted that for the usual type of blast load, the more flexible the frame, the smaller is the required resistance of the frame members. Therefore, it is often better to select a flexible frame (i.e., a frame with a longer fundamental natural period) if the deflections due to static loads are within the allowable limits.

STEP 4: Calculate the modified total impulse, I^* , of the blast load for the frame with the assumed natural period.

The modified total impulse, I^* , is calculated using Eq. 4-8. If the chart showing the relationship between the modified impulse per standard floor, i^* , and the fundamental natural period (similar to that shown in Fig. 4-20 or 4-21) is available, I^* can be calculated using Eq. 4-12.

STEP 5: Estimate the maximum base shear, Q_b .

The estimation of the maximum base shear, Q_b , is given by Eq. 4-11. When using this equation, the value of ρ between 4 and 5 may be selected depending upon the amount of damping expected and the type of frame. (The median for ρ is approximately 4.4.)

STEP 6: (For the first trial only.) Select the member sizes for the frame.

This step is initiated by calculating the required strength at the bottom story using Eq. 4-16. The column sizes for the bottom stories are first selected, then for the other stories in turn. The ratio of column stiffness at the bottom story to that at the top story should be approximately between 2 and 5 for ten-story frames or between 1 and 3 for five-story frames; and the average stiffness of the beam members should be slightly less (say, $1/2$ to 1) than the average stiffness of column members, as discussed in Sec. 4-6.

The natural period of the frame is then computed using the empirical formula given by Eq. 4-1. If this value of the natural period is approximately the same as that assumed in Step 3, proceed to Step 7. If the difference between the assumed and the calculated natural periods is rather large, go back to Step 4 with this new value of the natural period (it is also possible to select a new design at this stage and calculate the natural period of this frame; then go back to Step 4). Or else, if the difference is minor, the frame members may be modified (mainly the beams) so that the natural period of the frame becomes practically the same as that assumed in Step 3, and proceed to Step 7.

STEP 7: Check if the assumed frame is adequate with respect to strength.

Based on the maximum base shear, Q_b , obtained in Step 5, the maximum shears at other stories are estimated according to Curve A in Fig. 4-26 for ten-story frames or curve B in the same figure for five-story frames. For other structures the proportion may be obtained by interpolation.

When the maximum story shears are determined, it is possible to check if the required strength is within that provided, by following the procedure used in the example calculation in Sec. 4-7.

If the frame is adequate, the design then proceeds to Step 8. If not, a new set of member sizes is selected, the fundamental natural period is calculated using Eq. 4-1, and the design returns to Step 4.

STEP 8: Perform dynamic analysis.

It is always advisable to perform a dynamic analysis on a model which represents the actual frame reasonably well, in order to see if the frame designed above does behave as expected. (If the selection of frame conforms to the recommendations given in Secs. 4-6-1 and 4-6-2, the dynamic analysis may be omitted as the frames obtained in the above steps should behave satisfactory against given

blast loads.)

In practice, two or three possible designs may be compared here. The final selection should be based on the results of such an analysis as shown in Sec. 4-8.

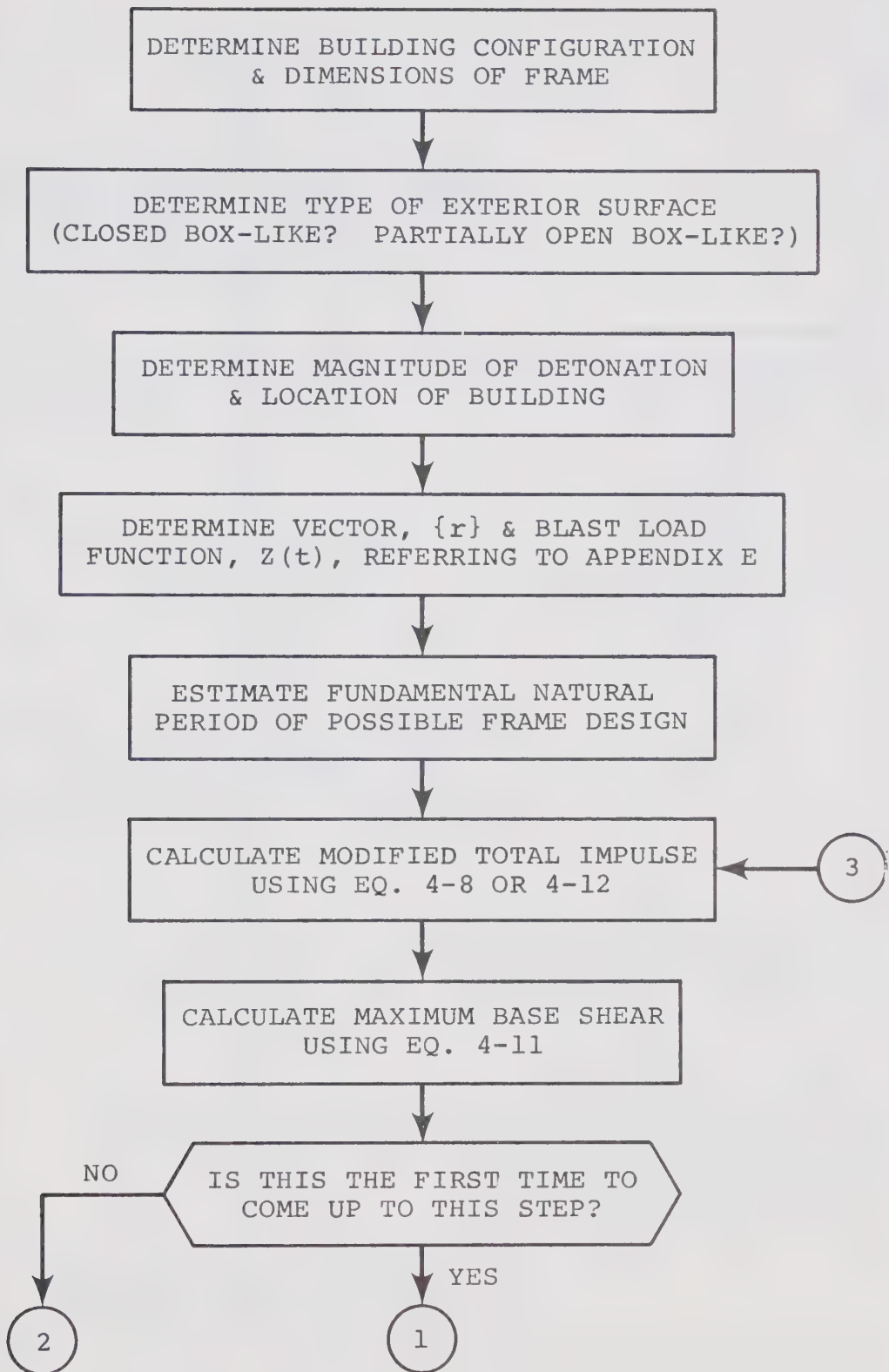


Fig. 5-1 Design Procedure (to be continued)

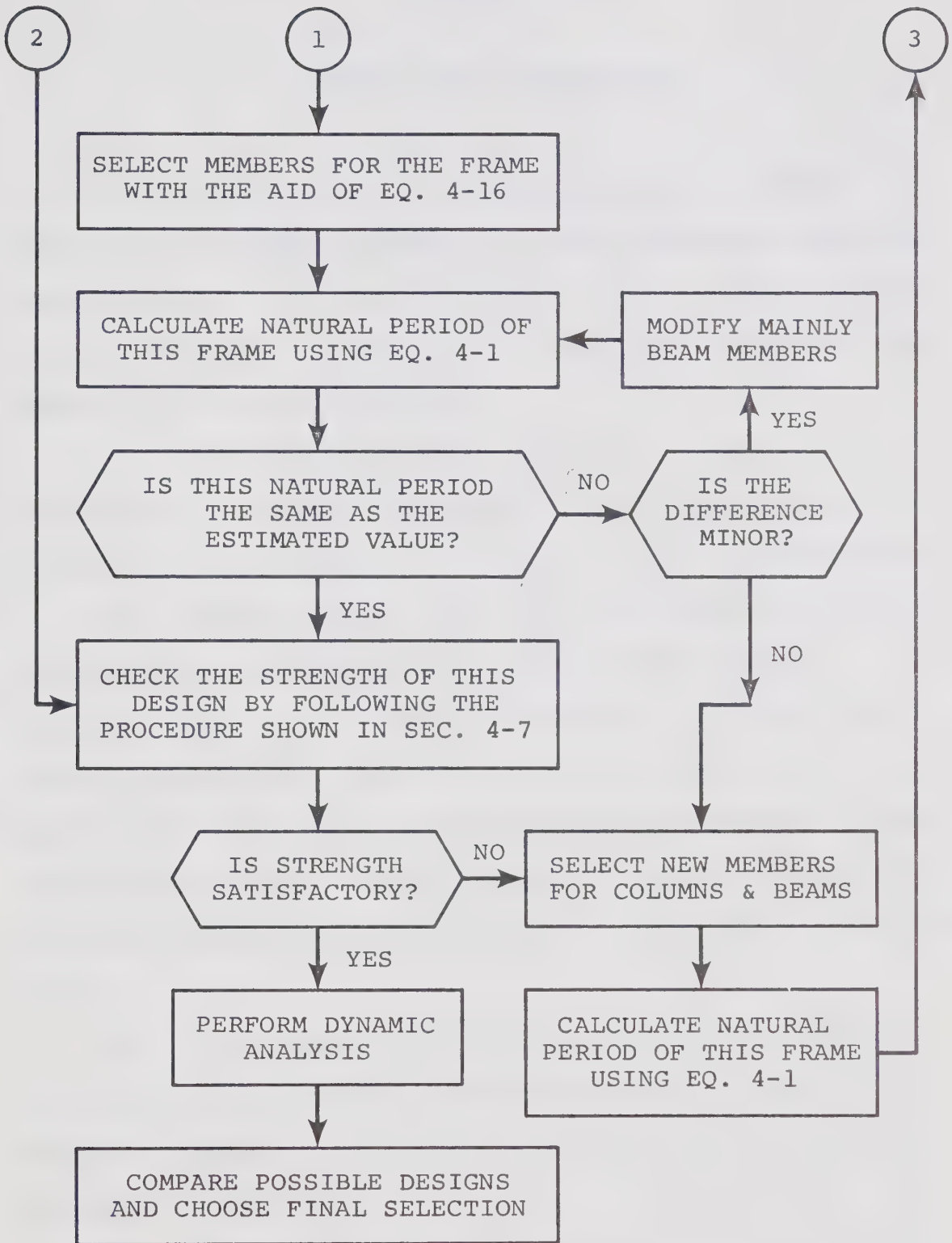


Fig. 5-1 (Continued) Design Procedure

Chapter 6.

SUMMARY AND CONCLUSIONS

In Chapters 2 and 3, a procedure for the dynamic analysis of a frame deformed into the inelastic range has been presented. A computer program based on this procedure is presented in Appendix D. The main features of this method are listed as follows:

- 1) The analytical model can have as many stories and bays as the actual frame has. The frame need not be symmetric. A shearwall structure can also be considered.
- 2) Either a blast load or an earthquake motion may be applied to the frame as an external disturbance.
- 3) Inelastic action and reversals of strain are taken into account. An equivalent rotational spring developed to consider these factors makes the inelastic dynamic calculation simpler, thus a dynamic analysis of multistory, multibay frame is performed within a reasonable computation time.
- 4) A trilinear moment-curvature relationship is assumed for all members. The hysteresis rule used in the analysis (shown in Fig. 2-15) is similar to that proposed by Kato and Akiyama³.
- 5) The $P-\Delta$ effect is considered in an approximate manner. The properties of an equivalent rotational spring

are prepared to include this effect.

6) The effect of shear deformations of beams and columns, the effect of semi-rigid joints, and the effect of shear deformations in the joint panels can be considered by modifying the characteristics of the equivalent rotational spring.

7) Uniformly distributed loads may be applied to beams. Thus, it is possible to analyze the combined effect of both gravity loads and dynamic loads.

8) The bases of the bottom story columns are attached to the foundations by elastic rotational springs.

9) The preparation of input data (determination of the characteristics of equivalent rotational springs) is simplified by using a separate program developed for this purpose (Computer Program I, Appendix B).

A behavioral study was performed in Chapter 4 using the above procedure. The study was focussed on the dynamic behavior of steel frames subjected to blast loads. Responses of such frames, designed under various conditions, were obtained in search of a suitable design procedure. The sizes of frames studied here were 5 or 10 stories in height and between 1 and 4 bays in width. (The empirical formula for the natural period was checked against frames ranging from 2 to 40 stories and 1 to 4 bays.) The connections between the lower ends of the bottom story columns

and the ground are assumed to be completely fixed. The effect of strain-hardening and the $P-\Delta$ effect were taken into account, but these effects were not evaluated specifically. Other secondary effects were ignored. The conclusions from this study are listed as follows.

1) The fundamental natural period, T_1 , of a frame can be estimated using Eq. 4-1; i.e.,

$$T_1 = T_0 h \sqrt{\beta/\alpha} \cdot N_s/10$$

in which symbols are as explained in Sec. 4-3.

2) The shape of blast load-time function, $Z(t)$, does not significantly affect the response; the response is mainly influenced by the modified total impulse of the blast load, I^* , which is defined in Eq. 4-8; i.e.,

$$I^* = \int_0^\infty f(t) Z(t) dt \sum_{i=1}^{N_s} r_i$$

where

$$f(t) = \begin{cases} \frac{1}{2} (1 + \cos \frac{2\pi}{T_1} t) & \text{for } \frac{T_1}{2} \geq t \geq 0 \\ 0 & \text{for } t > \frac{T_1}{2} \end{cases}$$

3) The maximum base shear developed, Q_b , can be estimated by Eq. 4-11; i.e.,

$$Q_b = \frac{\rho I^*}{T_1}$$

where ρ is approximately 4.4. This formula is valid in

the elastic range and for moderate inelastic action.

4) The variation in column stiffnesses along the height should be as small as possible. The recommended value for the ratio of stiffness at the bottom story to that at the top story ranges from 2 to 5 for ten-story frames and from 1 to 3 for five-story frames.

5) The average stiffness of beam members should be a little less (say, 50% to 100%) than the average stiffness of column members.

6) The maximum response shear for every story is distributed approximately as shown by curve A for ten-story frames and by curve B for five-story frames, both in Fig. 4-26.

7) It is possible to check if a frame has enough capacity to resist the assumed blast load in accordance with the procedure explained in Sec. 4-7. A crude estimate of required strength for the bottom story columns, M_b , (on the average) is given by Eq. 4-16; i.e.,

$$M_b = L \frac{Q_b}{N_b + 1} ,$$

where L may be taken equal to 70% to 100% of the bottom story height.

Based on the knowledge obtained from the behavioral study, a tentative procedure for a design of building against a blast load has been proposed in Chapter 5.

REFERENCES

1. Jennings, P.C. and Husid, P., "Collapse of Yielding Structures During Earthquakes," Proceedings of ASCE, Journal of the Engineering Mechanics Division, Vol. 94, No. EM5, October 1968, pp. 1045-1065.
2. Thomaidis, S.S., "Earthquake Response of Systems with Bilinear Hysteresis," Proceedings of ASCE, Journal of the Structural Division, Vol. 90, No. ST4, August 1964, pp. 123-143.
3. Kato, B. and Akiyama, H., "Inelastic Bar Subjected to Thrust and Cyclic Bending," Proceedings of ASCE, Journal of the Structural Division, Vol. 95, No. ST1, January 1969, pp. 33-56.
4. Arnold, P., Adams, P.F. and Lu, L.W., "The Effect of Instability on the Cyclic Behavior of a Frame," Report No. 297-24, Fritz Engineering Laboratory, Lehigh University, Bethlehem, Pa., September 1966.
5. Wakabayashi, M., et al, "Inelastic Behavior of Full Scale Steel Frames," Annual Bulletin No. 13-A, Disaster Prevention Research Institute, University of Kyoto, Japan, March 1970.
6. Jennings, P.C., "Response of Simple Yielding Structures to Earthquake Excitation," A thesis submitted in partial fulfillment of the requirement for the degree of Doctor of Philosophy, California Institute of Technology, Pasadena, Calif., 1963.
7. Goel, S.C. and Berg, G.V., "Inelastic Earthquake Response of Tall Steel Frames," Proceedings of ASCE, Journal of the Structural Division, Vol. 94, No. ST8, August 1968, pp. 1907-1934.
8. Oden, J.T., "Finite Elements of Nonlinear Continua," McGraw-Hill Book Co., New York, N.Y., 1972.
9. Rajasekaran, S. and Murray, D.W., "Solution Techniques for Nonlinear Equations," Structural Engineering Report, Dept. of Civil Engineering, University of Alberta, Edmonton, Alberta, to be published.

10. Yarimci, E., Yura, J.A. and Lu, L.W., "Techniques for Testing Structures Permitted to Sway," *Experimental Mechanics*, SESA, Vol. 7, No. 8, August 1967, p. 321.
11. Majumdar, S.N.G., MacGregor, J.G. and Adams, P.F., "Experimental and Analytical Study of the Behavior of Steel Frame-Shear Wall Structures," *Structural Engineering Report No. 27*, Department of Civil Engineering, University of Alberta, Edmonton, Alberta, August 1970.
12. Naka T., et al, "Static and Dynamic Behavior of Steel Beam-to-Column Connections," *Yawata Technical Report No. 256*, Yawata Iron & Steel Co. Ltd., Tokyo, Japan, September 1966, pp. 98-113 (in Japanese) and pp. 263-266 (in English).
13. Munse, W.H., Bell, N.G. and Cherson, E., Jr., "Behavior of Beam-to-Column Connections," *Transactions, ASCE*, Vol. 126, Part II, 1961, pp. 729-749.
14. "The Effects of Nuclear Weapons," edited by S. Glasstone, The U.S. Atomic Energy Commission, U.S. Government Printing Office, Washington 25, D.C., 1962, Revised Edition Reprinted 1964.
15. Brode, H.L., "Blast Wave from a Spherical Charge," *The Physics of Fluids*, Vol. 2, No. 2, March-April 1959, pp. 217-229.
16. Brode, H.L., "Numerical Solution of Spherical Blast Waves," *Journal of Applied Physics*, Vo. 26, No. 6, June 1955, pp. 766-775.
17. Henderson, G.H., "Dynamic Structural Analysis with Short Time History," *Proceedings of ASCE, Journal of the Structural Division*, Vol. 91, No. ST3, June 1965, pp. 1-24.
18. Norris, C.H., et al, "Structural Design for Dynamic Loads," *McGraw-Hill Book Co.*, New York, N.Y., 1959.
19. Newmark, N.M., "An Engineering Approach to Blast Resisting Design," *Transactions of ASCE*, Vol. 121, 1956, pp. 45-64.

20. "Design of Structures to Resist Nuclear Weapons Effects," prepared by the Committee on Structural Dynamics of the Engineering Mechanics Division, ASCE Manual of Engineering Practice No. 42, 1961.
21. Brode, H.L., "Review of Nuclear Weapons Effects," Annual Review of Nuclear Science, Vol. 18, 1968, pp. 153-202.
22. Newmark, N.M., "External Blast," Planning and Design of Tall Buildings, ASCE-IABSE International Conference Preprints: Reports Vol. Ib-8, ASCE, New York, N.Y., August 1972.
23. Strong Earthquake Response Analysis Committee (SERAC), "Digital Values Used for Analog Computation by SERAC," Preprint of SERAC Report No. 6, Tokyo, Japan, October 1964.
24. "Strong Motion Earthquake Accelerograms--Digitized and Plotted Data," Earthquake Engineering Research Laboratory, California Institute of Technology, Pasadena, Calif.
 Vol. I - Uncorrected Accelerograms
 Part A - Accelerograms IA1 through IA20, July 1969.
 Part B - Accelerograms IB21 through IB40, October 1970.
25. Strong Earthquake Response Analysis Committee (SERAC), "Nonlinear Response Analysis of Tall Buildings to Strong Earthquake and its Application to Dynamic Design," Tokyo, Japan.
 SERAC Report No. 6, October 1966.
 SERAC Report No. 7, July 1969.
26. Kurata, E., Ishizaka, T. and Tsuchida, H., "Annual Report on Strong-Motion Earthquake Records in Japanese Ports (1971)," Technical Notes of the Port and Harbour Research Institute, Ministry of Transport, Yokosuka, Japan, No. 136, March 1972.
27. Jennings, P.C., Housner, G.W. and Tsai, N.C., "Simulated Earthquake Motions," Earthquake Engineering Research Laboratory, California Institute of Technology, Pasadena, Calif., April 1968.

28. Gill, S., "A Process for the Step-by-Step Integration of Differential Equations in an Automatic Digital Computing Machine," Proceedings, Cambridge Philosophical Society, Vol. 47, 1951, pp. 96-108.
29. Milne, W.E., "Numerical Solution of Differential Equations," Second Revised and Enlarged Edition, Dover Publications Inc., New York, N.Y., 1970.
30. Newmark, N.M., "A Method of Computation for Structural Dynamics," Transactions of ASCE, Paper No. 3384, Vol. 127, 1962, Part I, pp. 1406-1435.
31. Ralston, A., "A First Course in Numerical Analysis," McGraw-Hill Book Co., New York, N.Y., 1965.
32. Penzien, J., "Dynamic Response of Elasto-Plastic Frames," Proceedings of ASCE, Journal of the Structural Division, Vol. 86, No. ST7, July 1960, pp. 81-94.
33. Veletsos, A.S. and Newmark, N.M., "Effect of Inelastic Behavior on the Response of Simple Systems to Earthquake Motions," Proceedings, Second World Conference on Earthquake Engineering, Vol. II, Tokyo, Japan, 1960, pp. 895-912.
34. Penzien, J., "Elasto-Plastic Response of Idealized Multi-Story Structures During Earthquakes," Proceedings, Second World Conference on Earthquake Engineering, Vol. II, Tokyo, Japan, 1960, pp. 739-760.
35. Hisada, T., Nakagawa, K. and Izumi, M., "Earthquake Response of Idealized Twenty Story Buildings Having Various Elasto-Plastic Properties," Proceedings, Third World Conference on Earthquake Engineering, Vol. II, Auckland and Wellington, New Zealand, 1965, pp. II-168 - II-184.
36. Clough, R.W., Benuska, K.L. and Wilson, E.L., "Inelastic Earthquake Response of Tall Buildings," Proceedings, Third World Conference on Earthquake Engineering, Vol. II, Auckland and Wellington, New Zealand, 1965, pp. II-68 - II-89.
37. Clough, R.W. and Benuska, K.L., "Nonlinear Earthquake Behavior of Tall Buildings," Proceedings of ASCE, Journal of the Engineering Mechanics Division, Vol. 93, No. EM3, June 1967, pp. 129-146.

38. Walpole, W.R. and Shepherd, R., "The Inelastic Response of a Steel Frame," Proceedings, Fourth World Conference on Earthquake Engineering, Vol. II, Santiago, Chile, 1969, pp. A4-195 - A4-204.
39. Goel, S.C., "P- Δ and Axial Column Deformation in Aseismic Frames," Proceedings of ASCE, Journal of the Structural Division, Vol. 95, No. ST8, August 1969, pp. 1693-1711.
40. Sun, C.K., "Gravity Effect on the Dynamic Stability of Inelastic Systems," A dissertation submitted in partial fulfillment of the requirement for the degree of Doctor of Philosophy, University of Michigan, Ann Arbor, Mich., August 1971.
41. Lionberger, S.R. and Weaver, W., Jr., "Dynamic Response of Frames with Nonrigid Connections," Proceedings of ASCE, Journal of the Engineering Mechanics Division, Vol. 95, No. EM1, February 1969, pp. 95-114.
42. Nielsen, N.N., "Vibration Tests of a Nine-Story Steel Frame Building," Proceedings of ASCE, Journal of the Engineering Mechanics Division, Vol. 92, No. EM1, February 1966, pp. 81-110.
43. Jennings, P.C., Matthiesen, R.B. and Hoerner, J.B., "Forced Vibration of a 22-story Steel Frame Building," Earthquake Engineering Laboratory, California Institute of Technology and Earthquake Engineering and Structures Laboratory, University of California at Los Angeles, February 1971.
44. Gulkan, P. and Sozen, M.A., "Response and Energy Dissipation of Reinforced Concrete Frames Subjected to Strong Base Motions," Structural Research Series No. 377, Civil Engineering Studies, University of Illinois, Urbana, Ill., May 1971.
45. Hoerner, J.B., "Modal Coupling and Earthquake Response of Tall Buildings," Thesis submitted in partial fulfillment of the requirements for the degree of Doctor of Philosophy, California Institute of Technology, Pasadena, Calif., May 1971.
46. Nigam, N.C., "Yielding in Framed Structures under Dynamic Loads," Proceedings of ASCE, Journal of the Engineering Mechanics Division, Vol. 96, No. EM5, October 1970, pp. 687-709.

47. Wen, R.K. and Farhoomand, F., "Dynamic Analysis of Inelastic Space Frames," Proceedings of ASCE, Journal of the Engineering Mechanics Division, Vol. 96, No. EM5, October 1970, pp. 667-686.
48. Toridis, T.G. and Khozeimeh, K., "Inelastic Response of Frames to Dynamic Loads," Proceedings of ASCE, Journal of the Engineering Mechanics Division, Vol. 97, No. EM3, June 1971, pp. 847-863.
49. Beedle, L.S., et al, "Structural Steel Design," The Ronald Press Co., New York, N.Y., 1964.
50. "General Information on Structural Steels," Canadian Institute of Steel Construction, Pub. No. 2074, March 1970.
51. Yokobori, T., "An Interdisciplinary Approach to Fracture and Strength of Solids," Wolters-Noordhoff Scientific Publications Ltd., Groningen, Netherlands, 1968.
52. Lessells, J.M., "Strength and Resistance of Metals," John Wiley & Sons, Inc., New York, N.Y., 1954.
53. Canadian Institute of Steel Construction, "Handbook of Steel Construction," C.I.S.C., Toronto, October 1970, pp. 6.28-6.41.
54. Nakamura, Y. and Litle, W.A., "Plastic Design Method of Multi-Story Planar Frames with Deflection Constraints," Report No. R68-12, Department of Civil Engineering, Massachusetts Institute of Technology, Cambridge, Mass., March 1968.
55. Goel, S.C., "Inelastic Behavior of Multistory Building Frames Subjected to Earthquake Motion," A dissertation submitted in partial fulfilment of the requirement for the degree of Doctor of Philosophy in the University of Michigan, Ann Arbor, Mich., December 1967.
56. Joint Committee of the WRC and the ASCE, "Plastic Design in Steel--A Guide and Commentary," ASCE - Manuals and Reports on Engineering Practice - No. 41, 1971.
57. Ketter, R.L., Kaminsky, E.L. and Beedle, L.S., "Plastic Deformation of Wide-Flange Beam Columns," Transactions, ASCE, Vol. 120, 1955, pp. 1028-1069.

58. Lay, M.G. and Gimsing, N., "Experimental Studies of the Moment-Thrust-Curvature Relationship," The Welding Journal, Vol. 44, February 1965, pp. 86s-96s.
59. Lay, M.G. and Smith, P.D., "Role of Strain Hardening in Plastic Design," Proceedings of ASCE, Journal of the Structural Division, Vol. 91, No. ST3, June 1965, pp. 25-43.
60. Driscoll, G.C., Jr., et al, "Plastic Design of Multi-story Frames," Lecture Notes, Fritz Engineering Laboratory Report No. 273.20, Lehigh University, Bethlehem, Pa., 1965.
61. Arnold, P., Adams, P.F. and Lu, L.W., "The Effect of Instability on the Cyclic Behavior of a Frame," Report No. 297.24, Fritz Engineering Laboratory, Lehigh University, Bethlehem, Pa., September 1966.
62. Carpenter, L.D. and Lu, L.W., "Behavior of Steel Frames Subjected to Repeated and Reversed Loads," Final Report of the 8th Congress of IABSE at New York, September 1968.
63. Hanson, R.D., "Comparison of Static and Dynamic Hysteresis Curves," Proceedings of ASCE, Journal of the Engineering Mechanics Division, Vol. 92, No. EM5, October 1966, pp. 87-113.
64. Wakabayashi, M., et al, "Inelastic Behavior of Full Scale Steel Frames," Bulletin No. 13-A, Disaster Prevention Research Institute, University of Kyoto, Japan, March 1970.
65. Tanabashi, R., et al, "Load Deflection Behaviors and Plastic Fatigue of Wide Flange Beams Subjected to Alternating Plastic Bending; Part I, Experimental Investigation," Transactions of Architectural Institute of Japan, No. 175, September 1970, pp. 17-26.
66. Tanabashi, R., Yokoo, Y. and Nakamura, T., "Load Deflection Behaviors and Plastic Fatigue of Wide Flange Beams Subjected to Alternating Plastic Bending; Part III, Steady State Theory," Transactions of Architectural Institute of Japan, No. 177, November 1970, pp. 35-44.

67. Igarashi, S., et al, "Inelastic Behaviors of Structural Steel Sections Under Alternative Loadings; (1) Method of Analysis and Examples," Transactions of Architectural Institute of Japan, No. 169, March 1970, pp. 53-60.
68. Igarashi, S., et al, "Inelastic Behaviors of Structural Steel Sections Under Alternative Loadings; (2) Final State of Resisting Moment and Experimental Study," Transactions of Architectural Institute of Japan, No. 170, April 1970, pp. 39-48.
69. Michael, D., "The Effect of Local Wall Deformations on the Elastic Interaction of Cross Walls Coupled by Beams," Tall Buildings, Proceedings of the Symposium held at the University of Southampton, Pergamon Press Ltd., April 1966, pp. 253-272.
70. Muto, K., "Dynamic Analyses of Structures," Aseismic Design Series No. 4, Maruzen Co., Tokyo, Japan, 1966 (in Japanese).
71. Jensen, C.D., et al, "Welded Interior Beam-to-Column Connections," A.I.A. File No. 13-C, American Institute of Steel Constructions, Inc., 1959.
72. Oden, J.T., "Mechanics of Elastic Structures," McGraw-Hill Book Co., New York, N.Y., 1967.
73. Forsythe, G.E. and Moler, C.B., "Computer Solutions of Linear Algebraic Systems," Prentice Hall, Inc., Englewood Cliffs, N.J., 1967.
74. Wilkinson, J.H., "The Algebraic Eigenvalue Problem," Oxford University Press, London, 1965.
75. Yarimci, E., "Incremental Inelastic Analysis of Framed Structures and Some Experimental Verification," Fritz Engineering Laboratory Report, No. 273-45, Lehigh University, Bethlehem, Pa., 1966.
76. Newmark, N.M. and Rosenblueth, E., "Fundamentals of Earthquake Engineering," Prentice-Hall, Inc., Englewood Cliffs, N.J., 1971.

77. Robertson, L.E. and Chen, P.W., "Application to Design of Research on Wind Effects," Proceedings of International Research Seminar on Wind Effects on Buildings and Structures, held in Ottawa, Canada, in September 1967, Vol. 1, University of Toronto Press, 1968, pp. 83-113.
78. Jourbert, P.N., et al, "The Drag of Bluff Bodies Immersed in a Turbulent Boundary Layer," Proceedings of International Research Seminar on Wind Effects on Buildings and Structures, held in Ottawa, Canada, in September 1967, Vol. 1, University of Toronto Press, 1968, pp. 297-336.
79. Wilson, E.L. and Clough, R.W., "Dynamic Analysis by Step-by-Step Matrix Analysis," Symposium on the Use of Computers in Civil Engineering, Vol. II, Paper No. 45, Lisbon, Portugal, October 1962, pp. 45.1-45.14.
80. Sharpe, R.L. and Kost, G., "Structural Response to Sonic Booms," Proceedings of ASCE, Journal of the Structural Division, Vol. 97, No. ST4, April 1971, pp. 1157-1174.
81. Maglieri, D.J., "Sonic Boom Ground Pressure Measurements for Flights at Altitudes in Excess of 70000 Feet and at Mach Numbers up to 3.0," Proceedings of the Second Conference on Sonic Boom Research, held at NASA, Washington, D.C., May 1968, NASA SP-180, U.S. Government Printing Office, Washington, D.C., 1968.
82. Blume, J.A., "Dynamic Characteristics of Multistory Buildings," Proceedings of ASCE, Journal of the Structural Division, Vol. 94, No. ST2, February 1968, pp. 377-402.
83. Wynhoven, J.H. and Adams, P.F., "Elastic Plastic Analysis of Three Dimensional Structures," Structural Engineering Report No. 29, Department of Civil Engineering, University of Alberta, Edmonton, Alberta, September 1970.

Appendix A

SUPPLEMENTARY EXPLANATION OF SECTION 2-5-1

The load-deflection ($Q-\Delta$) relationship for a cantilever column has been derived for both the elastic and inelastic range in Sec. 2-5-1. The column end is fixed at the base and the material is assumed to have a trilinear $M-\phi$ relationship. The derivation of Eqs. 2-35, 2-36 and 2-39 is explained in detail in this section. The load-deflection relationships for special cases are also demonstrated later in this section.

A-1 Derivation of Eqs. 2-35, 2-36 and 2-39.

The derivation of the $Q-\Delta$ relationship in the elastic range is trivial and the proof is omitted here.

When the moment at the base of the column reaches the plastic moment capacity, the system may be represented as shown in Fig. 2-11. This system will be described using two sets of coordinates as shown in Fig. A-1. The first set of coordinates ($x-y$ coordinates) have their origin at point A where the loads are applied and the second ($X-Y$ coordinates) at point C where the moment in the section is equal to the plastic moment capacity, M_{pc} .

The moment, M , at a distance X from point C is given

by:

$$M = M_{pc} + QX + PY \quad (A-1)$$

The corresponding curvature, ϕ ; i.e.,

$$\phi = -\ddot{Y} \quad (A-2)$$

is on the third branch of the moment-curvature relationship of Fig. 2-12. Therefore, the moment and the curvature are related as follows:

$$M = K_{st}\phi + (M_{pc} - M_i) \quad (A-3)$$

Substituting Eqs. A-1 and A-2 into Eq. A-3, the differential equation describing equilibrium of the portion BC is obtained as:

$$K_{st}\ddot{Y} + PY = -QX - M_i \quad (A-4)$$

As the boundary conditions are

$$\begin{aligned} Y &= 0 \quad \text{at} \quad X = 0 \\ \dot{Y} &= 0 \quad \text{at} \quad X = L_2 \end{aligned} \quad (A-5)$$

Eq. A-4 is solved as

$$Y = C_1 \cos vX + C_2 \sin vX - \frac{Q}{P}X - \frac{M_i}{P} \quad (A-6)$$

where,

$$C_1 = \frac{M_i}{P} \quad , \quad (A-7)$$

$$C_2 = \frac{1}{P} \left\{ M_i \tan vL_2 + \frac{Q}{v \cos vL_2} \right\} \quad , \quad (A-8)$$

and v is as defined in Eq. 2-37. The deflection at point C, Δ_p , is obtained by substituting $X = L_2$ in Eq. A-6, or

$$\begin{aligned}
\Delta_p &= C_1 \cos vL_2 + C_2 \sin vL_2 - \frac{Q}{P}L_2 - \frac{M_i}{P} \\
&= \frac{Q}{P} \left(\frac{\tan vL_2}{v} - L_2 \right) \\
&\quad + \frac{M_i}{P} (\sin vL_2 \tan vL_2 + \cos vL_2 - 1)
\end{aligned}$$

which is Eq. 2-36. The slope at point C, θ_c , is calculated as:

$$\begin{aligned}
\theta_c &= \dot{Y}_{X=0} \\
&= \frac{Q}{P} \left(\frac{1}{\cos vL_2} - 1 \right) + \frac{M_i}{P} v \tan vL_2
\end{aligned} \tag{A-9}$$

The differential equation describing the elastic portion AC is written as:

$$K\ddot{Y} + Py = -Qx \tag{A-10}$$

As the boundary conditions are

$$\left. \begin{aligned} y &= 0 \quad \text{at} \quad x = 0 \\ \dot{y} &= \theta_c \quad \text{at} \quad x = L_1 \end{aligned} \right\} \tag{A-11}$$

the equation is solved as:

$$y = C_3 \cos \mu x + C_4 \sin \mu x - \frac{Q}{P}x \tag{A-12}$$

where

$$C_3 = 0 \tag{A-13}$$

$$C_4 = (\theta_c + \frac{Q}{P}) / \mu \cos \mu L_1 \tag{A-14}$$

The condition that the moment at point C is equal to the plastic moment capacity, M_{pc} , yields the following equation:

$$M_{pc} = QL_1 + P\Delta_e \quad (A-15)$$

where Δ_e is the deflection of point A relative to point C, and is obtained by substituting $x = L_1$ into Eq. A-12; or

$$\Delta_e = C_4 \sin \mu L_1 - \frac{Q}{P} L_1 \quad (A-16)$$

Substituting Eq. A-16 into Eq. A-15 and also substituting Eq. A-14 for C_4 , the following equation results.

$$M_{pc} = (P\theta_c + Q) \tan \mu L_1 / \mu \quad (A-17)$$

If Eq. A-9 is substituted for θ_c in the above equation, the relationship between the applied load, Q , and the length of the inelastic portion, L_2 (or alternately the length of the elastic portion, L_1) is obtained as:

$$Q = \mu M_{pc} \frac{\cos \nu L_2}{\tan \mu L_1} - M_i \nu \sin \nu L_2$$

which is Eq. 2-39. Δ_e may be calculated using Eq. A-16; however, the following expression is simpler

$$\Delta_e = \frac{M_{pc} - QL_1}{P}$$

which is derived from Eq. A-15, and is given in Eq. 2-35.

Thus by assuming the length of inelastic portion, L_2 , the corresponding transverse load, Q , and the total deflection, Δ ; i.e.,

$$\Delta = \Delta_e + \Delta_p$$

as in Eq. 2-34, is determined. If by increasing the inelastic length, L_2 , the moment at the bottom of the column, M_b ,

$$M_b = QL + P\Delta \quad (A-18)$$

reaches the ultimate moment, M_{uc} , collapse of the column is assumed to occur.

A-2 Load-Deflection Relationship When Axial Load is Absent.

The load-deflection ($Q-\Delta$) relationship in the elastic range is given by:

$$\Delta = \frac{L^3}{3K} Q \quad (A-19)$$

for

$$Q \leq \frac{M_p}{L} \quad (A-20)$$

When the moment in the lower portion of the column exceeds the full plastic moment capacity, M_p , the system is similar to that shown in Fig. 2-11. The differential equations can be constructed in a similar manner and only the results are shown here. The notation is the same as that used in the main text.

The total deflection, Δ , is given by

$$\Delta = \Delta_e + \Delta_p ,$$

where

$$\Delta_e = \frac{QL_1^3}{3K} + L_1 \left(\frac{QL_2^2}{2K_{st}} + \frac{M_i L_2}{K_{st}} \right) \quad (A-21)$$

and

$$\Delta_p = \frac{QL_2^3}{3K_{st}} + \frac{M_i L_2^2}{2K_{st}} \quad (A-22)$$

The relationship between the load, Q , and the length of the inelastic portion, L_2 , (or the length of the elastic portion, L_1) is given by the next formula.

$$Q = \frac{M_p}{L_1} \quad (A-23)$$

The complete Q - Δ relationship is obtained as before except that Eqs. 2-35, 2-36 and 2-39 are now replaced by Eqs. A-21, A-22 and A-23.

A-3 Load-Deflection Relationship When the Moment-Curvature Relationship is Elastic-Perfectly Plastic.

The system shown in Fig. 2-11 is considered once more, however, the moment-curvature relationship is now assumed to be elastic-perfectly plastic. In the elastic range, the behavior of this column is the same as that described in Sec. 2-5-1.

After the moment at the bottom of the column reaches the plastic moment capacity, M_{pc} , it is usually assumed that an infinite rotation capacity is available at the bottom of the column. Then the load-deflection (Q - Δ) relationship is written as

$$QL + P\Delta = M_{pc}$$

or

$$Q = -\frac{P}{L}\Delta + \frac{M_{pc}}{L} \quad (A-24)$$

It is not possible, however, to relate the deflection to the curvature as in previous examples. Thus, in order to estimate the maximum deflection for a given value of the ductility ratio, additional factors must be taken into account.

A-4 Load-Deflection Relationship When the Base of the Column is Restrained by a Rotational Spring.

In Fig. 2-11, it is now assumed that the base of the column is now attached to the foundation by an elastic rotational spring having a spring constant, k . Otherwise, the conditions are the same as those in Sec. 2-5-1.

If the entire length of the column remains elastic, the Q - Δ relationship is given by:

$$\Delta = \frac{\frac{QL^3}{3K} \cdot \frac{3(\tan \mu L - \mu L)}{(\mu L)^3} + \frac{QL}{k} \cdot \frac{\tan \mu L}{\mu}}{1 - \frac{P}{k} \cdot \frac{\tan \mu L}{\mu}} \quad (A-25)$$

This formula is valid for Q such that

$$Q \leq M_{pc} \left(\frac{\mu}{\tan \mu L} - \frac{P}{k} \right) \quad (A-26)$$

Once the moment at the base of the column reaches the plastic moment capacity, the behavior is described as shown in Sec. A-1. The differential equation describing the elastic portion

is as shown in Eq. A-10 and that describing the inelastic portion is shown in Eq. A-4. The differences occur only in the boundary conditions. The resulting equations are shown below:

$$\Delta = \Delta_e + \Delta_p$$

as in Eq. 2-34, where

$$\Delta_e = \frac{M_{pc} - QL_1}{P} \quad (A-27)$$

which has the same expression as in Eq. 2-35. Δ_p is given by:

$$\Delta_p = C_1' \cos vL_2 + C_2' \sin vL_2 - \frac{Q}{P}L_2 - \frac{M_i}{P} \quad (A-28)$$

where

$$C_1' = \frac{M_i}{P}, \quad (A-29)$$

and

$$C_2' = \frac{\frac{M_i}{P} v \sin vL_2 + \frac{Q}{P} + \frac{1}{k} \{M_{pc} - M_i (1 - \cos vL_2)\}}{v \cos vL_2 - \frac{P}{k} \sin vL_2} \quad (A-30)$$

The equation describing the relationship between the length of the inelastic portion, L_2 , and the applied load, Q , is given as:

$$Q = \mu M_{pc} \frac{\cos vL_2}{\tan \mu L_1} - M_i v \sin vL_2 - \frac{P}{k} \{M_{pc} - M_i (1 - \cos vL_2) + \mu M_{pc} \frac{\sin vL_2}{\tan \mu L_1}\}$$

... (A-31)

Using these equations, the complete load-deflection curve is obtained as before. In the above equations, if the value of k is set equal to infinity, the equations shown in Sec. 2-5-1 are obtained.

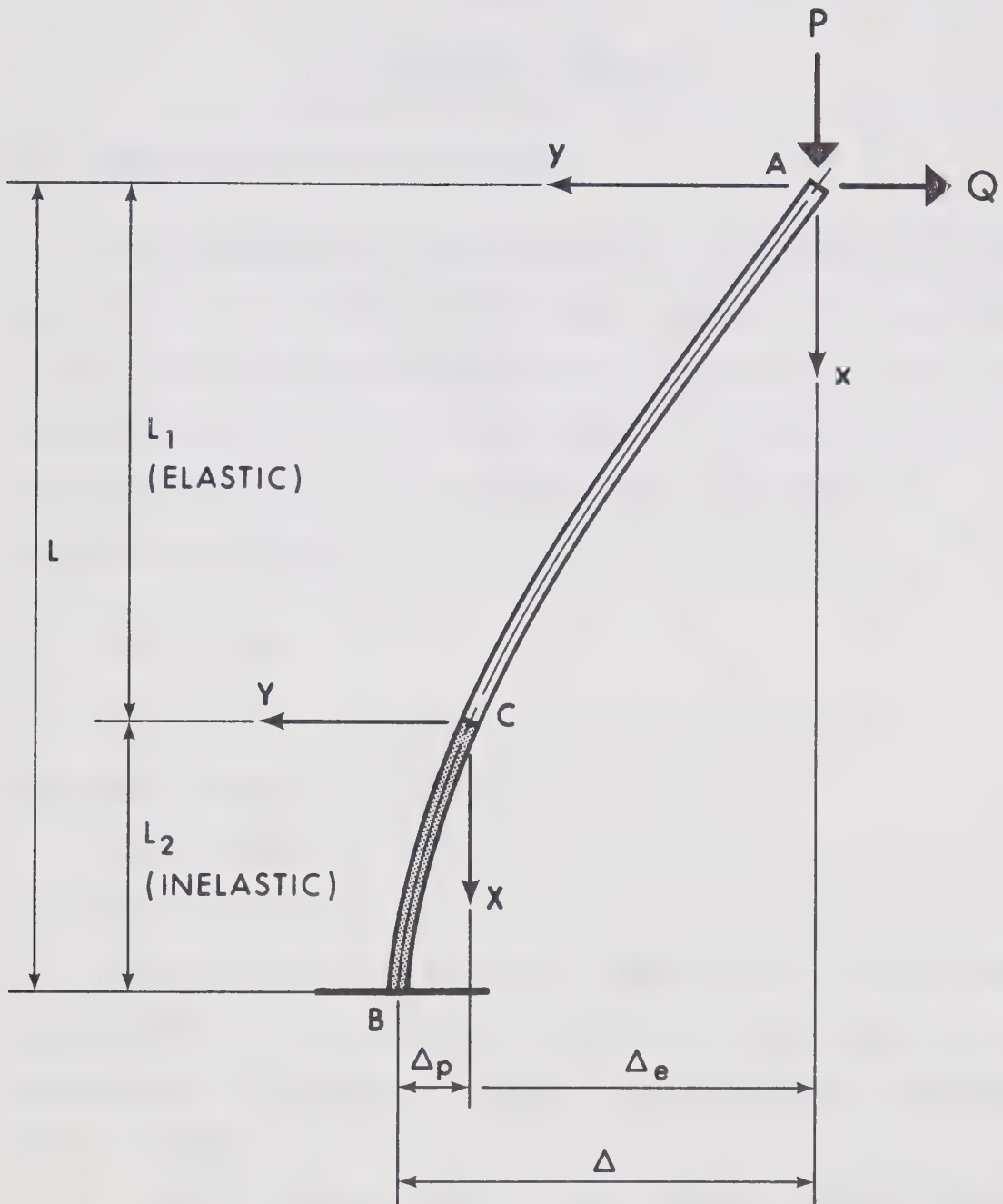


Fig. A-1 Coordinate Systems in Column

Appendix B.

COMPUTER PROGRAM I

B-1 Description of the Program.

This program has been developed to determine the properties of an equivalent rotational spring. The resulting $M_s - \delta\theta_s$ relationships together with the pertinent input data can be plotted by the CalComp Plotter as shown in Figs. 2-14a through 2-14d. The theoretical background is explained in Chapter 2.

B-2 Input Data.

First Card: SN, SI, P, H, STN, STK, D, YS

The input format is: (8F10.0)

Second Card: E, NDIV

The input format is: (F10.0, I5).

The above pair of cards are repeated for each system to be solved. To indicate the end of the problem, two blank cards are added at the end. The variables used here are as follows.

SN : Nominal size of wide flange section (inch),

SI : Moment of inertia (in^4),

P : Axial load. If $P > 1.0$, it indicates the axial load itself (kips); if $P \leq 1.0$, it

indicates the ratio of applied axial load to yield axial load,

- H : Height of the equivalent cantilever column,
 STN : s as in Eq. 2-12,
 STK : E_{st}/E , where E , E_{st} are defined in Sec. 2-2,
 D : σ_u/σ_y , where σ_y , σ_u are defined in Sec. 2-2,
 YS : Yield stress, σ_y (ksi),
 E : Modulus of elasticity (ksi), and
 NDIV : Any integer which is greater than about 50.
 The greater this number, the more accurate the result. (NDIV \leq 100 is usually satisfactory.)

B-3 Description of Subprograms and Flow Charts.

(1) MAIN PROGRAM.

Description: MAIN PROGRAM initiates CalComp Plotter, selects origin for the figure, calls subroutine KEISAN for the calculation of the $Q-\Delta$ relationship, and calls subroutine CHANGE to convert the $Q-\Delta$ relationship to the $M_s-\delta\theta_s$ relationship. Input data and the $M_s-\delta\theta_s$ relationship are plotted by calling subroutines DRAW1 and DRAW2.

Calls: KEISAN, CHANGE, DRAW1, DRAW2 and CalComp subroutines.

Flow Chart: Shown in Fig. B-1.

(2) SUBROUTINE KEISAN.

Description: KEISAN determines the cross sectional area and the plastic section modulus for the given values of the nominal depth and the moment of inertia based on Eqs. 2-3 and 2-5, respectively, and then the moment-curvature-thrust relationship in accordance with the description in Sec. 2-4-1. The $Q-\Delta$ relationship for the cantilever column is calculated using the procedure shown in Sec. 2-5-1 or Appendix A.

Called By: MAIN.

Calls: CalComp subroutines.

Flow Chart: Shown in Fig. B-2.

(3) SUBROUTINE CHANGE.

Description: CHANGE converts the $Q-\Delta$ relationship to the $M_s-\delta\theta_s$ relationship using the procedure shown in Sec. 2-5-2.

Called By: MAIN.

Flow Chart: Omitted.

(4) SUBROUTINE DRAW1.

Description: DRAW1 draws the $M_s-\delta\theta_s$ relationship as shown at the upper part of Fig. 2-14.

Called By: MAIN.

Calls: IFOX and CalComp subroutines.

Flow Chart: Omitted.

(5) SUBROUTINE DRAW2.

Description: DRAW2 draws the moment-curvature-thrust relationship as shown in the lower left-hand side in Fig. 2-14, then calls LABEL to enter the labels and titles and to show the column properties.

Called By: MAIN.

Calls: IFOX, LABEL and CalComp subroutines.

Flow Chart: Omitted.

(6) SUBROUTINE LABEL.

Description: LABEL puts labels on the moment-curvature-thrust relationship, and then draws the column with pertinent properties and loading situation as shown in the lower right-hand side of Fig. 2-14.

Called By: DRAW2.

Calls: CalComp subroutines.

Flow Chart: Omitted.

(7) FUNCTION IFOX

Description: IFOX defines the function $y = [x]$.

Called By: DRAW1 and DRAW2.

Flow Chart: Omitted.

B-4 Listing of the Program.

The listing of the program appears on page 215 through 227.

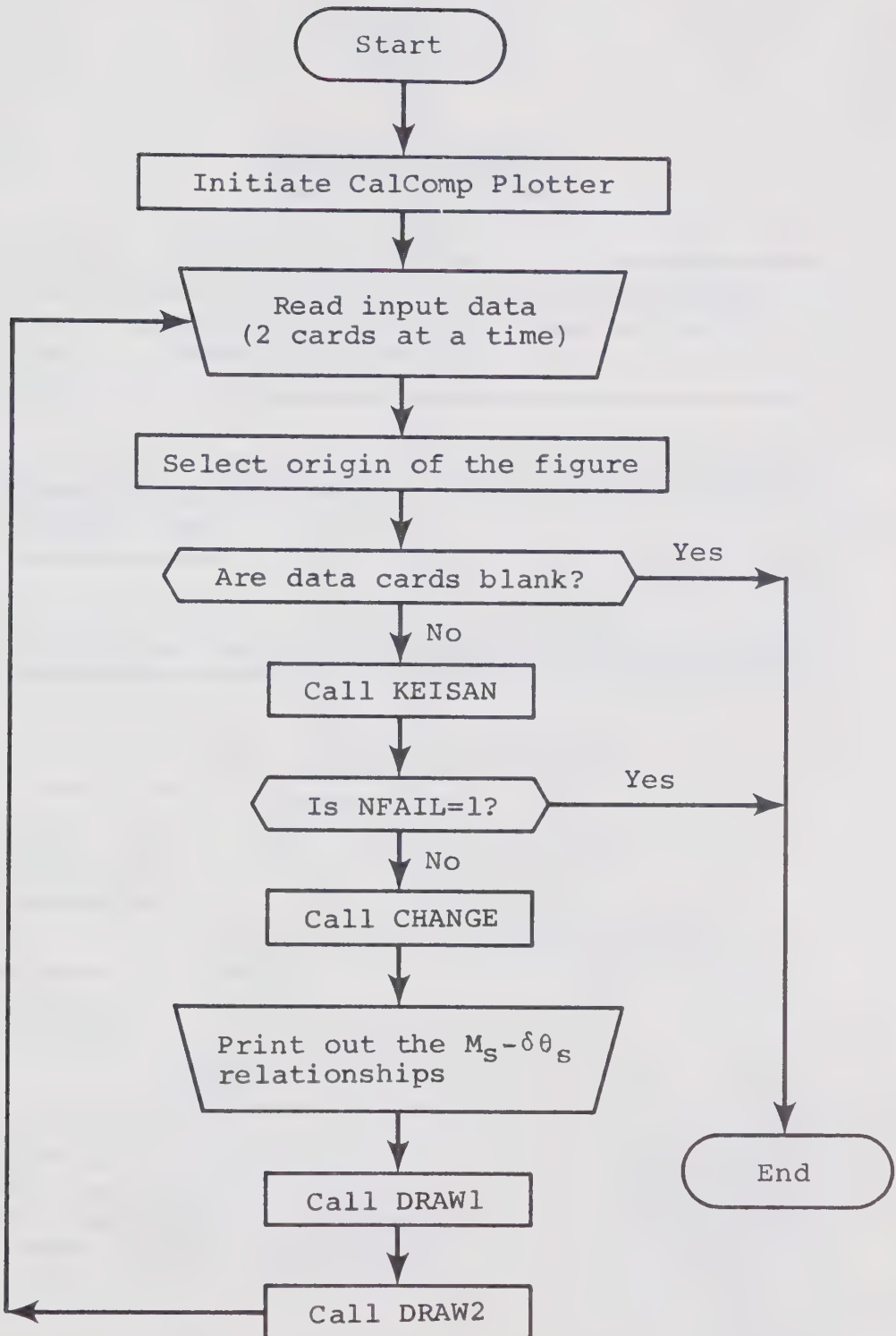


Fig. B-1 MAIN PROGRAM

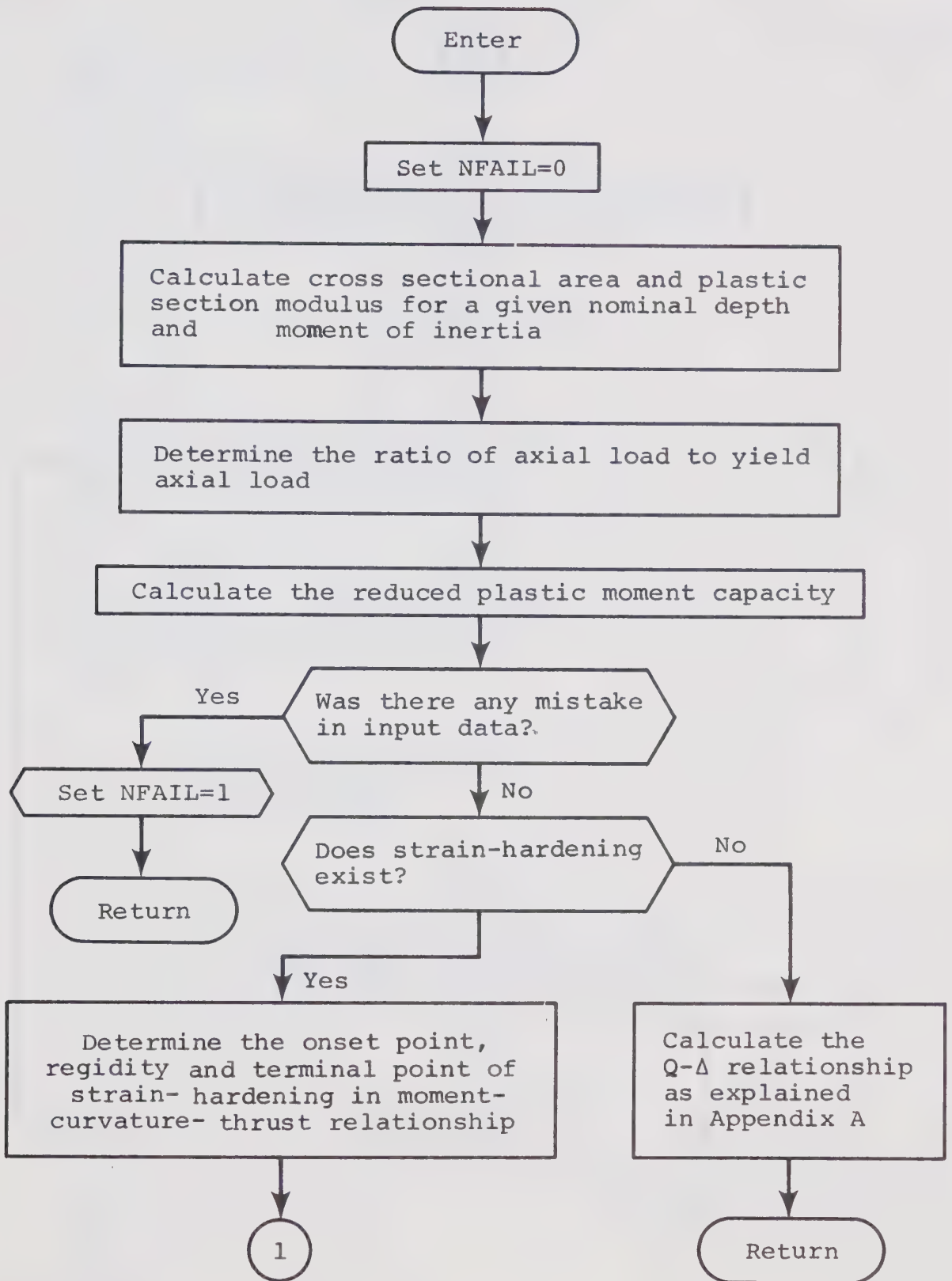


Fig. B-2 SUBROUTINE KEISAN (to be continued)

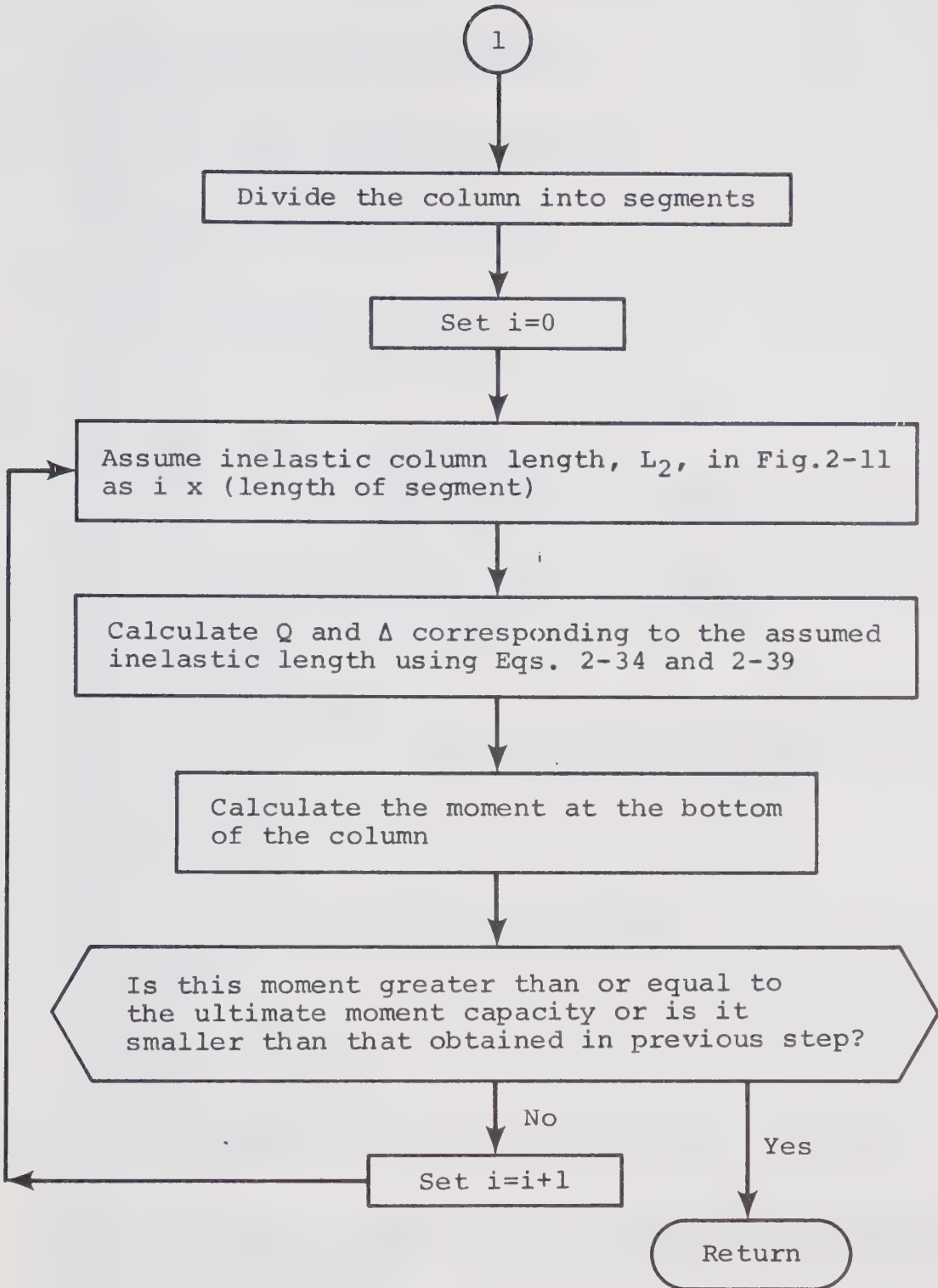


Fig. B-2 (Continued) SUBROUTINE KEISAN

LISTING OF PROGRAM I

```

      DIMENSION QL(201),DF(201),GRAPH(1024)
      CALL PLOTS (GRAPH,4096)
      NPLOT=0
100  NPLCT=NPLOT+1
      READ(5,110) SN,SI,P,H,STN,STK,D,YS,E,NDIV
110  FORMAT(8F10.0/F10.0,I5)
      IF(NPLOT .GE. 2) GO TO 120
      CALL SYMBOL (0.0,0.0,0.1,3,0.0,-1)
      CALL SYMBOL (8.5,0.0,0.1,3,0.0,-1)
      GC TO 140
120  ICH=2*(NPLOT/2)
      IF(NPLOT .EQ. ICH) GO TO 130
      CALL PLOT (6.6,-14.3,-3)
      CALL SYMBOL (8.5,0.0,0.1,3,0.0,-1)
      GO TO 140
130  CALL PLOT (-1.9,7.7,-3)
140  IF(SN .LT. 0.1) GO TO 200
      CALL SYMBOL (0.0,11.0,0.1,3,0.0,-1)
      CALL SYMBOL (8.5,11.0,0.1,3,0.0,-1)
      CALL SYMBOL (0.3,1.5,0.05,'PRODUCED WITH PROG#24, BY MASA AKI SUKO'
1,90.0,38)
      CALL KEISAN (IP,ISTH,NFAIL,STK,P,E,SI,EI,SN,Z,YS,FPM,CY,AREA,FAL,F
1P,FM,STN,STND,STKD,UM,D,PM,QMAX,QMIN,NDIV,H,NDEND,QL,DF,SPT)
      IF(NFAIL .EQ. 1) GO TO 200
      CALL CHANGE (QL,DF,QMAX,QMIN,NDEND,SPT,H,EI,P,IP)
      WEIGHT=3.4*AREA
      NSZ=IFIX(SN+0.5)
      NWT=IFIX(WEIGHT+0.5)
      WRITE(6,150) NSZ,NWT,SI,P
150  FORMAT(1H1, 1X,'** W',I3,'X',I3,4X,'MOMENT OF INERTIA=',F9.1,4X,
1'AXIAL LOAD=',F8.1//T17,'MOMENT',T28,'RELAXATION ANGLE')
      DO 170 K=1,NDEND
      WRITE(6,160) QL(K),DF(K)
160  FORMAT(10X,2E15.5)
170  CONTINUE
      WRITE(6,180) SPT
180  FORMAT(/1X,'SLCPE OF DASHED LINE =',E12.5)
      CALL DRAW1 (QL,DF,QMAX,QMIN,NDEND,SPT,ISTH,IP)
      CALL DRAW2 (IP,ISTH,STK,P,SI,EI,SN,FPM,CY,FP,FM,STN,STND,STKD,UM,D
1,PM,H,WEIGHT)
      CALL FACTOR(1.0)
      GO TO 100
200  IF(NPLOT .EQ. ICH) CALL PLOT (1.9,-11.0,-3)
      CALL PLOT(10.0,0.0,-3)
      PLNG=8.5*FLOAT(ICH/2+1)+3.5
      WRITE(6,300) PLNG
300  FORMAT(1H1,'REQUIRED PLOTTING PAPER LENGTH=',F4.0,'INCHES')
      CALL PLOT (0.0,0.0,999)
      STCF
      END
      SUBROUTINE KEISAN (IP,ISTH,NFAIL,STK,P,E,SI,EI,SN,Z,YS,FPM,CY,AREA
1,FAL,FP,FM,STN,STND,STKD,UM,D,PM,QMAX,QMIN,NDIV,H,NDEND,QL,DF,SPT)
      DIMENSION QL(201),DF(201)
      IP=1
      ISTH=1
      NFAIL=0
      IF(STK .LE. 0.000001) ISTH=0

```



```

IF(P .LE. 0.000001) IP=0
EI=E*SI
Z=1.79*SI**0.95/SN**0.8
FPM=Z*YS
CY=FPM/EI
AREA=3.4*SI**0.87/SN**1.5
FAI=AREA*YS
IF(P .GE. 1.000001) GO TO 150
FP=F
P=FP*FAL
GO TO 160
150 FP=P/FAL
160 SPI=-P/H
IF(FP .GT. 1.000001) GO TO 220
IF(FP .GE. 0.333333) GO TO 200
FM=1.0-1.8*FP**2
GO TO 230
200 FM=1.2*(1.0-FP)
GO TO 230
220 NFAIL=1
CALL SYMBOL (1.0,1.5,0.1,'GIVEN DATA ARE NOT PROPER',0.0,25)
RETURN
230 IF(ISTH .EQ. 0) GO TO 310
IF(STN .GE. 3.0) GO TO 260
UN=(3.0+STN*(2.0-STN))/4.0
IF(FM .GE. UN) GO TO 260
STND=FM+(STN-1.0)/2.0
GO TO 300
260 STND=SIN-0.5*SQRT(1.0-FM+1.0E-20)*(STN+1.0)
300 STKD=(2.0-FM)*STK
EIST=STKD*EI
UM=(FM+D-1.0)*FPM
SAM=STND*STKD*FPM
310 PM=FM*FPM
QMAX=0.0
QMIN=1.0E-20
IF(ISTH .EQ. 0) GO TO 410
IF(IF .EQ. 0) GO TO 320
A=SQRT(P/EI)
B=SQRT(P/EIST)
320 HD=H/FLOAT(NDIV)
ND=NDIV+1
GMOLD=0.0
DO 400 I=1,ND
NDEND=I-1
HB=HD*FLOAT(I-1)
HU=H-HB
IF(IF .EQ. 0) GO TO 350
SNA=SIN(A*HU)
CSA=CCS(A*HU)
SNB=SIN(B*HB)
CSE=COS(B*HB)
TNA=SNA/CSA
TNB=SNB/CSB
Q=A*FM*CSB/TNA-SAM*B*SNB
C1=SAM/P
C2=(C1*B*SNB+Q/P)/B/CSB
ALPHA=C2*B-Q/P
C4=C2*B/A/CSA
DU=C4*SNA-Q*HU/P

```



```

DB=C1*CSB+C2*SNB-Q*HB/P-SAM/P
DEI=DU+DB
GM=P*DEL+Q*H
GC TO 390
350 Q=FM/HU
DB=(Q*HB**3/3.0+SAM*HB**2/2.0)/EIST
ALPHA=(Q*HB**2/2.0+SAM*HB)/EIST
DU=Q*HU**3/3.0/EI+ALPHA*HU
DEI=DU+DB
GM=Q*H
390 IF (GM .GT. UM) RETURN
IF (GM .LT. GMOLD) RETURN
GMCID=GM
QL(I)=Q
DF(I)=DEL
IF (QMAX .LT. Q) QMAX=Q
IF (QMIN .GT. Q) QMIN=Q
400 CONTINUE
RETURN
410 NDEND=2
IF (IF .EQ. 0) GO TO 420
A=SQRT(P/EI)
QL(1)=A*PM*COS(A*H)/SIN(A*H)
DF(1)=(PM-QL(1)*H)/P
GC TO 430
420 QL(1)=FM/H
DF(1)=QL(1)*H**3/3.0/EI
430 DF(2)=20.0*DF(1)
QL(2)=QL(1)-P*19.0*DF(1)/H
IF (IF .EQ. 0) QL(2)=QL(1)
QMAX=QL(1)
IF (QL(2) .LT. 0.0) QMIN=QL(2)
RETURN
END
SUBROUTINE CHANGE (QL,DF,QMAX,QMIN,NEND,SPT,H,EI,P,IP)
DIMENSION QL(201),DF(201)
DO 100 I=1,NEND
X=DF(I)
Y=QL(I)
QL(I)=Y*H
DF(I)=X/H-Y*H**2/3.0/EI
100 CCNTINUE
IF (DF(1) .LE. 1.0E-25) DF(1)=0.0
QMAX=QMAX*H
QMIN=QMIN*H
IF (IF .EQ. 0) GO TO 110
SPT=-H/(H**2/3.0/EI+1.0/P)
RETURN
110 SPT=0.0
RETURN
END
SUBROUTINE DRAW1 (QL,DF,QMAX,QMIN,NEND,SPT,ISTH,IP)
DIMENSION QL(201),DF(201)
CALL FIOT (1.9,6.0,-3)
CALL FACTOR (0.9)
CALL SYMBOL (1.1,-0.57,0.1,'END MOMENT-RELAXATION ANGLE RELATIONSH
1IP',0.0,40)
IQ=IFOX (ALOG10 (QMAX-QMIN)-0.478)
NQA=IFIX (QMAX/10.0**IQ)+1
NQB=IFIX (QMIN/10.0**IQ)

```



```

UNL=4.0/FLOAT(NQA-NQB)
NQ=IFIX(0.3/UNL)+1
QLAB=FLOAT(NQ)
UNL=QLAB*UNL
BAIQ=QLAB*10.0**IQ/UNL
INTC=-NQB/NQ
YGEN=UNL*FLOAT(INTC)
IWA=-INTC*NQ
IF(IWA.NE.NQB) YGEN=YGEN+UNL/2.0
CALL PLOT(0.0,0.0,3)
CALL PLOT(0.0,4.0,2)
CALL PLOT(0.0,YGEN,-3)
IF(IQ.GE.3) GO TO 200
IF(IQ.LE.-2) GO TO 210
QLAB=QLAB*10.0**IQ
JO=C
GC TO 250
200 QLAB=QLAB*100.0
JO=IQ-2
GO TO 250
210 QLAB=QLAB/10.0
JO=IQ+1
250 CALL SYMBOL(0.0,0.0,0.1,16,90.0,-1)
IPTC=NQA/NQ+1
IF(IQ.LE.-1) GO TO 252
CALL SYMBOL(-0.6,-0.05,0.1,' 0',0.0,6)
GC TO 253
252 CALL SYMBOL(-0.6,-0.05,0.1,' 0.0',0.0,5)
253 INTC=INTC+1
DO 270 I=1,INTC
IF(UNL.LT.0.6) GO TO 255
YT=UNL*FLOAT(I-1)+UNL/2.0
IF(YT.GT.YGEN) GO TO 280
YT=-YT
CALL SYMBOL(0.0,YT,0.1,16,90.0,-1)
255 YT=UNL*FLOAT(I)
IF(YT.GT.YGEN) GO TO 280
YT=-YT
CALL SYMBOL(0.0,YT,0.1,16,90.0,-1)
YT=YT-0.05
YLA=QLAB*FLOAT(I)
IF(IQ.LE.-1) GO TO 256
KETA=IFIX(ALOG10(YLA+0.00001))+1
KBL=4-KETA
256 YIA=-YLA
CALL SYMBOL(-0.6,YT,0.1,' ',0.0,1)
IF(IQ.LE.-1) GO TO 266
IF(KBL.EQ.0) GO TO 265
DC 260 J=1,KBL
CALL SYMBOL(-0.0,-0.0,0.1,' ',0.0,1)
260 CONTINUE
265 CALL NUMBER(-0.0,-0.0,0.1,YLA,0.0,-1)
GC TO 270
266 CALL NUMBER(-0.0,-0.0,0.1,YLA,0.0,1)
270 CONTINUE
280 YPLUS=4.0-YGEN
DC 300 I=1,IPTC
IF(UNL.LT.0.6) GO TO 285
YT=UNL*FLOAT(I-1)+UNL/2.0
IF(YT.GT.YPLUS) GO TO 350

```



```

      CALL SYMBOL (0.0,YT,0.1,16,90.0,-1)
285  YT=UNL*FLOAT(I)
      IF(YT.GT. YPLUS) GO TO 350
      CALL SYMBOL (0.0,YT,0.1,16,90.0,-1)
      YT=YI-0.05
      YIA=QLAB*FLOAT(I)
      IF(IQ.LE. -1) GO TO 286
      KETA=IFIX(ALOG10(YIA+0.00001))+1
      KBL=5-KETA
286  CALL SYMBOL (-0.6,YT,0.1,' ',0.0,1)
      IF(IQ.LE. -1) KBL=1
      DC 290 J=1,KBL
      CALL SYMBOL (-0.0,-0.0,0.1,' ',0.0,1)
290  CCNTINUE
      IF(IQ.LE. -1) GO TO 295
      CALL NUMBER (-0.0,-0.0,0.1,YLA,0.0,-1)
      GO TO 300
295  CALL NUMBER (-0.0,-0.0,0.1,YLA,0.0,1)
300  CCNTINUE
350  IF(JO.EQ. 0) GO TO 400
      YJO=FLOAT(JO)
      YT=YPLUS+0.1
      CALL SYMBOL (-0.5,YT,0.1,'X10',0.0,3)
      YT=YI+0.07
      CALL NUMBER (-0.0,YT,0.08,YJO,0.0,-1)
400  YT=YPLUS
      CALL SYMBOL (0.1,YT,0.12,'M',0.0,1)
      CALL SYMBOL (-0.0,-0.0,0.1,' ( KIP-IN ) ',0.0,11)
      CALL FLOT (0.0,0.0,3)
      CALL FICT (5.8,0.0,2)
      DMAX=LF(NEND)
      ID=IFIX(ALOG10(DMAX)-0.478)
      NDA=IFIX(DMAX/10.0**ID)+1
      UND=5.8/FLOAT(NDA)
      ND=IFIX(0.4/UND)+1
      DLAB=FLOAT(ND)
      UND=DLAB*UND
      BAID=DLAB*10.0**ID/UND
      IF(ID.GE. 3) GO TO 410
      IF(ID.LE. -3) GO TO 420
      DLAB=DLAB*10.0**ID
      JO=0
      GO TO 450
410  DLAB=DLAB*100.0
      JO=ID-2
      GO TO 450
420  DLAB=DLAB/100.0
      JO=ID+2
450  IDIC=NDA/ND+1
      DO 500 I=1,IDIC
      IF(UND.LT. 0.8) GO TO 455
      XT=UND*FLOAT(I-1)+UND/2.0
      IF(XI.GT. 5.8) GO TO 510
      CALL SYMBOL (XT,0.0,0.1,15,-90.0,-1)
455  XT=UND*FLOAT(I)
      IF(XI.GT. 5.8) GO TO 510
      CALL SYMBOL (XT,0.0,0.1,15,-90.0,-1)
      XLA=DLAB*FLOAT(I)
      XT=XT-0.1
      IF(ID.EQ. 0.AND. XLA.LE. 9.99) XT=XT+0.05

```



```

      IF (ID .LE. -1) GO TO 460
      CALL NUMBER (XT,-0.2,0.1,XLA,0.0,-1)
      GO TO 500
460  CALL NUMBER (XT,-0.2,0.1,XLA,0.0,2)
500  CCNTINUE
510  IF (JO .EQ. 0) GO TO 550
      CALL SYMBOL (5.9,-0.05,0.1,'X10',0.0,3)
      XJO=FLOAT(JO)
      CALL NUMBER (-0.0,0.02,0.08,XJO,0.0,-1)
550  CALL SYMBOL (4.9,0.1,0.12,43,0.0,-1)
      CALL SYMBOL (-0.0,-0.0,0.12,37,0.0,-1)
      CALL SYMBOL (-0.0,-0.0,0.1,' ( RAD. ) ',0.0,9)
      QYLD=C1(1)
      DYID=DF(1)
      SLCFE=SPT*BAID/BAIQ
      CALL FLOT (0.0,0.0,3)
      DC 600 I=1,NEND
      QL(I)=QL(I)/BAIQ
      DF(I)=DF(I)/BAID
      CALL FLOT (DF(I),QL(I),2)
600  CCNTINUE
      XT=2.0*DF(1)+0.2
      YT=0.3
      IF (ISTH .EQ. 0) GO TO 620
      IF (IF .EQ. 0) GO TO 605
      YEND=-YGEN+0.3
      XEND=(YEND+SLOFE*DF(1)-QL(1))/SLOPE
      IF (XEND .LE. 5.5) GO TO 610
605  XEND=5.5
      YEND=SLOPE*(XEND-DF(1))+QL(1)
610  CALL FLOT (DF(1),QL(1),3)
      CALL DASHPT (XEND,YEND,0.06)
      CALL SYMBOL (XT,YT,0.1,'SLOPE OF DASHED LINE=',0.0,21)
      GC IC 630
620  CALL SYMBOL (XT,YT,0.1,'SLOPE OF SECOND BRANCH=',0.0,23)
630  IF (IF .EQ. 0) GO TO 635
      KETA=IFIX(ALOG10(-SPT))+1
      IF (KETA .GE. 6) GO TO 640
      IN=3-KETA
      IF (KETA .GE. 3) IN=-1
      KETA=0
      GO TO 645
635  IN=1
      KETA=0
      GO IC 645
640  IN=-1
      KETA=KETA-3
      FK=FLOAT(KETA)
      SPT=SPT/10.0**KETA
645  CALL NUMBER (-0.0,-0.0,0.1,SPT,0.0,IN)
      IF (KETA .EQ. 0) GO TO 649
      YIU=YT+0.07
      CALL SYMBOL (-0.0,-0.0,0.1,'X10',0.0,3)
      CALL NUMBER (-0.0,YTU,0.08,FK,0.0,-1)
649  YT=YT+0.25
650  YTD=YT-0.05
      CALL SYMBOL (XT,YT,0.12,43,0.0,-1)
      CALL SYMBOL (-0.0,-0.0,0.12,37,0.0,-1)
      CALL SYMBOL (-0.0,YTD,0.08,'S-YIELD',0.0,7)
      CALL SYMBOL (-0.0,YT,0.1,'=',0.0,1)

```



```

IF(IP .EQ. 1 .AND. DYLD .GT. 1.0E-25) GO TO 655
CALL SYMBOL (-0.0,-0.0,0.1,'0.0',0.0,3)
GO TO 690
655 KETA=IFOX(ALOG10(DYLD))+1
IF(KETA .LE. 1) GO TO 660
IN=-1
GO TO 680
660 IF(KETA .LE. -3) GO TO 670
IN=3-KETA
GO TO 680
670 IN=3
DYLD=DYLD/10.0**KETA
680 CALL NUMBER (-0.0,-0.0,0.1,DYLD,0.0,IN)
IF(KETA .GE. -2) GO TO 690
YTU=YI+0.07
DK=FLCAT(KETA)
CALL SYMBOL (-0.0,-0.0,0.1,'X10',0.0,3)
CALL NUMBER (-0.0,YTU,0.08,DK,0.0,-1)
690 YI=YI+0.25
YTD=YI-0.05
CALL SYMBOL (XT,YT,0.1,'M',0.0,1)
CALL SYMBOL (-0.0,YTD,0.08,'S-YIELD',0.0,7)
CALL SYMBOL (-0.0,YT,0.1,'=',0.0,1)
IN=-1
IF(IQ .LE. 1) IN=2-IQ
CALL NUMBER (-0.0,-0.0,0.1,QYLD,0.0,IN)
IF(YGEN .GE. 0.1) GO TO 710
CALL SYMBOL (0.0,0.0,0.1,15,-90.0,-1)
IF(ID .LE. -1) GO TO 700
CALL SYMBOL (-0.05,-0.2,0.1,'0',0.0,1)
GO TO 710
700 CALL SYMBOL (-0.1,-0.2,0.1,'0.0',0.0,3)
710 CALL FLOT (0.0,-YGEN,-3)
RETURN
END
SUBROUTINE DRAW2 (IP,ISTH,STK,P,SI,EI,SN,FPM,CY,FP,FM,STN,STND,STK
1D,UM,D,FM,H,WEIGHT)
CALL FLOT (0.0,-3.2,-3)
IF(ISTH .EQ. 0) D=1.0
IF(D .LE. 1.2) GO TO 150
Y3=2.0
Y1=2.0/D
GO TO 160
150 Y1=1.5
Y3=1.5*D
160 Y4=Y1*FM
IF(ISTH .EQ. 0) UM=FM
Y6=Y4*UM/PM
IF(ISTH .EQ. 0) GO TO 180
PHM=SIN+(D-1.0)/STK
X3=3.3
X1=3.3/PHM
X2=SIN*X1
X4=X1*FM
X5=X1*STND
PHMD=SIND+(D-1.0)/STKD
X6=X1*PHMD
GO TO 200
180 X3=3.3
X1=0.33

```



```

X4=0.33*FM
X6=3.3
200 CALL FLOT (0.0,2.1,2)
    CALL FLOT (3.5,0.0,3)
    CALL FLOT (0.0,0.0,2)
    CALL FLOT (X4,Y4,2)
    IF (IF .EQ. 0) GO TO 215
    CALL DASHPT (X1,Y1,0.06)
    CALL FLOT (X1,Y1,2)
    IF (ISTH .EQ. 0) GO TO 210
    CALL DASHPT (X2,Y1,0.06)
    CALL FLOT (X2,Y1,2)
210 CALL DASHPT (X3,Y3,0.06)
    CALL FLOT (X3,Y3,2)
    CALL FLOT (X4,Y4,3)
215 IF (ISTH .EQ. 0) GO TO 220
    CALL FLOT (X5,Y4,2)
220 CALL FLOT (X6,Y6,2)
    CALL SYMBOL (-0.2,-0.2,0.1,'O',0.0,1)
    CALL SYMBOL (0.0,Y1,0.1,16,90.0,-1)
    Z=Y1-0.05
    CALL SYMBOL (-0.3,Z,0.1,'M',0.0,1)
    Z=Z-0.05
    CALL SYMBOL (-0.0,Z,0.08,'P',0.0,1)
    IF (IF .EQ. 0) GO TO 240
    CALL SYMBOL (0.0,Y4,0.1,16,90.0,-1)
    YSA=Y1-Y4
    IF (YSA .LT. 0.15) GO TO 230
    Z=Y4-0.05
    GO TO 235
230 CALL FLOT (-0.06,Y4,3)
    Z=Y4-0.2
    CALL FLOT (-0.3,Z,2)
    Z=Z-0.1
235 CALL SYMBOL (-0.3,Z,0.1,'M',0.0,1)
    Z=Z-0.05
    CALL SYMBOL (-0.0,Z,0.08,'PC',0.0,2)
240 IF (ISTH .EQ. 0) GO TO 270
    CALL SYMBOL (0.0,Y3,0.1,16,90.0,-1)
    YSA=Y3-Y1
    IF (YSA .LT. 0.15) GO TO 250
    Z=Y3-0.05
    GO TO 255
250 CALL FLOT (-0.06,Y3,3)
    Z=Y3+0.2
    CALL FLOT (-0.3,Z,2)
255 CALL SYMBOL (-0.3,Z,0.1,'M',0.0,1)
    Z=Z-0.05
    CALL SYMBOL (-0.0,Z,0.08,'U',0.0,1)
    IF (IF .EQ. 0) GO TO 270
    CALL SYMBOL (0.0,Y6,0.1,16,90.0,-1)
    IF (Y6 .GE. Y1) GO TO 260
    YSA=Y1-Y6
    YYS=Y6-Y4
    IF (YSA .GE. 0.15 .AND. YYS .GE. 0.15) GO TO 265
    GO TO 270
260 YSA=Y3-Y6
    YYS=Y6-Y1
    IF (YSA .GE. 0.15 .AND. YYS .GE. 0.15) GO TO 265
    GO TO 270

```



```

265 Z=Y6-0.05
   CALL SYMBOL (-0.3,Z,0.1,'M',0.0,1)
   Z=Z-0.05
   CALL SYMBOL (-0.0,Z,0.08,'UC',0.0,2)
270 CALL SYMBOL (-0.05,2.15,0.12,'M',0.0,1)
   CALL SYMBOL (X1,0.0,0.1,15,-90.0,-1)
   CALL SYMBOL (X1,-0.2,0.1,36,0.0,-1)
   CALL SYMBOL (-0.0,-0.25,0.08,'P',0.0,1)
   IF(IP .EQ. 0) GO TO 280
   CALL SYMBOL (X4,0.0,0.1,15,-90.0,-1)
   XSA=X1-X4
   IF(XSA .LT. 0.1) GO TO 275
   XT=X4-0.05
   CALL SYMBOL (XT,-0.2,0.1,36,0.0,-1)
   CALL SYMBOL (-0.0,-0.25,0.08,'PC',0.0,2)
   GO TO 280
275 CALL PLOT (X4,-0.06,3)
   XT=X4-0.1
   CALL PLOT (XT,-0.2,2)
   XT=XT-0.1
   CALL SYMBOL (XT,-0.3,0.1,36,0.0,-1)
   CALL SYMBOL (-0.0,-0.35,0.08,'PC',0.0,2)
280 IF(ISTH .EQ. 0) GO TO 290
   XSA=X2-X1
   IF(XSA .LT. 0.3) GO TO 290
   CALL SYMBOL (X2,0.0,0.1,15,-90.0,-1)
   XT=X2-0.05
   CALL SYMBOL (XT,-0.2,0.08,'S',0.0,1)
   CALL SYMBOL (-0.0,-0.2,0.1,36,0.0,-1)
   CALL SYMBOL (-0.0,-0.25,0.08,'P',0.0,1)
   IF(IP .EQ. 0) GO TO 290
   CALL SYMBOL (X5,0.0,0.1,15,-90.0,-1)
   XSA=X2-X5
   IF(XSA .LT. 0.3) GO TO 285
   XT=X5-0.05
   CALL SYMBOL (XT,-0.2,0.1,36,0.0,-1)
   CALL SYMBOL (-0.0,-0.25,0.08,'ST',0.0,2)
   GO TO 290
285 CALL PLOT (X5,-0.06,3)
   XT=X5-0.1
   CALL PLOT (XT,-0.2,2)
   XT=XT-0.1
   CALL SYMBOL (XT,-0.3,0.1,36,0.0,-1)
   CALL SYMBOL (-0.0,-0.35,0.08,'ST',0.0,2)
290 CALL SYMBOL (X3,0.0,0.1,15,-90.0,-1)
   XT=X3-0.05
   CALL SYMBOL (XT,-0.2,0.1,36,0.0,-1)
   CALL SYMBOL (-0.0,-0.25,0.08,'U',0.0,1)
   IF(IF .EQ. 0 .OR. ISTH .EQ. 0) GO TO 300
   CALL SYMBOL (X6,0.0,0.1,15,-90.0,-1)
   XSA=X3-X6
   IF(XSA .LT. 0.25) GO TO 295
   XT=X6-0.05
   CALL SYMBOL (XT,-0.2,0.1,36,0.0,-1)
   CALL SYMBOL (-0.0,-0.25,0.08,'UC',0.0,2)
   GO TO 300
295 CALL PLOT (X6,-0.06,3)
   XT=X6-0.1
   CALL PLOT (XT,-0.2,2)
   XT=XT-0.1

```



```

CALL SYMBOL (XT,-0.3,0.1,36,0.0,-1)
CALL SYMBOL (-0.0,-0.35,0.08,'UC',0.0,2)
300 CALL SYMBOL (3.6,-0.05,0.12,36,0.0,-1)
    XI=EI/1000.0
    IF (FM .GT. 0.4) GO TO 310
    YT=(Y1+Y4)/2.0-0.1
    GC TO 315
310 YT=Y4/2.0-0.1
315 YTU=YT+0.07
    CALL SYMBOL (X1,YT,0.1,'EI=',0.0,3)
    CALL NUMBER (-0.0,-0.0,0.1,XI,0.0,-1)
    CALL SYMBOL (-0.0,-0.0,0.1,'X10',0.0,3)
    CALL SYMBOL (-0.0,YTU,0.08,'3',0.0,1)
    IF (ISTH .EQ. 0) GO TO 330
    IF (IF .EQ. 0) GO TO 320
    EST=EI*STKD/1000.0
    YT=(Y6+Y4)/2.0-0.3
    YTD=YT-0.05
    YTU=YT+0.07
    XT=X5+0.47
    CALL SYMBOL (XT,YT,0.1,'K',0.0,1)
    CALL SYMBOL (-0.0,YTD,0.08,'ST',0.0,2)
    CALL SYMBOL (-0.0,YT,0.1,'=',0.0,1)
    CALL NUMBER (-0.0,-0.0,0.1,EST,0.0,-1)
    CALL SYMBOL (-0.0,-0.0,0.1,'X10',0.0,3)
    CALL SYMBOL (-0.0,YTU,0.08,'3',0.0,1)
320 IF (FM .GT. 0.4) GO TO 325
    XT=X2+0.2
    YT=Y1-0.1
    GC TO 326
325 XT=X2-0.4
    YT=Y3+0.1
326 YTD=YT-0.05
    YTU=YT+0.07
    EST=EI*STK/1000.0
    CALL SYMBOL (XT,YT,0.1,'E',0.0,1)
    CALL SYMBOL (-0.0,YTD,0.08,'ST',0.0,2)
    CALL SYMBOL (-0.0,YT,0.1,'I=',0.0,2)
    CALL NUMBER (-0.0,-0.0,0.1,EST,0.0,-1)
    CALL SYMBOL (-0.0,-0.0,0.1,'X10',0.0,3)
    CALL SYMBOL (-0.0,YTU,0.08,'3',0.0,1)
330 CALL LABEL (IP,ISTH,P,SI,SN,FPM,CY,FP,FM,STN,STND,UM,D,PM,H,PHM,PH
1MD,X2,X1,WEIGHT)
    RETURN
    END
    SUBROUTINE LABEL (IP,ISTH,P,SI,SN,FPM,CY,FP,FM,STN,STND,UM,D,PM,H,
1FHM,PHMD,X2,X1,WEIGHT)
    YT=-0.5
    YTD=YT-0.05
    CALL SYMBOL (0.2,YT,0.1,'M',0.0,1)
    CALL SYMBOL (-0.0,YTD,0.08,'P',0.0,1)
    CALL SYMBOL (-0.0,YT,0.1,'=',0.0,1)
    CALL NUMBER (-0.0,-0.0,0.1,FPM,0.0,1)
    IF (ISTH .EQ. 0) GO TO 310
    CALL SYMBOL (-0.0,-0.0,0.1,'M',0.0,3)
    CALL SYMBOL (-0.0,YTD,0.08,'U',0.0,1)
    CALL SYMBOL (-0.0,YT,0.1,'=',0.0,1)
    UMD=D*FPM
    CALL NUMBER (-0.0,-0.0,0.1,UMD,0.0,1)
310 IF (IF .EQ. 0) GO TO 320

```



```

YT=YT-0.25
YTD=YT-0.05
CALL SYMBOL (0.2,YT,0.1,'M',0.0,1)
CALL SYMBOL (-0.0,YTD,0.08,'PC',0.0,2)
CALL SYMBOL (-0.0,YT,0.1,'=',0.0,1)
CALL NUMBER (-0.0,-0.0,0.1,FM,0.0,1)
IF(ISTH.EQ. 0) GO TO 320
CALL SYMBOL (-0.0,-0.0,0.1,' ',M',0.0,3)
CALL SYMBOL (-0.0,YTD,0.08,'UC',0.0,2)
CALL SYMBOL (-0.0,YT,0.1,'=',0.0,1)
CALL NUMBER (-0.0,-0.0,0.1,UM,0.0,1)
320 YT=YT-0.25
YTD=YT-0.05
YTU=YT+0.07
CALL SYMBOL (0.2,YT,0.1,36,0.0,-1)
CALL SYMBOL (-0.0,YTD,0.08,'P',0.0,1)
CALL SYMBOL (-0.0,YT,0.1,'=',0.0,1)
CYC=CY*1000.0
CALL NUMBER (-0.0,-0.0,0.1,CYO,0.0,3)
CALL SYMBOL (-0.0,-0.0,0.1,'X10',0.0,3)
CALL SYMBOL (-0.0,YTU,0.08,'-3',0.0,2)
XSA=X2-X1
IF(ISTH.EQ. 0) GO TO 330
IF(XSA.LT. 0.3) GO TO 325
CALL SYMBOL (-0.0,YT,0.1,' ',',0.0,2)
CALL SYMBOL (-0.0,-0.0,0.08,'S',0.0,1)
CALL SYMBOL (-0.0,-0.0,0.1,36,0.0,-1)
CALL SYMBOL (-0.0,YTD,0.08,'P',0.0,1)
CALL SYMBOL (-0.0,YT,0.1,'=',0.0,1)
CALL NUMBER (-0.0,-0.0,0.1,STN,0.0,1)
CALL SYMBOL (-0.0,-0.0,0.1,36,0.0,-1)
CALL SYMBOL (-0.0,YTD,0.08,'P',0.0,1)
325 CALL SYMBOL (-0.0,YT,0.1,' ',',0.0,2)
CALL SYMBOL (-0.0,-0.0,0.1,36,0.0,-1)
CALL SYMBOL (-0.0,YTD,0.08,'U',0.0,1)
CALL SYMBOL (-0.0,YT,0.1,'=',0.0,1)
CALL NUMBER (-0.0,-0.0,0.1,FHM,0.0,1)
CALL SYMBOL (-0.0,-0.0,0.1,36,0.0,-1)
CALL SYMBOL (-0.0,YTD,0.08,'P',0.0,1)
330 IF(IP.EQ. 0) GO TO 340
YT=YT-0.25
YTD=YT-0.05
YTU=YT+0.07
CYL=CY*FM*1000.0
CALL SYMBOL (0.2,YT,0.1,36,0.0,-1)
CALL SYMBOL (-0.0,YTD,0.08,'PC',0.0,2)
CALL SYMBOL (-0.0,YT,0.1,'=',0.0,1)
CALL NUMBER (-0.0,-0.0,0.1,CYD,0.0,3)
CALL SYMBOL (-0.0,-0.0,0.1,'X10',0.0,3)
CALL SYMBOL (-0.0,YTU,0.08,'-3',0.0,2)
IF(ISTH.EQ. 0) GO TO 340
IF(XSA.LT. 0.3) GO TO 335
SU=SINC/FM
CALL SYMBOL (-0.0,YT,0.1,' ',',0.0,2)
CALL SYMBOL (-0.0,-0.0,0.1,36,0.0,-1)
CALL SYMBOL (-0.0,YTD,0.08,'ST',0.0,2)
CALL SYMBOL (-0.0,YT,0.1,'=',0.0,1)
CALL NUMBER (-0.0,-0.0,0.1,SU,0.0,1)
CALL SYMBOL (-0.0,-0.0,0.1,36,0.0,-1)
CALL SYMBOL (-0.0,YTD,0.08,'PC',0.0,2)

```



```

335 SU=FHFD/FM
    CALL SYMBOL (-0.0,YT,0.1,' ',0.0,2)
    CALL SYMBOL (-0.0,-0.0,0.1,36,0.0,-1)
    CALL SYMBOL (-0.0,YTD,0.08,'UC',0.0,2)
    CALL SYMBOL (-0.0,YT,0.1,' ',0.0,1)
    CALL NUMBER (-0.0,-0.0,0.1,SU,0.0,1)
    CALL SYMBOL (-0.0,-0.0,0.1,36,0.0,-1)
    CALL SYMBOL (-0.0,YTD,0.08,'PC',0.0,2)
340 YT=YT-0.35
    CALL SYMBOL (0.4,YT,0.1,'MOMENT CURVATURE RELATIONSHIP',0.0,29)
    YT=YT-0.6
    CALL SYMBOL (1.0,YT,0.12,'CROSS SECTIONAL PROPERTIES AND M-',0.0,3
13)
    CALL SYMBOL (-0.0,-0.0,0.145,43,0.0,-1)
    CALL SYMBOL (-0.0,-0.0,0.145,37,0.0,-1)
    CALL SYMBOL (-0.0,-0.0,0.12,' RELATIONSHIP',0.0,13)
    CALL PLOT (0.0,-0.25,-3)
    CALL SYMBOL (4.3,-0.6,0.1,'UNIT OF FORCE: KIP.',0.0,19)
    CALL SYMBOL (4.3,-0.85,0.1,'UNIT OF LENGTH: IN.',0.0,19)
    CALL PLOT (4.5,0.0,3)
    CALL PLOT (5.3,0.0,2)
    CALL PLOT (4.8,0.0,3)
    CALL PLOT (4.8,1.8,2)
    CALL PLOT (4.9,1.8,2)
    CALL PLOT (4.9,0.0,2)
    DO 350 I=1,10
    XT=4.5+0.07*FLCAT(I)
    CALL SYMBOL (XT,0.0,0.1,15,-45.0,-1)
350 CCNTINUE
    CALL PLOT (4.85,-0.15,3)
    CALL PLOT (4.85,-0.3,2)
    CALL PLOT (5.15,-0.3,2)
    CALL PLOT (5.08,-0.27,2)
    CALL PLOT (5.08,-0.33,3)
    CALL PLOT (5.15,-0.3,2)
    CALL SYMBOL (5.25,-0.3,0.12,52,0.0,-1)
    IF (IF.EQ. 0) GO TO 360
    CALL PLOT (4.85,2.3,3)
    CALL PLOT (4.85,1.85,2)
    CALL PLOT (4.78,1.95,2)
    CALL PLOT (4.92,1.95,2)
    CALL PLOT (4.85,1.85,2)
    CALL SYMBOL (4.8,2.35,0.12,'P',0.0,1)
    CALL SYMBOL (-0.0,-0.0,0.1,' ',0.0,1)
    CALL NUMBER (-0.0,-0.0,0.1,P,0.0,1)
    CALL SYMBOL (4.9,2.15,0.1,' ',0.0,1)
    CALL NUMBER (-0.0,-0.0,0.1,FP,0.0,2)
    CALL SYMBOL (-0.0,-0.0,0.1,'P',0.0,1)
    CALL SYMBOL (-0.0,2.1,0.08,'Y',0.0,1)
360 CALL PLOT (4.3,1.8,3)
    CALL PLOT (4.75,1.8,2)
    CALL PLOT (4.65,1.87,2)
    CALL PLOT (4.65,1.73,2)
    CALL PLOT (4.75,1.8,2)
    CALL SYMBOL (4.3,1.9,0.12,'Q',0.0,1)
    CALL SYMBOL (5.3,1.8,0.3,16,90.0,-1)
    CALL PLOT (5.3,1.4,3)
    CALL PLOT (5.3,1.8,2)
    CALL PLOT (5.27,1.73,2)
    CALL PLOT (5.33,1.73,3)

```



```

CALL PLOT (5.3,1.8,2)
CALL PLOT (5.3,0.9,3)
CALL PLOT (5.3,0.0,2)
CALL PLOT (5.27,0.07,2)
CALL PLOT (5.33,0.07,3)
CALL PLOT (5.3,0.0,2)
CALL SYMBOL (5.2,1.1,0.1,'L=',0.0,2)
CALL NUMBER (-0.0,-0.0,0.1,H,0.0,-1)
CALL SYMBOL (5.4,0.5,0.1,'W',0.0,1)
CALL NUMBER (-0.0,-0.0,0.1,SN,0.0,-1)
CALL SYMBOL (-0.0,-0.0,0.1,'X',0.0,1)
CALL NUMBER (-0.0,-0.0,0.1,WEIGHT,0.0,-1)
CALL SYMBOL (5.4,0.25,0.1,'I=',0.0,2)
CALL NUMBER (-0.0,-0.0,0.1,SI,0.0,1)
CALL PLOT (0.0,0.45,-3)
RETURN
END
FUNCTION IFOX(X)
IF(X .LT. 0.0) GO TO 100
IFCX=IFIX(X)
RETURN
100 IFOX=IFIX(X)-1
RETURN
END

```


Appendix C.

DERIVATION OF MODIFIED SLOPE DEFLECTION EQUATIONS

The standard slope deflection equations have been modified in order to accommodate the special end conditions incurred during the modeling process of a frame for the dynamic analysis, as discussed in Chapter 3. In the model, a member end is restrained by a rotational spring. The member end may also consist of a rigid stub, as shown in Fig. 3-8. The final formats of such equations are shown in Eqs. 3-5 and 3.6. The derivation of these equations is shown in this appendix.

The sway rotation, ρ , between points a and b in Fig. 3-8 is temporarily assumed to be zero. If the joint rotations at points a and b are θ_a and θ_b , respectively, the end rotations of the member cd at points c and d are

$$\theta_a = \frac{M_{cd}^{-\beta_1}}{\alpha_1} ,$$

and

$$\theta_b = \frac{M_{dc}^{-\beta_2}}{\alpha_2}$$

respectively, as explained in Eqs. 3-3 and 3-4. If ρ is zero, the sway rotation between points c and d, ρ_{cd} , is given by:

$$\begin{aligned}\rho_{cd} &= - \frac{\lambda_1 L \theta_a + \lambda_2 L \theta_b}{\lambda_3 L} \\ &= - \frac{\lambda_1 \theta_a + \lambda_2 \theta_b}{\lambda_3} .\end{aligned}$$

Therefore the end moments, M_{cd} and M_{dc} , are expressed by:

$$\begin{aligned}M_{cd} &= \frac{2K}{\lambda_3 L} \left\{ 2 \left(\theta_a - \frac{M_{cd}^{-\beta_1}}{\alpha_1} \right) + \left(\theta_b - \frac{M_{dc}^{-\beta_2}}{\alpha_2} \right) \right. \\ &\quad \left. + 3 \frac{\lambda_1 \theta_a + \lambda_2 \theta_b}{\lambda_3} \right\} + C_{cd}\end{aligned}\quad (C-1)$$

$$\begin{aligned}M_{dc} &= \frac{2K}{\lambda_3 L} \left\{ \left(\theta_a - \frac{M_{cd}^{-\beta_1}}{\alpha_1} \right) + 2 \left(\theta_b - \frac{M_{dc}^{-\beta_2}}{\alpha_2} \right) \right. \\ &\quad \left. + 3 \frac{\lambda_1 \theta_a + \lambda_2 \theta_b}{\lambda_3} \right\} + C_{dc}\end{aligned}\quad (C-2)$$

where K , C_{cd} and C_{dc} are as defined in Eqs. 3-23, 3-7 and 3-8, respectively. Solving Eqs. C-1 and C-2 for M_{cd} and M_{dc} ,

$$\begin{aligned}M_{cd} &= \left[\frac{2K}{\lambda_3 L} \left\{ \left(2 + 3 \frac{\lambda_1}{\lambda_3} + \frac{6K}{\alpha_2 \lambda_3 L} + \frac{6\lambda_1 K}{\alpha_2 \lambda_3^2 L} \right) \theta_a \right. \right. \\ &\quad \left. + \left(1 + 3 \frac{\lambda_2}{\lambda_3} + \frac{6\lambda_2 K}{\alpha_2 \lambda_3^2 L} \right) \theta_b + \left(2 + \frac{6K}{\alpha_2 \lambda_3 L} \right) \frac{\beta_1}{\alpha_1} + \frac{\beta_2}{\alpha_2} \right\} \\ &\quad \left. + \left(1 + \frac{4K}{\alpha_2 \lambda_3 L} \right) C_{cd} - \frac{2K}{\alpha_2 \lambda_3 L} C_{dc} \right] / A_7\end{aligned}\quad (C-3)$$

$$\begin{aligned}
M_{dc} = & \left[\frac{2K}{\lambda_3 L} \left\{ \left(1 + 3 \frac{\lambda_1}{\lambda_3} + \frac{6\lambda_1 K}{\alpha_1 \lambda_3^2 L} \right) \theta_a + \left(2 + 3 \frac{\lambda_2}{\lambda_3} \right. \right. \right. \\
& + \left. \left. \frac{6K}{\alpha_1 \lambda_3 L} + \frac{6\lambda_2 K}{\alpha_1 \lambda_3^2 L} \right) \theta_b + \frac{\beta_1}{\alpha_1} + \left(2 + \frac{6K}{\alpha_1 \lambda_3 L} \right) \frac{\beta_2}{\alpha_2} \right\} \\
& \left. - \frac{2K}{\alpha_1 \lambda_3 L} C_{cd} + \left(1 + \frac{4K}{\alpha_1 \lambda_3 L} \right) C_{dc} \right] / A_7 \quad (C-4)
\end{aligned}$$

where A_7 is defined in Eq. 3-22.

The end moments, M_{ab} and M_{ba} , and the end moments, M_{cd} and M_{dc} , are related as follows.

In general, shear forces at the member ends (see Fig. C-1) are given, ignoring the secondary moments produced by axial force, by

$$Q_1 = -\frac{1}{L}(M_1 + M_2) + \frac{1}{2}wL \quad (C-5)$$

$$Q_2 = -\frac{1}{L}(M_1 + M_2) - \frac{1}{2}wL \quad (C-6)$$

Here the uniformly distributed load, w , is assumed to be applied throughout the member length, L . Therefore the shear force at the right end of member ac , Q_{ac} , is

$$Q_{ac} = -\frac{1}{\lambda_1 L}(M_{ab} + M_{ca}) - \frac{1}{2}w\lambda_1 L$$

and the shear force at the left end of member cd , Q_{cd} , is

$$Q_{cd} = -\frac{1}{\lambda_3 L}(M_{cd} + M_{dc}) + \frac{1}{2}w\lambda_3 L$$

The equilibrium condition at this point requires that the above two shear forces are the same. Thus,

$$M_{ab} = M_{cd} + \frac{\lambda_1}{\lambda_3}(M_{cd} + M_{dc}) - \frac{1}{2}w\lambda_1(1-\lambda_2)L^2 \quad (C-7)$$

In the above, the equilibrium of moments:

$$M_{ca} + M_{cd} = 0 \quad (C-8)$$

is used. A similar process at point d yields:

$$M_{ba} = M_{dc} + \frac{\lambda_2}{\lambda_3}(M_{cd} + M_{dc}) + \frac{1}{2}w\lambda_2(1-\lambda_1)L^2 \quad (C-9)$$

As M_{cd} and M_{dc} are calculated in Eqs. C-3 and C-4, the end moments M_{ab} and M_{ba} are obtained using Eqs. C-7 and C-9. Substituting Eqs. C-3 and C-4 into C-7, M_{ab} is obtained as:

$$M_{ab} = \frac{\frac{2K}{\lambda_3 L} (A_1 \theta_a + A_2 \theta_b + A_4 \frac{\beta_1}{\alpha_1} + A_5 \frac{\beta_2}{\alpha_2}) + A_6 C_{cd}}{A_7} + A_8 D_{ab} \quad \dots (C-10)$$

and similarly, M_{ba} as:

$$M_{ba} = \frac{\frac{2K}{\lambda_3 L} (A_2 \theta_a + A_1' \theta_b + A_5' \frac{\beta_1}{\alpha_1} + A_4' \frac{\beta_2}{\alpha_2}) + A_6' C_{dc}}{A_7} + A_8' D_{ba} \quad \dots (C-11)$$

where $A_1, A_1', A_2, A_4, A_4', A_5, A_5', A_6, A_6', A_7, A_8 D_{ab}$ and $A_8' D_{ba}$ are as defined in Sec. 3-5-1. When deriving these

equations, the relationship,

$$C_{cd} = -C_{dc} \quad (C-12)$$

was used.

If the sway rotation, ρ , is present, the end moments, M_{ab} and M_{ba} , will be expressed in the forms shown in Eqs. 3-5 and 3-6. The end moments observed when the joint rotations at both ends of the member are zero and only the sway rotation, ρ , exists are the same as the moments observed when the joint rotations at both ends are equal to $-\rho$ and the sway rotation is zero. Therefore the coefficients of ρ , A_3 and A'_3 , in Eqs. 3-5 and 3-6, respectively, are given by:

$$A_3 = -(A_1 + A_2)$$

and

$$A'_3 = -(A'_1 + A_2)$$

as shown in Eqs. 3-14 and 3-15. In other words, Eqs. 3-5 and 3-6 are the expressions for the end moments under an arbitrary member position as shown in Fig. 3-8.

The lower ends of the bottom story columns are connected to the foundation through elastic rotational springs. The slope deflection equations must be modified to accommodate this situation. The derivation of modified slope deflection equations for this case is, however, similar to that shown above, thus the explanation has been omitted here.

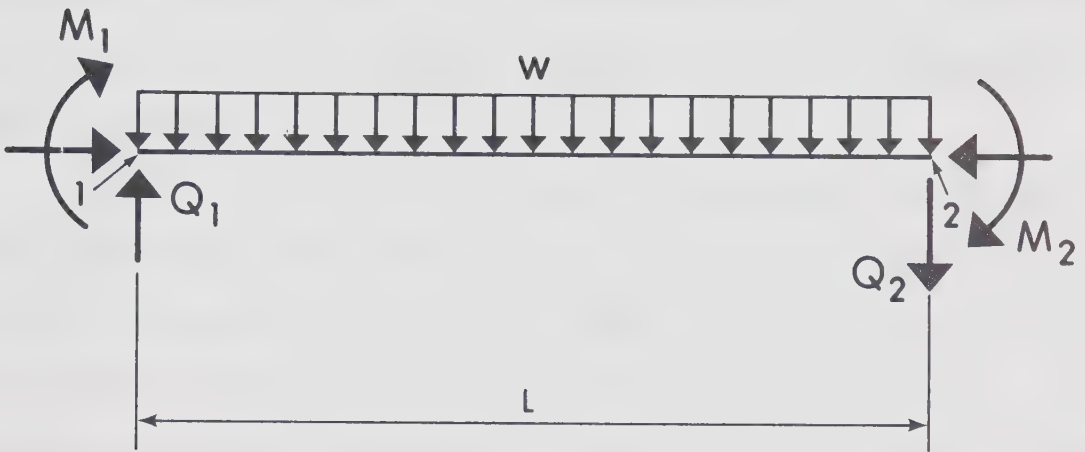


Fig. C-1 Equilibrium of Forces

Appendix D.

COMPUTER PROGRAM II

D-1 Description of the Program.

This program has been developed to perform an inelastic dynamic analysis of a multistory, multibay frame subjected to either a blast load or an earthquake motion. The procedure employed in the program complies with the statements made in Chapter 3.

The $M_s - \delta\theta_s$ relationship must be prepared beforehand for each member end. This may be done using PROGRAM I shown in Appendix B. In the present program, the input statement is made by assuming that the initial $M_s - \delta\theta_s$ relationships are the same at both ends of a member. The data describing the external disturbance may be input through a deck of cards or through a file stored in the computer disk.

The results of the entire response may be printed out or may be either punched out or stored in the disk so that the results can be plotted by CalComp Plotter using a program written especially for this purpose.

D-2 Input Data.

Card Group 1: NS, NB, NCAL, MXIT, NTOBU, NSAI, LTP,

IGPH, TIMELT, DELTAT, GOSA. The input format is (8I5, 10X, 3F10.0). The numbering convention and other symbols are as defined in Chapter 3. The variables used here are as follows.

- NS : Number of stories (N_s),
- NB : Number of bays (N_b),
- NCAL : Number of integration steps,
- MXIT : Maximum number of iterations allowed for each step of integration procedure.
($20 \leq \text{MXIT} \leq 50$),
- NTOBU : Results are printed out for every NTOBU-step of integration,
- NSAI : Number of subdivisions. If there is any change in the value of α_1 , β_1 , α_2 , or β_2 in the modified slope deflection equation or if the convergence was not obtained, the integration is done for smaller time increments as specified by this. ($2 \leq \text{NSAI} \leq 5$)
- LTP : Type of external disturbance.
 - $\text{LTP} \leq 4$... Earthquake
 - $\text{LTP} \geq 5$... Blast Load
- IGPH : Indicates the type of output.
 - $\text{IGPH} \geq 6$... Results are printed out; however they are neither punched out nor stored in the disk.

IGPH = 1 ... Results are punched out.

IGPH = 2 ... Results are stored in the disk.

Two files must be created in the disk, and the output code numbers must be assigned in the following manner.

2 = file name 1

3 = file name 2

In the file name 1, entire behavior is stored; and in file name 2, the maximum values are stored.

TIMELT : This value must be equal to the prepared total computation time minus 0.3 or 0.4 minutes. If the total computation time assigned for this job is not enough to perform all the response calculation, the response calculation is cut off after TIMELT (min) is spent, and the maximum values so far obtained are printed out and the results stored in the disk are saved in the tape.

DELTAT : Incremental time step in the integration step (Δt),

GOSA : Convergence limit. It is usually adequate to specify this value between 0.001 and 0.0001.

Card Group 2: EM, GR, SEICO, IDISC, THAJI, TOWA.

FORMAT (3F10.0, I5, 25X, 2F10.0).

- EM : Modulus of elasticity (E)
- GR : Acceleration of gravity (g)
- SEICO : Input data of external disturbance is multiplied by this value. If the input data for an earthquake is prepared so that the maximum value of acceleration is equal to the acceleration of gravity, SEICO corresponds to the seismic design coefficient in a static analysis. If the input data for a blast load is prepared so that the maximum value is 1.0, SEICO shows the maximum load at the standard floor.
- IDISC : Indicates if the data describing the external disturbance are input through a deck of cards (IDISC \neq 0) or through a file stored in the disk (IDISC = 0). If the data are given through the disk, the file must be called by the input code number 4.
- THAJI and TOWA : The results for every story are printed out regardless of the indication of IP(i) (See Card Group 4) for the time period from THAJI (sec) to TOWA (sec).
If these places are left blank, the function

is ignored.

Card Group 3: $SB(j)$, for $j = 1$ to N_b . FORMAT ((8F10.0)).

$SB(j)$: Length of the j -th bay (from column center to column center)

Card Group 4: For $i = 1$ to N_s ; $SM(i)$, $H(i)$, $SH(i)$, $IP(i)$. FORMAT (3F10.0, I5).

$SM(i)$: Weight concentrated at the i -th floor
($m_i \times g$)

$H(i)$: Damping factor (h_i)

$SH(i)$: Story height of the i -th story

$IP(i)$: Indicates if the print out of the result for the i -th floor is required ($IP(i) \geq 0$) or not ($IP(i) \leq -1$).

Card Group 5: For $i = 1$ to N_s ; $RP(i,j)$, for $j = 1$ to $N_b + 1$. FORMAT ((8F10.0)).

$RP(i,j)$: Length of the rigid stub at the right end of the beam at the i -th floor and the j -th bay which is assumed to be equal to the length of rigid stub at the left end of the beam at the i -th floor and the j -th bay.

Card Group 6: For $i = 1$ to N_s ; $BMI(i,j)$, for $j = 1$ to N_b . FORMAT ((8F10.0)).

$BMI(i,j)$: Moment of inertia of the beam at the i -th floor and the j -th bay.

Card Group 7: For $i = 1$ to N_s ; $CMI(i,j)$, for $j = 1$ to $N_b + 1$. FORMAT ((8F10.0)).

$CMI(i,j)$: Moment of inertia of the column at the i -th story and the j -th row.

Card Group 8: $SPR(j)$, for $j = 1$ to $N_b + 1$. FORMAT ((8F10.0)).

$SPR(j)$: Spring constant of the foundation at the bottom of the j -th column. (for fixed end $\rightarrow 1.0 \times 10^{30}$)

Card Group 9: For $i = 1$ to N_s ; $UDL(i,j)$, for $j = 1$ to N_b . FORMAT ((8F10.0)).

$UDL(i,j)$: Uniformly distributed load applied to the beam at the i -th floor and the j -th bay.

Card Group 10: Part a; $IKUTSU$, $NES(k)$, for $k = 1$ to $IKUTSU$. FORMAT ((16I5)).

Part b; $TEMPO(i)$, for $i = 1$ to 6, $SLPLS(k)$. FORMAT (7F10.0).

$IKUTSU$: Number of members which have the same $M_s - \delta\theta_s$ relationships.

$NES(k)$: Member number which was referred above.

$TEMPO(i)$: Temporary variable. Used to show the coordinates of points A, B and C in Fig. 3-9; i.e.,
 $(TEMPO(1), TEMPO(2))$... Point A
 $(TEMPO(3), TEMPO(4))$... Point B
 $(TEMPO(5), TEMPO(6))$... Point C

The next relationship must be satisfied.

$$\text{TEMPO}(5) > \text{TEMPO}(3) > \text{TEMPO}(1) > 0$$

If the theoretical value of $\text{TEMPO}(1)$ is zero, a value like 1.0×10^{-30} should be input in the computer.

$\text{SLPLS}(k)$: Quantity, ζ , defined in Eq. 2-48.

Part a and part b are repeated until the $M_s - \delta\theta_s$ relationships are input for all members.

Card Group 11 (Only when $\text{LTP} \geq 5$; i.e., for blast load):
 $\text{CSM}(i)$, for $i = 1$ to N_s . $\text{FORMAT} ((8\text{F}10.0))$.

$\text{CSM}(i)$: The i -th element of vector $\{r\}$ which is defined in Sec. 3-7-1.

Card Group 12 (Only when $\text{IGPH} = 1$ or 2): MSKIP , INSA , NPCH , $\text{IPCH}(j)$, for $j = 1$ to NPCH . $\text{FORMAT} (10\text{I}5)$.

MSKIP : Results are either punched out (if $\text{IGPH} = 1$) or stored in the disk (if $\text{IGPH} = 2$) for every MSKIP -steps of integration.

INSA : Indicates if the print out of results is required ($\text{INSA} \geq 5$) or not ($\text{INSA} \leq 4$) together with punched out cards or files stored in the disk.

NPCH : Number of floors for which results are punched out. ($\text{NPCH} \leq 5$).

$\text{IPCH}(j)$: Floor number for which the results are punched out.

If $IGPH = 2$, neither $NPCH$ nor $IPCH(j)$ need to be specified as the results of every floor is stored in the disk.

Card Group 12: $TSEI(i)$, for $i = 1$ to 20. FORMAT (20A4).

$TSEI(i)$: Identification of external disturbance.

Card Group 13: $GA(j)$, for $j = 1$ to $NCAL$. FORMAT ((7F10.0)).

$GA(j)$: Data of external disturbance. Seven data are input at a time.

Some general remarks are listed as follows:

1. One unit each for length, mass and time should be used throughout the preparation of data. As far as this regulation is observed, either customary (English) system or the SI (international) system may be used.
2. If $IDISC = 0$ in Card Group 2, the data given in Card Groups 12 and 13 are assumed to be stored in the disk in the same formats as shown here.
3. Total time for which the response calculation is performed is $NCAL \times DELTAT$.

D-3 Presentation of Results.

The results of response calculation are presented in various manners according to the specified values of $IGPH$ and $INSA$ in the preparation of input data.

- (1) Those which are printed out regardless of the values of IGPH and INSA.
 - a. First three natural periods and the smallest natural period.
 - b. Locations of member end where inelastic action was experienced.
 - c. Locations of member ends where collapse was indicated.
 - d. Maximum values in displacement relative to the ground, displacement relative to the lower floor, velocity relative to the lower floor, absolute acceleration, resisting force due to damping, resisting force due to frame action, shear coefficient and the total (damping and frame action combined) resisting force; for every floor.
- (2) Additional results which are printed out when $IGPH \geq 6$; or $IGPH = 1$ or 2 , and $INSA \geq 5$.
 - e. Displacement relative to the ground, displacement relative to the lower floor, velocity relative to the lower floor, absolute acceleration, resisting force due to damping, resisting force due to frame action and shear coefficient; for the specified floors by $IP(i)$, for every NTOBU-steps of integration.

(3) Results which are punched out when IGPH = 1.

- f. Floor number (counted from the bottom--only in this case), time, displacement relative to the ground, displacement relative to the lower floor, velocity relative to the lower floor, absolute acceleration, resisting force due to damping, resisting force due to frame action and shear coefficient; for the specified floors by IPCH(j), for every MSKIP-steps of integration. The output format is (I2, F8.3, 1P7E10.3).
- g. Maximum values in displacement relative to the lower floor, the time it was recorded, velocity relative to the lower floor, the time it was recorded, shear coefficient and the time it was recorded; for every floor starting from the bottom. The output format is (3(1PE10.4, 0PF10.3)).

(4) The results stored in the disk when IGPH = 2.

- h. The same variables as listed in article f above, by the same output format; except that they are recorded for every.floor.
- i. The same variables indicated in article g above, by the same output format.

D-4 Description of Subprograms and Flow Charts.

(1) MAIN PROGRAM.

Description: MAIN PROGRAM is functioned to set initial values for some variables and to assemble subroutines.

Calls: TIME, SAKURA, STIFF, SHUKI, KIKU and JISHIN.

Flow Chart: Shown in Fig. D-1.

Variables in Common Statements (in order of appearance):

NS, NB, SH(i), SPR(i), SB(i), RP(i,j), UDL(i,j) and
SLPLS(i) : As explained in the preparation of
input data,

STF(i) : Stiffness of the i-th member, $2EI/L$,
where L is either column length or bay
length (column center to center),

IOP(i,j) : Indicates if, in the $M_s-\delta\theta_s$ relationship in Fig. D-2, branch #2 exists (IOP = 1) or has been exhausted during the process of reversals of loading and branch #3 comes after branch #1 (IOP = 2); at the i-th member and the j-th end. End number 1 indicates the upper end of a column or the left end of a beam. End number 2 indicates the other end,

ION(i,j) : Similar to IOP(i,j); indicates if branch #4 still exists (ION = 1) or has been absorbed (ION = 2),

SLP(i,k) : α_1 or α_2 as appears in Eqs. 3-3 and 3-4 for the i-th member. If $k = 1$, the slope of branch #1; if $k = 2$, the slope of branch #2 or #4; and if $k = 3$, the slope of branch #3 or #5 in Fig. D-2,

BETA(i,j,k) : β_j as appears in Eq. 3-3 and 3-4, for the i-th member. Subscript k indicates the branch number as shown in Fig. D-2,

THETA(i,j,k) : The value of $\delta\theta_s$ at points A, B, C, A', B', and C', respectively, corresponding to $k = 1, \dots, 6$ at the i-th member and the j-th end,

IMA(i,j) : Indicates the branch in the M_s - $\delta\theta_s$ relationship where the present values of $(M_s, \delta\theta_s)$ lie, at the i-th member and the j-th end. If they are on branch #1, IMA = 0; if on branch #2, IMA = 1; if on branch #3, IMA = 2; if on branch #4, IMA = -1; and if on branch #5, IMA = -2, in Fig. D-2,

PMO(i,j,k) : The values of M_s at points A and A' in Fig. D-2, for $k = 1$ and 2, respectively, at the i-th member and the j-th end.

HXD(i) : Vector $\{\xi\}$ defined in Eq. 3-28, and

HNL(i) : Vector $\{\eta\}$ defined in Eq. 3-28.

Other Variables (Only the important ones):

GOSA, NCAL, MXIT, NTOBU, NSAI, GR, DELTAT, SEICO,

IP(i), THAJI, TOWA, LTP, IGPH and IDISC : As

explained in the preparation of input data,

C(i) : Identical to H(i) as explained in the preparation of input data until KIKU is called; thereafter, c_i as defined in Eq. 3-29,

SM(i) : Mass concentrated at the i-th floor,

CSM(i) : CSM_i as defined in Eq. 3-35 or $-CR_i$ as defined in Eq. 3-36, depending upon the type of external disturbance,

ITIME : TIMELT expressed in terms of milliseconds,

IA : Number of unknowns (dimension of $\{\theta\}$) in Eq. 3-24,

Q(i,i) : Stiffness matrix [G] in Eq. 3-28,

A(i,j) : Matrix [R] in Eq. 3-24. Stored for only the band width of $2N_b + 3$,

ISHUT : Indicates if the Gaussian elimination process was done without having numerical problems (ISHUT = 0) or not (ISHUT = 1), and

GOME : $1/\omega_1$, where ω_1 as defined in Sec. 3-7-1.

(2) SUBROUTINE SAKURA

Description: SAKURA reads in most of the input data and prints out the important frame properties necessary for the identification of the problem.

Called By: MAIN.

Flow Chart: Omitted.

New Variables:

SM(i) : Weight at first, later converted to mass, concentrated at the i-th floor, and
TEMPO(i) : Temporary variables.

(3) SUBROUTINE STIFF

Description: STIFF is called whenever a new stiffness matrix [G] as in Eq. 3-28 is necessary to be calculated. Matrix [R] as in Eq. 3-24 is constructed by calling FUJI. LU decomposition (Gaussian elimination) of matrix [R] using Doolittle's method (without pivoting) is performed. Then, by calling YURI, Eq. 3-24 is solved for the stiffness matrix in the manner as described in Sec. 3-5-2.

Called By: MAIN, JISHIN and SAIBUN.

Calls: FUJI and YURI.

Flow Chart: Shown in Fig. D-3.

New Variable:

INIT : Indicates if this subroutine is called to calculate the initial stiffness matrix by

MAIN (INIT = 0) or not (INIT = 1).

(4) SUBROUTINE FUJI.

Description: FUJI assembles the elements of matrix [R] defined in Sec. 3-5-2. The coefficients of θ_a and θ_b in the modified slope deflection equations as in Eqs. 3-5 and 3-6 are obtained by calling IZU.

Called By: STIFF.

Calls: IZU.

Flow Chart: Omitted.

New Variables:

VA : Coefficient of θ_a in Eq. 3-5 or 3-6,

VB : Coefficient of θ_b in Eq. 3-5 or 3-6,

MA : Member number indicating the column which connects from above to the joint where the equilibrium of moments is being considered,

ML : Member number indicating the beam which connects from left to such a joint,

MR : Member number indicating the beam which connects from right to such a joint,

MB : Member number indicating the column which connects from below to such a joint,

FR1 : λ_1 as defined in Sec. 3-5-1, and

FR2 : λ_2 as defined in Sec. 3-5-1.

(5) SUBROUTINE IZU.

Description: IZU calculates the coefficients of θ_a and θ_b in Eq. 3-5 or 3-6 when called by FUJI, or those in Eq. C-3 or C-4 when called by KYOTO. If IZU is called with respect to the equilibrium of story shears by FUJI, the corresponding values are calculated from the combined equation, $M_{ab} + M_{ba}$, obtained from Eqs. 3-5 and 3-6. The formulae used in the actual computation sometimes look different than given in the mentioned equations, depending upon the values of α_1 and α_2 .

Called By: FUJI and KYOTO.

Flow Chart: Omitted.

New Variables:

II : Indicates if the present calculation should be done using Eq. 3-5 or C-3 (II = 1), or using Eq. 3-6 or C-4 (II = 2). Further, if II = 3, the combined equation, $M_{ab} + M_{ba}$, should be used,

IASHI : Indicates if the member being considered is the column of bottom story (IASHI = -1) or not (IASHI = 1), and

IGO : Indicates if this subroutine was called by FUJI (IGO = 1) or by KYOTO (IGO = -1).

(6) SUBROUTINE YURI

Description: YURI assembles the right hand side, $\{B\}$, of Eq. 3-24 by calling B, and solves for $\{\theta\}$ by calling SOLVE. It then constructs the stiffness matrix $[G]$ as described in Sec. 3-5-2. If it is the calculation of the initial stiffness matrix, the vector $\{\eta_0\}$ defined in Sec. 3-5-2 is also evaluated.

Called By: STIFF.

Calls: B and SOLVE.

Flow Chart: Omitted.

(7) FUNCTION B

Description: B assembles the i -th element of vector $\{B\}$ in Eq. 3-24 by calling UHEN for given values of vector $\{x\}$.

Called By: YURI and KYOTO.

Calls: UHEN.

Flow Chart: Omitted.

New Variables:

MA, ML, MR, MB FR1 and FR2 : As defined in IZU,
 IJ : Indicates the element number in vector $\{B\}$,
 SXD(i) : Displacement relative to the ground;
 i.e., the vector $\{x\}$ defined in Sec. 3-7-1,
 and
 R : Sway rotation, ρ , as defined in Sec. 3-5-1.

(8) FUNCTION UHEN

Description: UHEN sums the rest of the terms that are excluded either by θ_a term or θ_b term in Eq. 3-5 or 3-6 when called by B, or the corresponding terms in Eq. C-3 or C-4 when called by KYOTO. If UHEN is called with respect to the equilibrium of story shears by B, the corresponding value is calculated from the combined equation, $M_{ab} + M_{ba}$, obtained from Eqs. 3-5 or 3-6. The formulae used in the actual computation, sometimes looks different than given in the mentioned equations depending upon the values of α_1 and α_2 .

Called By: B and KYOTO.

Flow Chart: Omitted.

New Variables:

II and IASH : as defined in IZU,

M : Member number,

S : Member length, and

IGO : Indicates if this function was called by B (IGO = 1) or by KYOTO (IGO = -1).

(9) SUBROUTINE SOLVE

Description: SOLVE solves for $\{\theta\}$ in Eq. 3-24 by back substitutions.

Called BY: YURI and KYOTO.

Flow Chart: Omitted.

New Variables:

$A(i,j)$: Lower and upper matrices that have been obtained by LU decomposition of matrix $[R]$ in Eq. 3-24 (done in STIFF) are now stored, instead of $[R]$ itself,

$W(i)$: Vector $\{B\}$ in Eq. 3-24 at the beginning; then changed to $[L]^{-1}\{B\}$ using forward elimination. When the calculation is finished, it is the solution $\{\theta\}$ in Eq. 3-24, and

$C(i)$: Story shear terms in the solution $\{\theta\}$ in Eq. 3-24.

(10) SUBROUTINE SHUKI

Description: SHUKI computes the first three undamped natural periods and the minimum natural period; and corresponding modes.

Called By: MAIN

Calls: TOKY01.

Flow Chart: Omitted.

(11) SUBROUTINE TOKY01

Description: TOKY01 is used to change a matrix to its inverse matrix as it goes through.

Called By: SHUKI and KIKU.

Flow Chart: Omitted.

(12) SUBROUTINE KIKU

Description: KIKU calculates the damping coefficients, c_i , as defined in Eq. 3-29. It also calculates

the initial deflection, $\{\xi_0\}$ as in Eq. 3-27.

Called By: MAIN.

Calls: TOKYO1.

Flow Chart: Omitted.

(13) SUBROUTINE JISHIN

Description: JISHIN is the most important subroutine as it solves the equations of motion by calling SUCHI, checks member end moments, M_s , and relaxation angles, $\delta\theta_s$, if they are within the assumed branches of the M_s - $\delta\theta_s$ relationship by calling KYOTO and if they are not, a new stiffness matrix is calculated in SAIBUN. The M_s - $\delta\theta_s$ relationships are updated in the manner as described in Sec. 2-5-4, by calling NARA. The results are output in various formats according to input specifications.

Called By: MAIN.

Calls: STIFF, SUCHI, SAIBUN, KYOTO, NARA and TIME.

Flow Chart: Shown in Fig. D-4.

New Variables:

GA(i), TSEI(i) : As defined in the preparation
of input data,

AX(i) : Acceleration relative to the ground
($\{\ddot{x}\}$ as in Sec. 3-7-1),

VX(i) : Velocity relative to the ground ($\{\dot{x}\}$),

XD(i) : Displacement relative to the ground ($\{x\}$),
 RX(i) : Displacement at the i-th floor relative to
 the i+1-th floor,
 RV(i) : Velocity at the i-th floor relative to the
 i+1-th floor,
 AA(i) : Absolute acceleration ($\{\ddot{x}\} + \ddot{y}_0\{1\}$ for an
 earthquake; $\{\ddot{x}\}$ for a blast load),
 CQ(i) : Shear coefficient,
 RESC(i) : Resisting force due to damping,
 RESQ(i) : Resisting force due to frame action,
 RXMX(i) : Maximum value in relative displacement,
 RVMX(i) : Maximum value in relative velocity,
 CQMX(i) : Maximum value in shear coefficient,
 XDMX(i) : Maximum value in displacement relative to
 the ground,
 AAMX(i) : Maximum value in absolute acceleration,
 RCMX(i) : Maximum value in resisting force due to
 damping,
 RQMX(i) : Maximum value in resisting force due to
 frame action,
 TRMX(i) : Maximum value in total resisting force,
 TRX(i) : Time when the maximum relative displacement
 was recorded,
 TRV(i) : Time when the maximum relative velocity was
 recorded,

TCQ(i) : Time when the maximum shear coefficient was recorded,
 OAX(i) : Acceleration ($\{\ddot{x}\}$) obtained in the previous step of integration,
 OVX(i) : Velocity ($\{\dot{x}\}$) obtained in the previous step of integration,
 OXD(i) : Displacement ($\{x\}$) obtained in the previous step of integration,
 FT(i,j) : Present value of relaxation angle, $\delta\theta_s$, at the i-th member and the j-th end,
 KOSAN(i,j) : Indicates if the rotational spring has experienced inelastic action (KOSAN = 1) or not (KOSAN = 0) at the i-th member and the j-th end,
 GA1 : External disturbance at $t = t_p - 2\Delta t$ where t_p is the value of time axis for which the present step of calculation is being done,
 GA2 : External disturbance at $t = t_p - \Delta t$,
 GA3 : External disturbance at $t = t_p$,
 GA4 : External disturbance at $t = t_p + \Delta t$, and
 TP : Value of time axis for which the present step of calculation is being done.

(14) SUBROUTINE SAIBUN

Description: SAIBUN reperforms the numerical integration by calling SUCHI with a smaller value of

time increment, when the calculations failed to converge with regular value of Δt or when the $M_s - \Delta \theta_s$ relationships at any member ends are being changed from one branch to another.

Called By: JISHIN.

Calls: SUCHI, KYOTO, STIFF and NARA.

Flow Chart: Shown in Fig. D-5.

New Variable:

GAP : Present value of external disturbance obtained by interpolating GA1, GA2, GA3 and GA4.

(15) SUBROUTINE SUCHI

Description: SUCHI solves the equations of motion using the linear acceleration method as explained in Sec. 3-7-2.

Called By: JISHIN and SAIBUN.

Calls: QQ.

Flow Chart: Shown in Fig. D-6.

New Variable:

ISAI : Indicates if the equations of motion were solved successfully; i.e., numerical integration procedure converged (ISAI = 10) or not (ISAI = -10).

(16) FUNCTION QQ

Description: QQ calculates $Q_i(\{x\})$ in Eq. 3-33.

Called By: SUCHI.

Flow Chart: Omitted.

(17) SUBROUTINE KYOTO

Description: KYOTO calculates the present value of relaxation angle at every member end and checks if it is within the assumed branch of the $M_s - \delta\theta_s$ relationship (set ICHI = 0) or not (Set ICHI \geq 1).

Called By: JISHIN and SAIBUN.

Calls: B, SOLVE, IZU and UHEN.

Flow Chart: Shown in Fig. D-7.

New Variables:

EM(j) : End moment at the j-th end of the member being considered; i.e., M_{cd} and M_{dc} as defined in Eqs. C-3 and C-4, and

IIQ : Indicates if this subroutine was called by JISHIN (IIQ = 1) or by SAIBUN (IIQ = 2).

(18) SUBROUTINE NARA

Description: NARA updates the $M_s - \delta\theta_s$ relationships by using the procedure described in Sec. 2-5-4. It also prints out the location of member end when it experiences the inelastic action for the first time or when the collapse is indicated.

Called By: JISHIN and SAIBUN.

Flow Chart: Shown in Fig. D-8.

New Variable:

KDIS : Indicates if any rotational springs have
indicated collapses (KDIS = -10) or not
(KDIS = 10).

(19) SUBROUTINE TIME

Description: TIME is a standard MTS (Michigan Terminal System - IBM/360 at the University of Alberta) subroutine which allows the user easy access to the elapsed time, CPU time used, time of day, and the date in convenient units.

Called By: MAIN and JISHIN.

D-5 Listing of Program.

The listing of the program appears on pages 271 through 300.

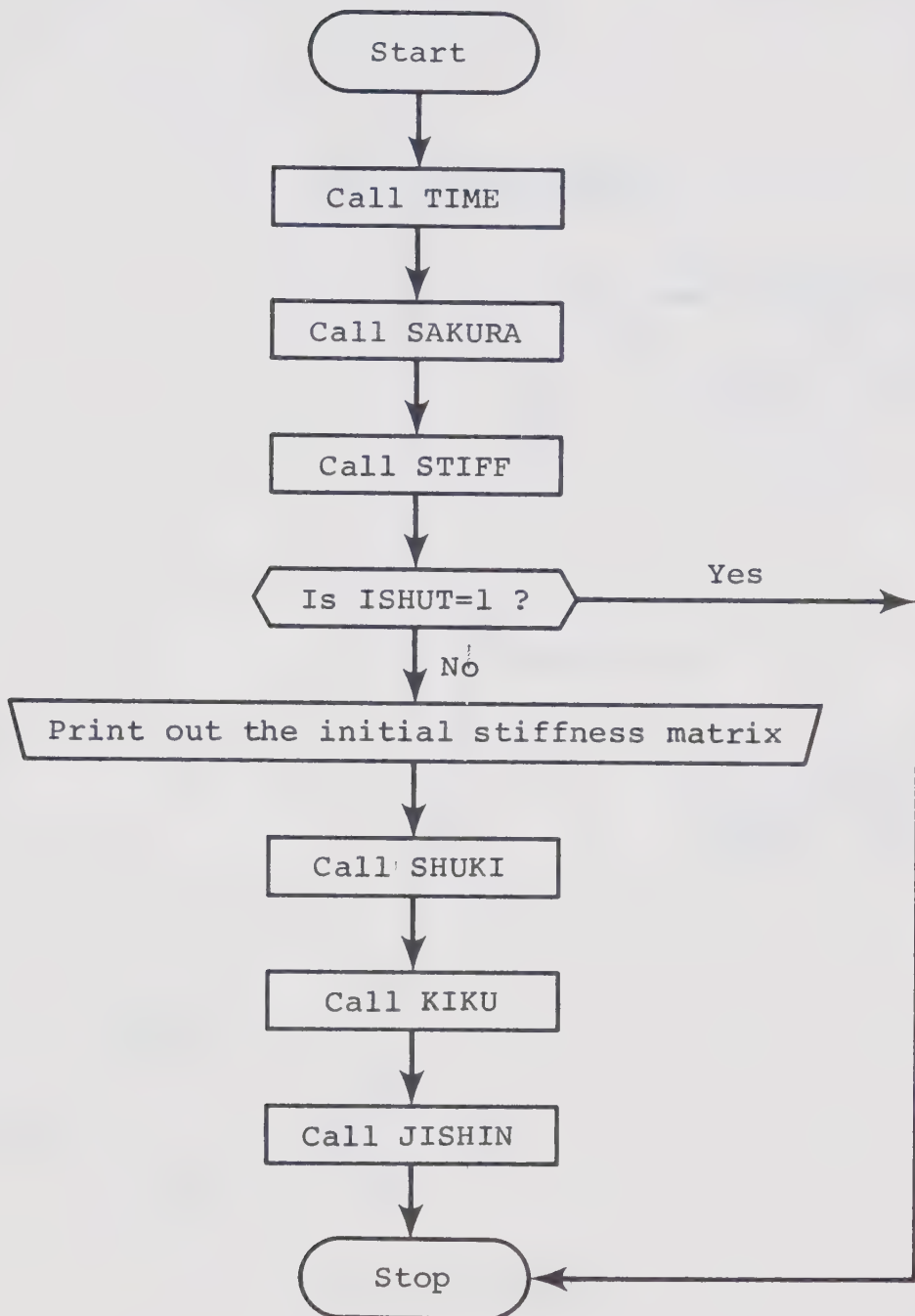


Fig. D-1 MAIN PROGRAM

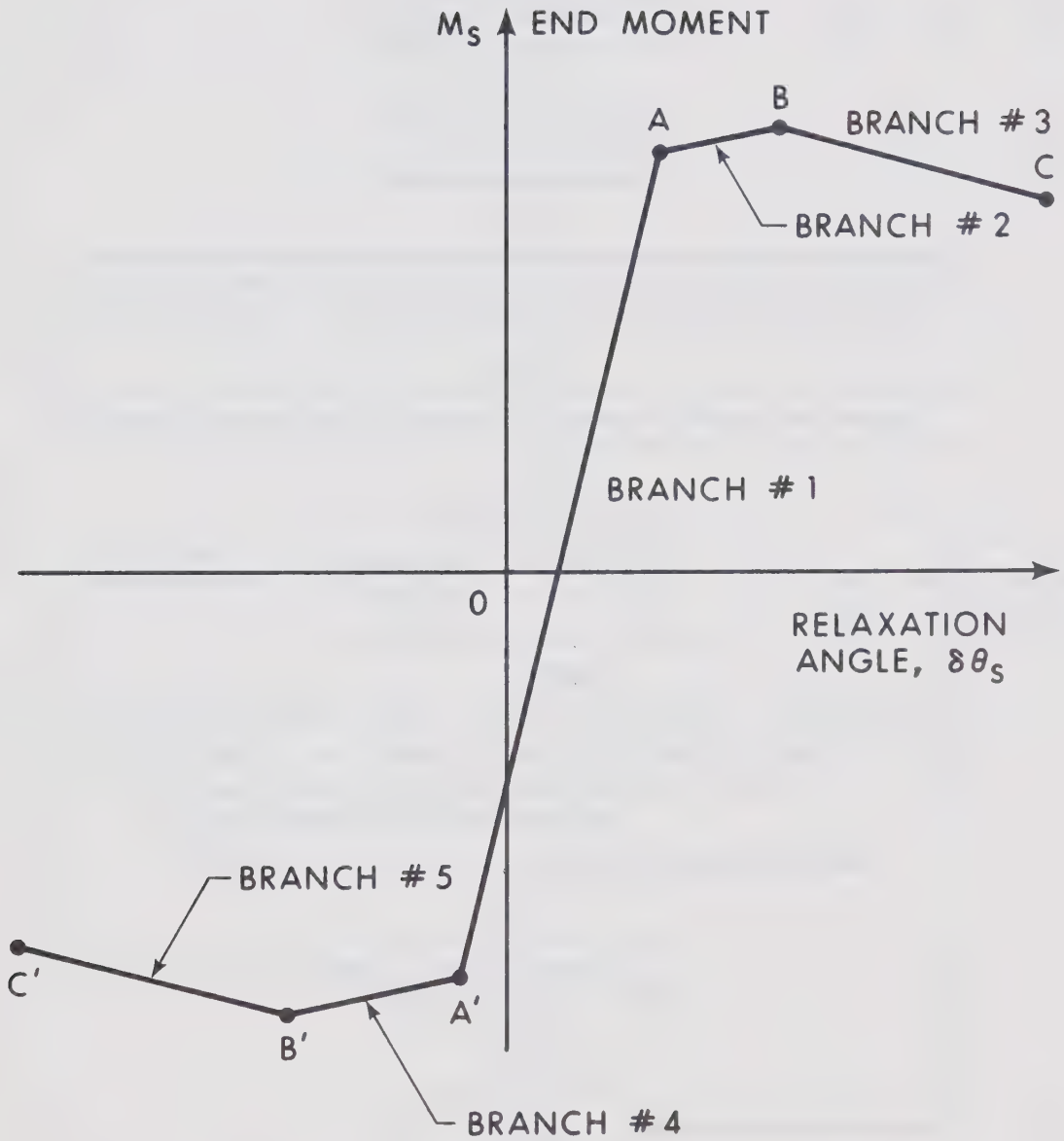


Fig. D-2 $M_s - \delta\theta_s$ Relationship in General Situation

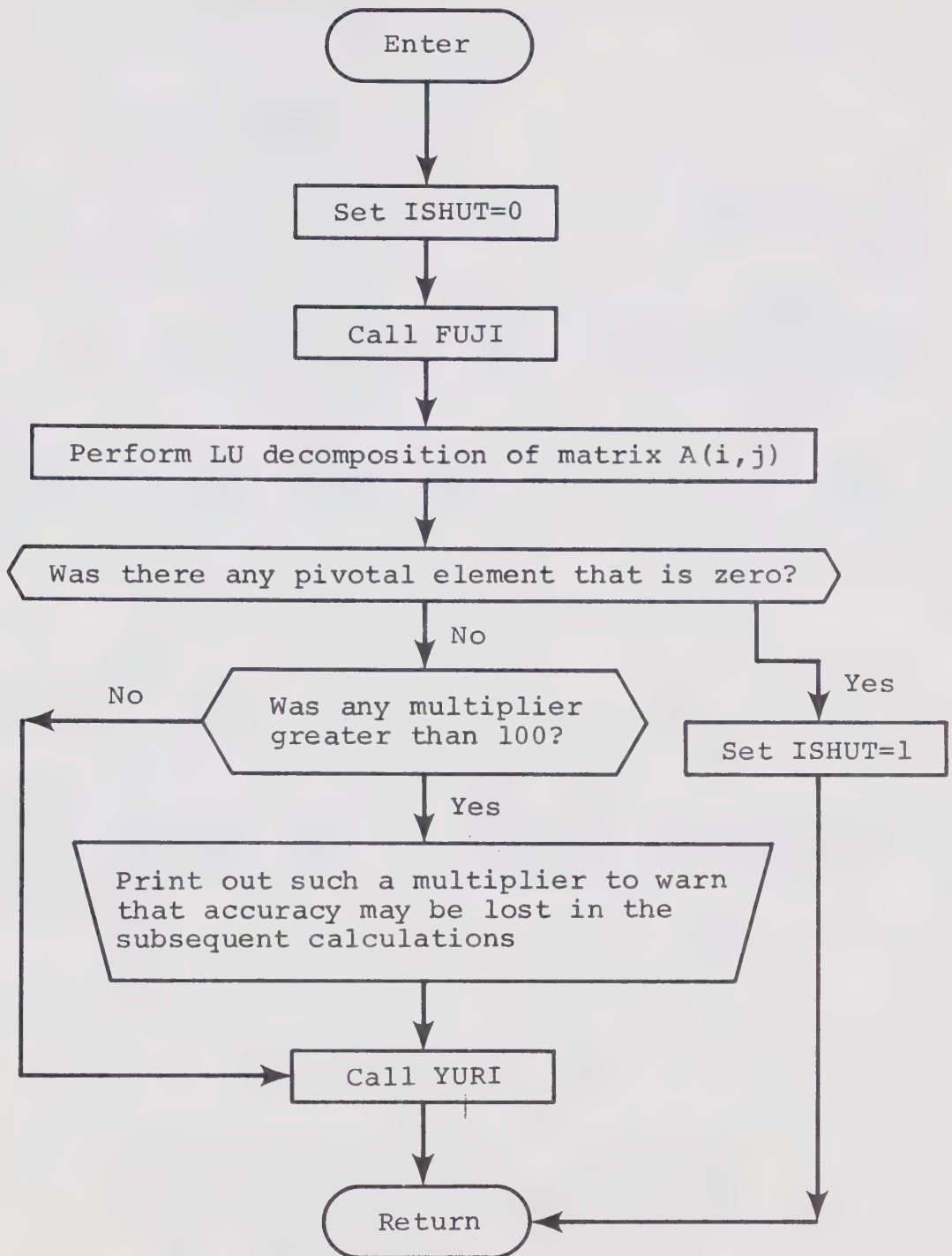


Fig. D-3 SUBROUTINE STIFF

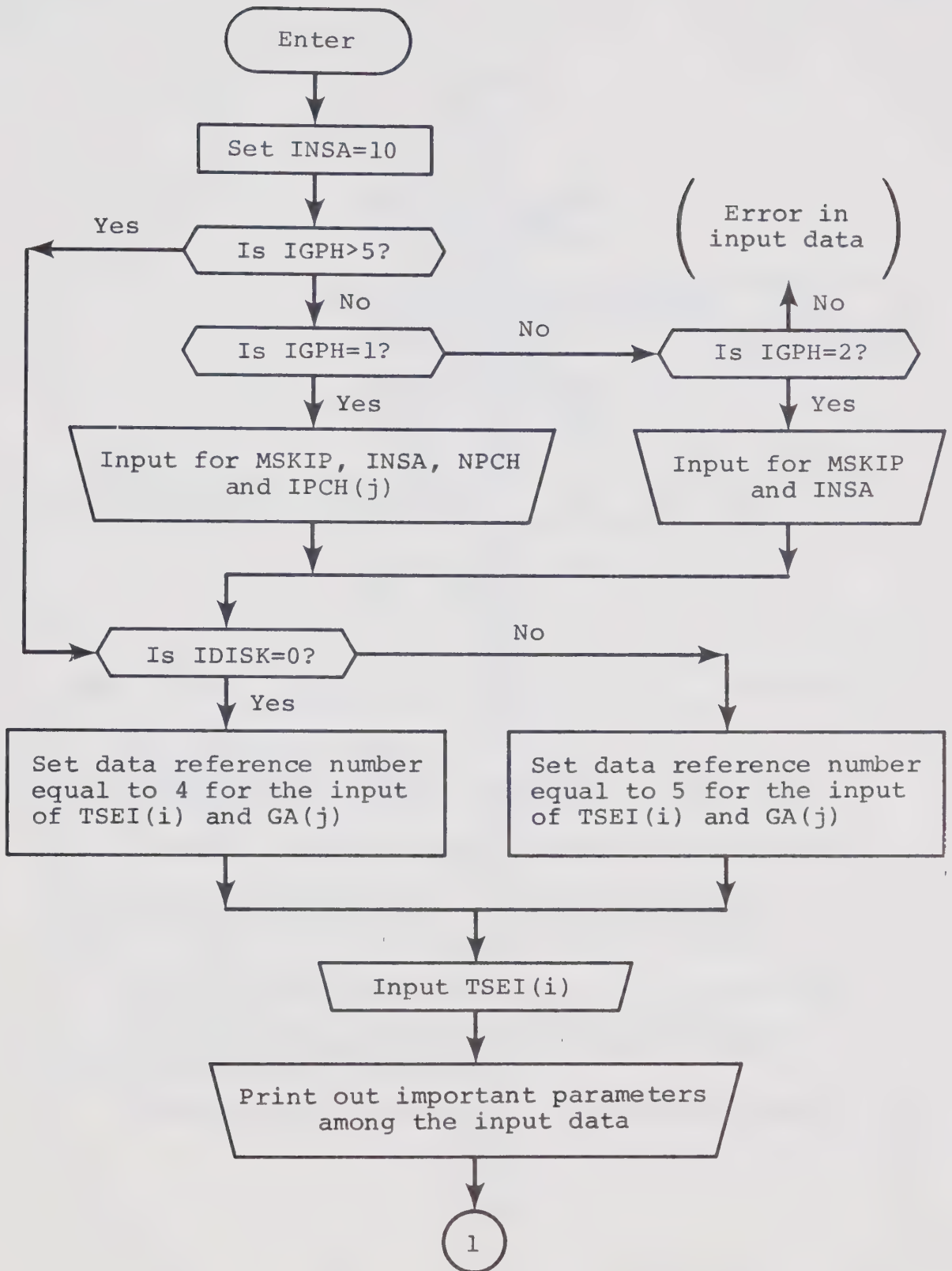


Fig. D-4 SUBROUTINE JISHIN (to be continued)

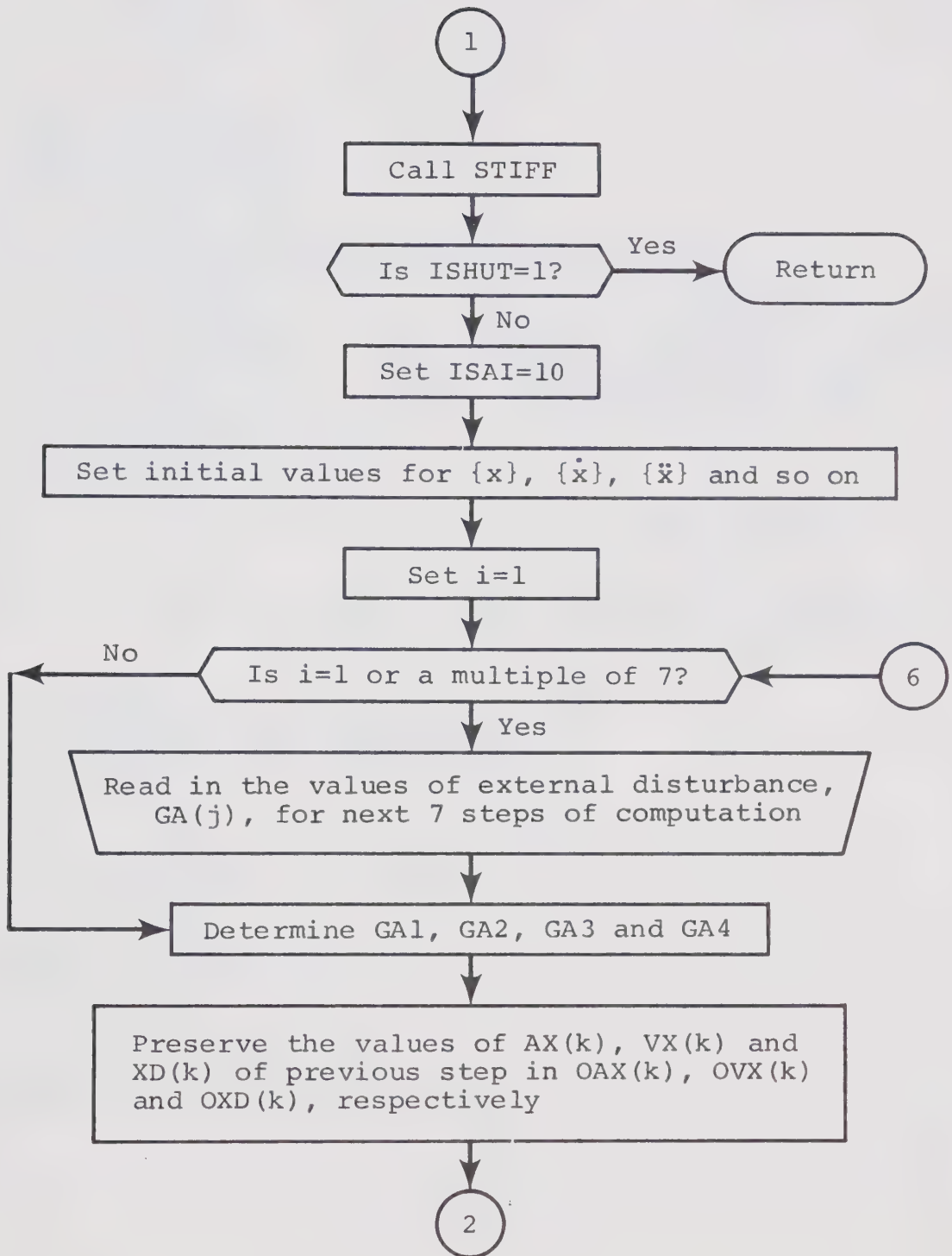


Fig. D-4 (continued) SUBROUTINE JISHIN

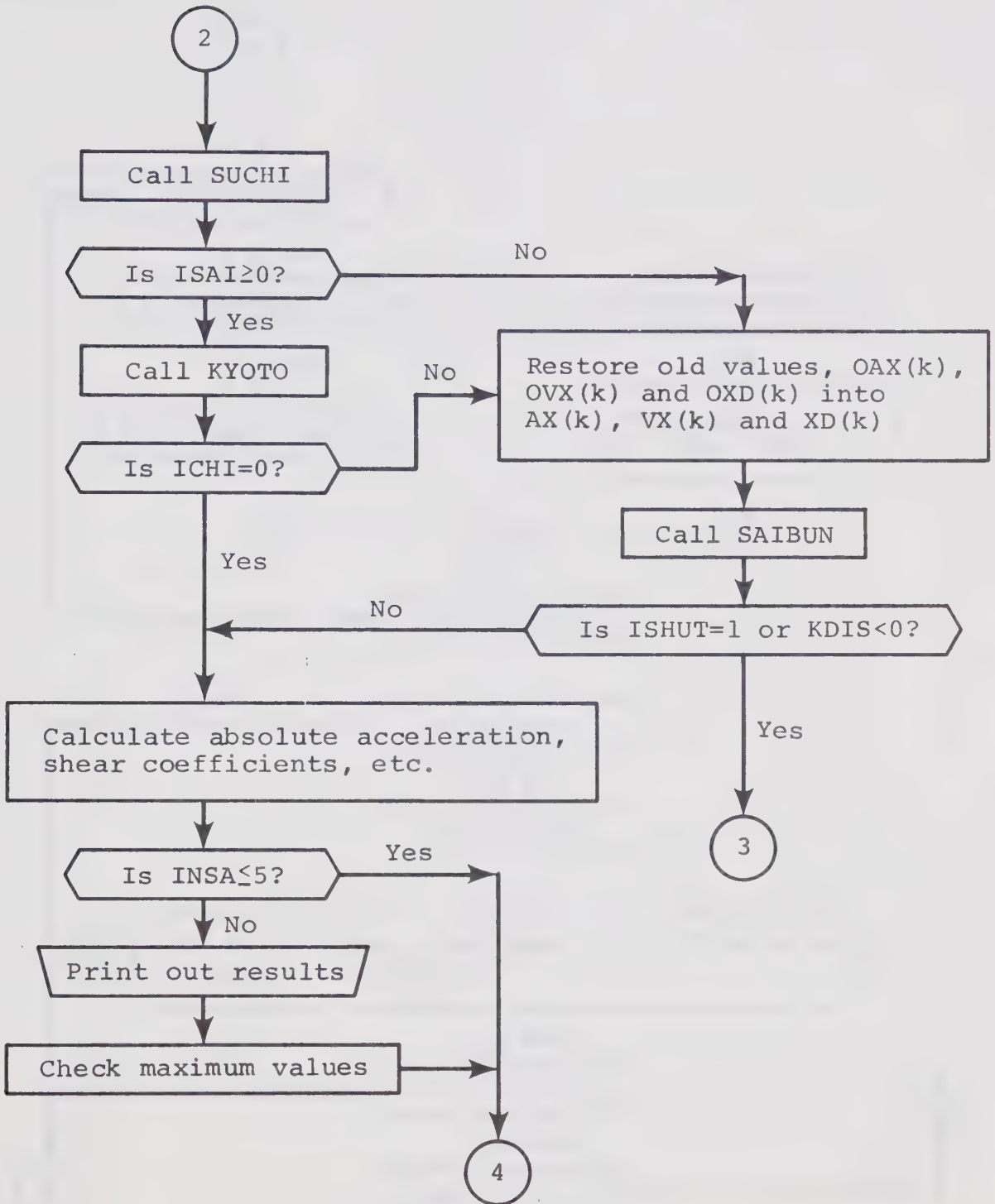


Fig. D-4 (continued) SUBROUTINE JISHIN

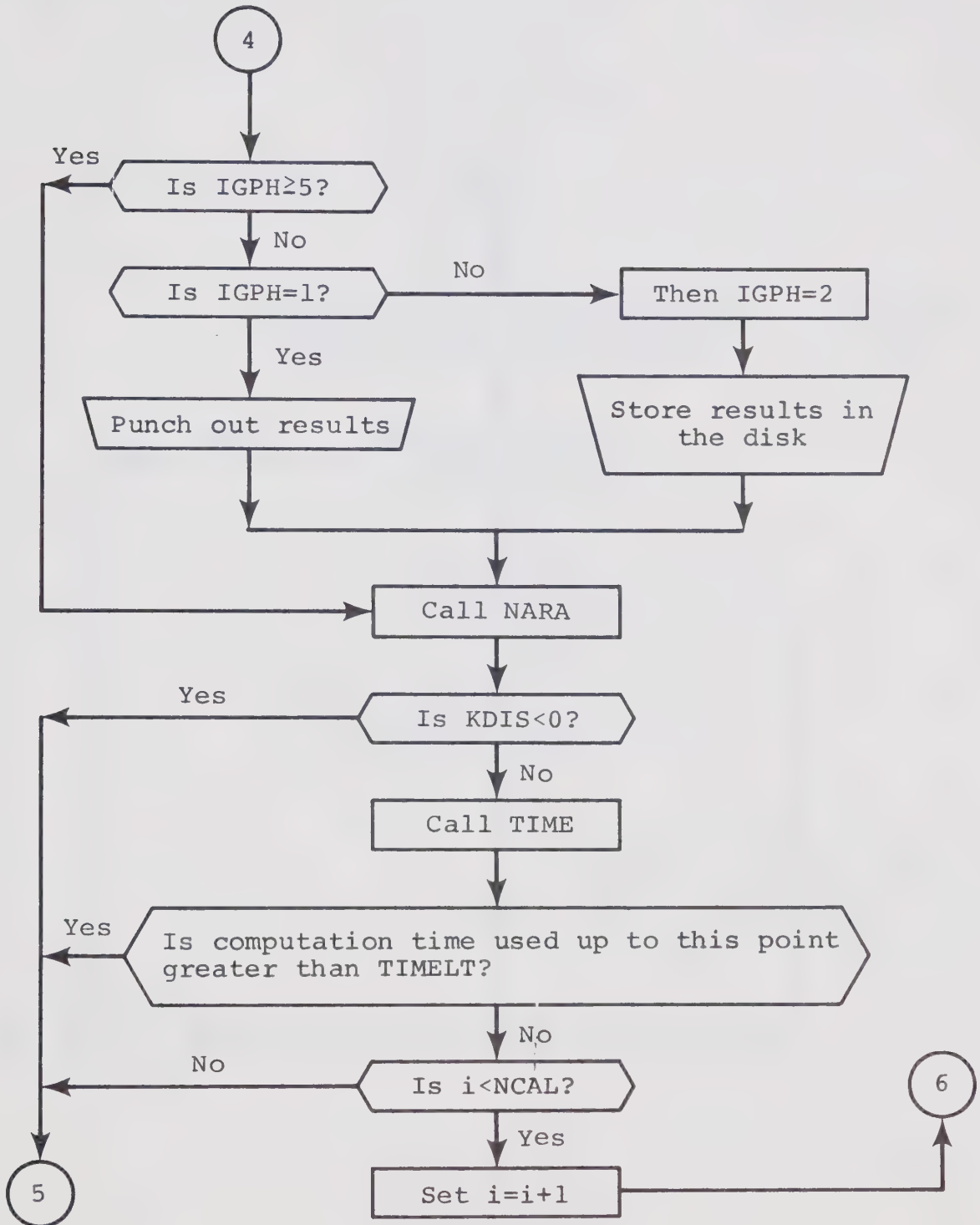


Fig. D-4 (continued) SUBROUTINE JISHIN

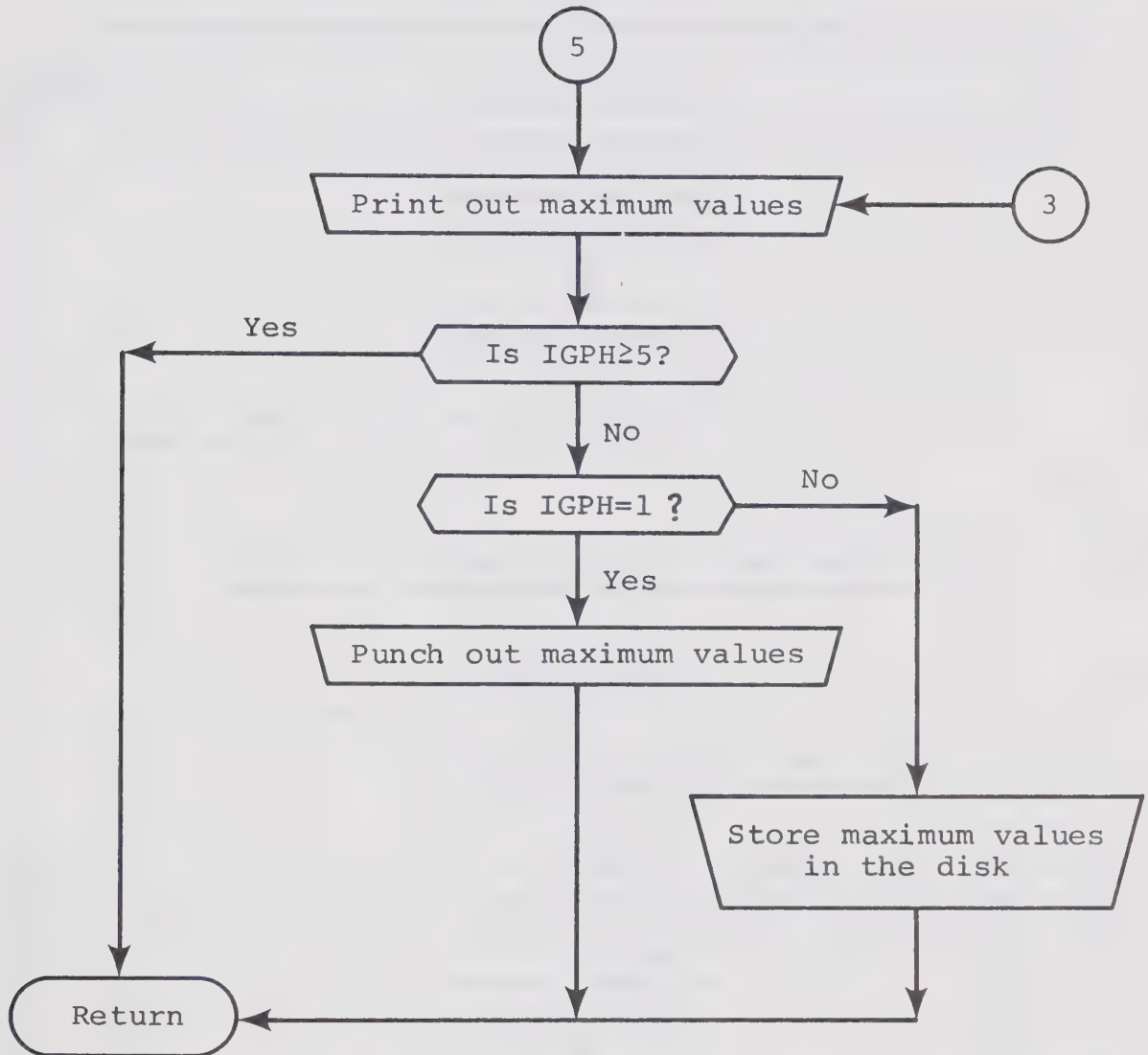


Fig. D-4 (continued) SUBROUTINE JISHIN

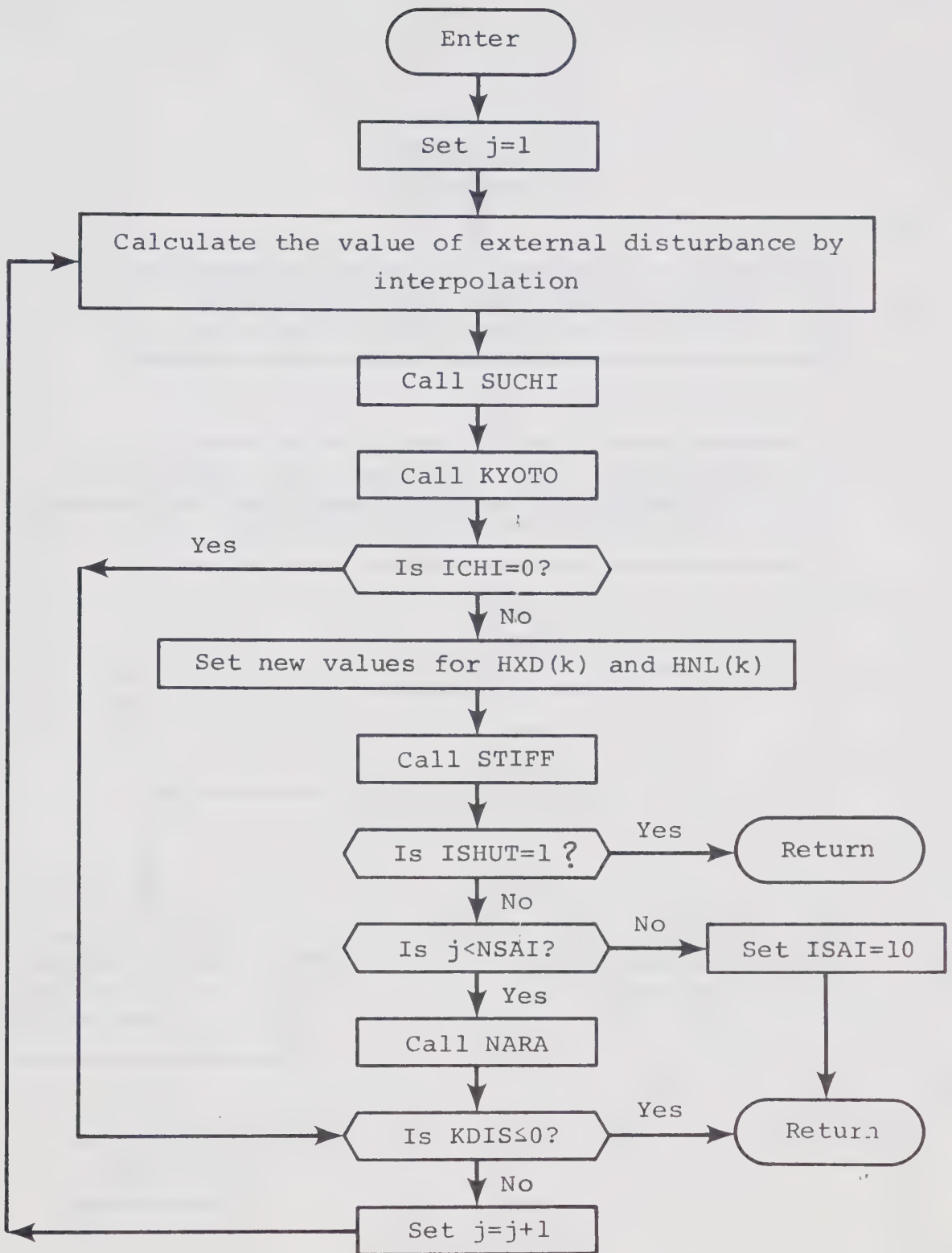


Fig. D-5 SUBROUTINE SAIBUN

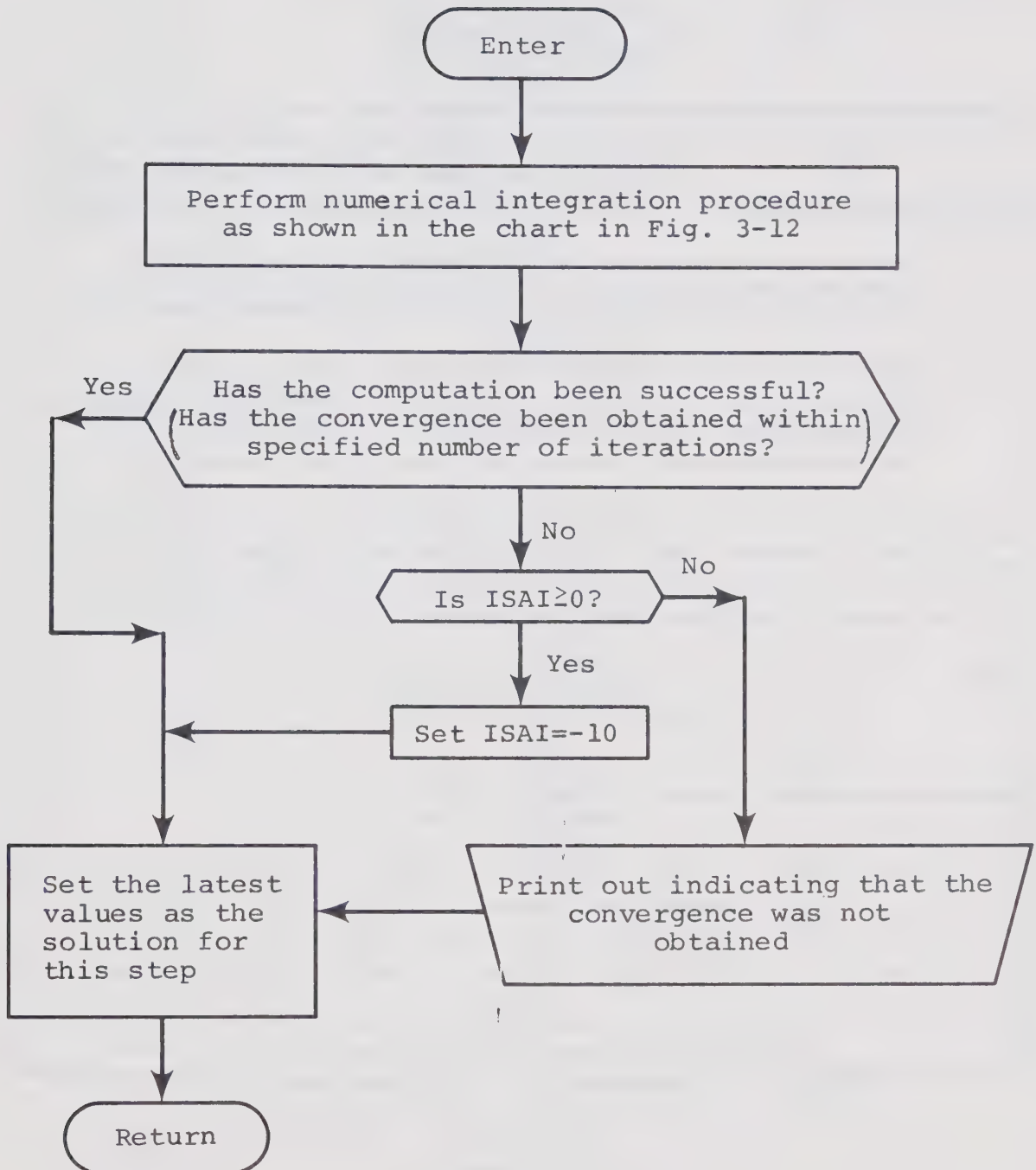


Fig. D-6 SUBROUTINE SUCHI

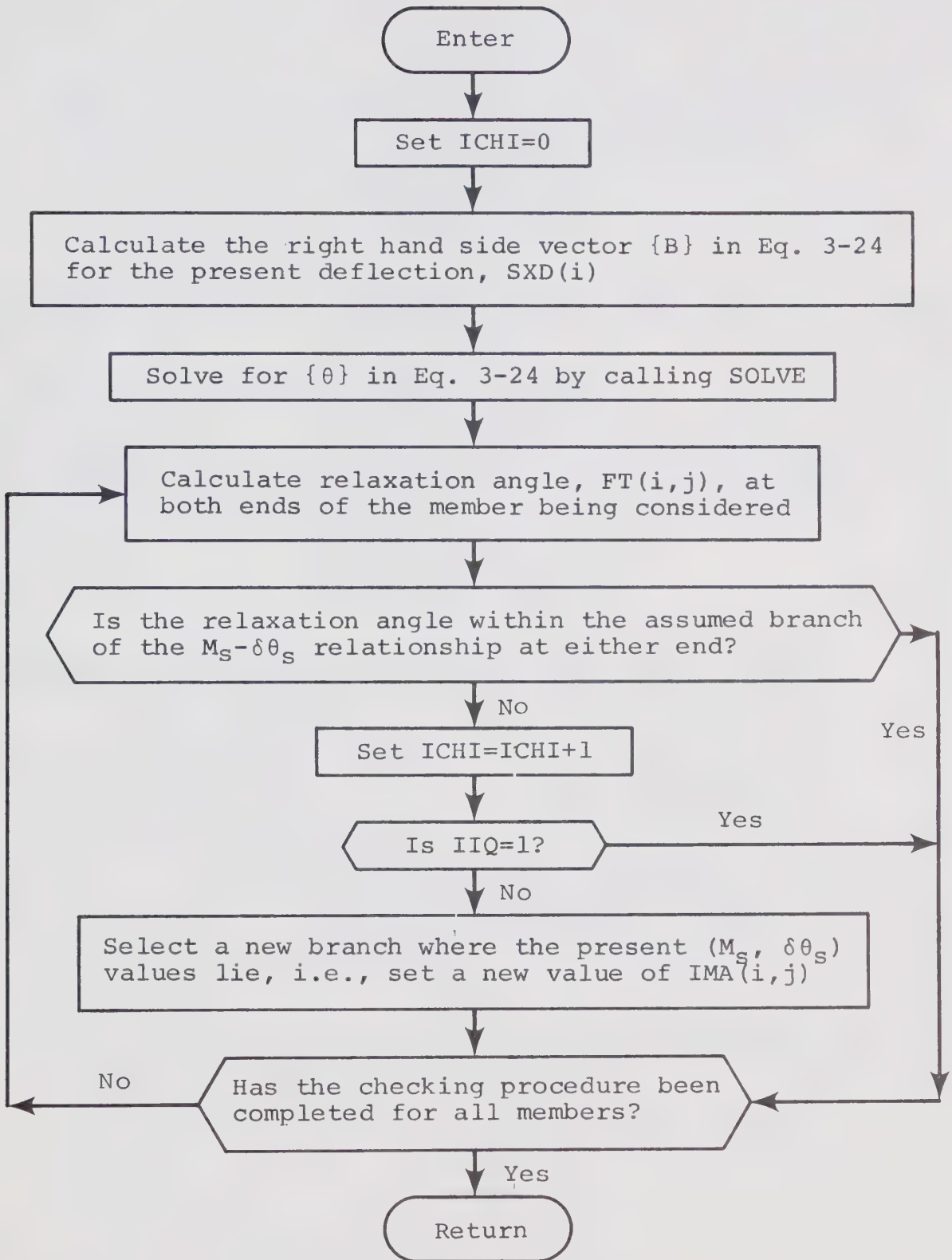


Fig. D-7 SUBROUTINE KYOTO

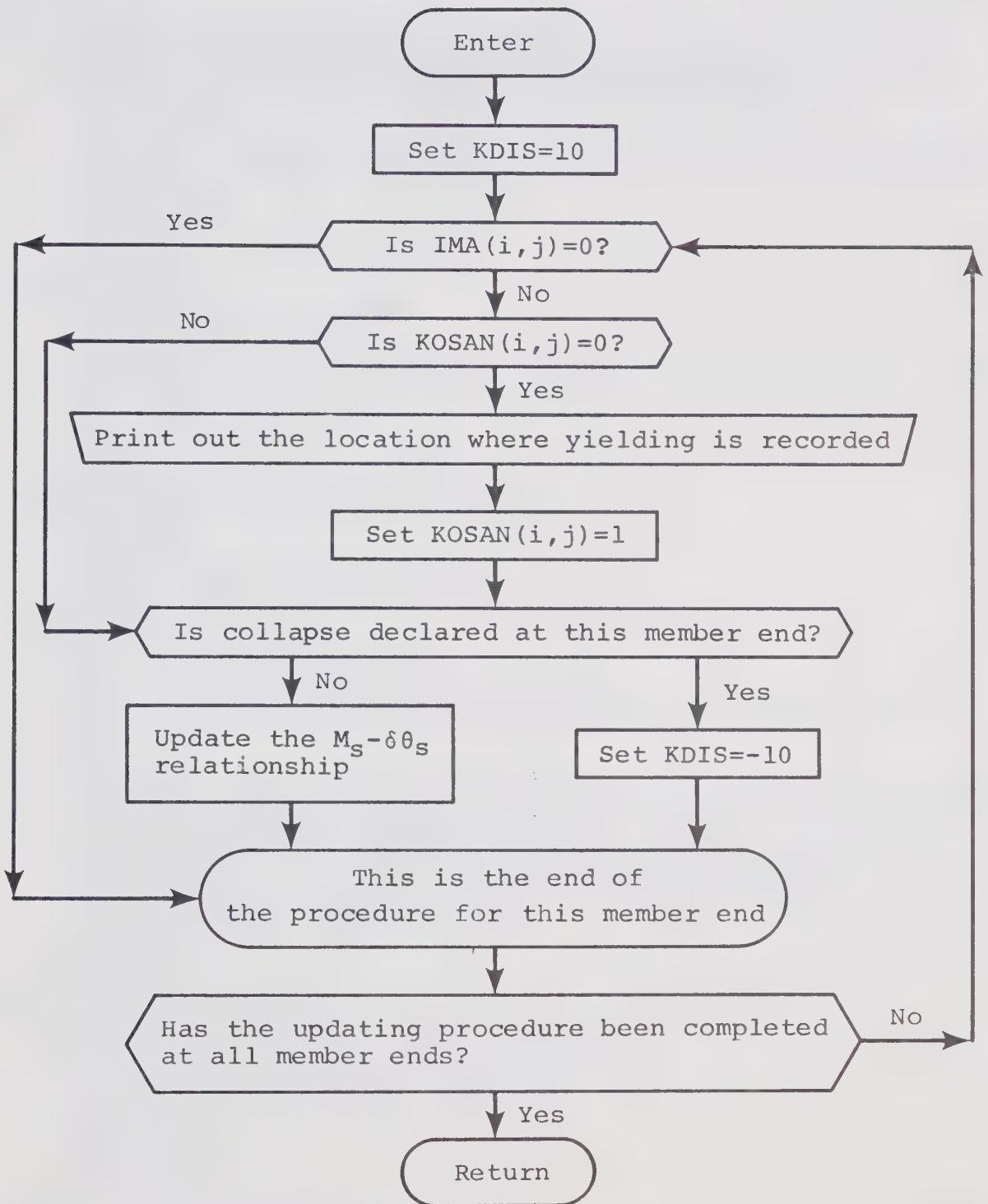


Fig. D-8 SUBROUTINE NARA

LISTING OF PROGRAM II

```

COMMON NS,NB,STF(225),SH(25),SPR( 5),SB( 4),RP(25, 5),UDL(25, 4)
CCMMCN IOP(225,2),ION(225,2),SLPLS(225),SLP(225,3),BETA(225,2,5),
1THETA(225,2,6),IMA(225,2),PMO(225,2,2),HXD(25),HNL(25)
DIMENSION A(150, 11),CSM(25),Q(25,25),C(25),SM(25),IP(25)
CALL TIME(0)
CALL SAKURA (GOSA,NCAL,MXIT,NTOB,NSAI,GR,DELTAT,SEICO,C,SM,IP,CSM
1,THAJI,TOWA,LTP,IGPH,ITIME,IDISC)
IA=(NB+2)*NS
DO 100 I=1,NS
  HXD(I)=0.0
  HNL(I)=0.0
100 CONTINUE
  CALL STIFF(Q,0,A,IA,ISHUT)
  IF(ISHUT.EQ. 1) STOP
  WRITE(6,200)
200 FORMAT(/1X,'STIFFNESS MATRIX FOR THE FRAME -- IN TERMS OF TOTAL ST
1OREY SHEAR.')
  IF(NS.LE. 8) GO TO 230
  DC 220 I=1,NS
  WRITE(6,210) I,(Q(I,J),J=1,NS)
210 FORMAT(3X,'ROW',I3,8E15.6/(9X,8E15.6))
220 CCNTINUE
  GO TO 260
230 DO 250 I=1,NS
  WRITE(6,240) I,(Q(I,J),J=1,NS)
240 FORMAT(3X,'ROW',I3,8E15.6)
250 CCNTINUE
260 CALL SHUKI(Q,SM,GOME)
  CALL KIKU (DELTAT,C,GOME,Q,GOSA,GR,NCAL)
  CALL JISHIN (SM,CSM,C,IP,IGPH,GR,GOSA,NCAL,DELTAT,MXIT,NSAI,NTOB,
1THAJI,TOWA,SEICO,Q,IA,A,LTP,ITIME,IDISC)
  STOP
  END
  SUEROUTINE SAKURA (GOSA,NCAL,MXIT,NTOB,NSAI,GR,DELTAT,SEICO,H,SM,
1IP,CSM,THAJI,TOWA,LTP,IGPH,ITIME,IDISC)
  CCMMCN NS,NB,STF(225),SH(25),SPR( 5),SB( 4),RP(25, 5),UDL(25, 4)
  CCMMCN IOP(225,2),ION(225,2),SLPLS(225),SLP(225,3),BETA(225,2,5),
1THETA(225,2,6),IMA(225,2),PMO(225,2,2),HXD(25),HNL(25)
  DIMENSION PMC(225),BMI(25, 4),CMI(25, 5),SM(25),IP(25),H(25),CSM(2
15),NES(225),TEMPO(225),NESS(225)
  10 FORMAT(1H1)
  20 FORMAT(1H )
COMMENT : INPUT STATEMENT
  READ(5,100) NS,NB,NCAL,MXIT,NTOB,NSAI,LTP,IGPH,TIMELT,
1DELTAT,GOSA,EM,GR,SEICO,IDISC,THAJI,TOWA
100 FORMAT( 8I5,10X,3F10.0/3F10.0,I5,25X,2F10.0)
  IF(TIMELT.LT. 0.000001) TIMELT=60.0
  ITIME=IFIX(TIMELT*60000.0)
  NE1=NB+1
  NBB=2*NB+1
  NEET=NBB*NS
COMMENT : INPUT STATEMENT
  READ(5,110) (SB(J),J=1,NB)
110 FORMAT((8F10.0))
  DC 130 I=1,NS
COMMENT : INPUT STATEMENT
  READ(5,120) SM(I),H(I),SH(I),IP(I)

```



```

120 FORMAT (3F10.0,I5)
130 CCNTINUE
    DC 140 I=1,NS
COMMENT : INPUT STATEMENT
    READ (5,110) (RP(I,J),J=1,NB1)
140 CCNTINUE
    DO 150 I=1,NS
COMMENT : INPUT STATEMENT
    READ (5,110) (BMI(I,J),J=1,NB)
150 CONTINUE
    EC 160 I=1,NS
COMMENT : INPUT STATEMENT
    READ (5,110) (CMI(I,J),J=1,NB1)
160 CONTINUE
    DO 190 I=1,NS
    DO 170 J=1,NB
    IJ=NBE*(I-1)+J
    STF(IJ)=2.0*EM*BMI(I,J)/SB(J)
170 CCNTINUE
    DC 180 J=1,NB1
    IJ=NBB*(I-1)+NB+J
    STF(IJ)=2.0*EM*CMI(I,J)/SH(I)
180 CCNTINUE
190 CCNTINUE
COMMENT : INPUT STATEMENT
    READ (5,110) (SFR(I),I=1,NB1)
    CSM(1)=SM(1)
    IF(NS.EQ.1) GO TO 220
    DO 210 I=2,NS
    CSM(I)=CSM(I-1)+SM(I)
210 CCNTINUE
220 DO 230 I=1,NS
COMMENT : INPUT STATEMENT
    READ (5,110) (UDL(I,J),J=1,NB)
230 CCNTINUE
    ITSU=0
    KUMI=0
COMMENT : INPUT STATEMENT
240 READ (5,241) IKUTSU, (NES(K),K=1,IKUTSU)
241 FORMAT ((16I5))
    K=10000000
    DO 231 J=1,IKUTSU
    IF(NES(J).GE.K) GO TO 231
    K=NES(J)
    IF(J.EQ.1) GO TO 231
    NES(J)=NES(1)
    NES(1)=K
231 CCNTINUE
COMMENT : INPUT STATEMENT
    READ (5,242) (TEMPO(I),I=1,6),SLPLS(K)
242 FORMAT (7E10.5)
    KUMI=KUMI+1
    DO 245 J=1,IKUTSU
    JJ=NES(J)
    NESS(JJ)=KUMI
245 CCNTINUE
    SLF(K,1)=TEMPO(2)/TEMPO(1)
    SLF(K,2)=(TEMPO(4)-TEMPO(2))/(TEMPO(3)-TEMPO(1))
    SLF(K,3)=(TEMPO(6)-TEMPO(4))/(TEMPO(5)-TEMPO(3))
    BETA(K,1,1)=0.0

```



```

      BETA(K,1,2)=(TEMPO(3)*TEMPO(2)-TEMPO(1)*TEMPO(4))/(TEMPO(3)-TEMPO(
11))
      BETA(K,1,3)=(TEMPO(5)*TEMPO(4)-TEMPO(3)*TEMPO(6))/(TEMPO(5)-TEMPO(
13))
      BETA(K,1,4)=-BETA(K,1,2)
      BETA(K,1,5)=-BETA(K,1,3)
      THETA(K,1,1)=TEMPO(1)
      THETA(K,1,2)=TEMPO(3)
      THETA(K,1,3)=TEMPO(5)
      THETA(K,1,4)=-TEMPO(1)
      THETA(K,1,5)=-TEMPO(3)
      THETA(K,1,6)=-TEMPO(5)
      PMC(K,1,1)=TEMPO(2)
      PMC(K,1,2)=-TEMPO(2)
      DC 270 I=1,IKUTSU
      KI=NES(I)
      DO 260 J=1,2
      ICF(KI,J)=1
      ICN(KI,J)=1
      IMA(KI,J)=0
      IF(I.EQ. 1 .AND. J.EQ. 1) GO TO 260
      DO 255 L=1,6
      THETA(KI,J,L)=THETA(K,1,L)
      IF(L.GE. 6) GO TO 255
      BETA(KI,J,L)=BETA(K,1,L)
      IF(L.GE. 3) GO TO 255
      PMC(KI,J,L)=PMC(K,1,L)
255  CCNTINUE
260  CCNTINUE
      IF(I.EQ. 1) GO TO 270
      SLPLS(KI)=SLPLS(K)
      DO 265 L=1,3
      SLF(KI,L)=SLP(K,L)
265  CCNTINUE
270  CCNTINUE
      THETA(K,1,5)=TEMPO(4)
      THETA(K,1,6)=TEMPO(6)
      ITSU=ITSU+IKUTSU
      IF(ITSU.EQ. NBBT) GO TO 275
      GO TO 240
275  WRITE(6,10)
      WRITE(6,280)
280  FORMAT(1X,'** INPUT DATA **')
      WRITE(6,290)
290  FORMAT(/1X,'BEAMS  ',5X,'PLASTIC MCMENT ** STIFFNESS(2EI/L) ** U.D
1.I. ')
      KAKU=1
300  JS=(KAKU-1)*3+1
      IF(NE.LE. KAKU*3) GO TO 301
      JE=JS+2
      KAKU=KAKU+1
      GO TO 302
301  JE=NB
      KAKU=-1
      JFS=JE+1-JS
      GO TO (304,303,302), JES
304  WRITE(6,307) (J,J=JS,JE)
      GO TO 308
303  WRITE(6,306) (J,J=JS,JE)
      GO TO 308

```



```

302 WRITE(6,305) (J,J=JS,JE)
305 FORMAT(3X,'FLCCR',3(10X,'---- BAY NO. (' ,I3,' ) ----',7X))
306 FORMAT(3X,'FLOCR',2(10X,'---- BAY NO. (' ,I3,' ) ----',7X))
307 FORMAT(3X,'FLOOR',10X,'---- BAY NO. (' ,I3,' ) ----')
308 DC 320 I=1,NS
      IJ=NBB*(I-1)+JS
      IJJ=IJ+JE-JS
      DO 310 K=JS,JE
      KK=IJ-JS+K
      TEMPO(KK)=UDL(I,K)
310 CONTINUE
      WRITE(6,315) I,((PMO(J,1,1),STF(J),TEMPO(J)),J=IJ,IJJ)
315 FORMAT(1X,I6,1X,3(2X,E13.5))
320 CCNTINUE
      WRITE(6,325) (SB(J),J=JS,JE)
325 FORMAT(3X,'BAY LENGTH',10X,E13.5,2(28X,E13.5))
      IF(KAKU.GE. 0) GO TO 300
      WRITE(6,330)
330 FORMAT(/1X,'COLUMNS',5X,'PLASTIC MOMENT ** STIFFNESS(2EI/H) ** LE
      NGTH OF RIGID ZONE (EACH SIDE OF CCOLUMN)')
      KAKU=1
340 JS=(KAKU-1)*3+1
      IF(NB1.LE. KAKU*3) GO TO 341
      JE=JS+2
      KAKU=KAKU+1
      GO TO 342
341 JE=NB1
      KAKU=-1
      JES=JE+1-JS
      GO TO (344,343,342), JES
344 WRITE(6,347) (J,J=JS,JE)
      GO TO 348
343 WRITE(6,346) (J,J=JS,JE)
      GO TO 348
342 WRITE(6,345) (J,J=JS,JE)
345 FORMAT(3X,'STOREY',3(9X,'--- COLUMN NO. (' ,I3,' ) ---',7X))
346 FORMAT(3X,'STOREY',2(9X,'--- COLUMN NO. (' ,I3,' ) ---',7X))
347 FORMAT(3X,'STOREY',9X,'--- COLUMN NO. (' ,I3,' ) ---')
348 DO 360 I=1,NS
      IJ=NBB*(I-1)+NB+JS
      IJJ=IJ+JE-JS
      DO 350 K=JS,JE
      KK=IJ-JS+K
      TEMPO(KK)=RP(I,K)
350 CCNTINUE
      WRITE(6,315) I,((PMO(J,1,1),STF(J),TEMPO(J)),J=IJ,IJJ)
360 CCNTINUE
      WRITE(6,370) (SPR(I),I=JS,JE)
370 FORMAT(3X,'BASE SPRING CONST.',2X,E13.5,2(28X,E13.5))
      IF(KAKU.GE. 0) GO TO 340
      WRITE(6,380)
380 FORMAT(/1X,'OTHER STRUCTURAL PROPERTIES')
      IF(LTF.GE. 5) GO TO 420
      WRITE(6,390)
390 FORMAT(3X,'STOREY',5X,'HEIGHT',9X,'WEIGHT',4X,'CUMULATIVE WT.',2
      1X,'DAMPING COEF.')
      DO 410 I=1,NS
      WRITE(6,400) I,SH(I),SM(I),CSM(I),H(I)
400 FORMAT(1X,I6,8E15.5)
      SM(I)=SM(I)/GR

```



```

      CSM(I)=CSM(I)/GR
410 CCNTINUE
      GC TO 445
COMMENT : INPUT STATEMENT (ONLY WHEN BLAST LOADING)
420 REAL(5,110) (CSM(I),I=1,NS)
      WRITE(6,430)
430 FORMAT( 3X,'STOREY',5X,'HEIGHT',9X,'WEIGHT',5X,'DAMPING CCEF.',3X
1,'ICAD FACTOR')
      DO 440 I=1,NS
      WRITE(6,400) I,SH(I),SM(I),H(I),CSM(I)
      SM(I)=SM(I)/GR
      CSM(I)=-CSM(I)
      IF(I.EQ. 1) GC TO 440
      CSM(I)=CSM(I-1)+CSM(I)
440 CCNTINUE
445 WRITE(6,450)
450 FORMAT(/,1X,'THE SPRING TO SIMULATE THE PLASTIC BEHAVIOUR AND/OR A
1XIAL LOAD EFFECT HAS A MOMENT-THETA RELATION GIVEN BELOW')
      DC 500 L=1,KUMI
      IKUTSU=0
      DO 460 LL=1,NBET
      IF(NESS(LL).NE. L) GO TO 460
      IKUTSU=IKUTSU+1
      NES(IKUTSU)=LL
460 CCNTINUE
      K=NES(1)
      IF(IKUTSU.LE. 22) GO TO 481
      WRITE(6,480) (NES(I),I=1,IKUTSU)
480 FORMAT(3X,'FOR THE MEMBER NO.',22(I4,',')/(6X,25(I4,','))
      GC TO 490
481 WRITE(6,482) (NES(I),I=1,IKUTSU)
482 FORMAT(3X,'FOR THE MEMBER NO.',22(I4,','))
490 WRITE(6,491) THETA(K,1,1),PMO(K,1,1),THETA(K,1,2),THETA(K,1,5),
1THETA(K,1,3),THETA(K,1,6),SLPLS(K)
491 FORMAT(3X,'THETA-MOMENT',3(2X,2E13.5,','),3X,'PLASTIC SLOPE',E14.5
1)
      THETA(K,1,5)=-THETA(K,1,2)
      THETA(K,1,6)=-THETA(K,1,3)
500 CCNTINUE
      RETURN
      END
      SUBROUTINE STIFF(Q,INIT,A,IA,ISHUT)
      COMMON NS,NB,STF(225),SH(25),SPR( 5),SB( 4),RP(25, 5),UDL(25, 4)
      COMMON IOP(225,2),ION(225,2),SLPIS(225),SLP(225,3),BETA(225,2,5),
1THETA(225,2,6),IMA(225,2),PMO(225,2,2),HXD(25),HNL(25)
      DIMENSION A(150,11),Q(25,25)
      ISHUT=0
      CALL FUJI(A,IA)
      N1=NB+1
      N2=NB+2
      N3=NB+3
      NE=2*NB+3
      DO 260 I=1,NS
      DO 250 J=1,N1
      IJ=N2*(I-1)+J
      DO 240 K=1,N2
      IK=IJ+K
      N2S=N2*NS+1
      IF(IK.GE. N2S) GO TO 250
      NK=N2-K

```



```

N3J=N3-J
IF(K .GE. N3J) NK=NK+1
IF(ABS(A(IK,NK)) .LT. 1.0E-30) GO TO 240
IF(ABS(A(IJ,N2)) .LT. 1.0E-30) GO TO 270
A(IK,NK)=-A(IK,NK)/A(IJ,N2)
IF(ABS(A(IK,NK)) .LT. 1.0E2) GO TO 220
WRITE(6,210) A(IK,NK)
210 FORMAT(/1X,'WARNING - ACCURACY LOSS IN CALCULATING STIFFNESS MATRI
1X - MULTIPLIER=',F12.4)
220 DO 230 L=N3,NE
    NL=NK+I-N2
    A(IK,NL)=A(IK,NL)+A(IK,NK)*A(IJ,L)
230 CCNTINUE
240 CCNTINUE
250 CCNTINUE
260 CCNTINUE
    GO TO 290
270 WRITE(6,280)
280 FORMAT(/1X,'DIVISION BY ZERO WHEN FINDING STIFFNESS MATRIX')
    ISHUT=1
    RETURN
290 CALL YURI(Q,A,IA,INIT)
    RETURN
    END
    SUERCUTINE FUJI(A,IA)
    CCMON NS,NB,STF(225),SH(25),SPR( 5),SB( 4),RP(25, 5),UDL(25, 4)
    CCMON IOP(225,2),ION(225,2),SLPLS(225),SLP(225,3),BETA(225,2,5),
1THEIA(225,2,6),IMA(225,2),PMO(225,2,2),HXD(25),HNL(25)
    DIMENSION A(150,11)
    N1=NB+1
    N2=NB+2
    N3=NB+3
    NEE=2*NB+1
    NE=NBE+2
    DO 100 I=1,IA
    DO 90 J=1,NE
    A(I,J)=0.0
90 CCNTINUE
100 CCNTINUE
    DO 260 I=1,NS
    DO 250 J=1,N2
    IJ=N2*(I-1)+J
    IF(J .EQ. N2) GO TO 200
    IF(I .EQ. 1) GO TO 110
    MA=NBE*(I-1)-N1+J
    CALL IZU(VA,VB,MA,2,0.0,0.0,1,1)
    A(IJ, 1)=VA
    A(IJ,N2)=VB
110 IF(J .EQ. 1) GO TO 120
    ML=NBB*(I-1)+J-1
    FR1=RF(I,J-1)/SB(J-1)
    FR2=RF(I,J)/SE(J-1)
    CALL IZU(VA,VB,ML,2,FR1,FR2,1,1)
    A(IJ,N1)=VA
    A(IJ,N2)=A(IJ,N2)+VB
120 IF(J .EQ. N1) GO TO 130
    MR=NBE*(I-1)+J
    FR1=RF(I,J)/SB(J)
    FR2=RF(I,J+1)/SB(J)
    CALL IZU(VA,VB,MR,1,FR1,FR2,1,1)

```



```

      A(IJ,N3)=VB
      A(IJ,N2)=A(IJ,N2)+VA
130  ME=NEB*I-N1+J
      IF(I.EQ. NS) GO TO 140
      CALL IZU(VA,VB,MB,1,0.0,0.0,1,1)
      A(IJ,NE)=VB
      A(IJ,N2)=A(IJ,N2)+VA
      GO TO 250
140  CALL IZU(VA,VB,MB,1,0.0,0.0,-1,1)
      A(IJ,N2)=A(IJ,N2)+VA
      GO TO 250
200  DC 220 K=1,N1
      KK=NBB*I-N1+K
      KE=N1+K
      IF(I.EQ. NS) GO TO 210
      CALL IZU(VA,VB,KK,3,0.0,0.0,1,1)
      A(IJ,K)=VA
      A(IJ,KE)=VB
      GO TO 220
210  CALL IZU(VA,VB,KK,3,0.0,0.0,-1,1)
      A(IJ,K)=VA
220  CCNTINUE
      A(IJ,NE)=SH(I)
250  CCNTINUE
260  CCNTINUE
      RETURN
      END
      SUBROUTINE IZU(VA,VB,M,II,FR1,FR2,IASHI,IGO)
      COMMON NS,NB,STF(225),SH(25),SPR(5),SB(4),RP(25,5),UDL(25,4)
      COMMON IOP(225,2),ION(225,2),SLPLS(225),SLP(225,3),BETA(225,2,5),
1 THETA(225,2,6),IMA(225,2),PMO(225,2,2),HXD(25),HNL(25)
      FR3=1.0-FR1-FR2
      FRA=FR1
      FRE=FR2
      IF(IGO.LT. 0 .AND. II.EQ. 1) FR1=0.0
      IF(IGO.LT. 0 .AND. II.EQ. 2) FR2=0.0
      IF(IASHI.LT. 0) J=M-(2*NB+1)*(NS-1)-NB
      IF(IMA(M,1).LE. -1) GO TO 111
      ICCN=IMA(M,1)+1
      W=SLF(M,ICON)
      GO TO 112
111  ICON=1-IMA(M,1)
      W=SLF(M,ICON)
112  IF(IMA(M,2).LE. -1) GO TO 113
      ICCN=IMA(M,2)+1
      Y=SLF(M,ICON)
      GO TO 120
113  ICCN=1-IMA(M,2)
      Y=SLF(M,ICON)
120  IF(ABS(W).LT. STF(M).OR. ABS(Y).LT. STF(M)) GO TO 130
      IF(W.LT. 1.0E30 .AND. Y.LT. 1.0E30) GO TO 105
      BUN=ALOG(W)+ALOG(Y)
      IF(BUN.LT. 150.0) GO TO 105
      DEN=1.0+2.0*STF(M)*(1.0/W+1.0/Y)/FR3
      GO TO 110
105  DEN=1.0+2.0*STF(M)*(1.0/W+1.0/Y)/FR3+3.0*(STF(M)/FR3/W)*(STF(M)/FR
13/Y)
110  IF(IASHI.LT. 0) GO TO 125
      VC=(1.0+3.0*(FR1+FR2)/FR3+6.0*FR1*FR2/FR3**2+3.0*STF(M)*(FR1/W+FR2
1/Y)/FR3**2+3.0*FR1*FR2*STF(M)*(1.0/W+1.0/Y)/FR3**3)*STF(M)/FR3/DEN

```



```

IF(II .EQ. 2) GO TO 122
VB=VC
IF(IGO .LT. 0) FR1=FRA
VA=2.0+3.0*FR1/FR3+3.0*STF(M)*(1.0+FR1/FR3)/FR3/Y
IF(IGC .LT. 0) GO TO 121
VA=VA+3.0*(1.0+2.0*FR1/FR3)*FR1/FR3+3.0*STF(M)*((1.0+FR1/FR3)*FR1/
1FR3**2/Y+FR1**2/FR3**3/W)
121 VA=VA*STF(M)/FR3/DEN
IF(II .EQ. 1) RETURN
VA=VA+VC
GO TO 123
122 VA=VC
IF(IGC .LT. 0) FR2=FRB
123 VB=2.0+3.0*FR2/FR3+3.0*STF(M)*(1.0+FR2/FR3)/FR3/W
IF(IGC .LT. 0) GO TO 124
VB=VB+3.0*(1.0+2.0*FR2/FR3)*FR2/FR3+3.0*STF(M)*((1.0+FR2/FR3)*FR2/
1FR3**2/W+FR2**2/FR3**3/Y)
124 VB=VB*STF(M)/FR3/DEN
IF(II .EQ. 2) RETURN
VB=VB+VC
RETURN
125 G=SPR(J)*DEN+STF(M)*(2.0+3.0*STF(M)/W)
VA=(2.0+3.0*STF(M)/Y-STF(M)/G)*STF(M)/DEN
IF(II .LE. 2) RETURN
IF(SPR(J) .GT. STF(M)) GO TO 126
VA=VA+SPR(J)*STF(M)/G
RETURN
126 G=DEN+STF(M)*(2.0+3.0*STF(M)/W)/SPR(J)
VA=VA+STF(M)/G
RETURN
130 IF(AES(W) .LE. STF(M)) GO TO 140
DEN=Y+2.0*STF(M)*(Y/W+1.0)/FR3+3.0*(STF(M)/FR3/W)*STF(M)/FR3
IF(IASHI .LT. 0) GO TO 135
VC=(Y*(1.0+3.0*(FR1+FR2)/FR3+6.0*FR1*FR2/FR3**2)+3.0*STF(M)*(FR1*Y
1/W+FR2)/FR3**2+3.0*FR1*FR2*STF(M)*(Y/W+1.0)/FR3**3)*STF(M)/FR3/DEN
IF(II .EQ. 2) GO TO 132
VB=VC
IF(IGO .LT. 0) FR1=FRA
VA=Y*(2.0+3.0*FR1/FR3)+3.0*STF(M)*(1.0+FR1/FR3)/FR3
IF(IGC .LT. 0) GO TO 131
VA=VA+3.0*Y*(1.0+2.0*FR1/FR3)*FR1/FR3+3.0*STF(M)*((1.0+FR1/FR3)*FR
11/FR3**2+Y*FR1**2/FR3**3/W)
131 VA=VA*STF(M)/FR3/DEN
IF(II .EQ. 1) RETURN
VA=VA+VC
GO TO 133
132 VA=VC
IF(IGC .LT. 0) FR2=FRB
133 VB=Y*(2.0+3.0*FR2/FR3+3.0*STF(M)*(1.0+FR2/FR3)/FR3/W)
IF(IGC .LT. 0) GO TO 134
VB=VB+3.0*Y*(1.0+2.0*FR2/FR3)*FR2/FR3+3.0*STF(M)*(Y*(1.0+FR2/FR3)*
1FR2/FR3**2/W+FR2**2/FR3**3)
134 VB=VB*STF(M)/FR3/DEN
IF(II .EQ. 2) RETURN
VB=VB+VC
RETURN
135 G=SPR(J)*DEN+Y*STF(M)*(2.0+3.0*STF(M)/W)
VA=(2.0*Y+3.0*STF(M)-Y**2*STF(M)/G)*STF(M)/DEN
IF(II .LE. 2) RETURN
IF(SPR(J) .GT. STF(M)) GO TO 136

```



```

    VA=VA+SPR(J)*Y*STF(M)/G
    RETURN
136 G=LEN+Y*STF(M)*(2.0+3.0*STF(M)/W)/SPR(J)
    VA=VA+Y*STF(M)/G
    RETURN
140 IF(ABS(Y) .LE. STF(M)) GO TO 150
    DEN=W+2.0*STF(M)*(1.0+W/Y)/FR3+3.0*(STF(M)/FR3)*(STF(M)/FR3/Y)
    IF(IASHI .LT. 0) GO TO 145
    VC=(W*(1.0+3.0*(FR1+FR2)/FR3+6.0*FR1*FR2/FR3**2)+3.0*STF(M)*(FR1+FR2*W/Y)/FR3**2+3.0*FR1*FR2*STF(M)*(1.0+W/Y)/FR3**3)*STF(M)/FR3/DEN
    IF(II .EQ. 2) GC TC 142
    VE=VC
    IF(IGO .LT. 0) FR1=FRA
    VA=W*(2.0+3.0*FR1/FR3+3.0*STF(M)*(1.0+FR1/FR3)/FR3/Y)
    IF(IGC .LT. 0) GC TO 141
    VA=VA+3.0*W*(1.0+2.0*FR1/FR3)*FR1/FR3+3.0*STF(M)*(W*(1.0+FR1/FR3)*FR1/FR3**2/Y+FR1**2/FR3**3)
141 VA=VA*STF(M)/FR3/DEN
    IF(II .EQ. 1) RETURN
    VA=VA+VC
    GC TO 143
142 VA=VC
    IF(IGC .LT. 0) FR2=FRB
143 VB=W*(2.0+3.0*FR2/FR3)+3.0*STF(M)*(1.0+FR2/FR3)/FR3
    IF(IGO .LT. 0) GO TO 144
    VB=VB+3.0*W*(1.0+2.0*FR2/FR3)*FR2/FR3+3.0*STF(M)*((1.0+FR2/FR3)*FR2/FR3**2+W*FR2**2/FR3**3/Y)
144 VE=VB*STF(M)/FR3/DEN
    IF(II .EQ. 2) RETURN
    VE=VB+VC
    RETURN
145 G=SPR(J)*DEN+STF(M)*(2.0*W+3.0*STF(M))
    VA=W*(2.0+3.0*STF(M)/Y-W*STF(M)/G)*STF(M)/DEN
    IF(II .LE. 2) RETURN
    IF(SPR(J) .GT. STF(M)) GO TO 146
    VA=VA+SPR(J)*W*STF(M)/G
    RETURN
146 G=DEN+STF(M)*(2.0*W+3.0*STF(M))/SPR(J)
    VA=VA+W*STF(M)/G
    RETURN
150 DEN=W*Y+2.0*STF(M)*(W+Y)/FR3+3.0*(STF(M)/FR3)**2
    IF(IASHI .LT. 0) GO TO 155
    VC=(W*Y*(1.0+3.0*(FR1+FR2)/FR3+6.0*FR1*FR2/FR3**2)+3.0*STF(M)*(FR1*Y+FR2*W)/FR3**2+3.0*FR1*FR2*STF(M)*(W+Y)/FR3**3)*STF(M)/FR3/DEN
    IF(II .EQ. 2) GO TC 152
    VE=VC
    IF(IGC .LT. 0) FR1=FRA
    VA=W*(Y*(2.0+3.0*FR1/FR3)+3.0*STF(M)*(1.0+FR1/FR3)/FR3)
    IF(IGC .LT. 0) GC TO 151
    VA=VA+3.0*W*Y*(1.0+2.0*FR1/FR3)*FR1/FR3+3.0*STF(M)*(W*(1.0+FR1/FR3)*FR1/FR3**2+Y*FR1**2/FR3**3)
151 VA=VA*STF(M)/FR3/DEN
    IF(II .EQ. 1) RETURN
    VA=VA+VC
    GC TC 153
152 VA=VC
    IF(IGO .LT. 0) FR2=FRB
153 VB=Y*(W*(2.0+3.0*FR2/FR3)+3.0*STF(M)*(1.0+FR2/FR3)/FR3)
    IF(IGC .LT. 0) GO TO 154
    VE=VB+3.0*W*Y*(1.0+2.0*FR2/FR3)*FR2/FR3+3.0*STF(M)*(Y*(1.0+FR2/FR3)

```



```

1) *FF2/FR3**2+W*FR2**2/FR3**3)
154 VB=VB*STF(M)/FF3/DEN
   IF(II .EQ. 2) RETURN
   VB=VB+VC
   RETURN
155 G=SPR(J)*DEN+Y*STF(M)*(2.0*W+3.0*STF(M))
   VA=W*(2.0*Y+3.0*STF(M)-W*Y**2*STF(M)/G)*STF(M)/DEN
   IF(II .LE. 2) RETURN
   IF(SPR(J) .GT. STF(M)) GO TO 156
   VA=VA+SPR(J)*W*Y*STF(M)/G
   RETURN
156 G=DEN+Y*STF(M)*(2.0*W+3.0*STF(M))/SPR(J)
   VA=VA+W*Y*STF(M)/G
   RETURN
   END
   SUBROUTINE YURI (Q,AI,IA,INIT)
   COMMON NS,NB,STF(225),SH(25),SPR( 5),SB( 4),RP(25, 5),UDL(25, 4)
   COMMON IOP(225,2),ION(225,2),SLPIS(225),SLP(225,3),BETA(225,2,5),
1 THETA(225,2,6),IMA(225,2),PMO(225,2,2),HXD(25),HNL(25)
   DIMENSION SXD(25),Q(25,25),AI(150,11),BH(150),BB(150),QTEM(25)
   IF(INIT .NE. 0) GO TO 130
   DO 100 I=1,NS
   SXL(I)=0.0
100 CCNTINUE
   DC 110 J=1,IA
   BB(J)=B(J,SXD)
110 CCNTINUE
   CALL SOLVE (AI,BB,QTEM)
   DC 120 I=1,NS
   HNI(I)=QTEM(I)
120 CCNTINUE
130 DO 140 I=1,NS
   SXL(I)=HXD(I)
140 CCNTINUE
   DC 150 I=1,IA
   BH(I)=B(I,SXD)
150 CCNTINUE
   DC 180 I=1,NS
   SXL(I)=HXD(I)+1.0
   DC 160 K=1,IA
   EE(K)=B(K,SXD)+BH(K)
160 CCNTINUE
   CALL SOLVE (AI,BB,QTEM)
   DC 170 J=1,NS
   Q(J,I)=QTEM(J)
170 CCNTINUE
   SXL(I)=HXD(I)
180 CCNTINUE
   RETURN
   END
   FUNCTION B(IJ,SXD)
   COMMON NS,NB,STF(225),SH(25),SPR( 5),SB( 4),RP(25, 5),UDL(25, 4)
   COMMON IOP(225,2),ION(225,2),SLPIS(225),SLP(225,3),BETA(225,2,5),
1 THETA(225,2,6),IMA(225,2),PMO(225,2,2),HXD(25),HNL(25)
   DIMENSION SXD(25)
   B=0.0
   NE1=NB+1
   NE2=NE+2
   I=(IJ-1)/NB2+1
   J=IJ-NE2*(I-1)

```



```

IF(J .EQ. NB2) GO TO 200
IF(I .EQ. 1) GO TO 110
MA=(2*NB+1)*(I-1)-NB1+J
S=SH(I-1)
R=(SXD(I-1)-SXD(I))/SH(I-1)
E=UHEN(MA,S,2,0.0,R,0.0,0.0,1,1)
110 IF(J .EQ. 1) GC TO 120
MI=(2*NB+1)*(I-1)+J-1
FR1=RF(I,J-1)/SB(J-1)
FR2=RF(I,J)/SB(J-1)
UL=UDL(I,J-1)
S=SE(J-1)
E=E+UHEN(MI,S,2,UL,0.0,FR1,FR2,1,1)
120 IF(J .EQ. NB1) GC TO 130
MR=(2*NB+1)*(I-1)+J
FR1=RF(I,J)/SB(J)
FR2=RF(I,J+1)/SB(J)
UL=UDL(I,J)
S=SE(J)
E=E+UHEN(MR,S,1,UL,0.0,FR1,FR2,1,1)
130 MB=(2*NB+1)*I-NB1+J
S=SH(I)
IF(I .EQ. NS) GO TO 140
R=(SXD(I)-SXD(I+1))/SH(I)
B=E+UHEN(MB,S,1,0.0,R,0.0,0.0,1,1)
RETURN
140 R=SXD(NS)/SH(NS)
B=E+UHEN(MB,S,1,0.0,R,0.0,0.0,-1,1)
RETURN
200 DO 220 K=1,NB1
KK=(2*NB+1)*I-NB1+K
S=SH(I)
IF(I .EQ. NS) GO TO 210
R=(SXD(I)-SXD(I+1))/SH(I)
B=E+UHEN(KK,S,3,0.0,R,0.0,0.0,1,1)
GC TO 220
210 R=SXD(NS)/SH(NS)
B=E+UHEN(KK,S,3,0.0,R,0.0,0.0,-1,1)
220 CCNTINUE
RETURN
END
FUNCTION UHEN(M,S,II,UL,R,FR1,FR2,IASHI,IGO)
CCMMON NS,NB,STF(225),SH(25),SPR(5),SB(4),RP(25,5),UDL(25,4)
CCMMCN IOP(225,2),ICN(225,2),SLPLS(225),SLP(225,3),BETA(225,2,5),
1TEETA(225,2,6),IMA(225,2),FMO(225,2,2),HXD(25),HNL(25)
UHEN=0.0
FR3=1.0-FR1-FR2
IF(IGC .LT. 0 .AND. II .EQ. 1) FR1=0.0
IF(IGO .LT. 0 .AND. II .EQ. 2) FR2=0.0
FEMD=UL*(FR3*S)**2/12.0
FEMC=-FEMD
AFC=-0.5*UL*FR1*(1.0-FR2)*S**2
AFD=0.5*UL*FR2*(1.0-FR1)*S**2
IF(IASHI .LT. C) J=M-(2*NB+1)*(NS-1)-NB
CER=2.01*STF(M)
IF(IMA(M,1) .LE. -1) GO TO 111
ICCN=IMA(M,1)+1
W=SLP(M,ICCN)
IF(IMA(M,1) .EQ. 0 .AND. W .GE. CER) GO TO 112
X=BETA(M,1,ICCN)

```



```

GC TO 112
111 ICCN=1-IMA(M,1)
    W=SLP(M,ICON)
    ICCN=ICON+2
    X=BETA(M,1,ICON)
112 IF(IMA(M,2) .IE. -1) GO TO 113
    ICCN=IMA(M,2)+1
    Y=SLP(M,ICCN)
    IF(IMA(M,2) .EQ. 0 .AND. Y .GE. CER) GO TO 115
    Z=BETA(M,2,ICON)
    GC TO 115
113 ICCN=1-IMA(M,2)
    Y=SLP(M,ICON)
    ICCN=ICCN+2
    Z=BETA(M,2,ICON)
115 CEF=2.0*STF(M)
    IF(ABS(W) .LT. STF(M) .OR. ABS(Y) .LT. STF(M)) GO TO 130
    IF(W .LT. 1.0E30 .AND. Y .LT. 1.0E30) GO TO 105
    EUN=ALOG(W)+ALCG(Y)
    IF(BUN .LT. 150.0) GO TO 105
    DEN=1.0+2.0*STF(M)*(1.0/W+1.0/Y)/FR3
    GC TO 110
105 DEN=1.0+2.0*STF(M)*(1.0/W+1.0/Y)/FR3+3.0*(STF(M)/FR3/W)*(STF(M)/FR
13/Y)
110 IF(IMA(M,1) .EQ. 0 .AND. W .GE. CER) GO TO 116
    XCW=X/W
    GC TO 117
116 IP=IOF(M,1)
    XCW=PMC(M,1,1)/W-THETA(M,1,IP)
117 IF(IMA(M,2) .EQ. 0 .AND. Y .GE. CER) GO TO 118
    ZCY=Z/Y
    GC TO 120
118 IF=ICF(M,2)
    ZOY=FMO(M,2,1)/Y-THETA(M,2,IP)
120 IF(IASHI .LT. C) GO TO 125
    IF(II .EQ. 2) GO TO 121
    VD=3.0*(1.0+STF(M)/Y)*R
    VD=VD-(2.0+3.0*FR1/FR3+3.0*STF(M)*(1.0+FR1/FR3)/FR3/Y)*XOW
    VD=VD-(1.0+3.0*FE1/FR3+3.0*STF(M)*FR1/FR3**2/W)*ZOY
    VD=VD*STF(M)/FE3
    UHEN=(VD-FEMC*(1.0+3.0*STF(M)*(1.0+FR1/FR3)/FR3/Y-3.0*STF(M)*FR1/F
1R3**2/W))/DEN-AFC
    IF(II .EQ. 1) FEIURN
121 VD=3.0*(1.0+STF(M)/W)*R
    VD=VD-(1.0+3.0*FR2/FR3+3.0*STF(M)*FR2/FR3**2/Y)*XOW
    VD=VD-(2.0+3.0*FE2/FR3+3.0*STF(M)*(1.0+FR2/FR3)/FR3/W)*ZOY
    VD=VD*STF(M)/FE3
    UHEN=UHEN+(VD-FEMD*(1.0+3.0*STF(M)*(1.0+FR2/FR3)/FR3/W-3.0*STF(M)*
1FR2/FR3**2/Y))/DEN-AFD
    RETURN
125 G=SPR(J)*DEN+STF(M)*(2.0+3.0*STF(M)/W)
    VD=3.0*(1.0+STF(M)/Y+STF(M)*(1.0+STF(M)/W)/G)*R
    VD=VD-(2.0+STF(M)*(3.0/Y-1.0/G))*XOW
    VI=VD-(1.0-STF(M)*(2.0+3.0*STF(M)/W)/G)*ZOY
    UHEN=VD*STF(M)/DEN
    IF(II .LE. 2) FEIURN
    VD=3.0*(1.0+STF(M)/W)*R-XOW-(2.0+3.0*STF(M)/W)*ZOY
    IF(SPR(J) .GT. STF(M)) GO TO 126
    UHEN=UHEN+VD*STF(M)*SPR(J)/G
    RETURN

```



```

126 G=DEN+STF(M)*(2.0+3.0*STF(M)/W)/SPR(J)
    UHEN=UHEN+VD*STF(M)/G
    RETURN
130 IF(ABS(W) .LE. STF(M)) GO TO 140
    DEN=Y+2.0*STF(M)*(Y/W+1.0)/FR3+3.0*(STF(M)/FR3/W)*STF(M)/FR3
    IF(IMA(M,1) .EQ. 0 .AND. W .GE. CER) GO TO 132
    XOW=X/W
    GO TO 133
132 IF=ICF(M,1)
    XCW=FMC(M,1,1)/W-THETA(M,1,IP)
133 IF(IASHI .LT. C) GO TO 135
    IF(II .EQ. 2) GO TO 131
    VD=3.0*(Y+STF(M))*R
    VD=VD-(Y*(2.0+3.0*FR1/FR3)+3.0*STF(M)*(1.0+FR1/FR3)/FR3)*XOW
    VL=VD-(1.0+3.0*FR1/FR3+3.0*STF(M)*FR1/FR3**2/W)*Z
    VD=VD*STF(M)/FR3
    UHEN=(VD-FEMC*(Y+3.0*STF(M)*(1.0+FR1/FR3)/FR3-3.0*Y*STF(M)*FR1/FR3
1**2/W))/DEN-AFC
    IF(II .EQ. 1) RETURN
131 VD=3.0*Y*(1.0+STF(M)/W)*R
    VD=VD-(Y*(1.0+3.0*FR2/FR3)+3.0*STF(M)*FR2/FR3**2)*XOW
    VL=VD-(2.0+3.0*FR2/FR3+3.0*STF(M)*(1.0+FR2/FR3)/FR3/W)*Z
    VD=VD*STF(M)/FR3
    UHEN=UHEN+(VD-FEMD*(Y*(1.0+3.0*STF(M)*(1.0+FR2/FR3)/FR3/W)-3.0*STF
1(M)*FR2/FR3**2))/DEN-AFD
    RETURN
135 G=SPR(J)*DEN+Y*STF(M)*(2.0+3.0*STF(M)/W)
    VD=3.0*(Y+STF(M)-Y**2*STF(M)*(1.0+STF(M)/W)/G)*R
    VL=VD-(2.0*Y+STF(M)*(3.0-Y**2/G))*XOW
    VD=VD-(1.0-Y*STF(M)*(2.0+3.0*STF(M)/W)/G)*Z
    UHEN=VD*STF(M)/DEN
    IF(II .LE. 2) RETURN
    VD=3.0*Y*(1.0+STF(M)/W)*R-Y*XOW-(2.0+3.0*STF(M)/W)*Z
    IF(SPR(J) .GT. STF(M)) GO TO 136
    UHEN=UHEN+VD*STF(M)*SPR(J)/G
    RETURN
136 G=DEN+Y*STF(M)*(2.0+3.0*STF(M)/W)/SPR(J)
    UHEN=UHEN+VD*STF(M)/G
    RETURN
140 IF(ABS(Y) .LE. STF(M)) GO TO 150
    DEN=W+2.0*STF(M)*(1.0+W/Y)/FR3+3.0*(STF(M)/FR3)*(STF(M)/FR3/Y)
    IF(IMA(M,2) .EQ. 0 .AND. Y .GE. CER) GO TO 142
    ZOY=Z/Y
    GO TO 143
142 IF=ICF(M,2)
    ZOY=FMC(M,2,1)/Y-THETA(M,2,IP)
143 IF(IASHI .LT. C) GO TO 145
    IF(II .EQ. 2) GO TO 141
    VD=3.0*W*(1.0+STF(M)/Y)*R
    VD=VD-(2.0+3.0*FR1/FR3+3.0*STF(M)*(1.0+FR1/FR3)/FR3/Y)*X
    VL=VD-(W*(1.0+3.0*FR1/FR3)+3.0*STF(M)*FR1/FR3**2)*ZOY
    VD=VD*STF(M)/FR3
    UHEN=(VD-FEMC*(W*(1.0+3.0*STF(M)*(1.0+FR1/FR3)/FR3/Y)-3.0*STF(M)*F
1R1/FR3**2))/DEN-AFC
    IF(II .EQ. 1) RETURN
141 VD=3.0*W*(1.0+STF(M)/Y)*R
    VD=VD-(1.0+3.0*FR2/FR3+3.0*STF(M)*FR2/FR3**2/Y)*X
    VL=VD-(W*(2.0+3.0*FR2/FR3)+3.0*STF(M)*(1.0+FR2/FR3)/FR3)*ZOY
    VD=VD*STF(M)/FR3
    UHEN=UHEN+(VD-FEMD*(W+3.0*STF(M)*(1.0+FR2/FR3)/FR3-3.0*W*STF(M)*FR

```



```

12/FF3**2/Y))/DEN-AFD
RETURN
145 G=SPR(J)*DEN+STF(M)*(2.0*W+3.0*STF(M))
VD=3.0*(W*(1.0+STF(M)/Y)-W*STF(M)*(W+STF(M))/G)*R
VD=VD-(2.0+STF(M)*(3.0/Y-W/G))*X
VD=VD-W*(1.0-STF(M)*(2.0*W+3.0*STF(M))/G)*ZOY
UHEN=VD*STF(M)/DEN
IF(II.LE.2) RETURN
VD=3.0*(W+STF(M))*R-X-(2.0*W+3.0*STF(M))*ZOY
IF(SPR(J).GT.STF(M)) GO TO 146
UHEN=UHEN+VD*STF(M)*SPR(J)/G
RETURN
146 G=DEN+STF(M)*(2.0*W+3.0*STF(M))/SPR(J)
UHEN=UHEN+VD*STF(M)/G
RETURN
150 DEN=W*Y+2.0*STF(M)*(W+Y)/FR3+3.0*(STF(M)/FR3)**2
IF(IA$HI.IT.0) GO TO 155
IF(II.EQ.2) GO TO 151
VD=3.0*W*(Y+STF(M))*R
VD=VD-(Y*(2.0+3.0*FR1/FR3)+3.0*STF(M)*(1.0+FR1/FR3)/FR3)*X
VD=VD-(W*(2.0+3.0*FR1/FR3)+3.0*STF(M)*FR1/FR3**2)*Z
VD=VD*STF(M)/FF3
UHEN=(VD-FEMC*(W*Y+3.0*W*STF(M)*(1.0+FR1/FR3)/FR3-3.0*Y*STF(M)*FR1
1/FF3**2))/DEN-AFC
IF(II.EQ.1) RETURN
151 VD=3.0*Y*(W+STF(M))*R
VD=VD-(Y*(1.0+3.0*FR2/FR3)+3.0*STF(M)*FR2/FR3**2)*X
VD=VD-(W*(2.0+3.0*FR2/FR3)+3.0*STF(M)*(1.0+FR2/FR3)/FR3)*Z
VD=VD*STF(M)/FR3
UHEN=UHEN+(VD-FEMD*(W*Y+3.0*Y*STF(M)*(1.0+FR2/FR3)/FR3-3.0*W*STF(M)
1)*FF2/FR3**2))/DEN-AFD
RETURN
155 G=SPR(J)*DEN+Y*STF(M)*(2.0*W+3.0*STF(M))
VD=3.0*(W*(Y+STF(M))-Y**2*W*STF(M)*(W+STF(M))/G)*R
VD=VD-(2.0*Y+STF(M)*(3.0-W*Y**2/G))*X
VD=VD-W*(1.0-Y*STF(M)*(2.0*W+3.0*STF(M))/G)*Z
UHEN=VD*STF(M)/DEN
IF(II.LE.2) RETURN
VD=3.0*Y*(W+STF(M))*R-X*Y-(2.0*W+3.0*STF(M))*Z
IF(SPR(J).GT.STF(M)) GO TO 156
UHEN=UHEN+VD*STF(M)*SPR(J)/G
RETURN
156 G=DEN+Y*STF(M)*(2.0*W+3.0*STF(M))/SPR(J)
UHEN=UHEN+VD*STF(M)/G
RETURN
END
SUBROUTINE SOLVE(A,W,C)
COMMON NS,NB,STF(225),SH(25),SPR(5),SB(4),RP(25,5),UDL(25,4)
COMMON IOP(225,2),ION(225,2),SLFIS(225),SLP(225,3),BETA(225,2,5),
1THETA(225,2,6),IMA(225,2),FMO(225,2,2),HXD(25),HNL(25)
DIMENSION A(150,11),W(150),C(25)
N1=NB+1
N2=NB+2
N3=NB+3
NE=2*NB+3
DO 300 I=1,NS
DO 290 J=1,N2
IJ=N2*(I-1)+J
K1=IJ-N2
IF(J.EQ.N2) K1=K1+1

```



```

      K2=K1+N1
      IF(I .EQ. 1 .AND. J .LE. N1) GO TO 240
      M=C
      L=0
      IS=N3-J
      IF(J .EQ. N2) LS=N2
      DC 230 K=K1,K2
      L=L+1
      IF(L .EQ. IS) GO TO 230
      M=M+1
      W(IJ)=W(IJ)+A(IJ,M)*W(K)
230  CCNTINUE
      GC TO 290
240  IF(J .EQ. 1) GO TO 290
      W(J)=W(J)+A(J,N1)*W(J-1)
290  CCNTINUE
300  CCNTINUE
      DC 500 II=1,NS
      I=NS-II+1
      DO 490 JJ=1,N2
      J=N3-JJ
      IJ=N2*(I-1)+J
      IF(I .EQ. NS) GO TO 450
      K1=IJ+1
      IF(J .EQ. N2) GO TO 440
      K2=IJ+N2
      L=N2
      M=N2
      LS=NE-J+1
      DC 430 K=K1,K2
      L=L+1
      IF(L .EQ. LS) GO TO 430
      M=M+1
      W(IJ)=W(IJ)-A(IJ,M)*W(K)
430  CCNTINUE
      W(IJ)=W(IJ)/A(IJ,N2)
      GC TO 490
440  K2=IJ+N1
      I=N1
      DC 445 K=K1,K2
      L=L+1
      W(IJ)=W(IJ)-A(IJ,L)*W(K)
445  CCNTINUE
      GO TO 480
450  IF(J .EQ. N2) GO TO 480
      K1=IJ+1
      K2=IJ+N1-J
      IF(J .EQ. N1) GO TO 470
      L=N2
      DO 460 K=K1,K2
      L=L+1
      W(IJ)=W(IJ)-A(IJ,L)*W(K)
460  CCNTINUE
470  W(IJ)=W(IJ)/A(IJ,N2)
      GC TO 490
480  W(IJ)=W(IJ)/A(IJ,NE)
      C(I)=W(IJ)
490  CCNTINUE
500  CCNTINUE
      RETURN

```



```

END
SUBROUTINE SHUKI(Q,SM,GOME)
CCMCN NS,NB,STF(225),SH(25),SPR( 5),SB( 4),RP(25, 5),UDL(25, 4)
CCMCN IOP(225,2),ION(225,2),SLPIS(225),SLP(225,3),BETA(225,2,5),
1THEIA(225,2,6),IMA(225,2),PMO(225,2,2),HXD(25),HNL(25)
DIMENSION SM(25),Y(25),YY(25),H(25,25),HH(25,25),C(25,25),D(25,25)
1,2(25),Q(25,25)
N=KS
FI=3.141593
IF(N.EQ. 1) GC TO 210
DO 110 I=1,N
DC 100 J=1,N
C(I,J)=Q(I,J)
D(I,J)=SM(J)
IF(J.GT. I) D(I,J)=0.0
100 CCNTINUE
110 CCNTINUE
CALL TCKY01 (N,C)
DC 140 I=1,N
DO 140 K=1,N
ABC=0.0
DC 150 J=1,N
AEC=AEC+C(I,J)*D(J,K)
150 CCNTINUE
HH(I,K)=ABC
H(I,K)=ABC
140 CCNTINUE
KK=0
NA=N
10 DC 20 I=1,NA
Y(I)=1.0
20 CCNTINUE
KK=KK+1
KA=2*(KK/2)
IF(KK.EQ. KA) Y(NA)=-1.0
E=C.000001
40 DC 50 I=1,NA
YY(I)=0.0
DC 60 J=1,NA
YY(I)=YY(I)+H(I,J)*Y(J)
60 CCNTINUE
IF(I.EQ. 1) A=YY(I)
50 CCNTINUE
IF(ABS(A).GT. 10.0E-15) GO TO 56
DC 55 I=1,NA
Y(I)=Y(I)+FLOAT(I)
55 CCNTINUE
GC TO 40
56 DC 70 I=1,NA
Y(I)=YY(I)/A
70 CCNTINUE
S=A/E
E=A
IF(S.GT. 1.00001) GO TO 40
IF(S.LT. 0.99999) GO TO 40
IF(KK.EQ. KA) GC TO 75
AA=A
DC 71 I=1,NA
Z(I)=Y(I)
71 CCNTINUE

```



```

      GO TO 10
75  IF (A .GE. AA) GO TO 80
      A=AA
      DO 76 I=1,NA
      Y(I)=Z(I)
76  CCNTINUE
80  IF (KK .EQ. 2) GO TO 200
      IF (KK .EQ. 4) GO TO 300
      IF (KK .EQ. 6) GO TO 400
      IF (KK .EQ. 12) GO TO 510
200  A1=A
      GCME=SQRT(A)
      GO TO 220
210  A=SM(1)/Q(1,1)
      GCME=SQRT(A)
220  T=2.0*PI*GCME
      WRITE(6,230) T
230  FORMAT(/1X,'NATURAL PERIOD OF FIRST MODE IS',F7.3,' SEC.')
      IF (N .EQ. 1) RETURN
      WRITE(6,240) (Y(I),I=1,N)
240  FCFMAT(3X,'CORRESPONDING MODE -- TOP TO BASE'/(3X,7E18.6))
      IF (N .EQ. 2) GO TO 280
      DC 260 I=1,NA
      DC 250 J=1,NA
      C(I,J)=H(I,J)
250  CCNTINUE
      C(I,I)=C(I,I)-A1
      Z(I)=E(1,I)
260  CCNTINUE
      NA=NA-1
      DC 275 I=1,NA
      DC 270 J=1,NA
      H(I,J)=H(I+1,J+1)-Y(I+1)*Z(J+1)
270  CCNTINUE
275  CCNTINUE
      GO TO 10
280  DO 285 I=1,NA
      B(I,I)=H(I,I)-A1
285  CCNTINUE
      GO TO 10
300  IF (N .EQ. 2) GO TO 375
      A2=A
      A=SQRT(A)
      T=2.0*PI*A
      WRITE(6,310) T
310  FORMAT(/1X,'NATURAL PERIOD OF SECCND MODE IS',F7.3,' SEC.')
315  DO 320 I=1,NA
      Z(I+1)=Y(I)
320  CCNTINUE
      Z(1)=0.0
      DC 340 I=1,N
      Y(I)=C.0
      DC 330 J=1,N
      Y(I)=Y(I)+C(I,J)*Z(J)
330  CCNTINUE
      IF (I .EQ. 1) A=Y(1)
      Y(I)=Y(I)/A
340  CCNTINUE
      WRITE(6,240) (Y(I),I=1,N)
      IF (KK .EQ. 6) GO TO 500

```



```

      IF(N .EQ. 3) GC TC 365
      DC 350 I=1,NA
      Y(I)=Z(I+1)
      DO 345 J=1,NA
      D(I,J)=H(I,J)
345  CCNTINUE
      D(I,I)=D(I,I)-A2
      Z(I)=H(1,I)
350  CCNTINUE
      NA=NA-1
      DO 360 I=1,NA
      DC 355 J=1,NA
      H(I,J)=H(I+1,J+1)-Y(I+1)*Z(J+1)
355  CCNTINUE
360  CCNTINUE
      GC TC 10
365  DO 370 I=1,NA
      H(I,I)=H(I,I)-A2
370  CCNTINUE
      GC TO 10
375  A=A+A1
      A=SQRT(A)
      T=2.0*PI*A
      WRITE(6,310) T
      WRITE(6,240) (Y(I),I=1,N)
      RETURN
400  IF(N .EQ. 3) GO TO 440
      A3=A
      A=SQRT(A)
      T=2.0*PI*A
      WRITE(6,410) T
410  FORMAT(/1X,'NATURAL PERIOD OF THIRD MODE IS',F7.3,' SEC.')
      DO 420 I=1,NA
      Z(I+1)=Y(I)
420  CCNTINUE
      Z(1)=0.0
      N2=NA+1
      DC 435 I=1,N2
      Y(I)=0.0
      DC 430 J=1,N2
      Y(I)=Y(I)+D(I,J)*Z(J)
430  CCNTINUE
435  CCNTINUE
      NA=N2
      GC TO 315
440  A=A+A2
      A=SQRT(A)
      T=2.0*PI*A
      WRITE(6,410) T
      GC TC 315
500  IF(N .LE. 3) RETURN
      CALL TCKYO1(N,HH)
      NA=N
      DC 506 I=1,N
      DC 505 J=1,N
      H(I,J)=HH(I,J)
505  CCNTINUE
506  CCNTINUE
      KK=10
      GC TC 10

```



```

510 A=SQRT(A)
    T=2.0*PI/A
    WRITE(6,520) T
520 FORMAT(/1X,'THE MINIMUM NATURAL PERIOD IS',F7.3,' SEC.')
    WRITE(6,240) (Y(I),I=1,N)
    RETURN
    END
    SUBROUTINE TOKYC1 (NO,A)
    DIMENSION AC(25),AE(25),A(25,25)
    NO1=NO-1
    A(1,1)=1.0/A(1,1)
    IF (NO.EQ. 1) RETURN
    DO 80 N=1, NO1
    DO 50 I=1, N
    AB(I)=0.0
    AC(I)=0.0
    DO 50 J=1, N
    AB(I)=AB(I)+A(I,J)*A(J,N+1)
    AC(I)=AC(I)+A(N+1,J)*A(J,I)
50 CCNTINUE
    ACE=0.0
    DO 60 I=1, N
    ACE=ACE+AC(I)*A(I,N+1)
60 CCNTINUE
    A(N+1,N+1)=1.0/(A(N+1,N+1)-ACE)
    DO 70 I=1, N
    A(N+1,I)=-A(N+1,N+1)*AC(I)
    A(I,N+1)=-AB(I)*A(N+1,N+1)
70 CCNTINUE
    DO 80 I=1, N
    DO 80 J=1, N
    A(I,J)=A(I,J)-A(I,N+1)*AC(J)
80 CCNTINUE
    RETURN
    END
    SUBROUTINE KIKU (DELTAT,C,GOME,Q,GOSA,GR,NCAL)
    COMMON NS,NB,STF(225),SH(25),SPR( 5),SB( 4),RP(25, 5),UDL(25, 4)
    COMMON IOP(225,2),ION(225,2),SLPLS(225),SLP(225,3),BETA(225,2,5),
1 THETA(225,2,6),IMA(225,2),PMO(225,2,2),HXD(25),HNL(25)
    DIMENSION C(25),Q(25,25)
    DO 100 I=1, NS
    C(I)=2.0*C(I)*Q(I,I)*GOME
100 CCNTINUE
    NCST=NS
    CALL TOKYO1(NOST,Q)
    DO 140 I=1, NS
    HXL(I)=0.0
    DO 130 J=1, NS
    HXD(I)=HXD(I)-Q(I,J)*HNL(J)
130 CCNTINUE
140 CCNTINUE
    DO 150 I=1, NS
    HNI(I)=0.0
150 CCNTINUE
    WRITE(6,160) (HXD(I),I=1,NS)
160 FORMAT(/1X,'INITIAL DEFORMATION -- TOP TO BOTTOM'/(6X,8E14.5))
    TLAST=DELTAT*FLOAT(NCAL)
    WRITE(6,340) DELTAT,TLAST,GR,GOSA
340 FORMAT(/1X,'CALCULATIONS WILL BE DONE EVERY',F6.3,' SEC. UNTIL',
    1F5.1,' SEC.',
    4X,'ACCE

```



```

2LEFATION OF GRAVITY IS',F8.3,4X,'CCONVERGENCE LIMIT IS',F9.6)
RETURN
END
SUBROUTINE JISHIN (SM,CSM,C,IP,IGPH,GR,GOSA,NCAL,DELTAT,MXIT,NSAI,
1NTCEU,THAJI,TOWA,SEICO,Q,IA,AI,LTF,ITIME,IDISC)
  COMMON NS,NB,STF(225),SH(25),SPR( 5),SE( 4),RP(25, 5),UDL(25, 4)
  COMMON IOP(225,2),ION(225,2),SLPIS(225),SLP(225,3),BETA(225,2,5),
1THETA(225,2,6),IMA(225,2),PMO(225,2,2),HXD(25),HNL(25)
  DIMENSION GA(7),SM(25),CSM(25),C(25),IP(25),TSEI(25),AX(25),VX(25)
1,XL(25),RX(25),RV(25),AA(25),CQ(25),RESC(25),RESQ(25),RXX(25),RVM
2X(25),CCMX(25),TRX(25),TRV(25),TCQ(25),OAX(25),OVX(25),OXD(25),
3C(25,25),AI(150, 11),FT(225,2),KOSAN(225,2),IPCH(5),XDMX(25),AAMX(
425),RCMX(25),RQMX(25),IR(25),TRMX(25),ZZ(25)
  INSA=10
  IF(IGPH .GT. 5) GO TO 10
  GO TO (1,2), IGPH
COMMENT : INPUT STATEMENT (ONLY WHEN PUNCHING OUT THE RESULTS)
  1 READ(5,100) MSKIF,INSA,NPCH,(IPCH(J),J=1,NPCH)
  GO TO 10
  2 READ(5,100) MSKIF,INSA
  NPCH=NS
  100 FORMAT(10I5)
COMMENT : INPUT STATEMENT
  10 INF=5
  IF(IDISC .EQ. C) INP=4
  READ(INP,15) (TSEI(I),I=1,20)
  15 FCFMAT(20A4)
  IF(LTF .LT. 5) GO TO 30
  WRITE(6, 20) (TSEI(I),I=1,20)
  20 FORMAT(/1X,'BLAST LOADING MODEL USED IN THIS CALCULATION : ',20A4)
  WRITE(6, 25) SEICO
  25 FORMAT(/1X,'MAXIMUM BLAST LOAD IS',F8.2,' AT THE LEVEL WHERE THE L
1CAL FACTOR IS EQUAL TO 1.0'/)
  GO TO 45
  30 WRITE(6, 35) (TSEI(I),I=1,20)
  35 FORMAT(/1X,'SEISMIC MODEL USED IN THIS CALCULATION : ',20A4)
  WRITE(6, 40) SEICO
  40 FCFMAT(/1X,'MAXIMUM GROUND ACCELERATION IS',F6.3,' OF GRAVITY ACCE
1LEFATION'/)
  45 IF(IGPH .GT. 5) GO TO 60
  TKAN=DELTAT*FLCAT(MSKIP)
  GO TO (46,56), IGPH
  46 WRITE(6,50) TKAN,(IPCH(J),J=1,NPCH)
  50 FCFMAT( 1X,'THIS PROGRAM PUNCHES OUT THE RESULTS OF EVERY',F6.3,
1' SEC. FOR THE STOREY NO.',5(I5,' ')/)
  WRITE(7,55) TKAN,NS,NPCH,(IPCH(J),J=1,NPCH)
  GO TO 60
  56 WRITE(6,57) TKAN
  57 FCFMAT(1X,'THE RESULT OF EVERY',F6.3,'SEC.,FOR EVERY STOREY IS STO
1RED IN THE DISK'/)
  WRITE(2,55) TKAN ,NS
  55 FCFMAT(F10.3, 9X,'PRODUCED BY PROG.# 40',5X,7I5)
  60 WRITE(6, 65)
  65 FCFMAT( /1X,'** RESPONSE **')
  IF(INSA .LT. 5) GO TO 111
  IF(LTF .GE. 5) GO TO 75
  WRITE(6, 70)
  70 FCFMAT(/2X,'TIME',3X,'GRND ACC',3X,'DISP TO GRND',3X,'RELTV DISP'
1,4X,'RELTV VELC',4X,'ABS ACCEL',3X,'RESIS (DAMP)',2X,'RESIS (SPRN)
2',3X,'SHEAR CCF',3X,'TIME',7X,'ITER')

```



```

      GC TO 85
75  WRITE(6, 80)
80  FORMAT(/2X,'TIME',3X,'BLAST LD/',3X,'DISP TO GRND',3X,'RELIV DISP'
      1,4X,'RELIV VELC',4X,'ABS ACCEL',3X,'RESIS (DAMP)',2X,'RESIS (SPRN)
      2',3X,'SHEAR CCEF',3X,'TIME',7X,'ITER')
85  WRITE(6, 90)
90  FORMAT(12X,'STOREY')
111 CALL STIFF(Q,1,AI,IA,ISHUT)
      IF(ISHUT .EQ. 1) RETURN
      ISAI=10
      DO 120 K=1,NS
      AX(K)=0.0
      VX(K)=0.0
      IF(ABS(HXD(K)) .LT. 1.0E-06) HXD(K)=0.0
      XD(K)=EXD(K)
      RXMX(K)=0.0
      TRX(K)=0.0
      RVMX(K)=0.0
      TRV(K)=0.0
      CQMX(K)=0.0
      TCQ(K)=0.0
      TRMX(K)=0.0
      XDMX(K)=0.0
      AAMX(K)=0.0
      RCMX(K)=0.0
      RQMX(K)=0.0
      ZZ(K)=GR/1.0E+15
120  CCNTINUE
      MEMB=(2*NB+1)*NS
      DC 125 I=1,MEMB
      DC 124 K=1,2
      KCSAN(I,K)=0
124  CCNTINUE
125  CCNTINUE
      DC 50C I=1,NCAL
      IF(I .EQ. 1) READ(INP,130) (GA(J),J=1,7)
130  FORMAT(7F10.0)
      IYOMU=7*(I/7)
      IF(I .EQ. IYOMU .AND. I .LT. NCAL) READ(INP,130) (GA(J),J=1,7)
      II=I-7*((I-1)/7)
      IF(I-1) 140,140,150
140  GA1=0.0
      GA2=0.0
      GA3=GA(II)*SEICO
      IF(NCAL .GT. 1) GO TO 141
      GA4=0.0
      GO TC 160
141  GA4=GA(II+1)*SEICO
      GO TC 160
150  GA1=GA2
      GA2=GA3
      GA3=GA4
      IF(I .EQ. NCAL) GC TO 151
      IF(II .EQ. 7) GO TO 152
      GA4=GA(II+1)*SEICC
      GC TC 160
151  GA4=0.0
      GC TC 160
152  GA4=GA(1)*SEICC
160  GAF=GA3

```



```

      TF=FLCAT(I)*DEITAT
      DC 190 K=1,NS
      CAX(K)=AX(K)
      OVX(K)=VX(K)
      CXI(K)=XD(K)
190  CCNTINUE
      CALL SUCHI (AX,VX,XD,RX,RV,SM,C,CSM,GAP,DELTAT,KAZU,RESC,RELQ,MXIT
1,TF,ISAI,GOSA,C,ZZ)
      IF(ISAI .GE. 0) GO TO 210
205  DC 206 K=1,NS
      AX(K)=CAX(K)
      VX(K)=CVX(K)
      XD(K)=OXD(K)
206  CCNTINUE
      CALL SAIBUN (ISAI,AX,VX,XD,NSAI,TP,DELTAT,RX,RV,SM,C,CSM,KAZU,RESC
1,RESQ,MXIT,GOSA,GA1,GA2,GA3,GA4,C,IA,AI,KDIS,FT,KOSAN,ISHUT,ZZ)
      IF(ISHUT .EQ. 1) GO TO 510
      IF(KDIS .LE. 0) GO TO 510
      GC TO 214
210  CALL KYOTO(XD,IA,AI,ICHI,FT,1)
      IF(ICHI .LE. 0) GO TO 214
      GC TO 205
214  IF(ITF .GE. 5) GO TO 225
      DC 215 K=1,NS
      AA(K)=AX(K)+GAP
215  CCNTINUE
      CQN=0.0
      DO 220 N=1,NS
      CQN=CQN-SM(N)*AA(N)
      TR(N)=CQN
      CQ(N)=RESQ(N)/CSM(N)/GR
220  CCNTINUE
      GC TO 230
225  DC 226 K=1,NS
      AA(K)=AX(K)
226  CCNTINUE
      TOTM=0.0
      CQN=0.0
      DO 228 N=1,NS
      TOTM=TOTM+SM(N)
      CQN=CQN-SM(N)*AA(N)
      TR(N)=CQN-CSM(N)*GAP
      CQ(N)=RESQ(N)/TOTM/GR
228  CCNTINUE
230  IF(INSR .LT. 5) GO TO 275
      IF(NICEU .EQ. 0) GC TO 239
      NTC=I/NTOBU
      NTC=NTC*NTOBU
      IF(NTC .NE. 1) GO TO 275
239  DC 270 K=1,NS
      IF(K .NE. 1) GC TO 250
      WRITE(6,240) TF,GAP,XD(1),RX(1),RV(1),AA(1),RESC(1),RESQ(1),CQ(1),
1TE,KAZU
240  FCFMAT(1X,F6.3,1X,F10.5,1P7E14.5,0PF7.3,I10)
      GO TO 270
250  IF(TP .GT. THAJI .AND. TP .LT. TOWA) GO TO 255
      IF(IF(K) .LT. C) GO TO 270
255  WRITE(6,260) K,XD(K),RX(K),RV(K),AA(K),RESC(K),RESQ(K),CQ(K)
260  FCFMAT(13X,I5,1P7E14.5)
270  CCNTINUE

```



```

275 DC 350 K=1,NS
    IF (ABS (RXMX (K)) .GE. ABS (RX (K))) GO TO 310
    RXMX (K) =RX (K)
    TRX (K) =TF
310 IF (ABS (RVMX (K)) .GE. ABS (RV (K))) GC TO 320
    RVMX (K) =RV (K)
    TRV (K) =TP
320 IF (ABS (TRMX (K)) .GE. ABS (TR (K))) GO TO 325
    TRMX (K) =TR (K)
325 IF (ABS (XDMX (K)) .GE. ABS (XD (K))) GC TO 326
    XDMX (K) =XD (K)
326 IF (ABS (AAMX (K)) .GE. ABS (AA (K))) GO TO 327
    AAMX (K) =AA (K)
327 IF (ABS (RCMX (K)) .GE. ABS (RESC (K))) GO TO 328
    RCMX (K) =RESC (K)
328 IF (ABS (RQMX (K)) .GE. ABS (RESQ (K))) GO TO 330
    RQMX (K) =RESQ (K)
    CQMX (K) =CQ (K)
    TCQ (K) =TP
330 IF (ZZ (K) .GE. ABS (AX (K))) GO TO 350
    ZZ (K) =ABS (AX (K))
350 CCNTINUE
    IF (IGFH .GT. 5) GO TO 450
    NTC =MSKIP* (I/MSKIP)
    IF (NTC .NE. I) GC TO 450
    DC 380 N=1,NPCH
    GC TO (335,360), IGPH
335 K=IFCH (N)
    KETM =NS-K+1
    WRITE (7,370) KETM,TP,XD (K),RX (K),RV (K),AA (K),RESC (K),RESQ (K),CQ (K)
    GC TO 380
360 K=NS-N+1
    KETM =N
    WRITE (2,370) KETM,TP,XD (K),RX (K),RV (K),AA (K),RESC (K),RESQ (K),CQ (K)
370 FCFMAT (I2,F8.3,1P7E10.3)
380 CCNTINUE
450 CALL NARA (KDIS,FI,KOSAN,IP)
    IF (KDIS .IE. 0) GC TO 510
    CALI TIME (1,0,itime)
    IF (itime .GE. itime) GO TO 510
500 CCNTINUE
510 WRITE (6,520)
520 FORMAT (//1X,'LIST OF MAXIMUM VALUES')
    WRITE (6,530)
530 FORMAT (/3X,'STRY',2X,'DISP TO GND',3X,'RELTV DISP - WHEN',4X,'RELT
1V VELC - WHEN',4X,'ABS ACCEL',3X,'DAMP RESIS',3X,'SPRN RESIS',3X,'
2SHEAR COEF-WHEN',2X,'TOTAL SHEAR')
    DC 550 K=1,NS
    WRITE (6,540) K,XDMX (K),RXMX (K),TRX (K),RVMX (K),TRV (K),AAMX (K),RCMX (
1K),RQMX (K),CQMX (K),TCQ (K),TRMX (K)
540 FCFMAT (2X,I4,1P2E13.3,2(0PF8.3,1PE13.3),1P2E13.3,0PF10.4,F8.3,
11PE13.3)
550 CCNTINUE
    IF (IGFH .GT. 5) GC TO 600
    IF (IGFH .EQ. 1) GO TO 553
    IXXXXX=0
    XXXXXX=0.0
    DC 552 J=1,NS
    DO 551 JJ=1,4
    WRITE (2,370) IXXXXX,XXXXXX

```



```

551 CCNTINUE
552 CCNTINUE
    WRITE(3,555)
    GC TO 557
553 WRITE(7,555)
555 FCRMAT(T55,'MAXIMUM VALUES, PROG.# 40')
557 DO 570 J=1,NS
    K=NS-J+1
    RXMX(K)=ABS(RXMX(K))
    RVMX(K)=ABS(RVMX(K))
    CQMX(K)=ABS(CQMX(K))
    IF(IGPH.EQ. 2) GO TO 558
    WRITE(7,560) RXMX(K),TRX(K),RVMX(K),TRV(K),CQMX(K),TCQ(K)
    GC TO 570
558 WRITE(3,560) RXMX(K),TRX(K),RVMX(K),TRV(K),CQMX(K),TCQ(K)
560 FCRMAT(3(1PE10.4,0PF10.3))
570 CCNTINUE
600 IF(LTIME.GE. ITIME) WRITE(6,610) TP
610 FCRMAT(/1X,'** CALCULATION OF RESPONSE WAS TERMINATED BECAUSE PRE
    1PARED COMPUTATION TIME HAD BEEN EXPIRED. **    TP=',F7.3/)
    WRITE(6,999)
999 FCRMAT(1H1)
    RETURN
    END
    SUBROUTINE SAIEUN (ISAI,AX,VX,XD,NSAI,TP,DELTAT,RX,RV,SM,C,CSM,
    1KAZU,RESC,RESQ,MXIT,GOSA,GA1,GA2,GA3,GA4,Q,IA,AI,KDIS,FT,KOSAN,
    2ISHUT,ZZ)
    CCMCN NS,NB,SIF(225),SH(25),SPR( 5),SB( 4),RP(25, 5),UDL(25, 4)
    CCMCN IOP(225,2),ION(225,2),SLPIS(225),SLP(225,3),BETA(225,2,5),
    1THETA(225,2,6),IMA(225,2),PMO(225,2,2),HXD(25),HNL(25)
    DIMENSION AX(25),VX(25),XD(25),RX(25),RV(25),SM(25),C(25),CSM(25),
    1RESC(25),RESQ(25),Q(25,25),AI(150, 11),FT(225,2),KOSAN(225,2),
    2ZZ(25)
    SAIN=FLOAT(NSAI)
    TF=TP-DELTAT
    DO 460 J=1,NSAI
    TBUN=FLOAT(J)/SAIN
    TF=TP+DELTAT/SAIN
    GAP=(GA4-3.0*GA3+3.0*GA2-GA1)*TBUN**3/6.0+(GA3-2.0*GA2+GA1)*TBUN**
    12/2.0-(GA4-6.0*GA3+3.0*GA2+2.0*GA1)*TBUN/6.0+GA2
    CALL SUCHI (AX,VX,XD,RX,RV,SM,C,CSM,GAP,DELTAT/SAIN,KAZU,RESC,RESQ
    1,MXIT,TP,ISAI,GOSA,Q,ZZ)
    CALL KYOTO(XD,IA,AI,ICHI,FT,2)
    IF(ICHI.LE. 0) GC TO 456
    DO 455 K=1,NS
    HXD(K)=XD(K)
    HNL(K)=RESQ(K)
455 CCNTINUE
    CALL STIFF(Q,1,AI,IA,ISHUT)
    IF(ISHUT.EQ. 1) RETURN
456 IF(J.EQ. NSAI) GO TO 460
    CALL NARA(KDIS,FT,KCSAN,TF)
    IF(KDIS.LE. 0) RETURN
460 CCNTINUE
    ISAI=10
    RETURN
    END
    SUBROUTINE SUCHI (SAX,SVX,SXD,RX,RV,SM,C,CSM,GAP,DELTAT,KAZU,RESC,
    1RESC,MXIT,TP,ISAI,GOSA,Q,ZZ)
    CCMCN NS,NB,SIF(225),SH(25),SPR( 5),SB( 4),RP(25, 5),UDL(25, 4)

```



```

      CCMCN IOP(225,2),ION(225,2),SLFIS(225),SLP(225,3),BETA(225,2,5),
      1THETA(225,2,6),IMA(225,2),PMO(225,2,2),HXD(25),HNL(25)
      DIMENSION UX(25),UA(25),RX(25),RV(25),SAX(25),SXD(25),SVX(25),
      1SM(25),C(25),CSM(25),ICOL(25),RESC(25),RESQ(25),UV(25),U(25),
      2Q(25,25),ZZ(25)
      KAZU=0
      MXIJ=MXIT/2
      DO 100 N=1,NS
      UA(N)=SAX(N)
100  CCNTINUE
110  KAZU=KAZU+1
      DO 120 N=1,NS
      UV(N)=SVX(N)+(SAX(N)+UA(N))*DELTAT/2.0
      UX(N)=SXD(N)+(SVX(N)+(SAX(N)/3.0+UA(N)/6.0)*DELTAT)*DELTAT
120  CCNTINUE
      DO 200 N=1,NS
      NN=N-1
      CMA=0.0
      IF(N.EQ. 1) GO TO 140
      DO 130 K=1,NN
      CMA=CMA+SM(K)*UA(K)
130  CCNTINUE
140  IF(N.NE. NS) GO TO 150
      ST=CMA+GAP*CSM(N)
      GO TO 160
150  ST=CMA+GAP*CSM(N)-C(N)*UV(N+1)
160  RESQ(N)=QQ(N,Q,UX)
      U(N)=-(C(N)*UV(N)+RESQ(N)+ST)/SM(N)
200  CCNTINUE
      JHAN=0
      DO 400 N=1,NS
      ICCI(N)=0
      EUNBO=ABS(U(N)-UA(N))/GOSA/100.0+1.0E-35
      SHI=1.01*ABS(U(N)-UA(N))/(ABS(U(N))+EUNBO)
      IF(SHI.LT. GOSA) GO TO 400
      SHI=10.0*ABS(U(N)-UA(N))/ZZ(N)
      IF(SHI.LT. GOSA) GO TO 400
      JHAN=JHAN+1
      ICCL(N)=ICOL(N)+1
400  CCNTINUE
      IF(JHAN.EQ. 0) GO TO 450
      IF(KAZU.LT. MXIT) GO TO 420
      IF(ISAI.LT. 0) GO TO 405
      ISAI=-10
      GO TO 450
405  MXII=MXIT+1
      IF(KAZU.EQ. MXII) GO TO 411
      DO 410 N=1,NS
      IF(ICOL(N).EQ. 0) GO TO 410
      WRITE(6,406) N
406  FORMAT(1X,'CONVERGENCE IS NOT ENOUGH AT STOREY NO.',I3)
410  CCNTINUE
411  DO 415 N=1,NS
      IF(ICCL(N).EQ. 0) GO TO 415
      WRITE(6,412) TP,N,UX(N),UV(N),U(N),RESQ(N),KAZU
412  FORMAT(1X,F6.3,6X,I5,1PE14.5,7X,E14.5,7X,E14.5,14X,E14.5,21X,0PI10
      1)
415  CCNTINUE
      IF(KAZU.EQ. MXII) GO TO 450
420  IF(KAZU.EQ. MXIJ) GO TO 440

```



```

      DC 430 N=1,NS
      UA(N)=U(N)
430  CCNTINUE
      GC TO 110
440  DC 445 N=1,NS
      UA(N)=(UA(N)+U(N))/2.0
445  CCNTINUE
      MXIJ=MXIJ+(MXII-MXIJ)/2
      GC TO 110
450  DO 455 N=1,NS
      SAX(N)=U(N)
      SVX(N)=UV(N)
      SXD(N)=UX(N)
455  CCNTINUE
      DC 470 N=1,NS
      IF(N.EQ. NS) GO TO 460
      RX(N)=SXD(N)-SXD(N+1)
      RV(N)=SVX(N)-SVX(N+1)
      GC TO 465
460  RX(NS)=SXD(NS)
      RV(NS)=SVX(NS)
465  RESC(N)=C(N)*RV(N)
470  CCNTINUE
      RETURN
      END
      FUNCTION QQ (N,Q,SXD)
      COMMON NS,NB,SIF(225),SH(25),SPR( 5),SB( 4),RP(25, 5),UDL(25, 4)
      COMMON IOP(225,2),ION(225,2),SLPIS(225),SLP(225,3),BETA(225,2,5),
1THETA(225,2,6),IMA(225,2),FMO(225,2,2),HXD(25),HNL(25)
      DIMENSION Q(25,25),SXD(25)
      QQ=C.C
      DC 100 I=1,NS
      SHXI=SXD(I)-HXD(I)
      QQ=QQ+C(N,I)*SHXI
100  CCNTINUE
      QQ=HNI(N)+QQ
      RETURN
      END
      SUBROUTINE KYOTO (SXD,IA,AI,ICHI,FT,IIQ)
      COMMON NS,NB,SIF(225),SH(25),SPR( 5),SB( 4),RP(25, 5),UDL(25, 4)
      COMMON IOP(225,2),ION(225,2),SLPIS(225),SLP(225,3),BETA(225,2,5),
1THETA(225,2,6),IMA(225,2),FMO(225,2,2),HXD(25),HNL(25)
      DIMENSION SXD(25),EB(150),AI(150,11),FT(225,2),EM(2),CCC(25)
      ICHI=C
      DO 100 I=1,IA
      EE(I)=E(I,SXD)
100  CCNTINUE
      NE1=NB+1
      NE2=NB+2
      NEE=2*NB+1
      CALL SOLVE(AI,EB,CCC)
      DC 300 I=1,NS
      IF(I.EQ. NS) GO TO 110
      R=(SXI(I)-SXD(I+1))/SH(I)
      GC TO 120
110  R=SXI(NS)/SH(NS)
120  DC 250 J=1,NBB
      M=NEE*(I-1)+J
      IF(STF(M).LT. 1.0E-30) GO TO 250
      JJ=J-NB

```



```

      IF(J .GE. NB1) GO TO 130
      KA=NB2*(I-1)+J
      KE=KA+1
      GC TC 140
130   KA=NB2*(I-1)+J-NB
      IF(I .EQ. NS) GO TC 140
      KE=KA+NB2
140   FA=BE(KA)
      IF(I .EQ. NS .AND. J .GE. NB1) GO TO 150
      FE=EB(KB)
150   IF(J .GE. NB1) GO TO 160
      SS=SB(J)
      FR1=RF(I,J)/SS
      FR2=RF(I,J+1)/SS
      FR3=1.0-FR1-FR2
      UI=UDI(I,J)
      DC 155 K=1,2
      CALL IZU (VA,VE,M,K,FR1,FR2,1,-1)
      EM(K)=VA*PA+VB*PE-UHEN(M,SS,K,UL,0.0,FR1,FR2,1,-1)
155   CCNTINUE
      FEM=-UL*(FR3*SS)**2/12.0
      FT(M,1)=- (2.0*EM(1)-EM(2)-3.0*FEM)*FR3/STF(M)/3.0+(1.0+FR1/FR3)*PA
      1+FF2*FE/FR3
      FT(M,2)=- (2.0*EM(2)-EM(1)+3.0*FEM)*FR3/STF(M)/3.0+FR1*PA/FR3+(1.0+
      1FR2/FF3)*PB
      GC TO 180
160   SS=SH(I)
      IF(I .EQ. NS) GO TO 170
      DC 165 K=1,2
      CALL IZU (VA,VE,M,K,0.0,0.0,1,-1)
      EM(K)=VA*PA+VE*PE-UHEN(M,SS,K,0.0,R,0.0,0.0,1,-1)
165   CCNTINUE
      GC TC 175
170   CALL IZU (VA,VE,M,1,0.0,0.0,-1,-1)
      EM(1)=VA*PA-UHEN(M,SS,1,0.0,R,0.0,0.0,-1,-1)
      CALL IZU (VA,VE,M,3,0.0,0.0,-1,-1)
      EM(2)=VA*PA-UHEN(M,SS,3,0.0,R,0.0,0.0,-1,-1)-EM(1)
      IF(SPR(JJ) .LE. 1.0E-5) GO TO 175
      FB=-EM(2)/SPR(JJ)
175   FT(M,1)=- (2.0*EM(1)-EM(2))/STF(M)/3.0+PA-R
      IF(I .EQ. NS .AND. SPR(JJ) .LE. 1.0E-5) GO TO 180
      FT(M,2)=- (2.0*EM(2)-EM(1))/STF(M)/3.0+PB-R
180   DC 220 K=1,2
      IF(I .EQ. NS .AND. J .GE. NB1 .AND. SPR(JJ) .LE. 1.0E-5) GO TO 220
      IF(IMA(M,K)) 210,200,190
190   ICCN=IMA(M,K)
      IF(FT(M,K) .GE. THETA(M,K,ICON) .AND. FT(M,K) .LE. THETA(M,K,ICON+
      11)) GC TO 220
      IF(FT(M,K) .GE. THETA(M,K,ICON+1)) GO TO 195
      ICHI=ICHI+1
      IF(IIQ .EQ. 1) GO TC 220
      IMA(M,K)=IMA(M,K)-IOP(M,K)
      GC TC 220
195   IF(IMA(M,K) .EQ. 2) GO TO 220
      ICHI=ICHI+1
      IF(IIQ .EQ. 1) GO TO 220
      IMA(M,K)=IMA(M,K)+1
      GO TO 220
200   IF(EM(K) .GE. FMC(M,K,2) .AND. EM(K) .LE. PMO(M,K,1)) GO TO 220
      ICHI=ICHI+1

```



```

IF(IIQ .EQ. 1) GO TO 220
IF(EM(K) .LE. PMO(M,K,2)) IMA(M,K)=-ION(M,K)
IF(EM(K) .GE. PMO(M,K,1)) IMA(M,K)=IOP(M,K)
GO TO 220
210 ICCN=3-IMA(M,K)
IF(FT(M,K) .GE. THETA(M,K,ICON+1) .AND. FT(M,K) .LE. THETA(M,K,ICO
1N)) GO TO 220
IF(FT(M,K) .LE. THETA(M,K,ICON+1)) GO TO 215
ICHI=ICHI+1
IF(IIQ .EQ. 1) GO TO 220
IMA(M,K)=IMA(M,K)+ION(M,K)
GO TO 220
215 IF(IMA(M,K) .EQ. -2) GO TO 220
ICHI=ICHI+1
IF(IIQ .EQ. 1) GO TO 220
IMA(M,K)=IMA(M,K)-1
220 CCNTINUE
250 CCNTINUE
300 CCNTINUE
RETURN
END
SUBROUTINE NARA (KDIS,FT,KOSAN,TP)
CCMMCN NS,NB,STF(225),SH(25),SPR( 5),SB( 4),RP(25, 5),UDL(25, 4)
CCMMCN IOP(225,2),ION(225,2),SLPIS(225),SLP(225,3),BETA(225,2,5),
1THETA(225,2,6),IMA(225,2),PMO(225,2,2),HxD(25),HNL(25)
DIMENSION FT(225,2),KOSAN(225,2)
KDIS=10
NE1=NB+1
NE2=NB+2
NBB=2*NB+1
DO 360 I=1,NS
DO 350 J=1,NBB
M=NEE*(I-1)+J
CEF=2.5*STF(M)
DO 340 K=1,2
IF(IMA(M,K)) 100,340,100
100 IF(KOSAN(M,K) .EQ. 0) GO TO 110
IF(IMA(M,K) .GT. 0) GO TO 130
GO TO 170
110 KOSAN(M,K)=1
IF(J .GE. NB1) GO TO 120
GO TO (111,115), K
111 WRITE(6,112) I,J,TP
112 FORMAT(1X,'YIELD AT THE LEFT END OF THE BEAM -- STOREY NO.',I3,',
1 EAY NO.',I3,'; TIME',F7.3,' SEC.')
GO TO 128
115 WRITE(6,116) I,J,TP
116 FORMAT(1X,'YIELD AT THE RIGHT END OF THE BEAM -- STOREY NO.',I3,',
1 EAY NO.',I3,'; TIME',F7.3,' SEC.')
GO TO 128
120 JC=J-NB
GO TO (121,125), K
121 WRITE(6,122) I,J,TP
122 FORMAT(1X,'YIELD AT THE TOP OF THE COLUMN -- STOREY NO.',I3,',
1 CCL. NO.',I3,'; TIME',F7.3,' SEC.')
GO TO 128
125 WRITE(6,126) I,J,TP
126 FORMAT(1X,'YIELD AT THE BCTTCM OF THE COLUMN -- STOREY NO.',I3,',
1 CCL. NO.',I3,'; TIME',F7.3,' SEC.')
128 IF(IMA(M,K) .GT. 0) GO TO 130

```



```

GO TO 170
130 IF (FT(M,K) .GE. THETA(M,K,3)) GO TO 210
    IF=IMA(M,K)
    IOF(M,K)=IP
    IN=ICK(M,K)+3
    THETA(M,K,IP)=FT(M,K)
    YB=SLF(M,IP+1)*FT(M,K)+BETA(M,K,IP+1)
    FMC(M,K,1)=YB
    IF(SLP(M,1) .GE. STF(M)) GO TO 140
    DX=(SLP(M,1)*(FT(M,K)-THETA(M,K,IN))-YB+PMO(M,K,2))/(SLP(M,1)-SLPL
1S(M))
    GC TO 150
140 DX=(FT(M,K)-THETA(M,K,IN)-(YB-PMO(M,K,2))/SLP(M,1))/(1.0-SLPLS(M)/
1SLF(M,1))
150 DY=SLPLS(M)*DX
    FMC(M,K,2)=PMO(M,K,2)+DY
    IF(SLF(M,1) .GT. CER) GO TO 155
    EETA(M,K,1)=YB-SLF(M,1)*FT(M,K)
155 DO 160 KK=IN,6
    THETA(M,K,KK)=THETA(M,K,KK)+DX
    IF(KK .EQ. 6) GO TO 160
    INN=IN-2
    DE=DY-DX*SLP(M,INN)
    EETA(M,K,IN)=BETA(M,K,IN)+DB
160 CCNTINUE
    GO TO 340
170 IF (FT(M,K) .LE. THETA(M,K,6)) GO TO 210
    IN=-IMA(M,K)
    ICK(M,K)=IN
    IF=IOF(M,K)
    THETA(M,K,IN+3)=FT(M,K)
    YB=SLF(M,IN+1)*FT(M,K)+BETA(M,K,IN+3)
    FMC(M,K,2)=YB
    IF(SLP(M,1) .GE. STF(M)) GO TO 180
    DX=(SLP(M,1)*(FT(M,K)-THETA(M,K,IP))-YB+PMO(M,K,1))/(SLP(M,1)-SLPL
1S(M))
    GC TO 190
180 DX=(FT(M,K)-THETA(M,K,IP)-(YB-FMC(M,K,1))/SLP(M,1))/(1.0-SLPLS(M)/
1SLF(M,1))
190 DY=SLPLS(M)*DX
    FMC(M,K,1)=FMC(M,K,1)+DY
    IF(SLP(M,1) .GT. CER) GO TO 195
    BETA(M,K,1)=YB-SLF(M,1)*FT(M,K)
195 DC 200 KK=IP,3
    THETA(M,K,KK)=THETA(M,K,KK)+DX
    IF(KK .EQ. 3) GO TO 340
    DB=DY-DX*SLF(M,IP+1)
    EETA(M,K,IP+1)=BETA(M,K,IP+1)+DB
200 CCNTINUE
    GO TO 340
210 KDIS=-10
    IF(J .GE. NB1) GO TO 260
    GO TO (220,240), K
220 WRITE(6,230) I,J,TP
230 FORMAT(/1X,'COLLAPSE AT THE LEFT END OF THE BEAM -- STOREY NO.',I
13,',', 'EAY NO.',I3,',', 'TIME',F7.3,' SEC.')
    GC TO 340
240 WRITE(6,250) I,J,TP
250 FORMAT(/1X,'COLLAPSE AT THE RIGHT END OF THE BEAM -- STOREY NO.',I
13,',', 'EAY NO.',I3,',', 'TIME',F7.3,' SEC.')

```



```
GC TO 340
260 JC=J-AB
GO TO (270,290), K
270 WRITE(6,280) I,JC,TP
280 FORMAT(/1X,'COLLAPSE AT THE TOP OF THE COLUMN -- STOREY NO.',I
13,', COL. NO.',I3,'; TIME',F7.3,' SEC.')
GC TO 340
290 WRITE(6,300) I,JC,TP
300 FORMAT(/1X,'COLLAPSE AT THE BOTTOM OF THE COLUMN -- STOREY NO.',I
13,', COL. NO.',I3,'; TIME',F7.3,' SEC.')
340 CCNTINUE
350 CCNTINUE
360 CCNTINUE
RETURN
END
```


Appendix E.

BLAST LOADS ON A STRUCTURE

E-1 Determination of Blast Loads on a Structure.

The blast loads considered in this dissertation are assumed to be caused by blast waves accompanying a nuclear explosion in the air. The characteristics of blast waves have been investigated by the United States Department of Defence and other affiliated agencies and research institutes. Refs. 14 through 22 provide useful information concerning the nature of blast waves and the magnitude of the blast loads which could be applied to a structure at a particular site.

Summarizing the available information, the following steps are used to determine the blast loads acting on structures for the purpose of the present investigation.

STEP 1: Estimate the size of burst, W (KT, TNT), height of burst, h (feet), the location of the building from G.Z. (ground zero), d (feet), and the orientation of the building. Here G.Z. is the point on the earth's surface immediately below the point of detonation.

The objective of Steps 2 to 9 is to find the over-pressure, $p(t)$ (psi), dynamic pressure, $q(t)$ (psi), and the shock front velocity, U (ft/sec), at the site of the building. These values do not depend upon the shape or type of building.

STEP 2: Find the scaled height of burst, h_1 (feet),
as:

$$h_1 = \frac{h}{W^{1/3}} \quad (E-1)$$

A 1 KT (TNT equivalent) burst at height h_1 would produce the same effect as a W KT burst at height h when observed at the site immediately below the point of detonation, according to the scaling law.

STEP 3: Find the scaled distance from G.Z., d_1 (feet),
as:

$$d_1 = \frac{d}{W^{1/3}} \quad (E-2)$$

The pressure at the distance d_1 from G.Z. for a 1 KT burst at height h_1 would be the same as the pressure obtained at the distance d from G.Z. for a W KT burst at height h , according to the scaling law.

STEP 4: Find the maximum overpressure, p (psi), using the pertinent graph prepared for a 1 KT burst. Depending upon the values of scaled height and distance, the following figures are used.

For $d_1 < 1200$, $h_1 < 1000$... Fig. E-1a

For $d_1 < 7000$, $h_1 < 500$... Fig. E-1b

For surface burst, $h_1=0$... Fig. E-2

STEP 5: Find the horizontal component of the peak dynamic pressure, q (psi), using Fig. E-3, prepared for a

1 KT burst, by entering with the scaled height and distance.

The values p and q obtained in the preceding two steps are also the peak overpressure and the horizontal component of the peak dynamic pressure, respectively, for the burst and building location described in Step 1.

STEP 6: Find the positive phase duration of the overpressure, t_{+p1} (sec), and the dynamic pressure, t_{+q1} (sec), for an equivalent 1 KT burst using Fig. E-4. Then apply the scaling law to find the actual durations of the overpressure, t_{+p} (sec), and the dynamic pressure, t_{+q} (sec), for the W KT burst as:

$$t_{+p} = t_{+p1} W^{1/3} \quad (E-3)$$

$$t_{+q} = t_{+q1} W^{1/3} \quad (E-4)$$

STEP 7: Determine the overpressure, $p(t)$ (psi), and the horizontal component of dynamic pressure, $q(t)$ (psi), as functions of time using Fig. E-5 and Fig. E-6, respectively. Both are functions of peak overpressure, p , and are expressed by:

$$p(t) = p \left(1 - \frac{t}{t_{+p}}\right) e^{-t/t_{+p}} \quad (E-5)$$

and

$$q(t) = q \left(1 - \frac{t}{t_{+q}}\right)^2 e^{-2(t/t_{+q})} \quad (E-6)$$

respectively, which are valid approximately when the peak

overpressure is less than about 10 psi. In the above equations, t (sec) is the elapsed time after the arrival of the shock front. The peak overpressure is assumed to occur almost instantaneously with the arrival of the shock front.

STEP 8: Find the shock front velocity, U (ft/sec), using Fig. E-7. This is also a function of the peak overpressure, p .

STEP 9: The arrival time is obtained from Fig. E-8. This value is not necessary to find the blast loads on a structure but it may give useful information in designing the building. For instance, the availability of warning time may change the design attitude.

Knowing both the overpressure function, $p(t)$, and the dynamic pressure function, $q(t)$, at the location of the building, the blast loads on the building, assumed in this case to be a closed box-like structure oriented parallel to the direction of the wave, are calculated as follows.

Steps 10 to 12 determine the average horizontal load to be applied to a structure.

STEP 10: Find the reflected overpressure, p_r (psi), from Fig. E-9. The angle of incidence, α , is as shown in Fig. E-10. For the present investigation, α is assumed to be zero.

STEP 11: Find the time required for stagnation, t_s (sec), as:

$$t_s = 3S/U , \quad (E-7)$$

where S (feet) is equal to H or $B/2$, whichever is less. H , L , and B denote the height, depth and width of the building in feet as shown in Fig. E-11.

STEP 12: Plot the average pressure, p_1 , applied to the front surface as shown in Fig. E-12. The reflected overpressure, p_r , is developed instantaneously with the arrival of the shock front; this corresponds to the origin of the time axis. This pressure decays to stagnation pressure, p_s , which is given by:

$$p_s = p(t_s) + q(t_s) \quad (E-8)$$

in a linear manner in time t_s , calculated in the preceding step. Beyond a time t_s , the front surface pressure is the sum of the overpressure and the dynamic pressure. The drag coefficient, C_d , is taken equal to 1 in this case. This curve is expressed mathematically as follows:

For $t_s \geq t \geq 0$:

$$p_1 = p_r - (p_r - p_s) \frac{t}{t_s} , \quad (E-9)$$

For $t > t_s$:

$$p_1 = p(t) + q(t) . \quad (E-10)$$

The average loading on the back surface is determined according to the following two steps.

STEP 13: Compute the time, t_2 , required for the shock front to travel the length (depth) of the building as:

$$t_2 = L/U . \quad (E-11)$$

At this time, the loading on the back surface is initiated. Compute the time, t_b , required for the pressure to build up to the surrounding overpressure and dynamic pressure as:

$$t_b = 4S/U \quad (E-12)$$

where S is as defined before.

STEP 14: Plot the average pressure, p_2 , applied to the back surface of the building as shown in Fig. E-13. The loading starts at $t = t_2$ and increases linearly up to p_b which is given by:

$$p_b = p(t_b) + C_d q(t_b) , \quad (E-13)$$

by taking an additional time t_b . Beyond this time, the pressure is the sum of the overpressure and the dynamic pressure multiplied by the drag coefficient, C_d (tabulated in Table E-1). The curve is represented mathematically as follows:

For $t_2 \leq t \leq 0$:

$$p_2 = 0 , \quad (E-14)$$

For $t_2 + t_b \geq t \geq t_2$:

$$p_2 = p_b \cdot \frac{t-t_2}{t_b}, \quad (\text{E-15})$$

For $t > t_2 + t_b$:

$$p_2 = p(t-t_2) + C_d q(t-t_2). \quad (\text{E-16})$$

The net horizontal load is calculated as follows.

STEP 15: Subtract the back surface pressure, p_2 , from the front surface pressure, p_1 , to obtain the net horizontal load, p_n , applied to the structure. This corresponds to the shaded area in Fig. E-14a or equivalently in Fig. E-14b. The total load on the structure is obtained by multiplying the surface area, $H \times B$, by the above pressure. The load may be distributed at each floor level in proportion to the tributary surface area. It is seen from Fig. E-14a or E-14b that the most substantial loading is applied within (t_2+t_b) sec. or $(L+4S)/U$ sec., thus it may be regarded as a shock or an impulse.

The loading on the sides or roof may be found in a similar manner. The loading on a partially open structure, open frame structure, or cylindrical structure can also be calculated by consulting the same references.^{14,18,19,20}

E-2 Example Calculation of the Blast Load on a Structure.

The building considered in this example is the one shown in Fig. 4-3. It is a ten-story building and has four bays in either direction. The plan is a square with its sides 100 feet long. Story height is constant throughout the stories and is 12 feet, thus the total height is 120 feet. Exterior surfaces are assumed to be covered with concrete panels with relatively small openings for windows. Thus this building may be classified as a closed box-like structure.

The blast load on this building will be determined as follows in accordance with the steps described in the previous section.

STEP 1: Estimated size of burst: $W = 1 \text{ MT} = 1000 \text{ KT}$.

Estimated height of burst: $h = 5000 \text{ ft}$.

Assumed location of the building from G.Z.:

$d = 42,000 \text{ ft}$. (about 8 miles).

STEP 2: Scaled height of burst: $h_1 = 5000/(1000)^{1/3} = 500 \text{ ft}$.

STEP 3: Scaled distance from G.Z.:

$d_1 = 42000/(1000)^{1/3} = 4200 \text{ ft}$.

STEP 4: Maximum overpressure (use Fig. E-1b):

$p = 1.47 \text{ psi}$.

STEP 5: Horizontal component of the peak dynamic pressure (use Fig. E-3): $q = .32 \text{ psi}$.

STEP 6: Positive phase duration of the overpressure and the dynamic pressure for an equivalent 1 KT burst (use Fig. E-4): $t_{+p1} = .4$ sec. and $t_{+q1} = .45$ sec. respectively. Apply scaling law to obtain actual duration of positive phase of each pressure: $t_{+p} = .4 \cdot (1000)^{1/3} = 4.0$ sec. and $t_{+q} = .45 \cdot (1000)^{1/3} = 4.5$ sec.

STEP 7: Use the pertinent curves from Fig. E-5 and Fig. E-6 to obtain the overpressure function, $p(t)$, and the dynamic pressure function, $q(t)$, respectively.

STEP 8: Shock front velocity (use Fig. E-7):
 $U = 1170$ ft/sec.

STEP 9: Arrival time for an equivalent 1 KT burst (use Fig. E-8): $t_{a1} = 3.2$ sec.
 Apply scaling law to obtain the actual arrival time:
 $t_a = 3.2 \cdot (1000)^{1/3} = 32$ sec.

STEP 10: Angle of incidence: $\alpha = 0$.
 Reflected overpressure (use Fig. E-9): $p_r/p = 2.07$,
 therefore $p_r = 2.07 \cdot 1.47 = 3.05$ psi.

STEP 11: $H = 120$ ft., $B = 100$ ft., therefore $S = 50$ ft.
 Time required for stagnation: $t_s = 3 \cdot 50/1170 = .13$ sec.

STEP 12: Average pressure applied to the front surface is plotted as shown by curve A in Fig. E-15. Here the stagnation pressure, p_s , is given as follows:

$$t_s/t_{+p} = 0.13/4.0 = 0.0325.$$

Using Fig. E-5, $p(t_s)/p = 0.95$, therefore $p(t_s) = 1.40$ psi and

$$t_s/t_{+q} = 0.13/4.5 = 0.029 .$$

Using Fig. E-6, $q(t_s)/q = 0.9$, therefore $q(t_s) = .30$ psi.

Stagnation pressure is then: $p_s = p(t_s) + q(t_s) = 1.70$ psi.

STEP 13: Time required for the shock front to travel the depth of the building: $t_2 = 100/1170 = 0.085$ sec.

Time required for the pressure to build up to the surrounding pressure at the back surface of the building:

$$t_b = 4 \cdot 50/1170 = 0.17 \text{ sec.}$$

STEP 14: Average pressure applied to the back surface is plotted as shown by curve B in Fig. E-15. Here p_b is calculated as follows:

$$t_b/t_{+p} = 0.17/4.0 = 0.043 .$$

Using Fig. E-5, $p(t_b)/p = 0.93$, therefore $p(t_b) = 1.37$.

And, $t_b/t_{+q} = 0.17/4.5 = 0.038$.

Using Fig. E-6, $q(t_b)/q = .85$, therefore $q(t_b) = .27$ psi.

Therefore: $p_b = 1.37 - 0.4 \cdot .27 = 1.26$ psi

where the drag coefficient, C_d , is -0.4 in this case (Table E-1).

STEP 15: Net horizontal load (in terms of average pressure) shown in Fig. E-16 is obtained by taking the difference between curve A and curve B in Fig. E-15.

If it is assumed that the pressure is distributed uniformly over the exterior surface and that each of the five bents takes an equal amount of horizontal load at any instant, the loading to any one bent is determined as follows: The tributary area per floor per bent for the 2nd floor to the 10th floor is $12 \cdot \frac{100}{5} = 240 \text{ ft}^2$, or $34,560 \text{ in}^2$. At the first floor (top floor), the tributary area is one half of the other. Therefore the loading at the 2nd floor to the 10th floor is obtained by the net horizontal pressure in Fig. E-16 multiplied by 34.56 (in terms of kips) and at the 1st floor, by 17.28. In accordance with the description in Sec. 3-7-1, the vector $\{r\}$ is:

$$r_i = 0.5, \quad \text{for } i = 1,$$

$$r_i = 1.0, \quad \text{for } i = 2, 3, \dots, 10,$$

and the function, $Z(t)$, is expressed by the curve in Fig. E-16 where the quantity in ordinate is multiplied by 34.56; or as shown in Fig. 4-5.

Table E-1 Drag Coefficient : C_d

Dynamic Pressure	Drag Coefficient (Side, Top, Back)
0 - 25 psi	-.4
25 - 50 psi	-.3
50 - 130 psi	-.2

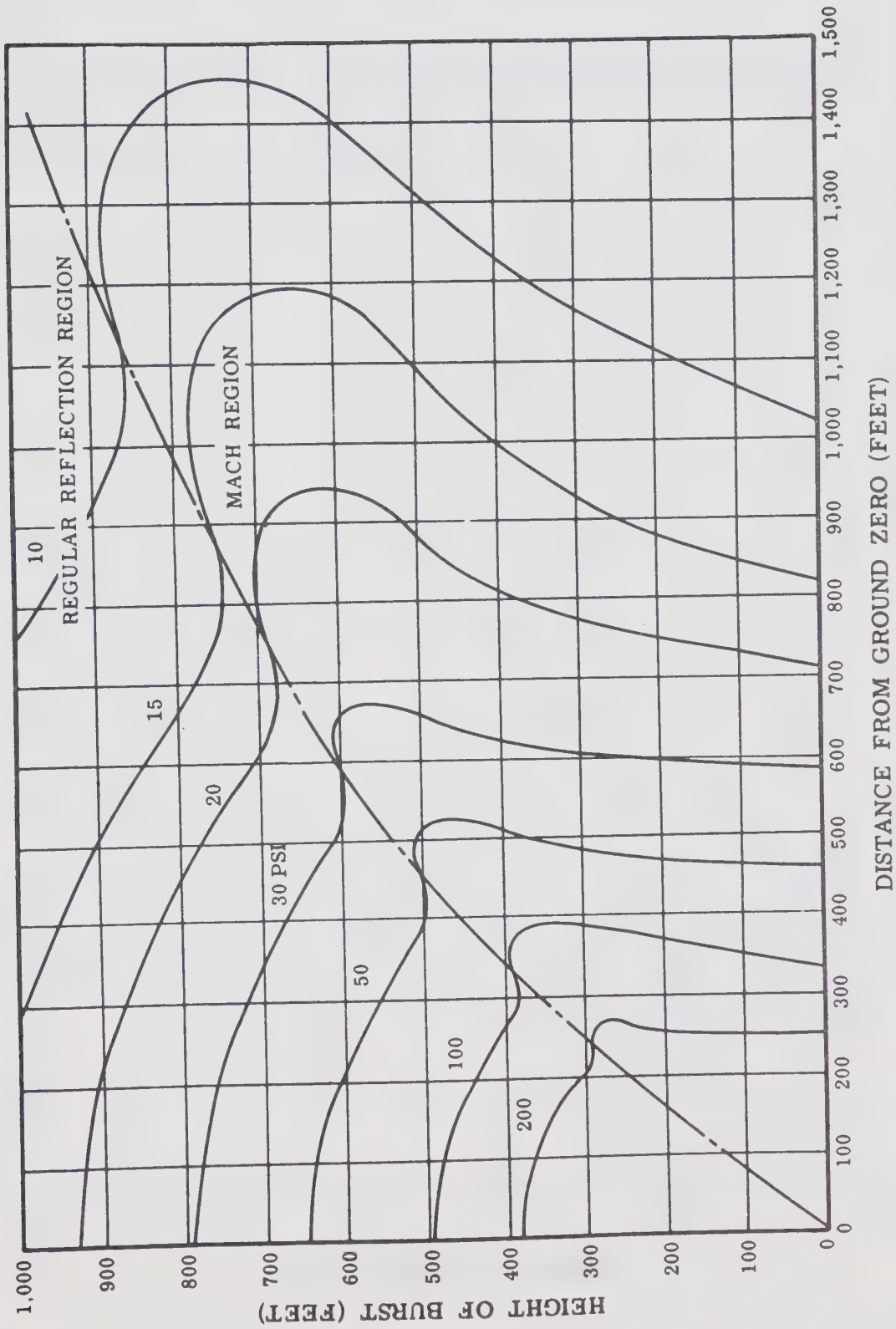


Fig. E-1a Peak Overpressures on the Ground for 1-KT Burst (High-Pressure Range)
Due to Ref. 14

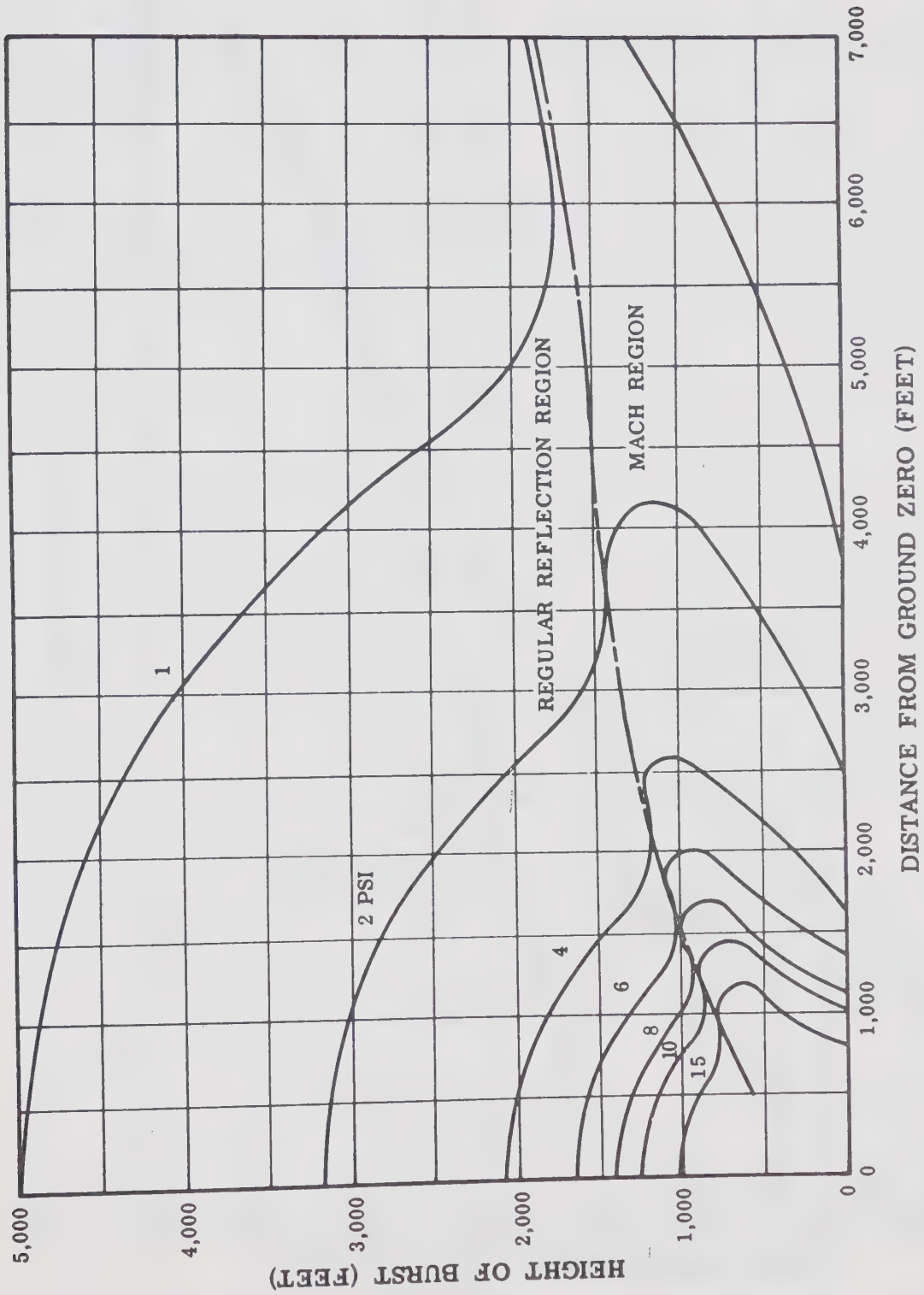


Fig. E-1b Peak Overpressure on the Ground for 1-KT Burst (Low Pressure Range)
Due to Ref. 14

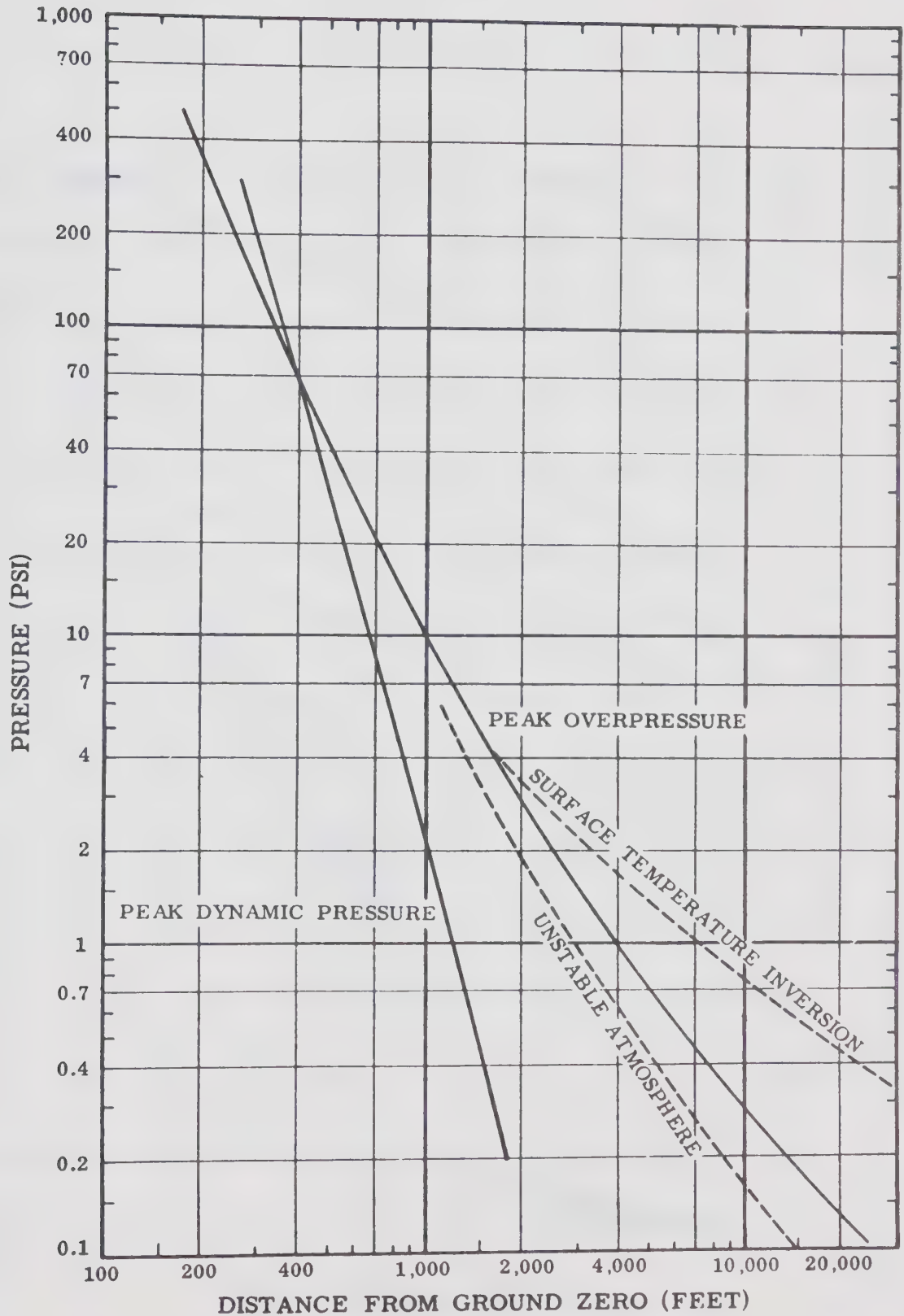


Fig. E-2 Peak Overpressure and Peak Dynamic Pressure for 1-KT Surface Blast
Due to Ref. 14

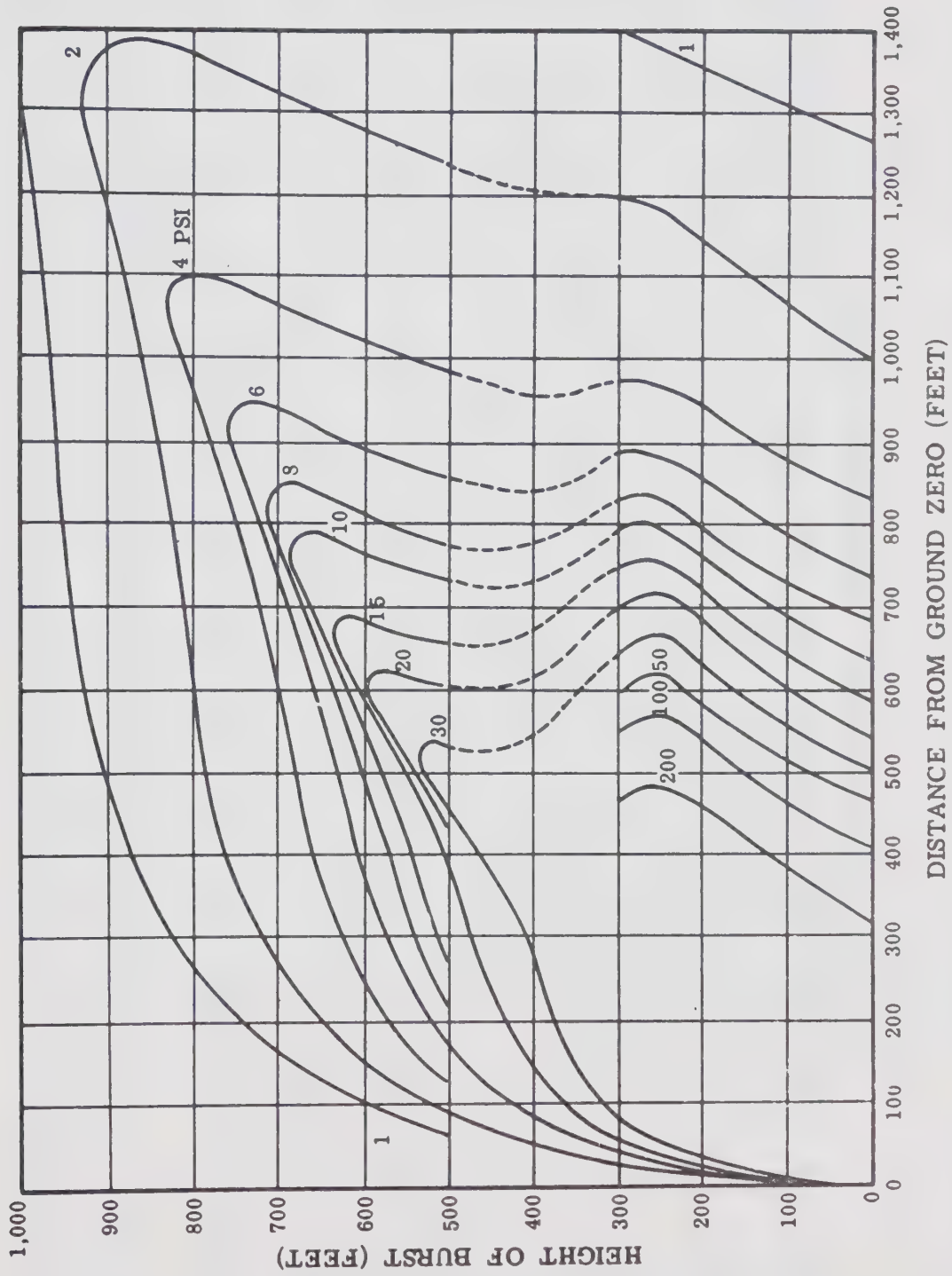


Fig. E-3 Horizontal Component of Peak Dynamic Pressure for 1-KT Burst
Due to Ref. 14

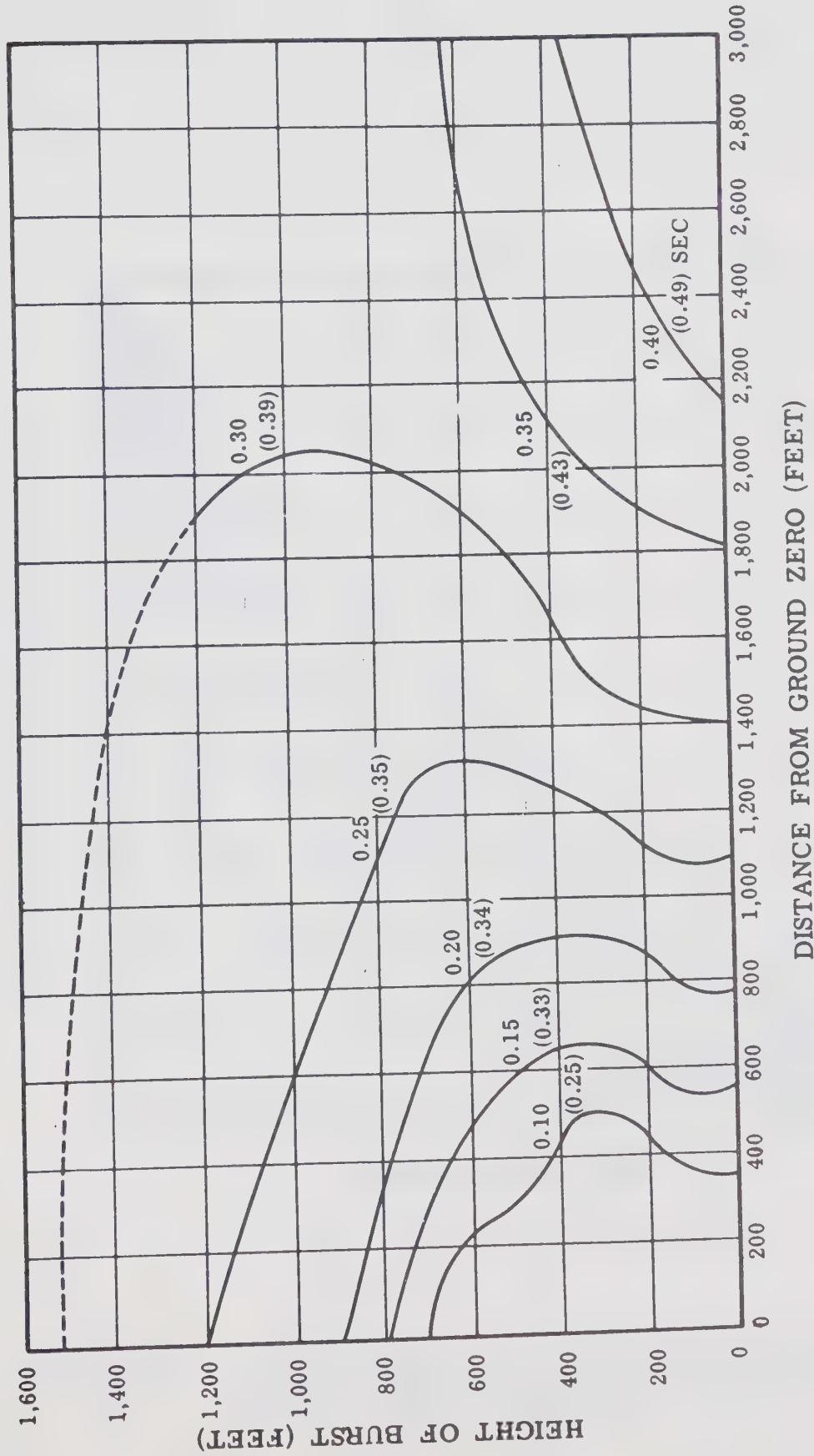


Fig. E-4 Positive Phase Duration on the Ground of Overpressure and Dynamic Pressure (in parenthesis) for 1-KT Burst Due to Ref. 14

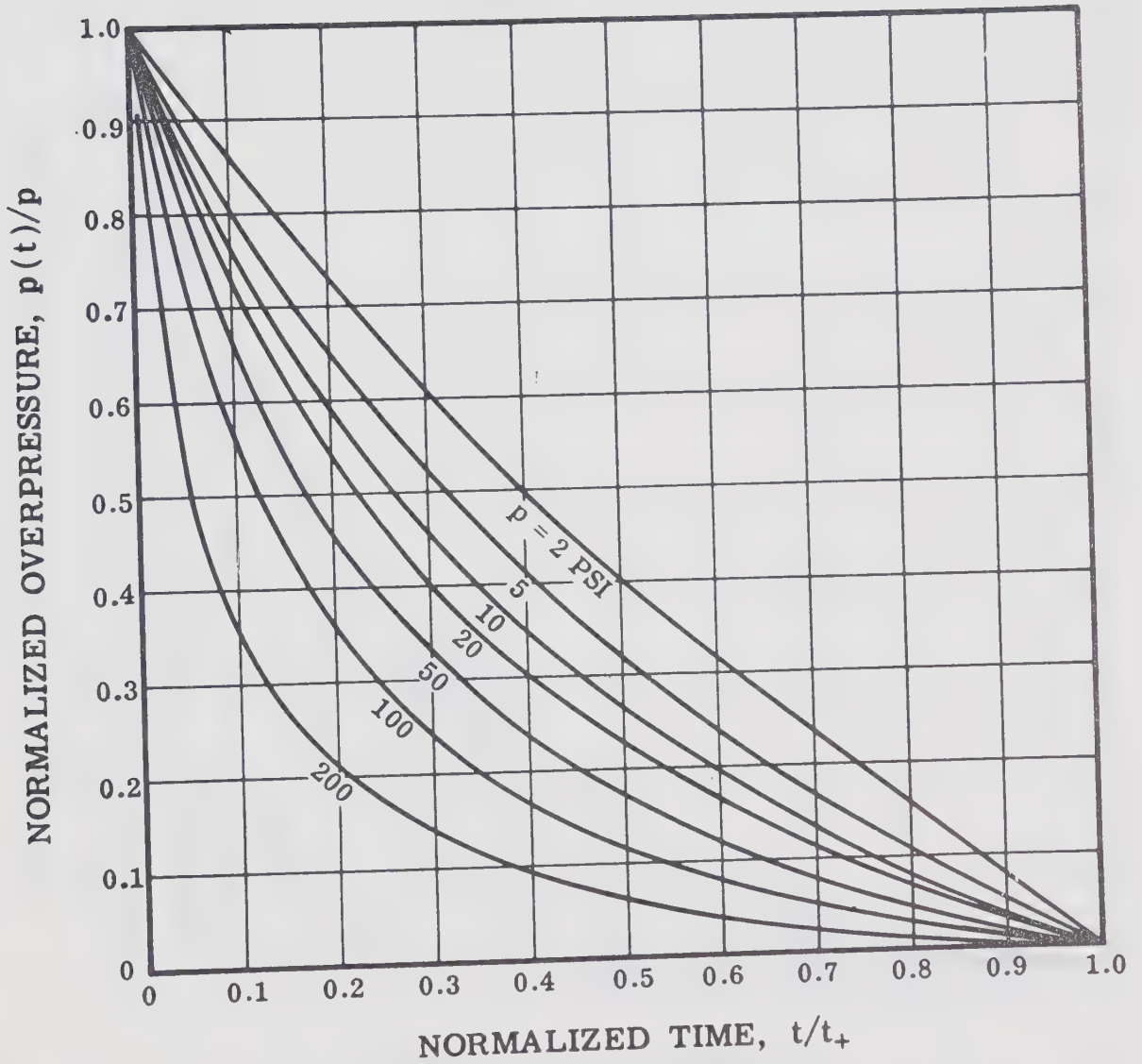


Fig. E-5 Rate of Decay of Pressure with Time for
Various Values of the Peak Overpressure
Due to Ref. 14

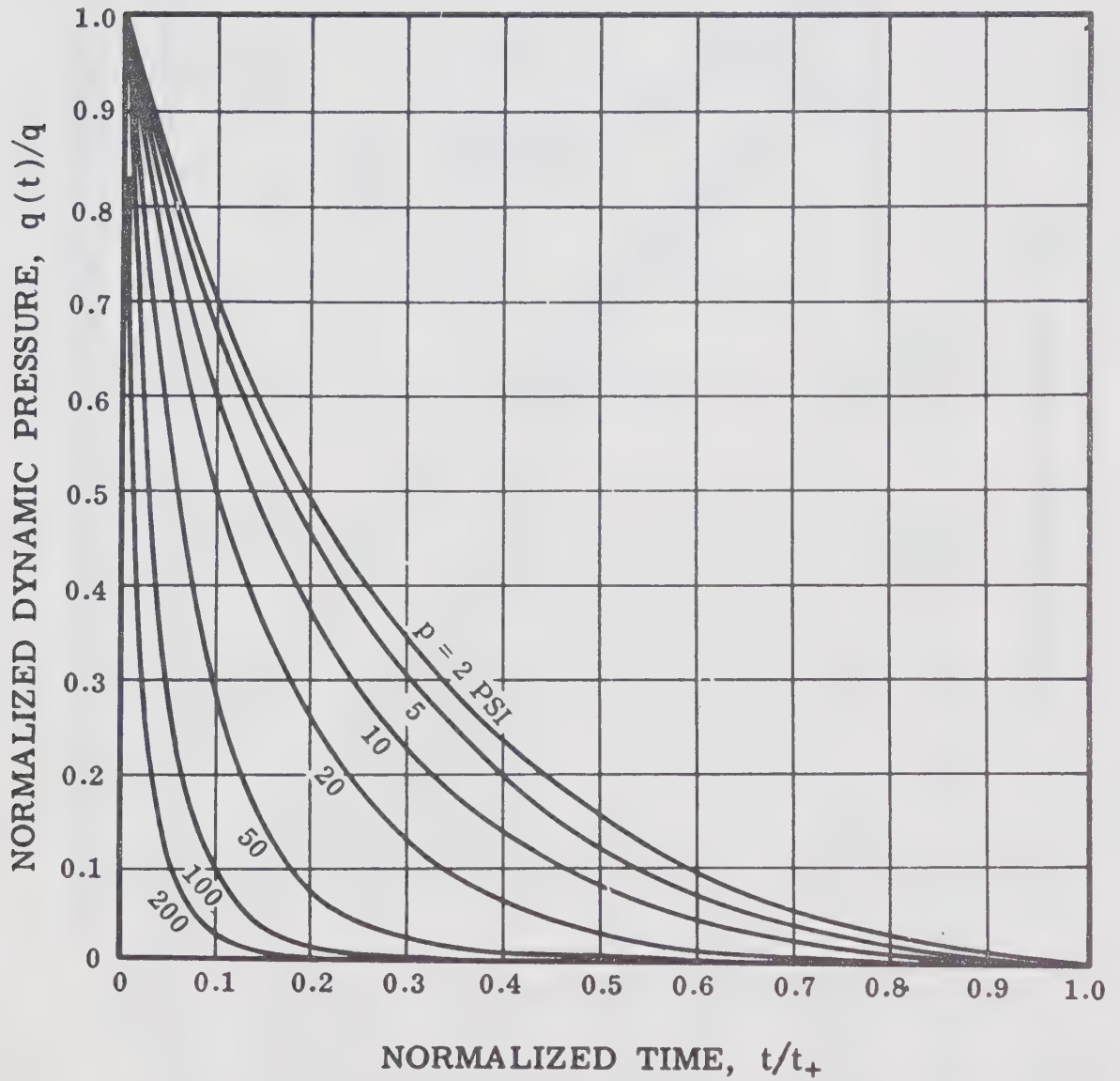


Fig. E-6

Rate of Decay of Dynamic Pressure with Time
for Various Values of the Peak Overpressure
Due to Ref. 14

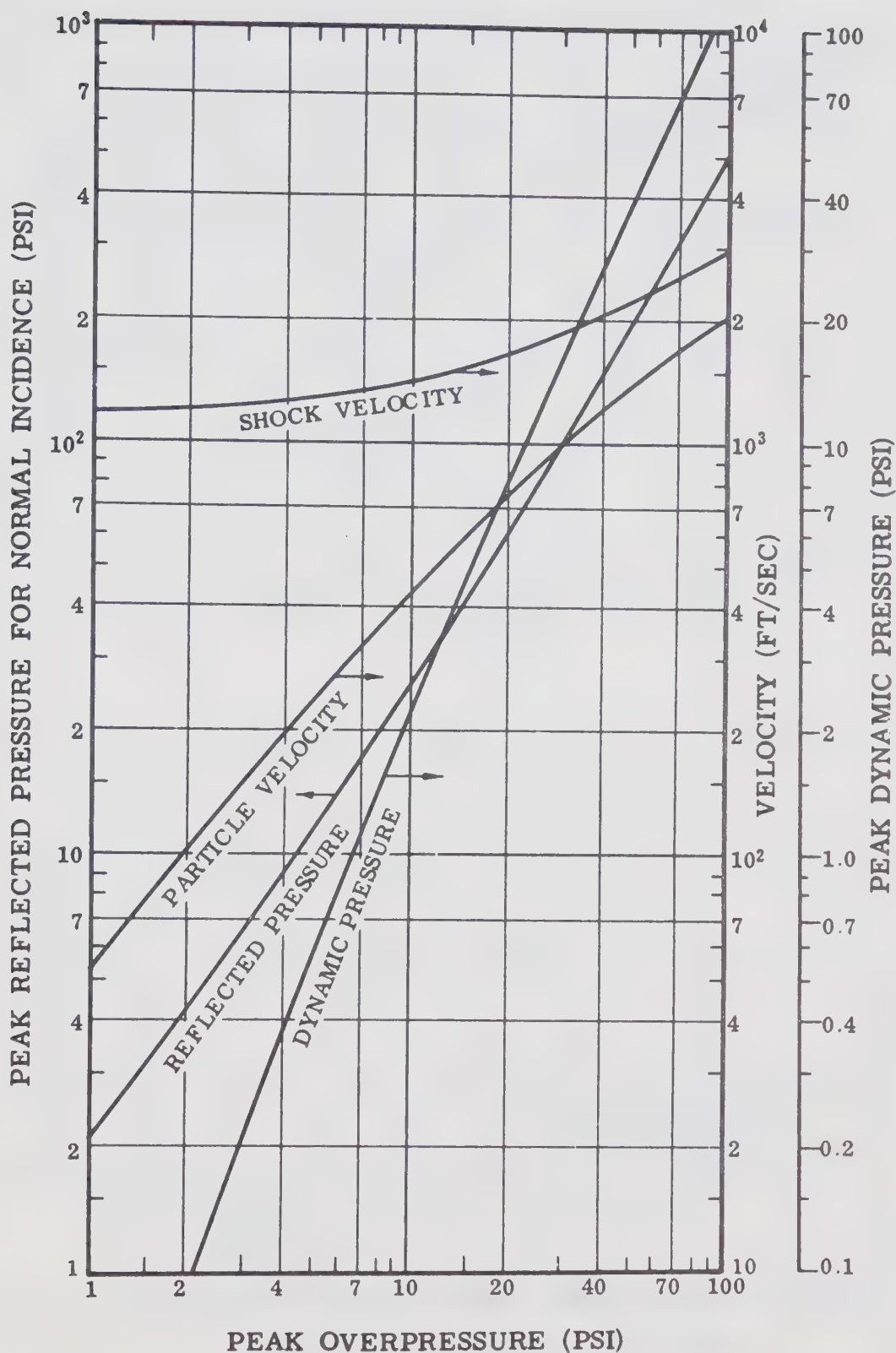


Fig. E-7 Relation of Ideal Blast Wave Characteristics at the Shock Front to the Peak Overpressure
Due to Ref. 14

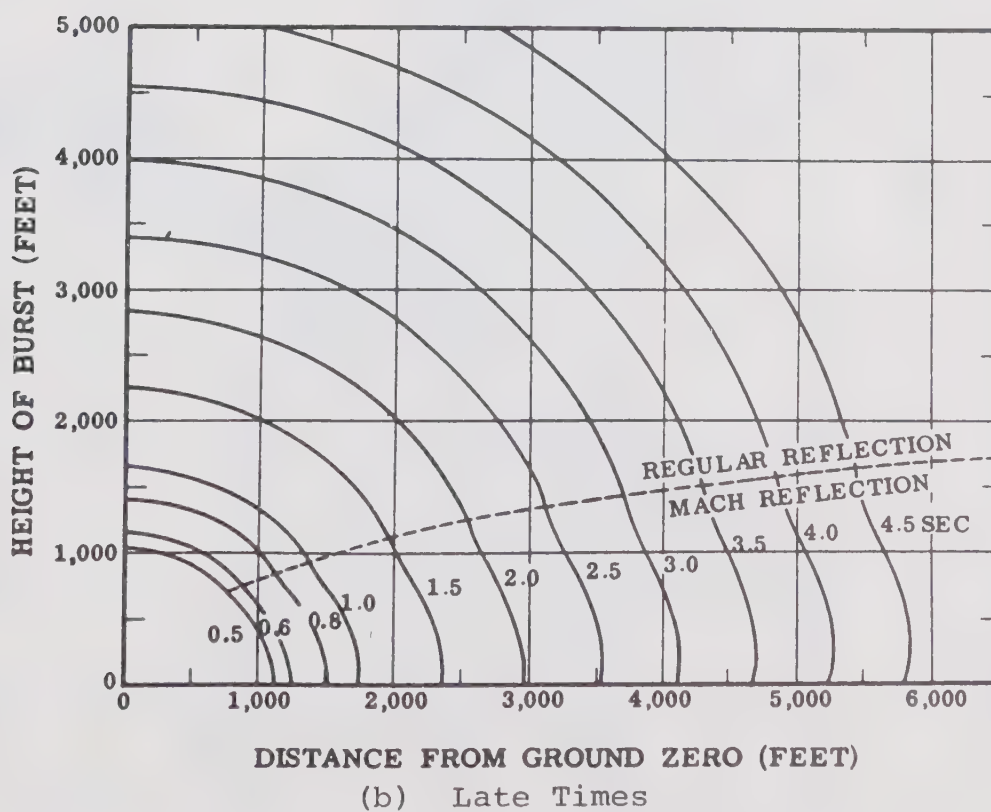
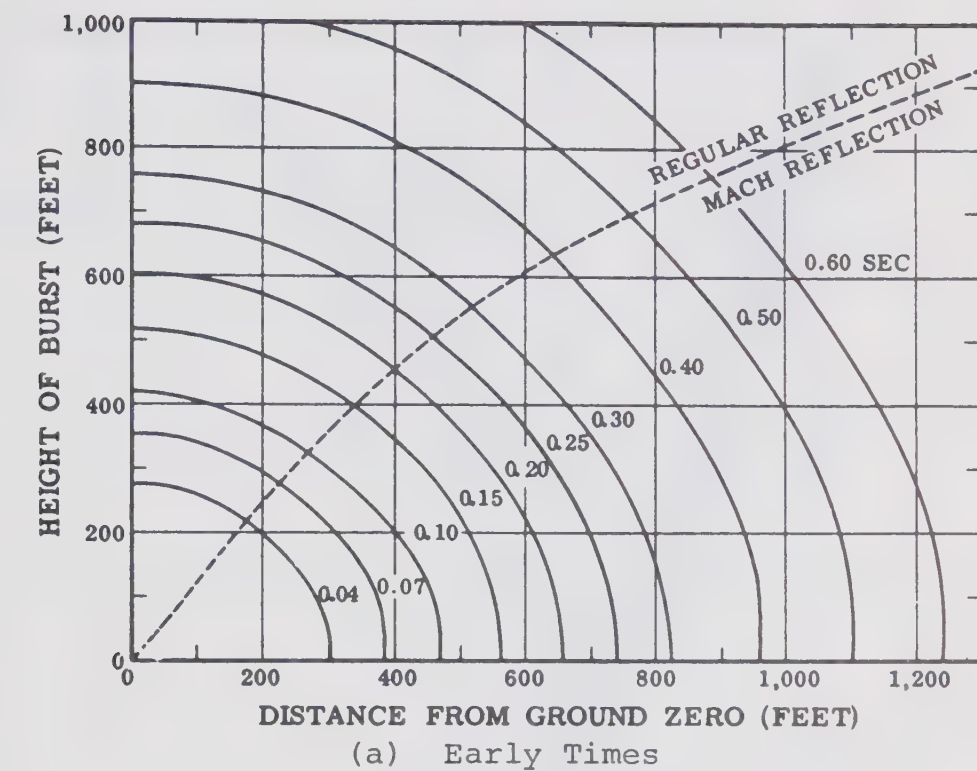


Fig. E-8 Arrival Time on the Ground of Blast Wave for 1-KT Burst. Due to Ref. 14

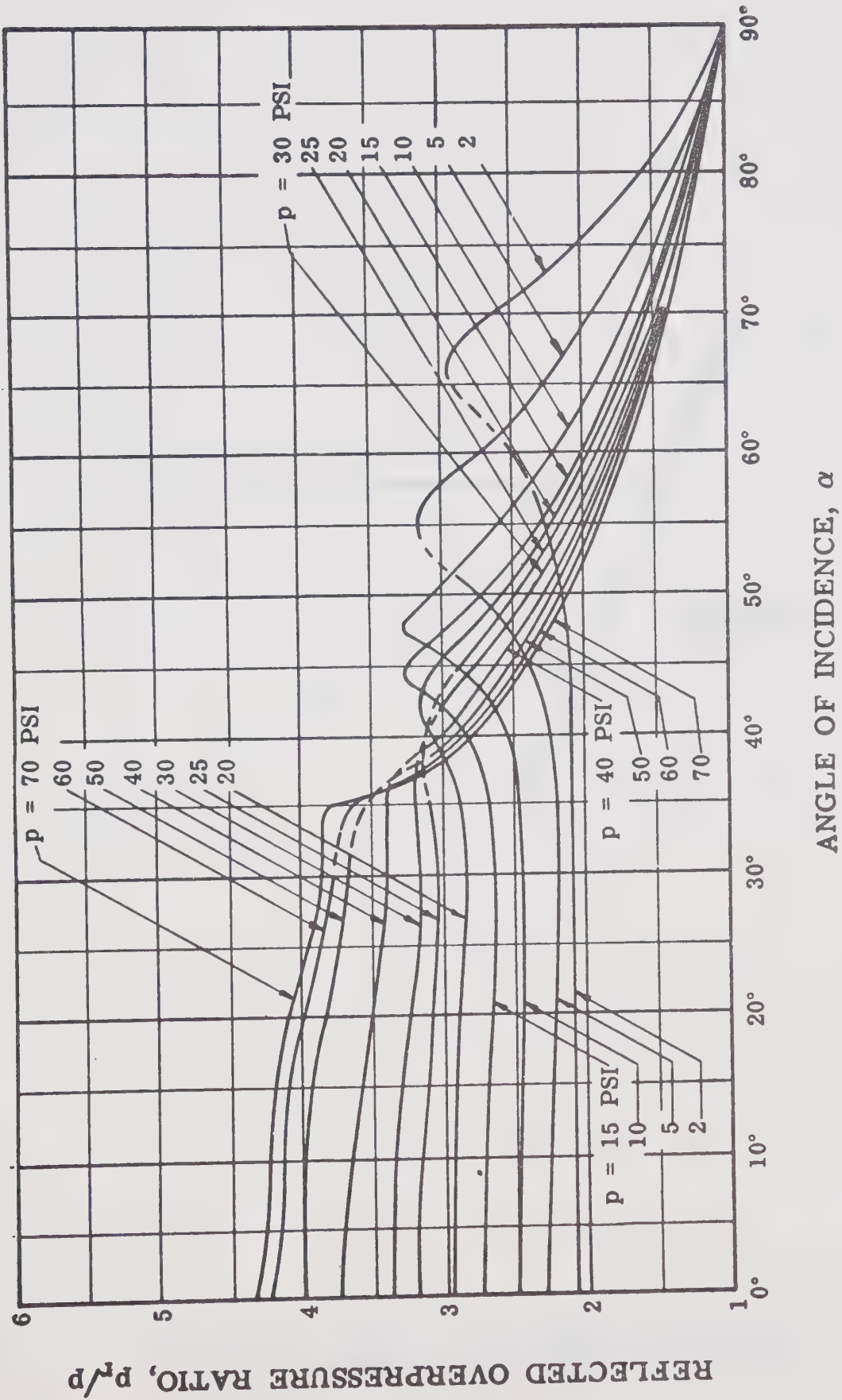


Fig. E-9 Reflected Overpressure Ratio as Function of Angle of Incidence
for Various Side-on Overpressures
Due to Ref. 14

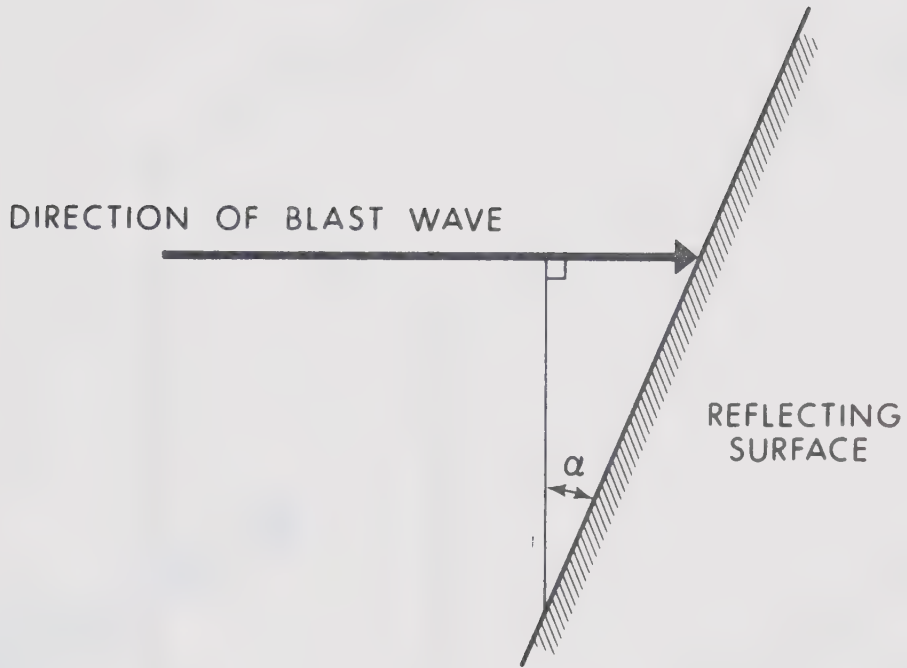


Fig. E-10 Angle of Incidence, α , of Blast Wave with Reflecting Surface

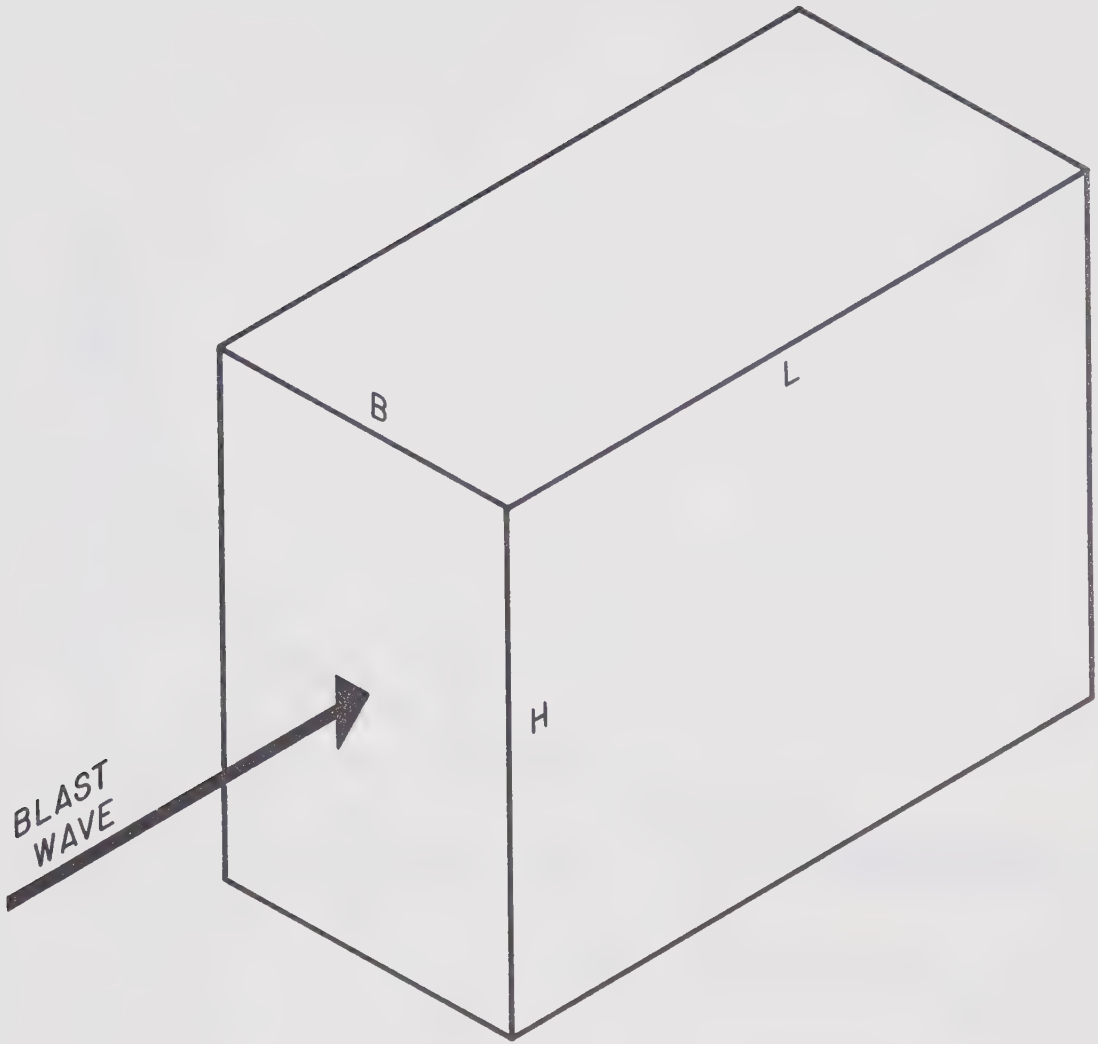


Fig. E-11 Closed Box-Like Structure

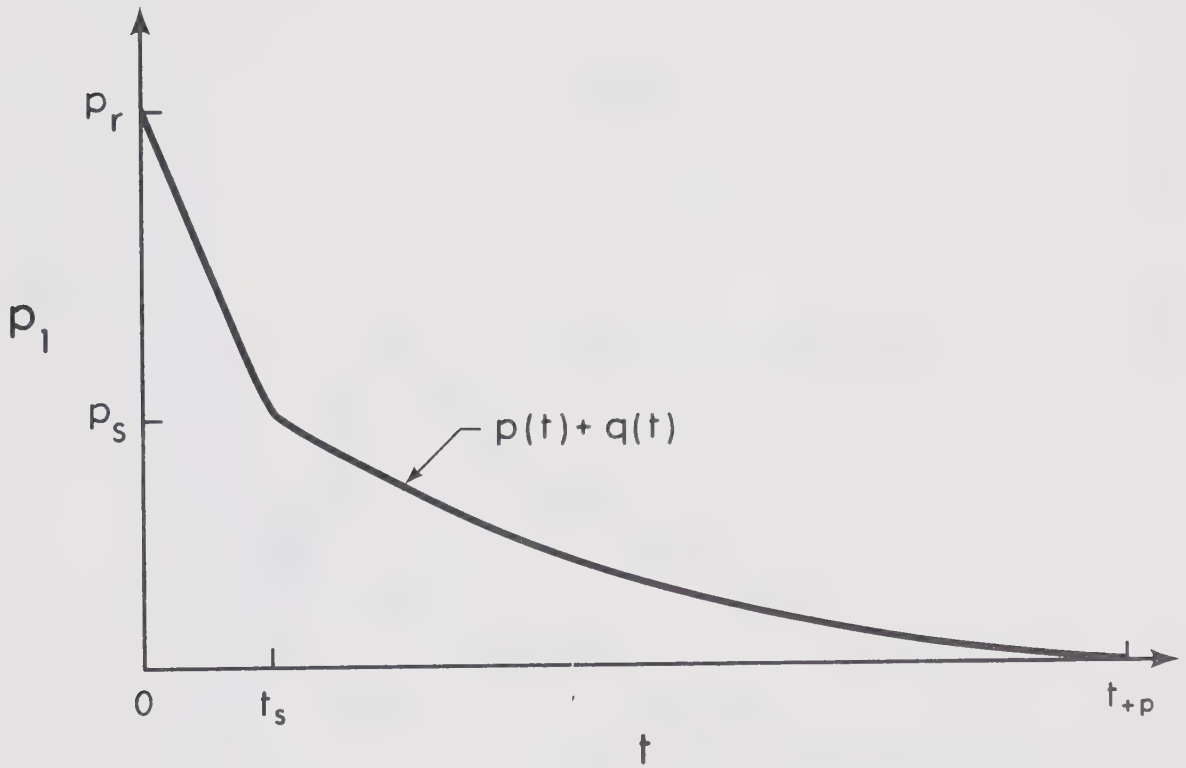


Fig. E-12 Average Front Surface Pressure, p_1

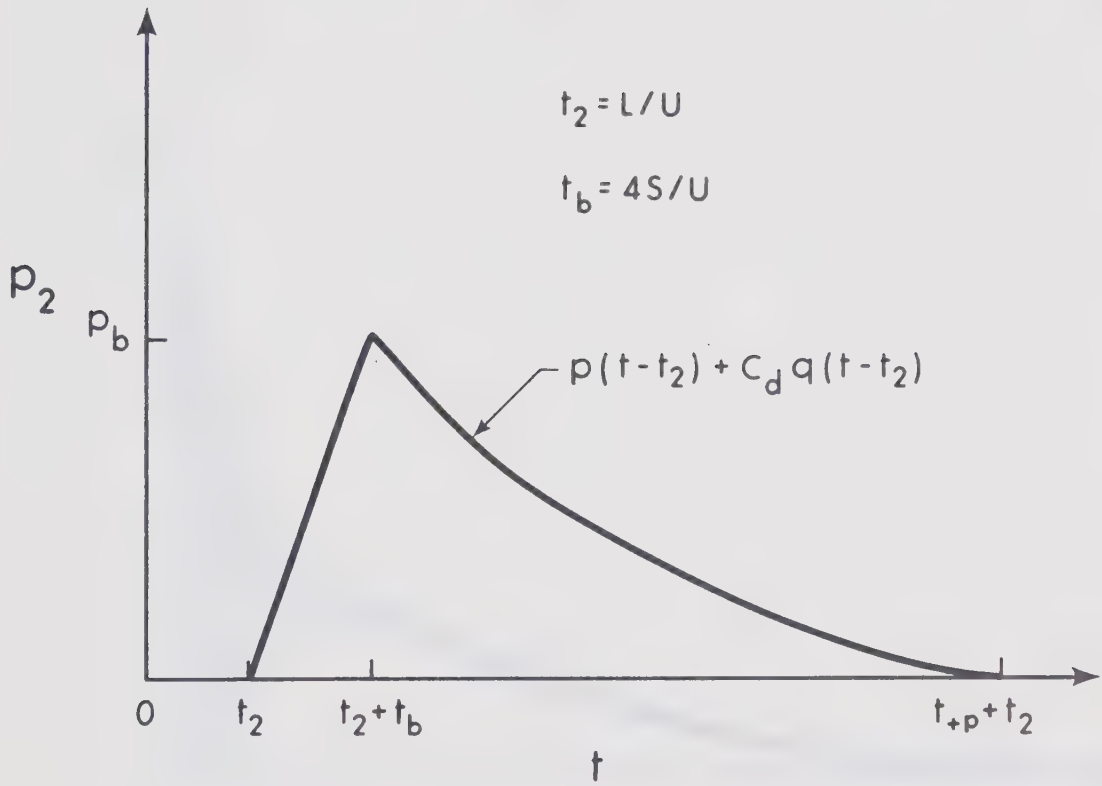


Fig. E-13 Average Back Surface Pressure, p_2

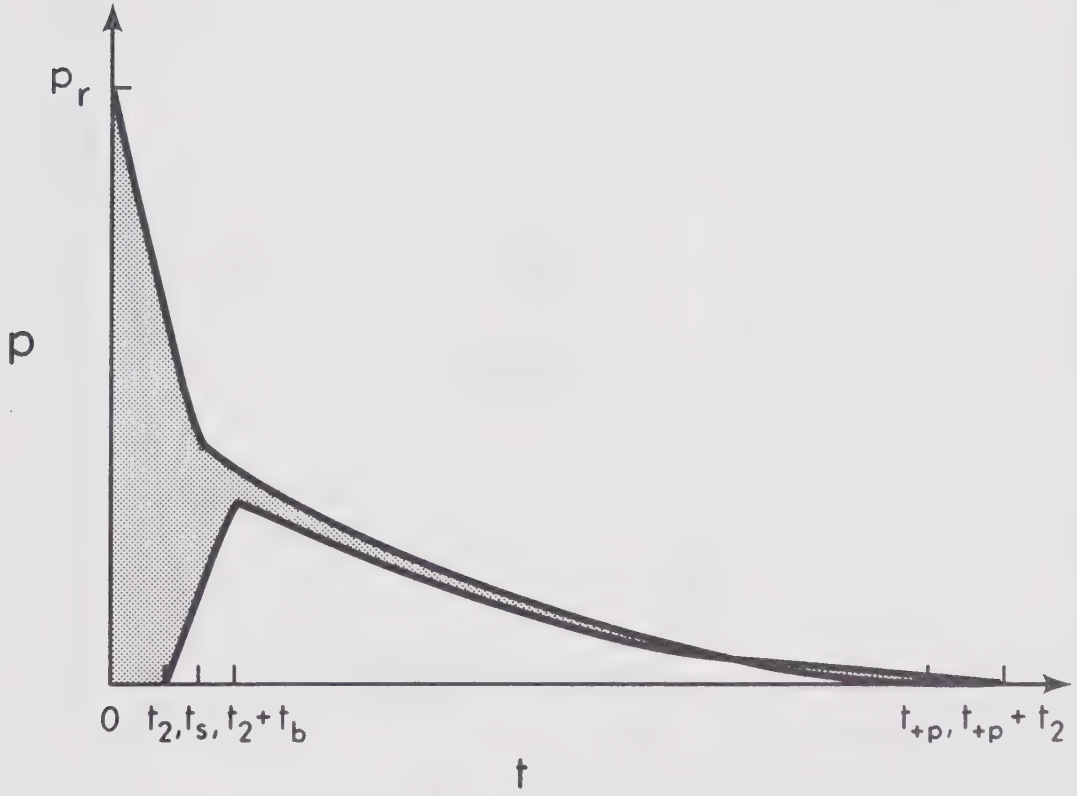


Fig. E-14a Net Horizontal Load (Pressure)

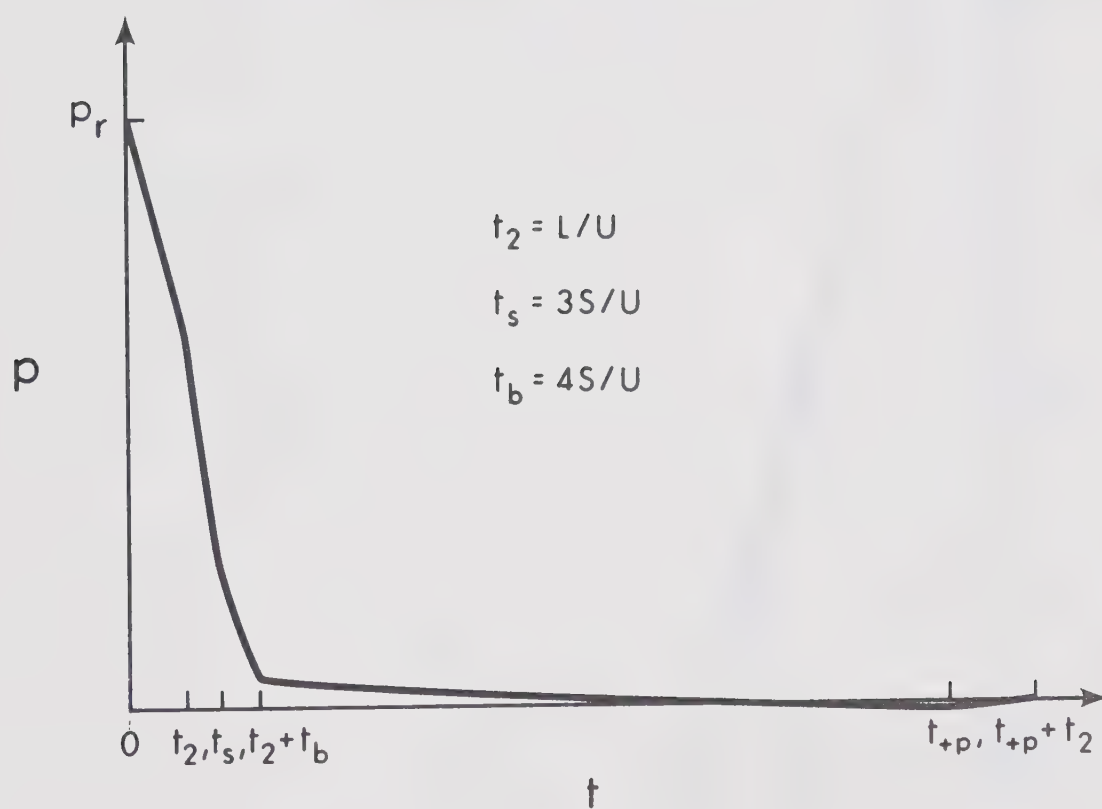


Fig. E-14b Net Horizontal Load (Pressure)

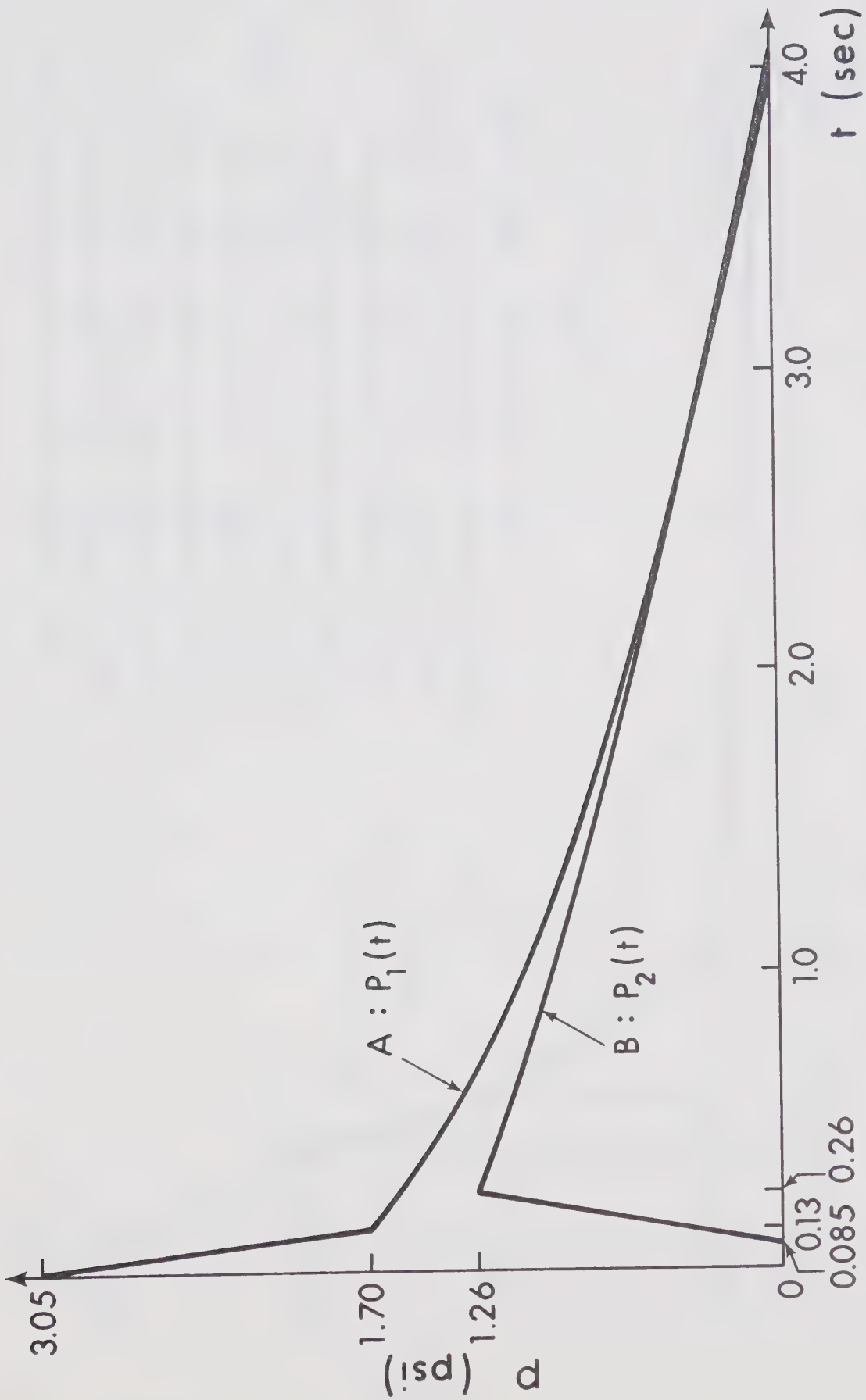


Fig. E-15 Average Pressure Applied to Front Surface (A) and to Back Surface (B)

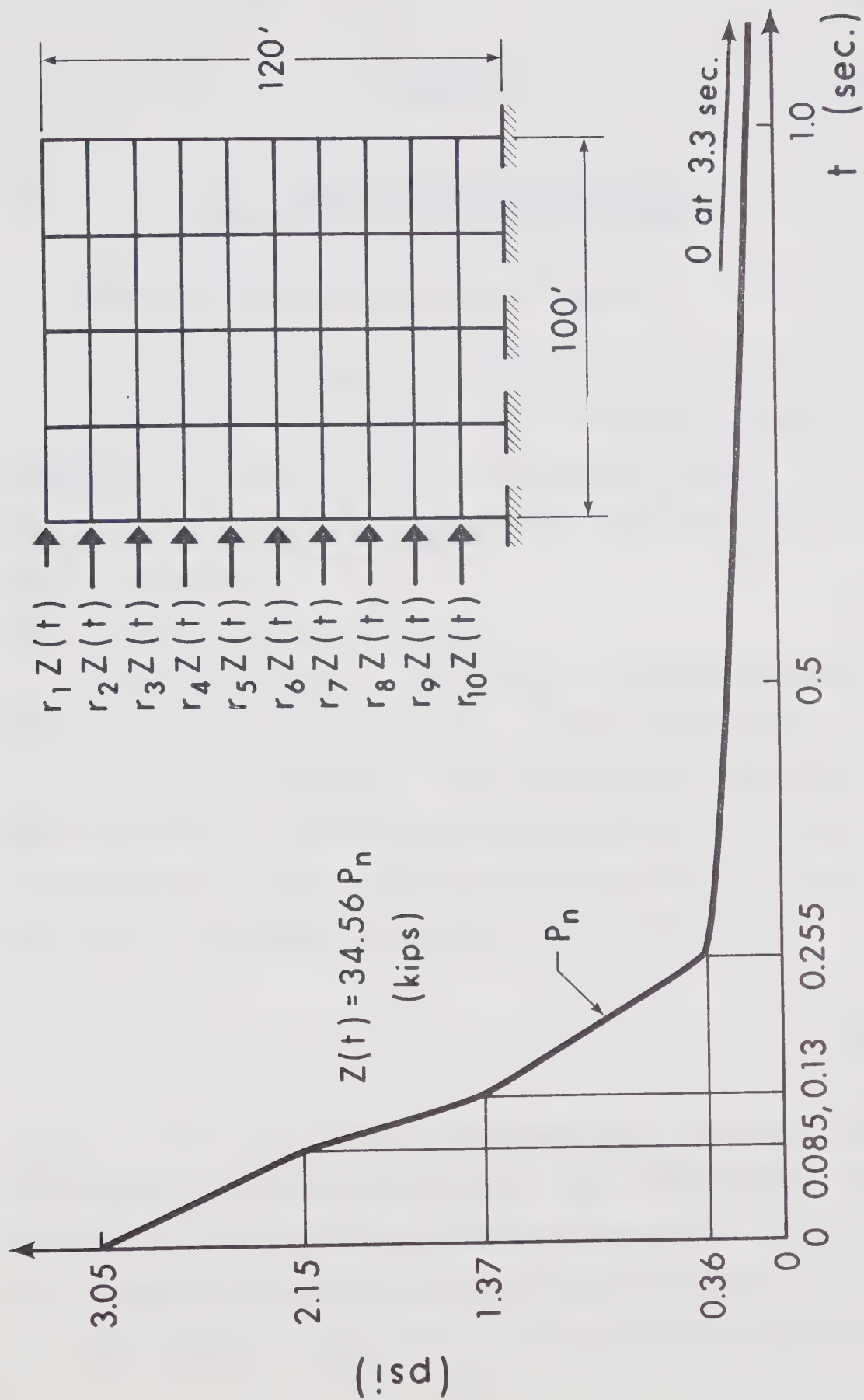


Fig. E-16 Average Net Horizontal Load on the Structure

Appendix F.

EMPERICAL METHOD FOR THE DETERMINATION OF THE NATURAL PERIOD

F-1 Empirical Formula for Natural Period.

In Sec. 4-3 an empirical formula for the calculation of the fundamental natural period of a regular frame was proposed. If the frame contains shearwalls and/or non-rigidly framed members, the quantities defined in Sec. 4-3 must be modified.

(1) Frame Containing Shearwalls.

Such a frame may be represented by the model shown in Fig. F-1. Rigid stubs simulate the wall width effect. In this case, the stiffness of the beam members attached to the shearwall is calculated using the effective length, L_e , instead of the column center to center length, L , used in Sec. 4-3. The effective length, L_e , is defined as:

$$L_e = \left(1 - 2 \sum_{j=1}^2 \lambda_j\right) L \quad (F-1)$$

where $\lambda_1 L$ and $\lambda_2 L$ represent the lengths of the rigid stubs at the left and right ends of the beam, respectively. The natural period may then be determined using Eq. 4-1.

(2) Frame Containing Non-Rigidly Framed Members.

If a beam is connected to its supporting columns by

pinned joints, the bending stiffness of this beam is taken as zero. If only one end has a pinned connection, the stiffness of the beam may be calculated using an effective length, L_e , equal to twice the actual length.

If interior columns have pinned ends as shown in Fig. F-2a, these columns may completely be ignored. Therefore the example in Fig. F-2a may be regarded as a single bay frame ($N_b = 1$ is assumed in Eq. 4-1). The beam stiffness is based on the average moment of inertia of left and right beams with the length of beam equal to the total of the two beam lengths.

If exterior columns have pinned ends as shown in Fig. F-2b, the example is again considered as a single bay frame ($N_b = 1$ in Eq. 4-1). The average beam stiffness, K_b , is calculated as:

$$\begin{aligned}
 K_b = & \left[\sum_{\substack{\text{for all beams} \\ \text{in regular bays}}} \left(\frac{EI}{L} \right)_b \right. \\
 & + \left. \sum_{\substack{\text{for all beams in} \\ \text{special bays}}} \left(\frac{EI}{L_e} \right) \right] / N_s \cdot N_b
 \end{aligned} \tag{F-2}$$

in which a special bay is the exterior bay where the exterior ends of the beams are pinned. Regular bays are all other bays. The effective beam lengths, L_e , in special bays

are taken as twice the actual beam lengths. N_b is the number of bays which is equal to the actual number of bays minus the number of special bays.

F-2 Examples.

(1) Example Calculation on FRAME#1AA.

The properties necessary in Eq. 4-1 are found in Table 4-1. The calculations proceed as follows:

$$\begin{aligned} K_b &= \Sigma \left(\frac{EI}{L} \right)_b / N_s N_b \\ &= .1973 \times 10^6 \text{ kip}\cdot\text{in} \end{aligned}$$

$$\begin{aligned} K_c &= \Sigma \left(\frac{EI}{L} \right)_c / N_s (N_b + 1) \\ &= .5266 \times 10^6 \text{ kip}\cdot\text{in} \end{aligned}$$

Thus,

$$\gamma = \frac{K_b}{K_c} = .375$$

Then T_0 is read from the chart in Fig. 4-1a, as

$$T_0 = 1.83 \text{ sec.}$$

The average story height is 144", thus,

$$h = \frac{144}{144} = 1.0.$$

The quantity, α , is given by:

$$\alpha = 2K_c \times 10^{-6} = 1.053$$

The average weight per story, per column is 95 kips and $N_b = 4$, then β is calculated as:

$$\beta = \frac{95}{70} \times \frac{4 + 0.4}{4} = 1.49$$

Substituting above values in Eq. 4-1, the fundamental natural period of the frame is calculated as:

$$\begin{aligned} T_1 &= T_0 h \sqrt{\frac{\beta}{\alpha}} \cdot \frac{N_s}{10} \\ &= 1.83 \times 1.0 \times \sqrt{\frac{1.49}{1.053}} \times \frac{10}{10} \\ &= 2.18 \text{ sec.} \end{aligned}$$

The rigorous calculation resulted in $T_1 = 2.25$ sec., which indicates the error in empirical formula is about 3% in this case.

(2) Example Calculation on a Frame Shown in Fig. F-3.

The frame shown in Fig. F-3 contains a shearwall as well as exterior columns whose ends are pin connected. Dimensions and necessary properties are inserted in the figure. The empirical formula is used to estimate the fundamental natural period in the following manner.

$$\begin{aligned} K_b &= \left[\sum_{\text{left bay}} \left(\frac{EI}{L} \right)_b + \sum_{\text{right bay}} \left(\frac{EI}{L} \right)_e \right] / N_s N_b \\ &= (2.651 + 1.326) \times 10^6 / 10 \times 1 \\ &= .3977 \times 10^6 \text{ kip}\cdot\text{in} \end{aligned}$$

In the above, the effective length, L_e , for the beams in

the left hand bay is taken, according to Eq. F-1, as

$$L_e = 300 - 2 \times 60 = 240 \text{ inches}$$

and for the beams in the right hand bay:

$$L_e = 2 \times (300 - 2 \times 60) = 480 \text{ inches,}$$

respectively.

$$\begin{aligned} K_c &= \Sigma \left(\frac{EI}{L} \right)_c / N_s (N_b + 1) \\ &= 4.736 \times 10^6 \text{ kip} \cdot \text{in} \end{aligned}$$

Thus,

$$\gamma = \frac{K_b}{K_c} = \frac{.3977}{4.736} = .084$$

Then, T_0 is read from the chart in Fig. 4-1b, as

$$T_0 = 3.34 \text{ sec.}$$

The quantity, α , is given by:

$$\alpha = 2K_c \times 10^{-6} = 9.472 .$$

The average weight per story per column is 87 kips and

$N_b = 1$, therefore;

$$\beta = \frac{87}{70} \times \frac{1 + 0.4}{1} = 1.74$$

The average story height is 144", thus

$$h = 1.0$$

Substituting these values into Eq. 4-1, the fundamental natural period for this frame is calculated as:

$$\begin{aligned}
 T_1 &= T_0 h \sqrt{\frac{\beta}{\alpha}} \cdot \frac{N_s}{10} \\
 &= 3.34 \times 1.0 \times \sqrt{\frac{1.74}{9.472}} \times \frac{10}{10} \\
 &= 1.43 \text{ sec.}
 \end{aligned}$$

The rigorous calculation indicated the natural period to be 1.54 sec. The error in the empirical formula when applied to this rather irregular type of frame is approximately 7%.

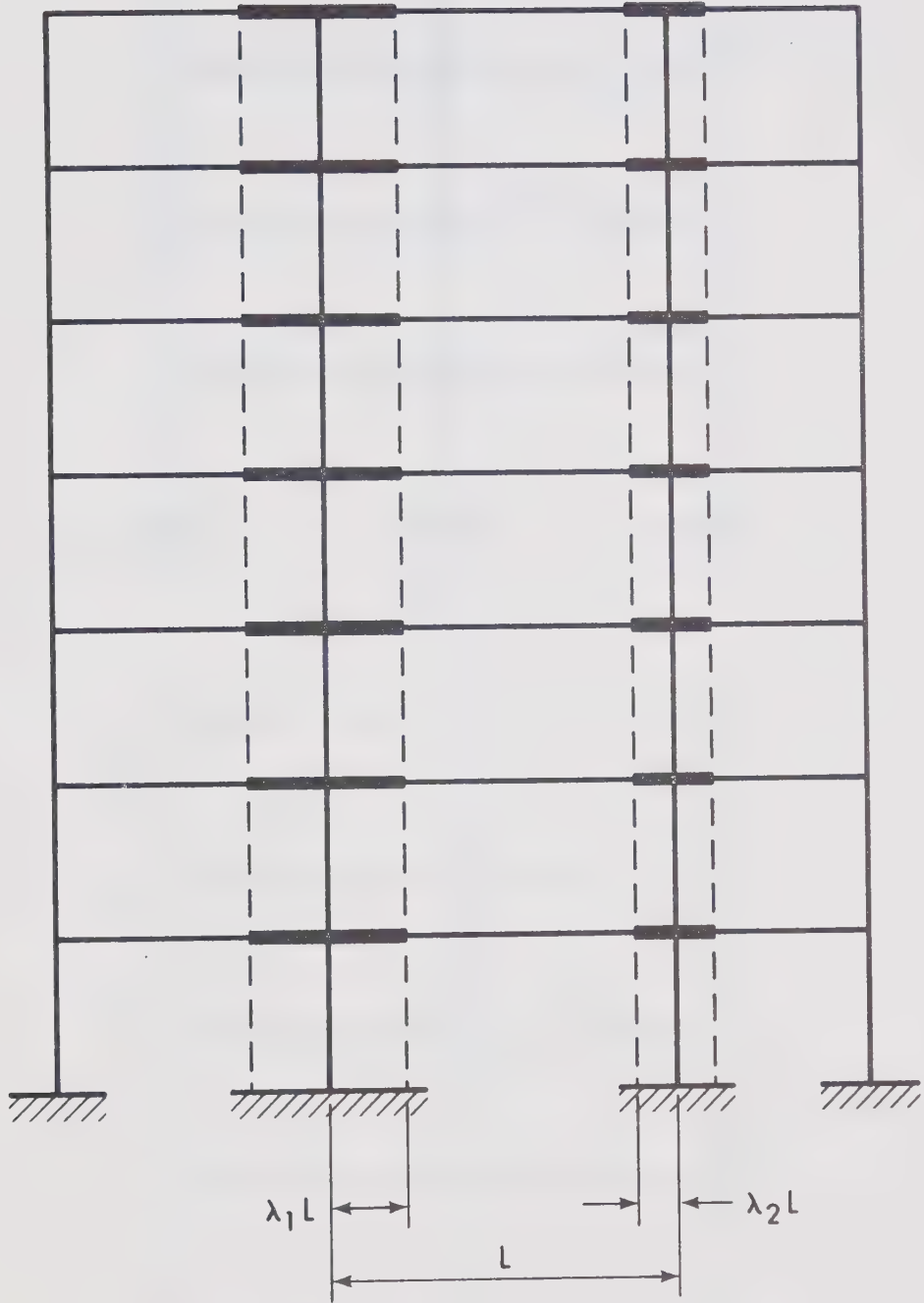
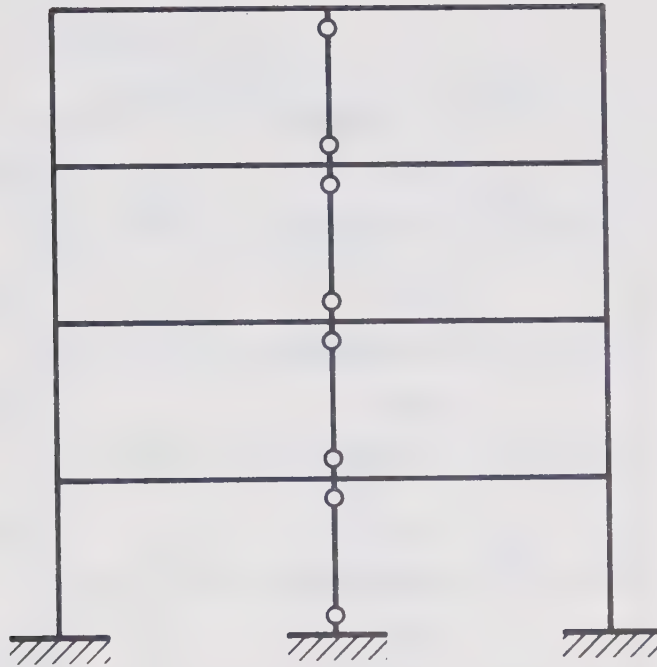
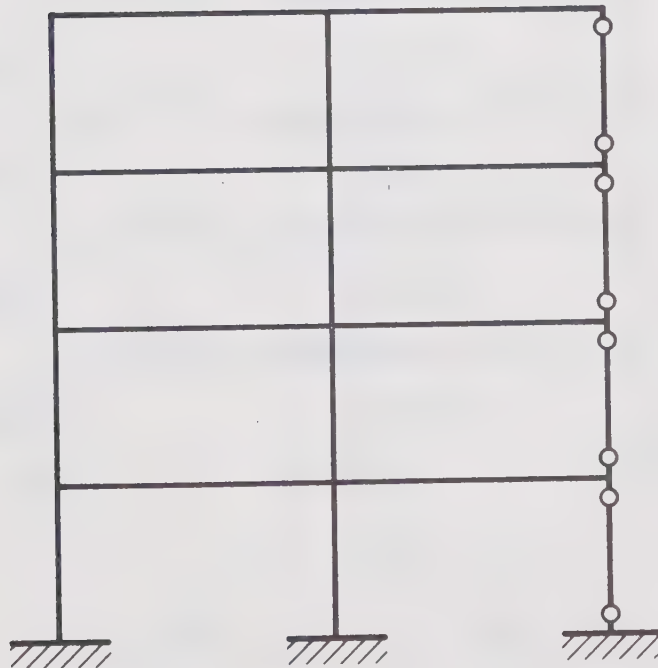


Fig. F-1 Frame with Shearwalls



(a)



(b)

Fig. F-2 Frames with Pinned-End Columns

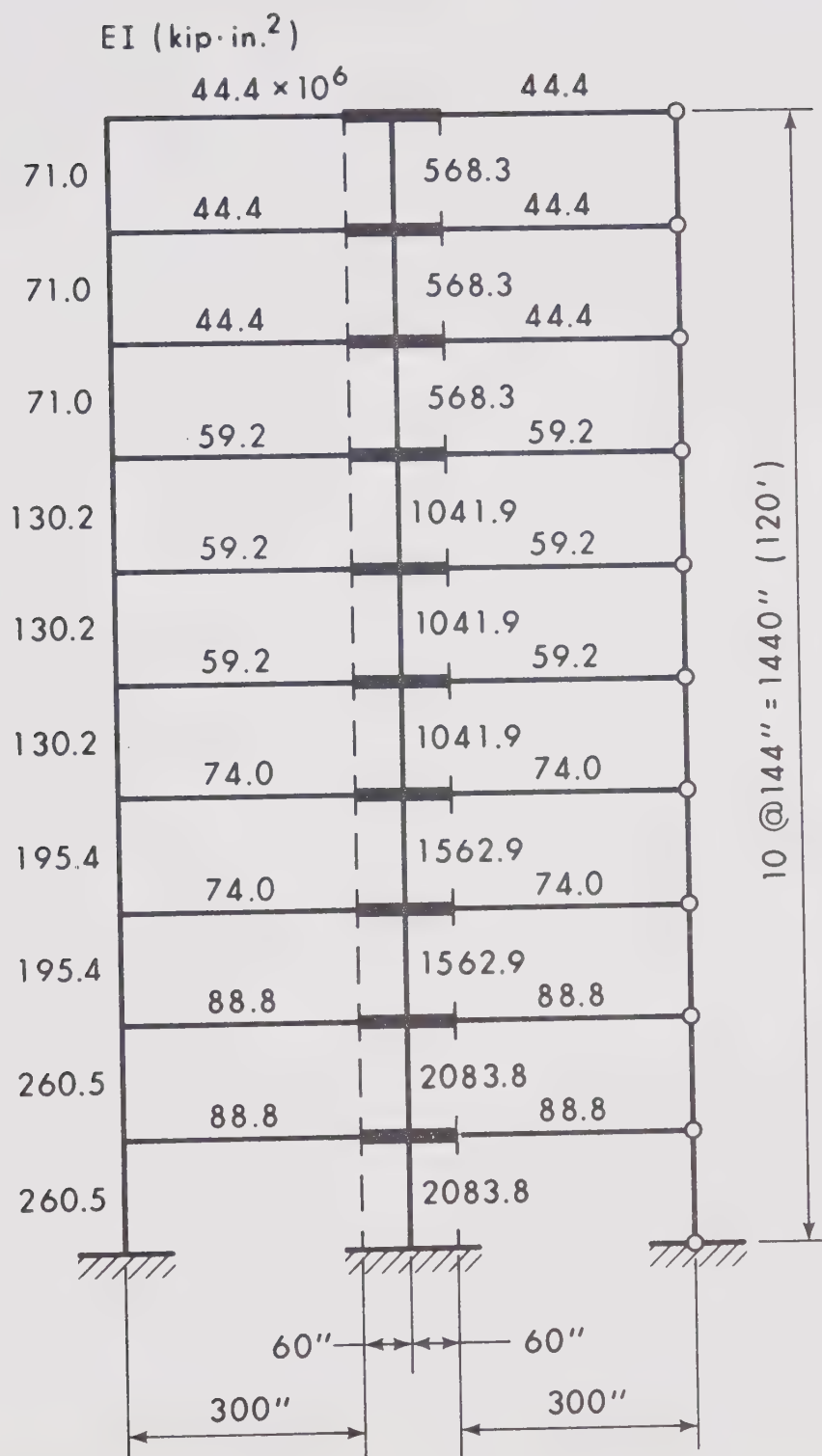


Fig. F-3 Example Frame

B30078